REPORT DOCUMENTATION PAGE

Form Approved
OMB No. 0704-0188

1. AGENCY USE ONLY (Leave blank)	2. REPORT DATE	3. REPORT TYPE AND DATES COVERED
	8/25/04	Final Report 6/30/02 – 6/30/04

4. TITLE AND SUBTITLE

Long-Range, High Coverage Rate Synthetic Aperture Sonar for ASW and MCM Phase I: SAS Validation Experiments

5. FUNDING NUMBERS

N00014-00-D-0108
Delivery Order 0011

6. AUTHOR(S)

Angela Putney, Matt Nelson, James Campbell, Eric S.H. Chang

7. PERFORMING ORGANIZATION NAME(S) AND ADDRESS(ES)

Dynamics Technology, Inc.
21311 Hawthorne Blvd. #300
Torrance, CA 90503

8. PERFORMING ORGANIZATION REPORT NUMBERS

DTW-0223-04007

9. SPONSORING/MONITORING AGENCY NAME(S) AND ADDRESS(ES)

Douglas Abraham
Office of Naval Research
800 N. Quincy Street
Arlington, VA 22217-5660

10. SPONSORING/MONITORING AGENCY REPORT NUMBER

N00014-00-D-0108
Delivery Order 0011

11. SUPPLEMENTARY NOTES

12a. DISTRIBUTION / AVAILABILITY STATEMENT

Approved for Public Release; distribution unlimited

13. ABSTRACT *(Maximum 200 words)*

In October 2003, Dynamics Technology, Inc. (DTI) and L-3 Communications Ocean Systems (L-3OS) took the L-3OS Seahawk 1.4 kHz variable depth sonar with twin-line receive array to sea and collected active sonar data against the Ex-USS Salmon (SS-573, diesel submarine) and M/S Bidevind (freighter sunk by torpedo) off the NJ/NY coast. DTI processed the data as synthetic aperture sonar (SAS) imagery. The limits of effective SAS processing were set by array motion and not by characteristics of the environment. Image resolutions for the Ex-USS Salmon of 6.5 m at 500 m range, 12 m at 4500 m range, and 13 m at 8000 m range were achieved. For the Bidevind our resolutions were 5 m at 500 m and 9 m at 4000 m. The system characteristics afforded us the opportunity to provide SAS imagery from multiple aspects. This imagery demonstrated potential classification clues for distinguishing targets from clutter. The data set collected against the Salmon is the most complete set to date against a submarine in terms of data at multiple aspects and multiple ranges in an uncluttered environment; it is an ideal data set for developing an automatic target recognition system (classifier). Additionally, the SAS images were processed to investigate frequency responses of the Ex-USS Salmon and Bidevind. Despite the small, 400 Hz bandwidth, there were indications that this could be a useful classification tool.

14. SUBJECT TERMS	15. NUMBER OF PAGES
Synthetic Aperture Sonar, Anti-Submarine Warfare, Mine Countermeasures, towed array, classification, Ex-USS Salmon, multi-aspect	223
	16. PRICE CODE

17. SECURITY CLASSIFICATION	18. SECURITY CLASSIFICATION OF THIS PAGE	19. SECURITY CLASSIFICATION OF ABSTRACT	20. LIMITATION OF ABSTRACT
Unclassified	Unclassified	Unclassified	SAR

NSN 7540-01-280-5500

Standard Form 298 (Rev. 2-89)
Prescribed by ANSI/NISO Std. Z39.18
298-102

DTW-0223-04007

dynamics technology, inc.

Long-Range, High Coverage Rate Synthetic Aperture Sonar for ASW and MCM
Phase I: SAS Validation Experiments

Final Report

August 2004

Prepared By:

Angela Putney
Matt Nelson
James Campbell
Eric S.H. Chang

Contract No.: N00014-00-D-0108, Delivery Order 0011
In fulfillment of
Contract Deliverable: CDRL #A0002

Dynamics Technology, Inc.
21311 Hawthorne Blvd., Suite 300
Torrance, CA 90503
(310) 543-5433

ABSTRACT

In October 2003, Dynamics Technology, Inc. (DTI) and L-3 Communications Ocean Systems (L-3OS) took the L-3OS Seahawk 1.4 kHz variable depth sonar with twin-line receive array to sea and collected active sonar data against the Ex-USS Salmon (SS-573, diesel submarine) and M/S Bidevind (freighter sunk by torpedo) off the NJ/NY coast. DTI processed the data as synthetic aperture sonar (SAS) imagery. It was determined that the limits of effective SAS processing were set by array motion and not by characteristics of the environment, which would have implied limitations in a practical application of the SAS technique. Image resolutions for the Ex-USS Salmon of 6.5 m at 500 m range, 12 m at 4500 m range, and 13 m at 8000 m range were achieved. For the Bidevind our resolutions were 5 m at 500 m and 9 m at 4000 m. The wide transmit and receive beams of the system provided us with the opportunity to steer beams in individual runs and provide SAS imagery from multiple aspects. This imagery demonstrated potential classification clues for distinguishing targets from clutter. The data set collected against the Salmon is the most complete set to date against a submarine in terms of data at multiple aspects and multiple ranges in an uncluttered environment; it is an ideal data set for developing an automatic target recognition system (classifier). Additionally, the SAS images were processed to investigate frequency responses of the Ex-USS Salmon and Bidevind. Despite the small, 400 Hz bandwidth, there were indications that this could be a useful classification tool.

This report contains a detailed description of the preparations, deployment, and results of the October 2003 trial. Twenty-four data sets were collected. With the funds available, five data sets representing a cross-section of the system capabilities were identified and SAS processed. All SAS images processed under the program are included in this report, along with the corresponding side-look sonar processed images.

TABLE OF CONTENTS

LIST OF FIGURES

LIST OF TABLES

SUMMARY

The Naval Transformational Roadmap requires surface combatants to protect themselves and support battle group assets using area denial and transit route sanitization from threat submarine platforms. This requirement forces the Navy to locate and hold at risk the quiet diesel-electric, and upcoming air-independent propulsion, submarines found in the fleets of potentially hostile nations. The current passive-only sonar anti-submarine warfare (ASW) techniques are becoming increasingly ineffective against such targets. These problems are compounded by anticipated operation in the littorals, areas known to have poor sound propagation and high levels of ambient noise from coastal shipping traffic. Traditional active search and localization techniques produce excessive false targets overwhelming the ability of both operators and information processors to discriminate valid threats from other objects. Additionally, current active techniques are rarely effective against zero- and low-Doppler targets. In order to overcome these shortcomings, the Navy needs to develop revolutionary surveillance technologies.

Dynamics Technology, Inc. (DTI) demonstrates a revolutionary active sonar technique for ASW in this study. Synthetic Aperture Sonar (SAS) is a technique that is revolutionizing the mine countermeasure community with its fine range-independent resolution. This resolution has significantly improved our ability to detect and classify sea mines. Extending these capabilities to lower frequencies and thus longer ranges, SAS has been demonstrated here in a sea trial as a viable ASW technique. An ASW sonar system optimized for SAS has the potential to achieve 5 m resolution out to 25 km range or further. It is important to note that SAS is the only currently known active acoustic ASW technique that can distinguish a zero/low-Doppler target such as a bottomed, quiet conventional submarine (SSK). DTI performed a proof-of-concept at-sea trial to demonstrate the feasibility of just such an ASW SAS system. The 1.4 kHz L-3 Communications Ocean Systems (L-3OS) Seahawk variable depth sonar (VDS) with twin-line towed arrays required only minor modifications for SAS compatibility and provided us with an inexpensive sonar system for the trial.

DTI previously demonstrated the feasibility of SAS out to 10's of kilometers utilizing systems of opportunity that were not well matched to SAS processing. Under the DARPA-funded program presented here, DTI used the L-3OS SAS-compatible Seahawk system to conduct a trial at-sea. DTI successfully created SAS images of a bottomed submarine and a sunken ship from the trial. The respective images contained some similar characteristics such as size, but, more importantly, they contained distinguishable characteristics which would be useful to an operator or other classifier. Our multi-aspect processing of the data appears to increase this potential classification usage.

Additionally, we investigated the potential of an additional classification tool, namely the frequency response of a target. The 400 Hz bandwidth of the system was large enough to evaluate the potential for such a tool, although a deployed system would most like use a larger bandwidth. The Ex-USS Salmon and Bidevind each demonstrated differences in the frequency responses amongst different aspect angles and between one another.

We have investigated several ASW scenarios and developed a concept of operations (CONOPS) for these scenarios involving SAS. In all cases the carrier battle group could be protected from zero/low Doppler submarines using a small number of assets with SAS ASW systems installed.

This proof of concept program indicates the potential for a SAS ASW system. However, for a deployable system, the impact of clutter at these tactically useful frequencies needs to be further investigated and assessed. With the knowledge of how targets and clutter are both similar and different, we can determine the classification effectiveness, i.e., probability of detection, correct classification, and false alarms, of such a system. Additionally we can calculate the related receiver operating characteristic (ROC) curves and create a design for optimal performance.

We recommend to advance this proof of concept program into a technically mature and tactically valuable SAS ASW capability. Specifically, we recommend to develop an ASW SAS processor, upgrade the L-3OS Seahawk VDS/twin-line towed array system used in the 2003 at sea test for longer arrays with motion sensors, collect data against clutter in multiple sea trials, and produce ROC curves for the system. By the end of such a future program we expect to have a system ready for transition into the Navy.

We also recommend using the data set for developing an automated target recognition (ATR) system (classifier) for ASW using the LRSAS data set for development and testing of the target models. The data collected against the Ex-USS Salmon was from all around the submarine, i.e., multiple aspects, and multiple ranges. The lack of clutter and the favorable ocean conditions on the data collection days make this data set is the most comprehensive set collected against an actual submarine, albeit over a small frequency range. It is comparable to the data sets collected on platters for mine countermeasures work.

1. INTRODUCTION

Our Navy's surface ships are often significantly challenged to protect themselves or other ships from submarine attack with the current suite of sonar systems installed. A foreign submarine that can come to within 10 km of one of our Navy surface ships has a good chance of achieving a firing solution sufficient to launch weapons. A bottomed or slowly moving submarine, providing a low or zero Doppler target is extremely difficult to detect, localize, and classify. Such a submarine can act as an intelligent, mobile, homing mine waiting for a battle group to pass by before attacking. Even when deployed by third world navies in small numbers, the threat of undetectable SSKs to battle groups can exceed the potential for force on force exchange by the impact of area denial on US fleet operations and planning.

Over the last several decades the submarines of the world have become quieter while the oceans of the world have not. The US Navy will in all likelihood have to take the battle into their opponents' waters conducting sustained operations in shallower and more varied ocean environments than was expected during the cold war period. Thus passive sonar by itself, which achieved extraordinary detection ranges for several decades, can no longer be relied on to deliver tactically useful detections against modern submarines, especially if the submarines are bottomed or barely moving. During the decades of ascendancy of passive sonar, active Anti-Submarine Warfare (ASW) fell into disfavor and research in warship-borne active sonar suffered commensurately.

There are valid reasons for avoiding conventional tactical active sonar. Current fleet hull-array active systems achieve only a little better than 9 degrees of azimuth resolution. This yields a resolution cell of ~4 km wide at 25 km ranges. A detection in such a large cell cannot be effectively classified without additional information. A second issue is that in many environments the downward-refracting acoustic propagation from existing hull-array sonars does not lead to illumination of the target. The littoral regions additionally suffer from severe reverberation and false contact problems. A third issue is that the method used to distinguish a submarine from clutter relies on the Doppler shift of the returning signal off a moving target. If the detected object is not moving or moving extremely slowly, these Doppler shifts are absent and the object may be declared not a target or it remains unclassified until it is much closer and possibly within shooting range of the surface ships. The potential for large numbers of these possible targets can easily overwhelm the ability of the host platform to classify. This means that conventional active sonar ASW is only useful for locating moving submarines.

However, there is an active sonar technique that could overcome the conventional active ASW problems. Dynamics Technology, Inc. (DTI) has adapted synthetic aperture radar (SAR) techniques to the ocean environments. Our synthetic aperture sonar (SAS) processing techniques were developed for the mine countermeasures (MCM) community and our real-time SAS processor, PRO*SAS*^{TM}, is used on unmanned underwater vehicles. In the program reported here, DTI has demonstrated the feasibility for using the same basic processing techniques in the more stressful ASW arena.

SAS processing can greatly enhance the ability of the operators to sort targets from clutter. By coherently combining returns from multiple pings a large synthetic aperture is formed. This large aperture allows the creation of an image of constant resolution at all ranges. Thus, instead of 4 km wide cells at 25 km range, 5-10 m cells at 25 km range can be formed. At this resolution, for example, an oil rig could be distinguished from a submarine-like object. SAS works best for non-moving targets which makes it the only active sonar technique that can discriminate low or zero-Doppler targets. For moving targets, SAS can be combined with more conventional techniques to form images. In this case, the velocity of a detected object can be determined from conventional sonar processing and then fed into the SAS processor to change the processing reference frame and allow for an image of the detected object to be formed.

The program reported upon herein, as the title suggests, is a validation of SAS for long range ASW and MCM usage. This validation consisted of at-sea trials using an existing sonar, the L-3 Communications Ocean Systems (L-3OS) Seahawk variable depth sonar, that required only minor modifications to be SAS ready. The results of the three day SAS trial in October 2003 at the Shallow Water Diesel Test Facility near Hudson Canyon off the coast of New York/New Jersey, DTI demonstrated that SAS images could be formed out to 8 km range and a submarine, the Ex-USS Salmon (SS-573), could be resolved at this range. Thus also verifying the classification potential of SAS. An additional classification tool for SAS was also demonstrated in the trial results. Namely the ability to form images from multiple aspects of a detection thus increasing the number of looks and possibility of correct classification. All these results are presented in this report.

This report is the final scientific and technical report required by Contract Number N00014-00-D-0108, Task Order 0011. Section 2 describes the methods, assumptions, and procedures used for the validation sea trials and subsequent data processing. Section 3 presents the results of the October 2003 sea trial and discusses these results. Section 4 summarizes our conclusions. Section 5 delineates our recommendations for the next stages of this work.

2. METHODS, ASSUMPTIONS, AND PROCEDURES

The overall plan for this program was to conduct a sea trial to collect SAS-compatible data, SAS process the data, and analyze the SAS images. This section describes the processes involved in this plan. The results of the trial and analyzes are shown in Section 3.

All aspects of this program required preparation. In Section 2.1 we describe the L-3OS Seahawk sonar system. In Section 2.2 we describe the process for choosing the trial location. In Section 2.3 we delineate the aspects of planning the actual trial. In Section 2.4 we explain the acoustic data processing. In Section 2.5 we illustrate the clutter and target analyses we conducted.

2.1 L-3OS Seahawk Sonar

Several years ago L-3OS built a variable depth sonar (VDS) with a twin line towed array, now designated Seahawk. While not fully SAS compatible, only a few adjustments were required to make it so. The existence and availability of this system was a key enabler for the Long Range SAS (LRSAS) program. The basic description of this system is in Section 2.1.1.

The Seahawk system had not been used for several years and required a full set of laboratory tests and maintenance[1]. Some key results of these tests, such as the functionality of the receivers, are delineated in Section 2.1.2. The array testing indicated that there were some dead channels. Section 2.1.3 details the simulations conducted in order to determine if the lack of these channels would impact the SAS imagery enough to require repairs to the array (i.e., a costly proposition). Additionally in this section, we investigate the effects on SAS imagery of where in the data stream a time stamp indicating the start of ping is placed. Using the results of these simulations, Section 2.1.4 summarizes the PingNow circuit. Given all the parameters for the system, Section 2.1.5 describes the boundaries for SAS with the Seahawk system.

2.1.1 Seahawk System Description

As stated above, Seahawk is a VDS with a twin line towed array. Table 2-1 lists key system characteristics. The VDS transmitter is an array of 16 projector elements. These are retracted during deployment and recovery (Figure 2-1) and extended at depth (Figure 2-2). These 16 elements allow the transmitter to have one of two

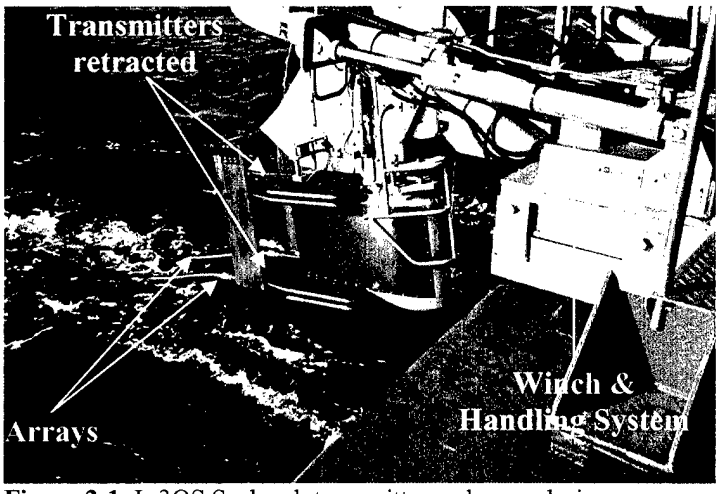

Figure 2-1. L-3OS Seahawk transmitter and array during deployment.

[1] Some activities involved in "dusting off" the system and improvements to the system were L-3OS internal research and development activities. They are described in this document since they are very much related to the DARPA/ONR funded work.

horizontal transmit patterns: omnidirectional (360°) or directional (120°, steerable to one of four directions). The VDS towbody contains devices to measure several non-acoustic parameters (see Table 2-2 for list of those potentially useful to SAS). The receive arrays attach directly to the rear of the VDS. This arrangement stabilizes the array motion. The system was designed to deploy a total of four fluid-filled arrays, but we use only two. Seahawk is deployed using a compact winch and handling system (seen in Figure 2-1). It was designed to operate off of various sized ships, including frigates, corvettes, small patrol craft. For our trials, we deployed off an 95 ft (28.96 m) and a 110 ft (33.53 m) vessel.

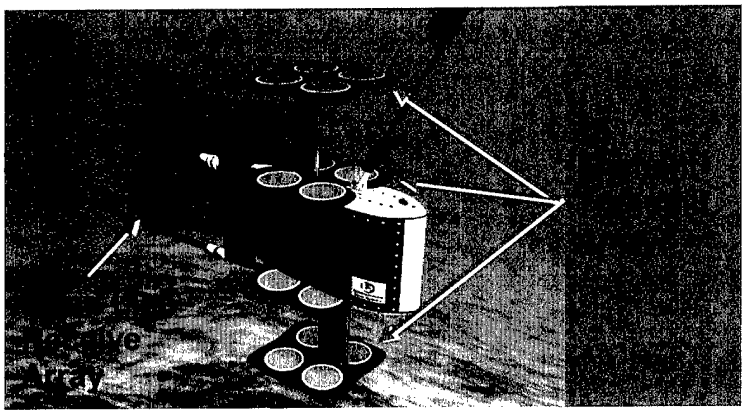

Figure 2-2. L-3OS Seahawk transmitter and array schematic during use. The transmitter is fully extended in this drawing. Note also the start of the fairing on the tow cable. This schematic shows the optional additional receiver array pair in the upper position. Our trials only used the lower arrays as seen in Figure 2-1.

Table 2-1. Seahawk system parameters.

Characteristic	**Value**
Operating frequency	1400Hz
Bandwidth	400 Hz
Max source level (omni transmit)	219 dB re 1 μPa @ 1m
Max source level (directional transmit)	221 dB re 1 μPa @ 1m
Vertical beam	Cardioid-like with null towards surface
Horizontal beam	120 ° steerable
Planned pulse length	0.25 s, 0.5 s
Planned pulse repetition interval (PRI)	6 s, 12 s
Operational Depths	15-300 m (50-985 ft)
Operational Speeds	3-15 kts
Receive arrays	Two 48 element arrays
Array length	23.5 m
Array separation	0.3 m
Array and handling system	3250 kg weight; 2.5x3.5x2.3 m size
Shipboard electronics	880 kg weight; ~2.1x1.7x1.8 m size (multiple units, this is one possible configuration)

The sonar controls and transmit amplifiers are located topside. From the operator console the various parameters of the system (e.g., pulse repetition interval/range scale, waveform,

and source level) are set, the transmitter is turned on and off, and the receive array and non-acoustic data are set to record. All communications to and from the sonar pass through an optical fiber on the 50% faired tow cable, which also provides power for the sonar. The transmit waveforms are programmable. For our trials we used either a 0.25 s or a 0.5 s LFM chirp. The source level could be set to the maximum shown in Table 2-1 or stepped down by 3, 6, 9, 12, or 18 dB.

Seahawk required several alterations to make it SAS compatible. The native Seahawk processing did not require knowledge of the exact moment of transmission of the ping; however, SAS requires this knowledge or at least a repeatable time and phase knowledge of the ping cycle. An additional circuit, the PingNow circuit, was added to the system to sense the ping start time and set and indicator bit in the topside telemetry. This is described in more detail in Section 2.1.4. The second alteration was to write the data to disk before decimation. To keep this change reasonably priced, we lost some Seahawk processing capabilities, described below. There was a possible third alteration - increase the number of ping repetition interval (PRI) choices to allow faster tow speeds - but since it did not inhibit SAS processing and the required changes and testing were not feasible within the program scope, the change was not made. Thus the system PRI and range scale remained tied together with only a few settings, e.g., 6 s PRI for 5000 m range.

Table 2-2. Summary of non-acoustic data sensors with possible SAS usage.

Parameter	**Range**
Water temperature	[~-37.0°C,~+70°C]
Heading (magnetic compass)	[0.0°, 360.0°)
Depth	[0 m, ~480 m]
Body Roll	[~-32.0°, ~+32.0°]
Body Pitch	[~-32.0°, ~+32.0°]
Cable Pitch	[~22.0°, ~106.0°]
GPS Time*	[00h00m00s, 99h99m99s]
GPS Latitude *	[00d00.000m,99d99.999m], with N or S label
GPS Longitude*	[000d00.000m,999d99.999m], with E or W label
GPS course direction*	[0°, 360°)
GPS course speed*	[0.000 kt, 999.9 kt]

*Global positioning system (GPS) values are recorded topside by L-3OS and added to the data stream.

For this program, all data (acoustic and non-acoustic) were recorded to disk for post-trial SAS processing. The data were tapped out of the Seahawk processing stream at a point where the L-3OS standard processing could not occur. It was possible to passively view the data during the trial, but no active sonar processing was available on the L-3OS console. It was also impossible to replay the data through the L-3OS software.

2.1.2 Seahawk Health

In preparation for sea trials, L-3OS conducted a series of laboratory tests on the arrays, transmitter, and topside equipment to ensure that they were working within tolerance. This

was especially necessary since the system had not been used in several years and some standard maintenance (such as refilling fluids) was required. If simple repairs were required, they were completed, however, dead receivers were not repaired due to the cost and risk associated with opening the arrays.

L-3OS conducted their standard tests on the arrays. These tests mostly consisted of electrical and mechanical environmental tests. The electrical tests included resistance, electrical power, multiplexers, band pass, linearity, and audible tone injection. The mechanical environmental tests included tension, reeling, pressure, and vibration, all followed by an electric test with an injected sine wave. Table 2-3 summarizes the receiver elements which failed tests. Due to the order of the tests, the receivers which failed all tests were flagged first and we (DTI) used that information for simulations (see Section 2.1.3). The status of the elements which failed the audible tone test was not made known until after simulations were completed, however, the effects of a couple of additional non-functional channels would not be large, based upon simulations (Section 2.1.3).

Table 2-3. Summary of failed receivers.

Array	Receiver	Test failed
002 (port)	31	All electrical
002 (port)	48	Audible tone injection
003 (starboard)	11	All electrical
003 (starboard)	12	All electrical
003 (starboard)	48	Audible tone injection

L-3OS also conducted tests on the topside equipment (power amplifier, operator console, winch and handling system), the towbody, and the transmitter. Some of the towbody and transmitter testing were related to the addition of the PingNow circuit (described below). As for the arrays, mechanical and electrical tests were conducted on all parts. All parts passed laboratory testing.

2.1.3 Timing and Dead Channel Impact on SAS

Early plans put forth by engineers at L-3OS proposed maintaining ping-to-ping coherence in the Seahawk SAS demonstration by setting a flag (dubbed "PingNow") in the sonar data stream indicating when the projector was active (i.e., when the ping was transmitted). In principle, this would provide the information needed to properly register multiple pings together. Although this plan embodied the correct concept, the data frame headers in which the PingNow flag would be stored were generated at a rate of only 5120 per second. DTI suspected that this would not provide enough precision to accurately register the phase of the 1400 Hz signal from ping to ping (1/5120 s corresponds to approximately 1/3 wavelength of the carrier).

After discussions with L-3OS engineers, an alternate method for increasing the precision at which the PingNow information could be stored in the sonar data stream was proposed. The new concept would store the PingNow flag in the *sonar data itself*, not in the headers. This would be done by sacrificing the least significant bit (LSB) of the 16-bit hydrophone

output words. Although this slightly degrades the precision at which the sonar data is stored, it allows the Ping Now information to be updated at the rate at which the hydrophone channels are read – (192 X 5120) 983,040 per second. Our experience shows that proper phase is the most important contributor to good SAS images, and that the new scheme was an appropriate compromise.

Before moving forward with the new PingNow flag storage scheme, it was important to quantitatively assess the impact of both timing precision and hydrophone output storage precision. DTI therefore performed a series of simulations of the Seahawk array that incorporated the effects we expected to see in the Seahawk data.

The simulation consisted of the following steps:

1) **Ideal simulation**: simulation of the 48-element Seahawk array (1400 Hz center frequency, 43 cm hydrophone spacing, etc.). This is an ideal simulation, with no unwanted motion errors or any other corruption.
2) **Introduction of timing jitter**: add a random time jitter to each *ping* of data. When simulating the original scheme with the PingNow flag in the data frame headers, a random time uniformly distributed between 0 - 1/5120 s was added to the data. For the new method, the time error ranged from 0 - 1/983040 s.
3) **Conversion to 16-bit representation**: conversion of floating-point I/Q format into 16-bit integer magnitude-only values, as supplied by Seahawk. During conversion, the simulation output is scaled by a gain factor and converted to 16-bit values. The gain factor is important when dealing with limited-precision data representations, so was scalable to represent cases where the full dynamic range and precision of the 16-bit word was optimally used, and also cases simulating poor gain settings that result in all the sonar information being stored in the last few bits of the word (resulting in very low dynamic range and poor precision). The LSB was optionally blanked to simulate the loss of precision due to the modified PingNow scheme.
4) **Blank-out dead channels**: L-3OS indicated that there were two dead channels in the array, although at the time of the simulations did not inform us of exactly which ones. The effect of dead channels was included by zeroing-out randomly-selected channels.
5) **Form super-elements**: adjacent hydrophones were combined together into "super elements" appropriate for the cross-range resolution at which we planned to process the data.
6) **Image formation and analysis**: the final data, with expected Seahawk artifacts is processed with the usual scallop correction, Range Migration Algorithm (RMA) image formation and diagnostics.

A comprehensive set of simulations were generated and analyzed, resulting in the following conclusions:

1) The original scheme of having the PingNow flag set in the data frame headers results in unacceptable phase jitter that precludes high-quality SAS imagery.

2) The new proposed PingNow scheme is very good. The timing precision is more than adequate to maintain good phase registration from ping to ping, and the corruption of the hydrophone data from the presence of the embedded PingNow flag is negligible in all but the most contrived cases (e.g., those where the gain setting forces all sonar information into the last few bits of the 16-bit word).
3) The presence of a few dead channels causes negligible degradation in the final SAS imagery.

Samples of the simulation results are presented below. For all of these simulations, groups of 12 channels were combined into super elements, supporting an along track resolution of 2.58 m. No unwanted motion was injected into any of the simulations. Similar results are obtained when larger super-elements are used. Results for an ideal simulation with no timing jitter and no dead channels are shown in Figure 2-3. This case resulted in good quality SAS images and ideal point response (IPR). The integrated side-lobe ratio (ISLR) for this case was –10.5 dB. Introduction of two dead channels into an otherwise ideal simulation resulted in similar results, as shown in Figure 2-4. The image quality remained good, with barely measurable degradation in IPR and an ISLR of –10.4 dB.

The original PingNow scheme was evaluated by introducing 1/5120 s random timing jitter into the simulation (while retaining two dead channels). The results, shown in Figure 2-5, show a somewhat degraded SAS image and degraded IPR. The ISLR for this case was an unacceptable –4.3 dB. The level of degradation varied from realization to realization, and typically ranged from about –3 dB to –9 dB. The new PingNow scheme results, in contrast, are shown in Figure 2-6. This simulation introduced 1/983040 s random timing jitter in each ping, and produced good SAS images and IPR. The ISLR for this case was –10.4 dB. These results are essentially indistinguishable from the baseline case shown in Figure 2-4.

Based on these results, we recommended that the new PingNow scheme be implemented, since the original plan resulted in unacceptable image quality, even if the theoretical limits of performance were achieved. The new scheme was implemented, and was used during the sea trials.

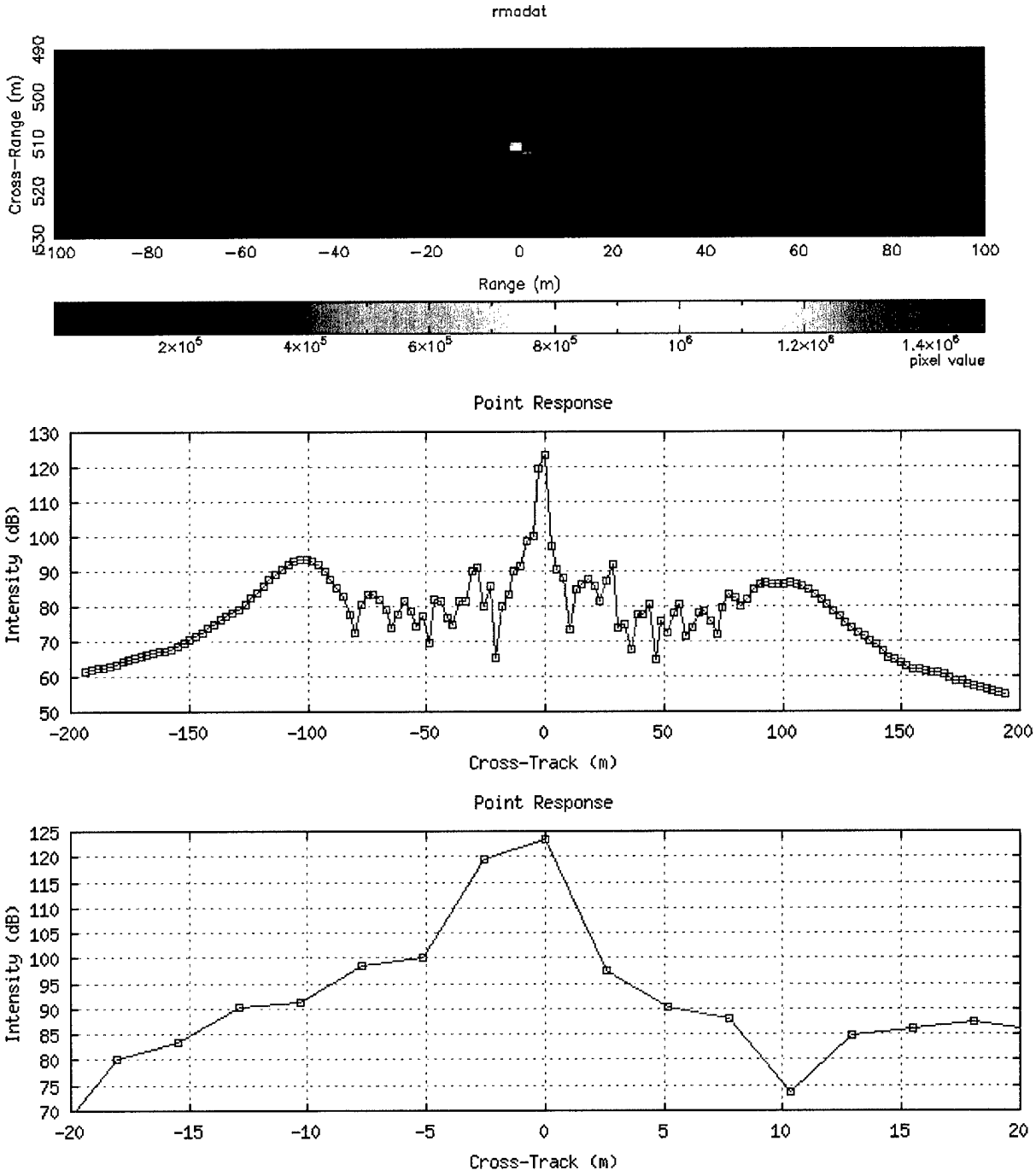

Figure 2-3. Ideal simulation results. Ideal simulation with no timing jitter and no dead channels results in good quality SAS image (top) and relatively good IPR (middle and bottom; bottom is close-up of middle image). The ISLR for this case was –10.5 dB.

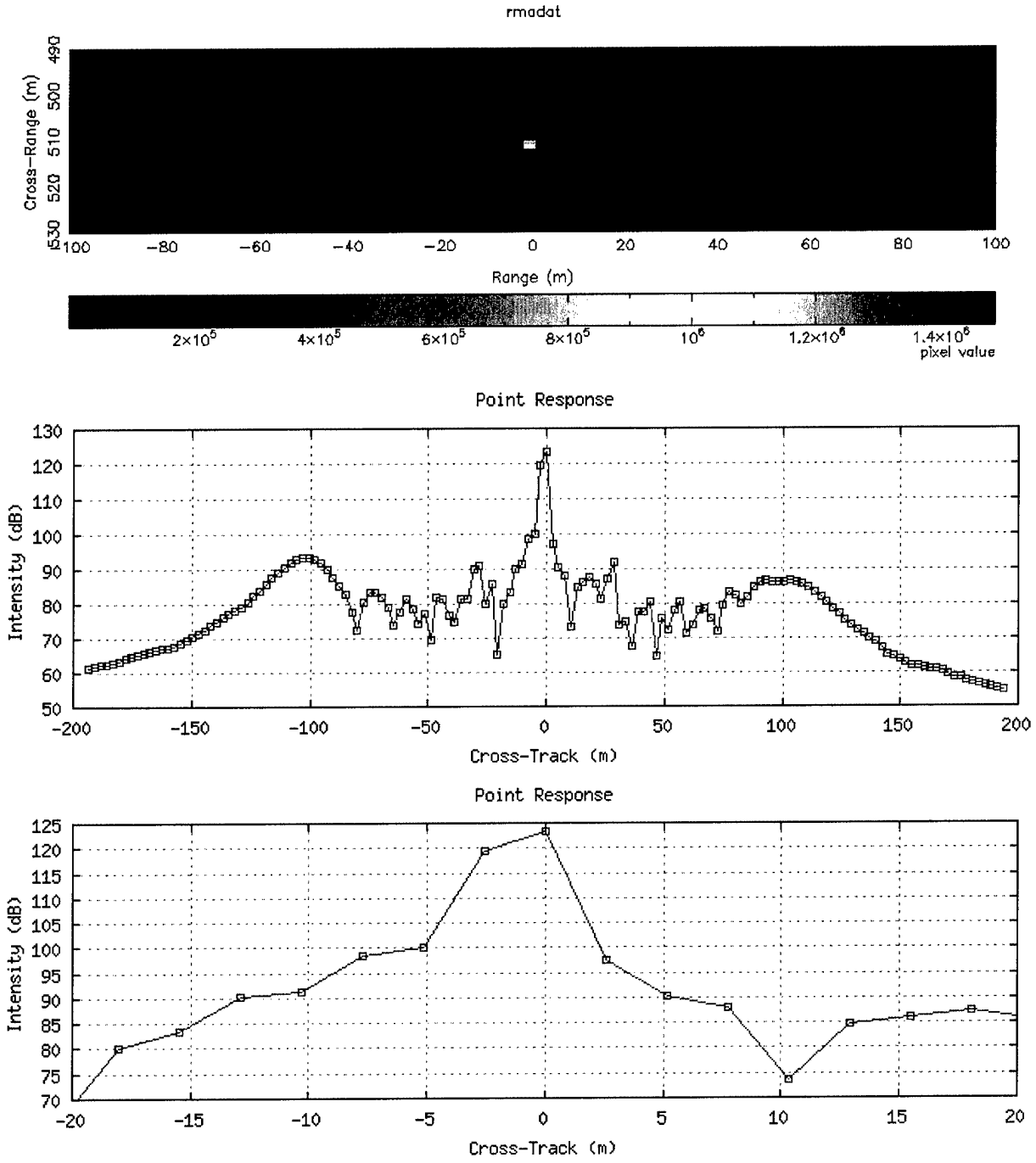

Figure 2-4. Dead channel simulation results. Simulation with no timing jitter and only two dead channels results in good quality SAS image (top) and negligibly degraded IPR (middle and bottom). The ISLR for this case was –10.4 dB.

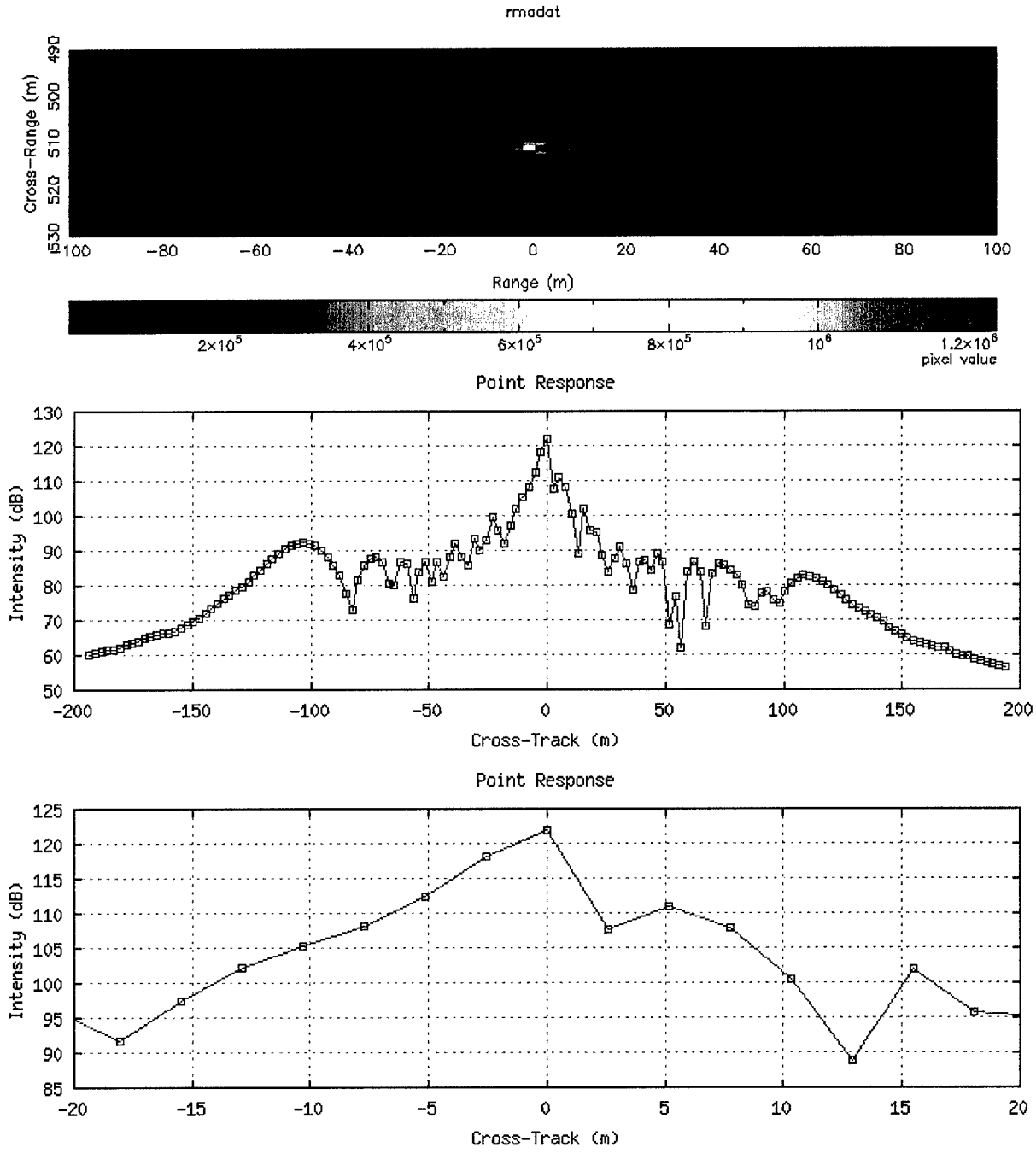

Figure 2-5. Large time-jitter simulation results. Simulation with 1/5120 s random timing jitter (as expected in the old PingNow flag scheme) and two dead channels results in a somewhat degraded SAS image (top) and degraded IPR (middle and bottom). The ISLR for this case was –4.3 dB. The level of degradation varies from realization to realization, and typically ranges from about –3 dB to –9 dB.

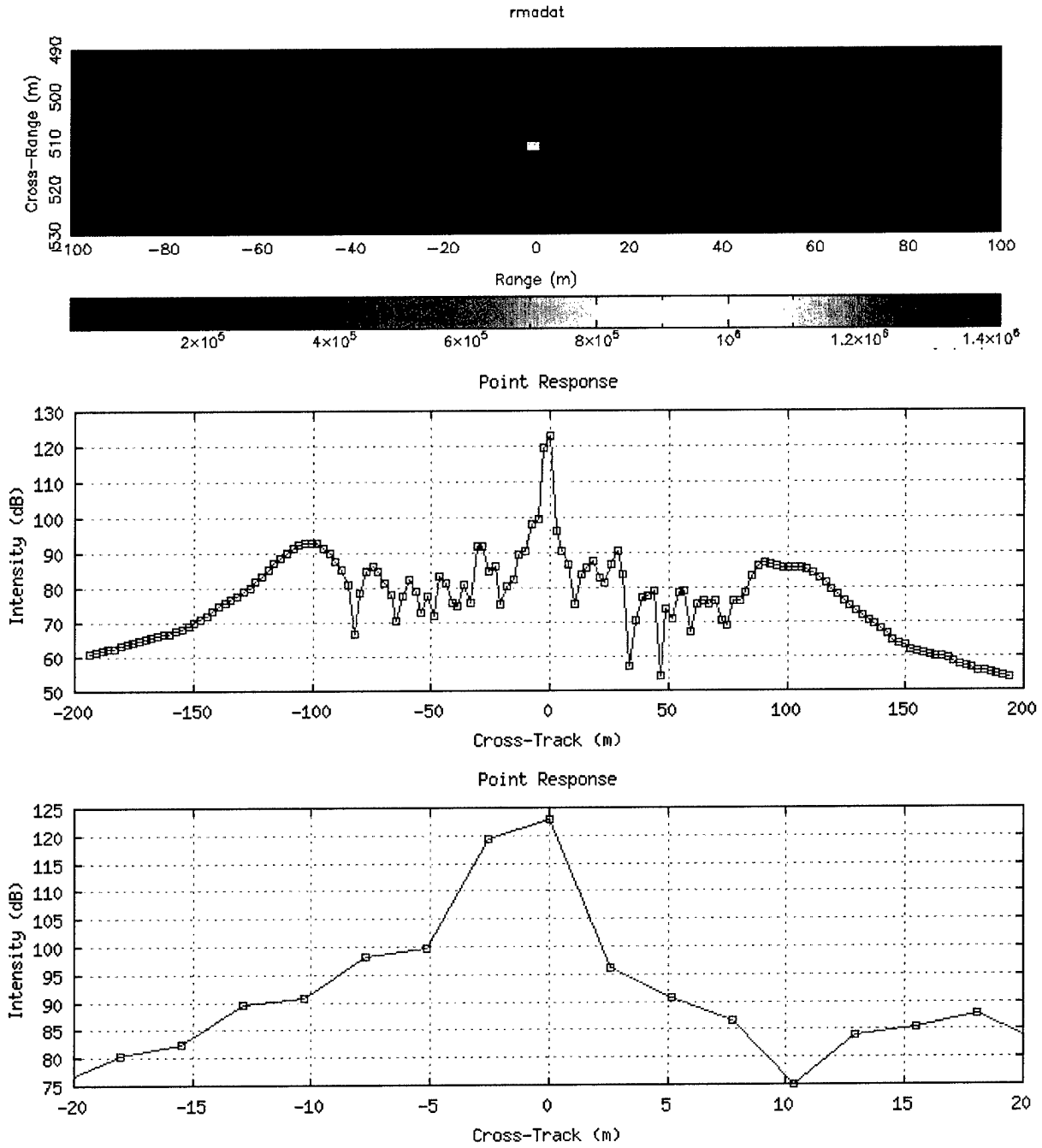

Figure 2-6. Small time-jitter simulation results. Simulation with 1/983040 s random timing jitter (as expected in the new PingNow flag scheme) and two dead channels results in a good SAS image (top) and negligibly degraded IPR (middle and bottom). The ISLR for this case was –10.4 dB. These results are essentially indistinguishable from the baseline case shown in Figure 2-4.

2.1.4 PingNow

In order to coherently processes data from multiple pings, the time intervals between pulse transmission and digitization of hydrophone data must be known very precisely. As was shown in Section 2.1.3, even small timing fluctuations can significantly degrade the ultimate SAS image. The mechanism implemented in Seahawk for accurately indicating the moment at which transmission occurs is to set the least-significant bit of the acoustic data to "1" during transmission, which is a sufficiently accurate method for SAS image processing. Due to various random latencies in the controlling computer systems, the time of transmission can not be accurately determined by simply monitoring the high-level software command logic. In fact, due to the system architecture, there was no method available for accurately determining when the projector was active. To remedy this situation, L-3OS designed and implemented a hardware monitoring circuit that measures the drive current in the projector amplifiers. This circuit would trigger when the current exceeded a critical threshold, causing the "PingNow" bit to be populated in the acoustic data. This system provided very good timing accuracy, but unfortunately failed early into the sea test.

2.1.5 Seahawk and SAS

In order to produce data that is amenable to SAS processing, the sonar system design must satisfy certain requirements, including:

- *Recording of individual hydrophone channel data.* Such systems may achieve an along-track resolution of approximately one-half the channel spacing (or approximately one wavelength, whichever is greater). Systems that beamform the array data prior to recording are effectively creating a single, large hydrophone element, and thus will have an along-track resolution limited to one-half of the array length. Although this may still provide benefit over the system's conventional resolution, it is clearly not as optimal as what is available when data from all channels are recorded.

- *Waveform generation that is repeatable from ping to ping.* Variations in waveform result in variations in the phase of the returned signal, and are thus not acceptable for coherent processing such as SAS.

- *Constant time delay between initiation of the transmitted pulse and the first ADC sample of the hydrophone.* This ensures that the relative phases of all pings are the same – a basic criteria for coherent processing of multiple pings.

The Seahawk system was chosen for this research in part because it satisfies all of the above requirements[2].

[2] To record the individual hydrophone data a minor modification of the system was required as alluded to in Section 2.1.1.

In addition to sonar design, operational methods must be considered during SAS data collection. The most fundamental requirement for SAS operations is that the sonar system advance no farther than one-half of the array length during each ping interval. This places strict speed limits on the survey vessel – often referred to as the "SAS speed limit". For the Seahawk system, the speed limit versus imaging ranges is shown in Figure 2-7.

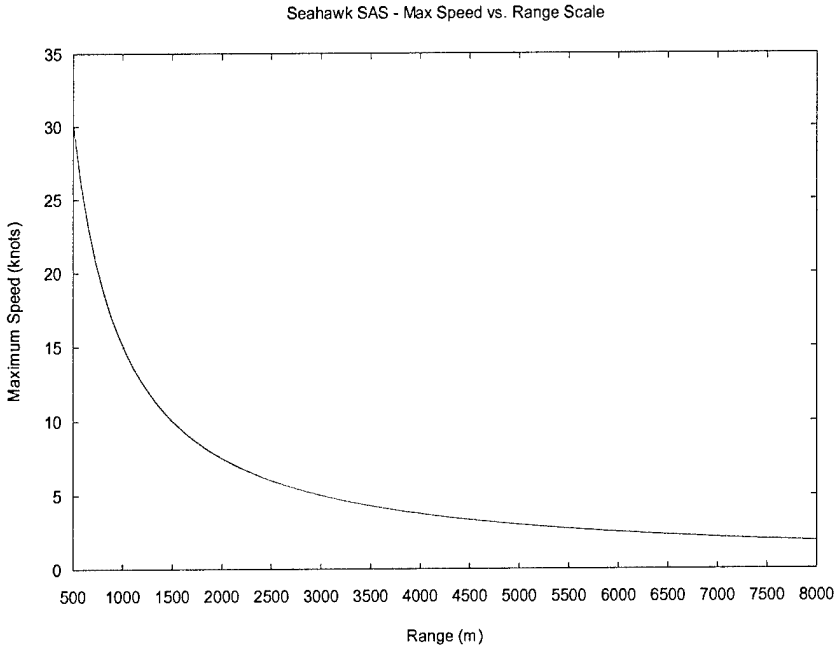

Figure 2-7. Speed limit versus range. The maximum allowable speed of advance is dependent on the range scale setting of the sonar. For the Seahawk system, the maximum speed at 4 km range is about 3.7 knots, and at 8 km is approximately 1.8 knots.

2.2 Trial location

The choice of the trial location is an important one. The location must allow us to fulfill the scientific goals of the experiment while being one that can work on a practical level. An appropriate vessel must be available that is able to maintain a steady course and slow speed (1.54 m/s = 3 kt) in the expected sea states. Since we are using sonar, we must be able to operate without harming the environment and the mammals therein. Thus the location choice must promote operations without harming the environment nor sacrificing test requirements.

Section 2.2.1 delineates the requirements for the site. Section 2.2.2 describes the site investigations. There is some description of the sites not chosen to aid in understanding the choice and for future reference should we decide to return. Section 2.2.3 contains simulations of two sites.

2.2.1 Site Requirements

For this trial we have a relatively simple set of requirements for the site. In order to prove the concept with the Seahawk sonar, we must be able to collect data off a submarine-sized target at 4-5 km range. A secondary requirement is to collect data of meter sized clutter. This requires: a region with appropriate targets of opportunity, preferably a submarine or similar sized vessel, other man-made objects from the few meter scale to submarine size or larger, and geological clutter – ground truth would be ideal; an appropriate combination of depth, sound velocity profile (SVP), and bottom profile that supports acoustic propagation to 5 km; the accessibility to appropriate vessels from which to operate; the expected sea states for the time of operation must allow the vessel to operate at 3 kts; and finally, we must be able to get permission to operate in the region. Since we expect this system to operate in the shallow water, and generally on the continental shelf, we have a maximum depth constraint of order 100 fathoms (~200 m). This constraint yields an advantage in terms of targets of opportunity since the locations of ship wrecks under 200 m depths are often well known (i.e., coordinates known, marked on charts, and often ground truth available) by divers and fishermen. Previous experience had shown us that for the sound propagation to reach and return from the desired range, a flat or shallow sloped region is required, which adds another constraint.

We planned to use targets of opportunity rather than laying our own target field, thus our site selections were dictated by the requirement of appropriate targets of opportunity. All other requirements were given nearly equal weighting in decisions as discussed in the following section.

2.2.2 Trial Location Investigation

Our initial plan was to conduct two active trials. One off the Southern California coast against targets with good ground truth available via high frequency side scan sonar images. This site had the advantage of being local to both DTI and L-3OS. This first test was to be an engineering trial where we would test the equipment and processing. The second test would be located off the New York/New Jersey coast to collect data against the Ex-USS Salmon, a diesel submarine that was converted into a sonar target. This second trial would feature more extensive data processing, incorporating any enhancements or additions resulting from the first trial, and would collect data against a tactically significant target. We investigated both sites for suitability. The results of this investigation led us to alter our plans to a non-active test off the Southern California coast and a full test off the NY/NJ coast. These investigations are discussed below.

While each investigation consisted of site specific work, there were general methods and sources of information for each site. Wreck information, for potential targets of opportunity, came from a variety of sources, mostly web based, but the National Oceanographic and Atmospheric Administration (NOAA) Office of Coast Survey Hydrographic Division's Automated Wreck and Obstruction Information System (AWOIS) was used to verify those located from other sources such as scuba diver web sites. NOAA Office of Coast Survey nautical charts were used for all depth and bottom contour information as well as additional information on wrecks, obstructions, shipping

lanes, 3 nm and 12 nm distances from shore, etc. To determine if a locale could satisfy our sound propagation requirements, we used average SVPs of a given region[3] and depth information from the NOAA nautical charts for inputs to PCSWAT[4]. While we required ~5 km range for propagation, we typically checked for ~10 km as well to allow for more stressing data collection runs should the trial run smoothly enough.

Southern California Site Investigation

The continental shelf ends very close to shore on the western coast of North America with the 100 fathom (~200 m, 600 ft) depth within the 3 nm (5.6 km) line at times. Since we require relatively shallow slopes and depths for the first tests of the system, we are very limited in choice of location. A region in the San Pedro Channel (see Figure 2-8) is relatively flat and shallow; this region also contains several sunken vessels and other items of which L-3OS previously collected high frequency sonar images. The Santa Monica Bay also has relatively shallow slopes and depths, although no imaged targets of opportunity. Both of these regions are close (<12 nm) to shore. Through Southwest Division Naval Facilities Engineering Command, Science Applications International Corporation (SAIC) prepared an environmental issues report on these two locations. From this report it was clear that there is significant marine mammal activity near the Southern California shore throughout the year. Expected mammal mitigation measures would not allow us to run an effective proof of concept trial in either of these locations.

[3] We used the average profile for a given region and month from the Generalized Digital Environment Model Variable resolution (GDEMV) database.

[4] Personal Computer Shallow Water Acoustic Tool-set (PCSWAT) is a computer code written by Gary Sammelmann at the Naval Warfare Surface Center, Dahlgren Division, Panama City (formerly Coastal Systems Station). We used version 7.0.

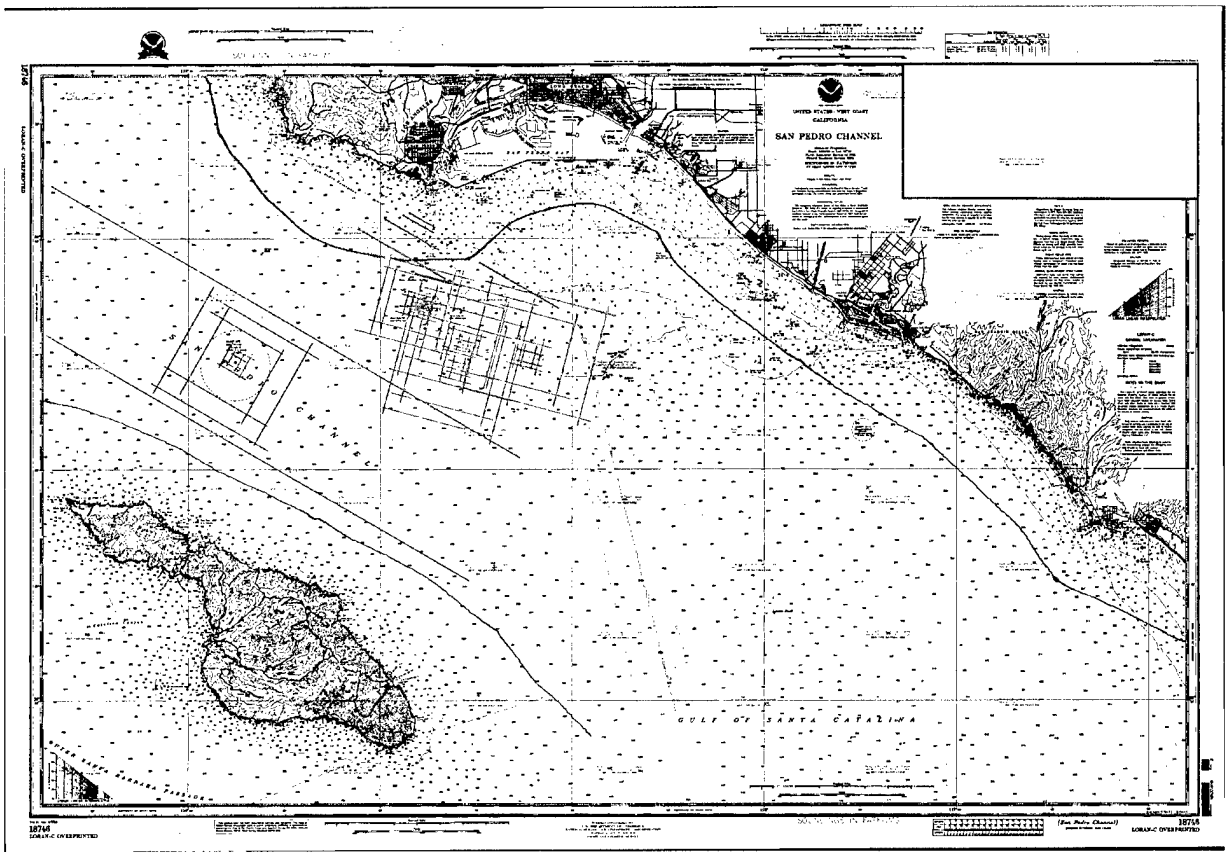

Figure 2-8. San Pedro Channel Chart showing region of interest for first trial. This is an annotated NOAA chart. The gray boxes mark possible runs around objects with SLS imagery. The red lines mark the approximate 3 nm line from shore.

We additionally investigated the Tanner/Cortez Banks area approximately 100 nm west of San Diego. This is a region of shallow (< 100 fathom) water far from shore where the depths are otherwise typically much larger (>500 fathom) depths. There is some geologic clutter, a few ship wrecks (for targets), and low mammal activity. However, we intended to test in the spring when the significant wave heights are typically largest (>3 m). The captain of the vessel we planned to use, Three Aces[5], felt that being able to steer the boat in a straight line at 3 kt would be very difficult under these conditions. We thus expected the towbody and array motion to be too large for a proof-of-concept system that did not have all the motion sensors an acquisition system would.

From these investigations, we determined that an active sonar trial was not possible off the Southern California coast. However, the proximity of DTI and, more importantly, L-3OS to the region made it useful for a passive sonar trial. The sonar system had not been used in several years and we could not pass up the chance to deploy, to collect sample passive acoustic data, and to retrieve the sonar while close to L-3OS facilities. Should there have

[5] The Three Aces is a vessel owned and operated by L-3OS.

been a problem, this proximity allows rapid repairs and re-testing. All active sonar testing was done either in the laboratory at L-3OS or the location of the active sonar trial.

East Coast Site Investigation

The continental shelf ends approximately 100 nm from shore along the eastern coast of North America. This yields a large, shallow sloping, shallow depth region. There are a large number of sunken vessels on the shelf, especially near the port of New York. Approximately 80 nm from the Long Island, NY and New Jersey shore is the Naval Undersea Warfare Center (NUWC) Shallow Water Diesel Submarine Test Facility. The Navy sank the Ex-USS Salmon (SS-573; see Figure 2-9) here as an environmentally safe target[6]. As far as targets of opportunity are concerned, this is the ultimate target since it is a bottomed (thus non-moving) diesel submarine and may have contained some air. However, we wanted more than one target to collect data against, in particular, we desired man-made clutter. Table 2-4 lists the objects in the AWOIS database in an approximately 1° x 1° region containing the Salmon. Clearly there are additional man-made items in the vicinity. We chose the Bidevind (Figure 2-10) and Texas Tower #4 (Figure 2-11) as potential additional targets for the trial. Both sites would contain small and large man-made objects for clutter studies.

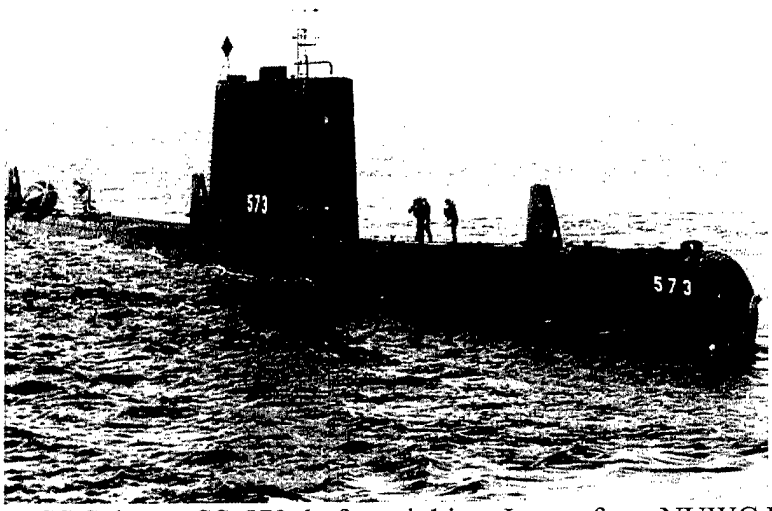

Figure 2-9. Ex-USS Salmon, SS-573, before sinking. Image from NUWC Division, Newport (2003).

[6] The Ex-USS Salmon was air filled when sunk in the early 1990s, but recent surveys indicate that it may now be partially filled .

Table 2-4. Wrecks in AWOIS database near Ex-USS Salmon. The named wrecks are also found in most scuba divers' databases. Record number is from AWOIS database (Office of Coast Survey 2004).

Rec No	Description	Latitude Longitude	Depth	Type/ Material	Comments
1283	Isabel B. Wiley	+39° 10' 00.43" –73° 06' 58.35"	222 ft	Schooner / Wood	Loran-C: 26472.5 / 429143.9
1306	Rio Tercero	+39° 15' 00.44" –72° 29' 58.28"	462 ft		
1315	Unknown	+39° 18' 20.68" –72° 38' 10.91"			
2757	Kenneback	+39° 26' 00.42" –72° 49' 58.33"			
1356	Winneconne	+39° 26' 00.42" –72° 49' 58.33"			
1384	Jacob Haskell	+39° 36' 00.42" –73° 01' 28.36"	216 ft		
1394	Herbert Parker	+39° 38' 00.41" –73° 02' 58.36"	156 ft		
1399	Corvallis	+39° 39' 00.42" –73° 12' 58.38"	126 ft		
1401	Unknown	+39° 39' 30.41" –72° 34' 28.30"			
7771	Canton Mouth	+39° 41' 02.95" –72° 29' 00.87"			
7768	Unknown	+39° 47' 55.43" –72° 40' 02.31"			
7733	Texas Tower #4	+39° 47' 56.43" –72° 40' 08.00"	70-180 ft	NORAD listening post / Steel	Intact, launched 1957, sunk 1961, storm, 50 mi offshore Loran-C: 26313.0 / 43267.8
7769	Stephen W.	+39° 48' 19.72" –72° 53' 03.47"			
1438	Bidevind	+39° 48' 30.40" –72° 48' 58.34"	190 ft	Freighter / Steel	Broken up, 414ft long, launch 1938, sunk1942 by torpedo Loran-C: 26357.6 / 43280.5
1437	Unknown	+39° 48' 30.40" –72° 44' 58.33"			
7776	Unknown	+39° 49' 22.52" –72° 52' 37.18"			
1449	Unknown	+39° 50' 00.40" –72° 52' 58.35"			
1448	Sagun	+39° 50' 00.41" –72° 10' 18.26"			
7770	Unknown	+39° 50' 12.44" –72° 39' 55.31"			
1456	Sea King	+39° 54' 43.58" –72° 01' 24.10"			

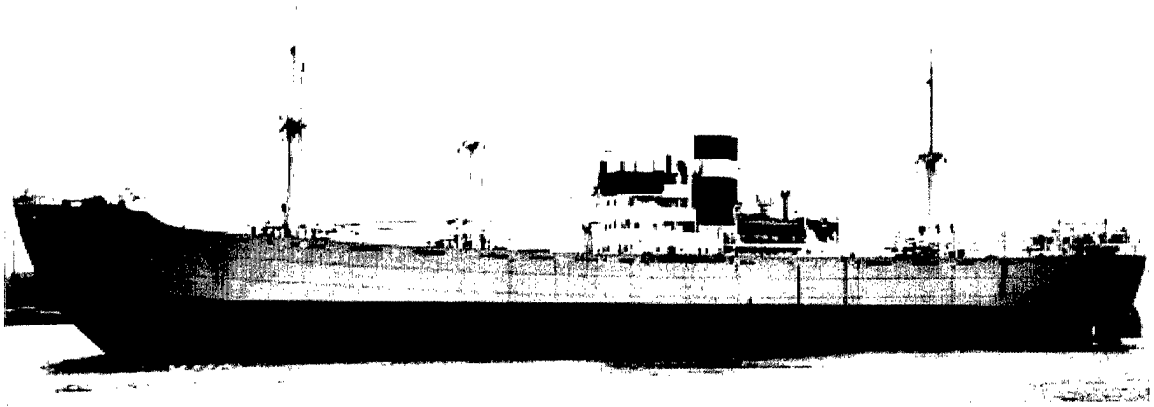

Figure 2-10. M/S Bidevind, Norwegian freighter. Image from NJ Scuba Diver (2004a).

The Salmon site passed all of our requirements. Sound propagation simulations indicated that we would be able to detect objects on the bottom past a 10 km range for the September-October time period (see Section 2.2.3). The site is far enough from shore that we could not be based on shore, thus the operations vessel needed to be large enough to accommodate all staff to live on board for several days. Several such vessels were available on the eastern seaboard, in particular in the NY/NJ area. The size of the vessel and the average wind speeds and wave heights for the region were amenable to 3 kt vessel speeds. The distance of the site from shore and the planned trial dates meant lower marine mammal activity. Through ONR, Marine Acoustics, Inc. performed an Overseas Environmental Assessment (OEA) for our planned work at the Salmon site. This OEA, endorsed by the Navy, required mitigation measures that did not greatly impact our plans for the proof-of-concept trial. We were additionally able to receive permission to use the Salmon site for testing over a time period in early October. Figure 2-12 shows the region of planned operation.

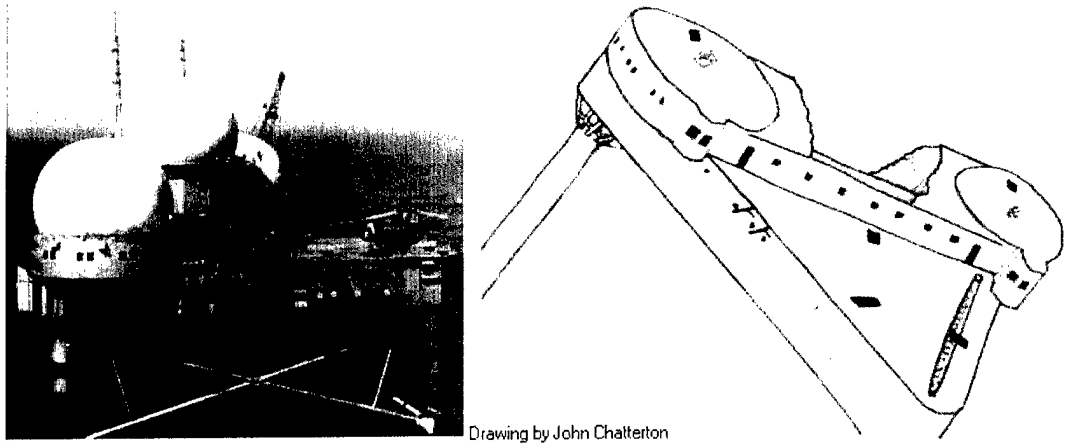

Figure 2-11. Texas Tower #4. While operational on left, scuba diver's drawing since sinking on right. Images from NJ Scuba Diver (2004b).

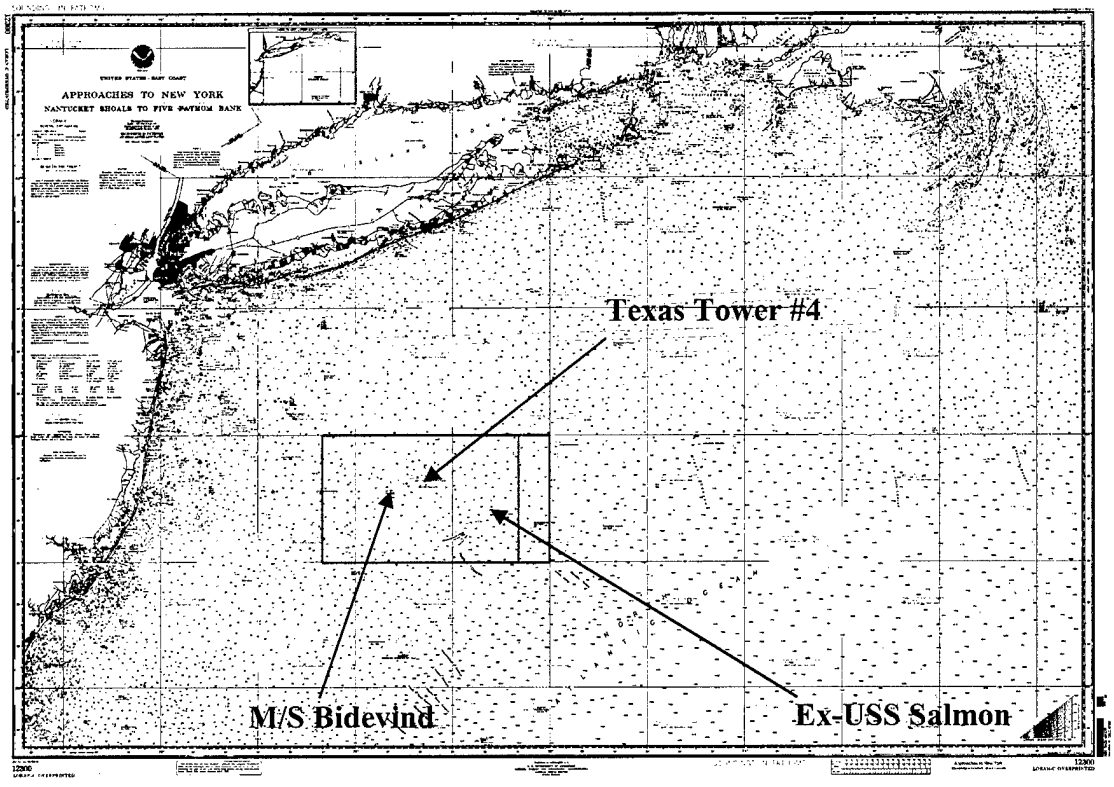

Figure 2-12. East coast region of planned operation. This is an annotated NOAA chart. The red boxes mark areas of planned operations. The three potential targets are labeled.

2.2.3 Simulations

As part of our trial site location survey, we simulated expected results to determine if there were any fundamental sound propagation issues with each site. We used two different methods to investigate each site, the first for SNR levels and the second for SAS imagery. We undertook a more extensive study for the west coast site. This was partly due to the fact that it was the first site studied and thus the east coast site simulations were a confirmation that it was not a worse location. Due to the slope of the proposed test areas for the west coast site, up-slope and down-slope propagation simulation were required, thus doubling the effort.

The two approaches yielded consistent results. For SNR studies we used PCSWAT 7.0 to calculate the signal, bottom, surface, and volume reverberation, ambient noise, and the resultant SNRs. The calculations demonstrated that sufficient SNR would be available for ASW and most MCM targets. For the SAS imagery we used a parabolic equation solver to calculate the propagation between the sonar and target, including multipath, and simulated the data Seahawk would receive under such conditions. We were able to SAS process the simulated images and to focus all multipath imagery. The details of the simulations are

described below with representative results. More complete results can be found in Appendix B.

SNR Study

Our SNR calculations were made using PCSWAT 7.0. The Seahawk frequency of 1.4 kHz is lower than the standard models used in PCSWAT, however, the documentation states that the high-frequency model, in terms of propagation, is adequate if the water depth is of order 100 wavelengths or more. There could be a question of the validity of the ambient noise, bottom types, etc. in this frequency range. We validated the PCSWAT output against sonar equation calculations using appropriate values for our frequency regime. In any SNR plot shown, note that the PCSWAT definition of SNR is signal to non-signal ratio, meaning ambient noise, bottom, surface, and volume reverberation are combined as noise. We are interested in imaging the bottom, thus we are interested in the bottom reverberation strength with respect to the remaining "noise" sources in addition to the SNR. Note also that the PCSWAT calculation was made assuming SAS processing. This means that the ambient noise has been reduced due to array gain in most figures (it is noted if otherwise). Our array motion estimation techniques operate on the data before this gain is achieved. Thus, the bottom reverberation needs to be ~20 dB larger than the noise if we hope to image the bottom. Additionally, our eventual acoustic data processing used less than a full aperture, so the PCSWAT produced ambient noise is optimistic.

The SNR study was undertaken to confirm that we would receive a signal. We also did parameter studies to understand the range of pulse lengths, transmission type (omnidirectional or directional), and source levels that would allow us to operate. We also varied depths (bottom and sonar), sound velocity profiles, and bottom types. The bottom was always considered to be flat. Many calculations merely confirmed our expectations, but all bolstered our choices for operational parameters in the trial. Table 2-5 lists most of our SNR calculations. The runs listed are grouped in a way that should indicate the parameters being studied. Runs 1 through 36 were set for the San Pedro site, although the isovelocity SVP could be valid in either locale. Runs 37-42 were specifically made for the Salmon region using an SVP for the Salmon region from the GDEMV database (Tamul 2001). Certain parameters, such as the transmission mode, were not varied often either because the few calculations made confirmed expectations or other considerations precluded our exercising the choice in a sea trial. The initial target strength of –10 dB was chosen as a typical MCM target strength since this would be the limiting target-type in terms of SNR. The target strength was later changed to 0 dB to simplify conversion of SNR to other targets.

Table 2-5. Summary of PCSWAT calculations.

Run	Source Level	Pulse length	Water depth	Sonar depth	Target strength	Bottom type	SVP	Mode
1	219 dB	0.25 s	400 m	100 m	–10 dB	Coarse sand	Isovelocity	Directional
2	219 dB	0.25 s	400 m	100 m	–10 dB	Coarse sand	Isovelocity	Omni-dir.
3	219 dB	2.00 s	400 m	100 m	–10 dB	Coarse sand	Isovelocity	Directional
4	219 dB	0.25 s	400 m	100 m	–10 dB	Fine sand	Isovelocity	Directional

Run	Source Level	Pulse length	Water depth	Sonar depth	Target strength	Bottom type	SVP	Mode
5	219 dB	0.25 s	100 m	50 m	–10 dB	Coarse sand	Isovelocity	Directional
6	160 dB	0.25 s	100 m	50 m	0 dB	Sandy silt	Isovelocity	Directional
7	170 dB	0.25 s	100 m	50 m	0 dB	Sandy silt	Isovelocity	Directional
8	180 dB	0.25 s	100 m	50 m	0 dB	Sandy silt	Isovelocity	Directional
9	190 dB	0.25 s	100 m	50 m	0 dB	Sandy silt	Isovelocity	Directional
10	200 dB	0.25 s	100 m	50 m	0 dB	Sandy silt	Isovelocity	Directional
11	210 dB	0.25 s	100 m	50 m	0 dB	Sandy silt	Isovelocity	Directional
12	220 dB	0.25 s	100 m	50 m	0 dB	Sandy silt	Isovelocity	Directional
13	203 dB	0.25 s	100 m	50 m	0 dB	Sandy silt	Isovelocity	Directional
14	203 dB	0.50 s	100 m	50 m	0 dB	Sandy silt	Isovelocity	Directional
15	203 dB	1.00 s	100 m	50 m	0 dB	Sandy silt	Isovelocity	Directional
16	203 dB	2.00 s	100 m	50 m	0 dB	Sandy silt	Isovelocity	Directional
17	209 dB	0.25 s	100 m	50 m	0 dB	Sandy silt	Isovelocity	Directional
18	209 dB	0.50 s	100 m	50 m	0 dB	Sandy silt	Isovelocity	Directional
19	209 dB	1.00 s	100 m	50 m	0 dB	Sandy silt	Isovelocity	Directional
20	209 dB	2.00 s	100 m	50 m	0 dB	Sandy silt	Isovelocity	Directional
21	212 dB	0.25 s	100 m	50 m	0 dB	Sandy silt	Isovelocity	Directional
22	212 dB	0.50 s	100 m	50 m	0 dB	Sandy silt	Isovelocity	Directional
23	212 dB	1.00 s	100 m	50 m	0 dB	Sandy silt	Isovelocity	Directional
24	212 dB	2.00 s	100 m	50 m	0 dB	Sandy silt	Isovelocity	Directional
25	215 dB	0.25 s	100 m	50 m	0 dB	Sandy silt	Isovelocity	Directional
26	215 dB	0.50 s	100 m	50 m	0 dB	Sandy silt	Isovelocity	Directional
27	215 dB	1.00 s	100 m	50 m	0 dB	Sandy silt	Isovelocity	Directional
28	215 dB	2.00 s	100 m	50 m	0 dB	Sandy silt	Isovelocity	Directional
29	218 dB	0.25 s	100 m	50 m	0 dB	Sandy silt	Isovelocity	Directional
30	218 dB	0.50 s	100 m	50 m	0 dB	Sandy silt	Isovelocity	Directional
31	218 dB	1.00 s	100 m	50 m	0 dB	Sandy silt	Isovelocity	Directional
32	218 dB	2.00 s	100 m	50 m	0 dB	Sandy silt	Isovelocity	Directional
33	221 dB	0.25 s	100 m	50 m	0 dB	Sandy silt	Isovelocity	Directional
34	221 dB	0.50 s	100 m	50 m	0 dB	Sandy silt	Isovelocity	Directional
35	221 dB	1.00 s	100 m	50 m	0 dB	Sandy silt	Isovelocity	Directional
36	221 dB	2.00 s	100 m	50 m	0 dB	Sandy silt	Isovelocity	Directional
37	203 dB	0.25 s	110 m	55 m	0 dB	Medium sand	Salmon	Directional
38	209 dB	0.25 s	110 m	55 m	0 dB	Medium sand	Salmon	Directional
39	212 dB	0.25 s	110 m	55 m	0 dB	Medium sand	Salmon	Directional
40	215 dB	0.25 s	110 m	55 m	0 dB	Medium sand	Salmon	Directional
41	218 dB	0.25 s	110 m	55 m	0 dB	Medium sand	Salmon	Directional
42	221 dB	0.25 s	110 m	55 m	0 dB	Medium sand	Salmon	Directional

We are only showing two small groupings of SNR results here for brevity. The remaining results can be found in Appendix B. Figure 2-13 contains the results of a source level study for conditions in the San Pedro Bay. All the source levels used are not achievable by the Seahawk in its current configuration. This study aided our decision not to alter the system in order to reduce source level. From an SNR standpoint, a minimum of 200 dB source level is needed to achieve 20 dB SNR[7] for a 0 dB target. However, at 200 dB, the bottom reverberation is not above the ambient noise out to 5 km, our maximum planned range. A source level of 220 dB is needed for the bottom reverberation to be above the noise for the whole range.

Figure 2-14 contains the results of the source level study for the Salmon region. The source levels chosen are the possible Seahawk settings for the directional transmitter mode. The shape of the received signal and, thus, SNR are due to the expected multipaths from the SVP and flat bottom. These graphs indicate that the SNR is approximately 20 dB for the whole range for all source levels. Also, the bottom reverberation is more than 20 dB stronger than the ambient noise (or at least at the non-SAS ambient noise level) for source levels of 215 dB and larger, although 212 dB is marginal. Thus the transmissions can be safely reduced by 6 dB if needed, as it was, during the trial.

[7] We use 20 dB as a cut-off for a detectable target since that is the condition where one typically believes that a detection has been made. Lower values may be acceptable in some circumstances.

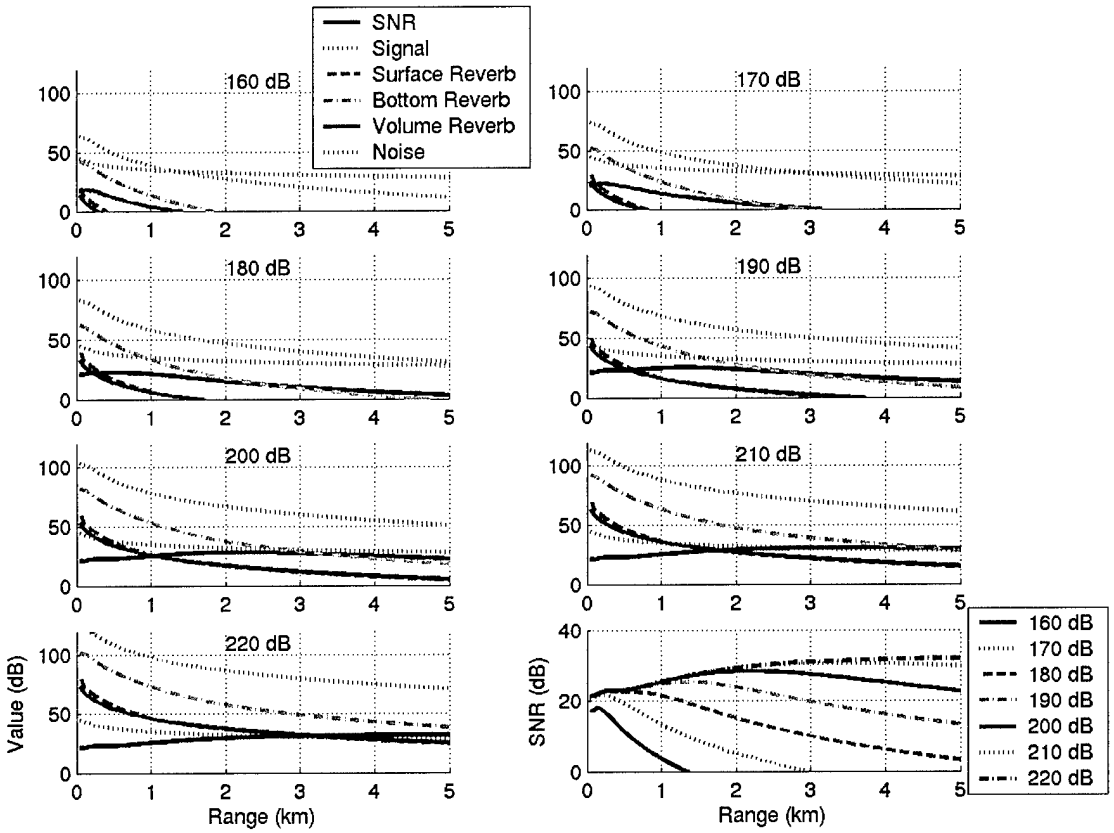

Figure 2-13. PCSWAT results for seven different source levels and the SNRs for all seven. Water depth of 100 m, sonar depth of 50 m, 0.25 s LFM chirp from 1.18 – 1.58 kHz, and a 0 dB target strength for a bottom type of "sandy silt."

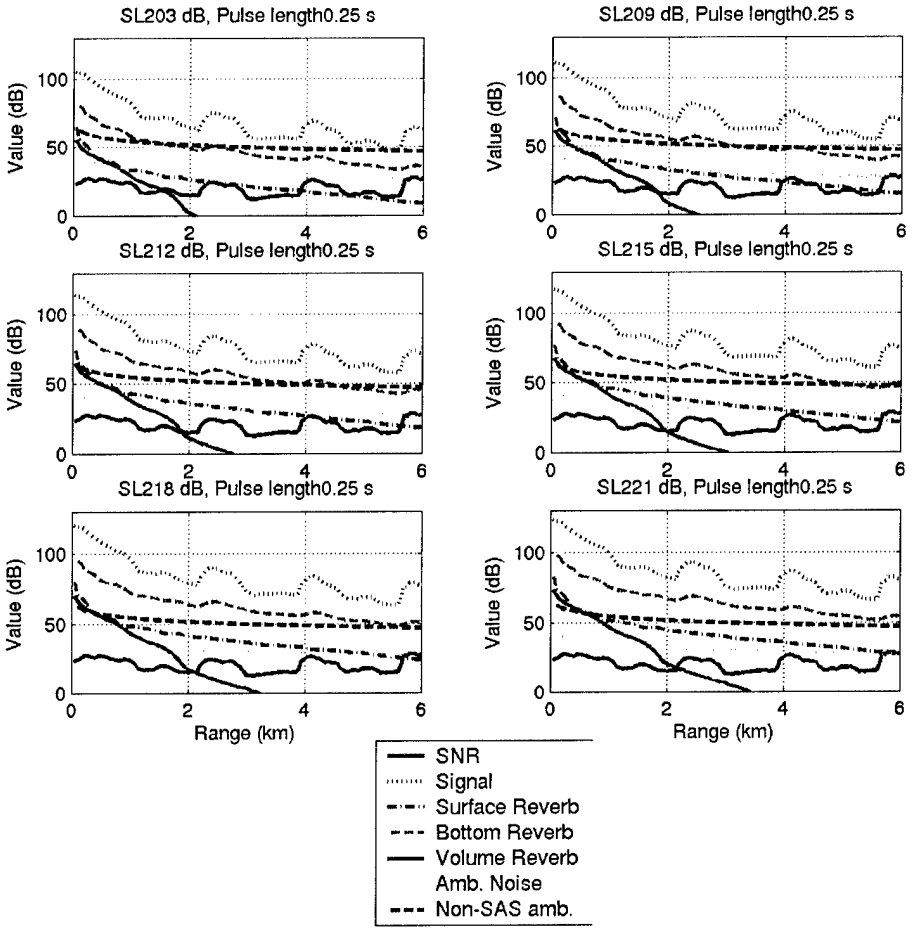

Figure 2-14. PCSWAT results for 6 source levels and 0.25 s pulse length. The source levels are those available on the Seahawk for the directional transmit mode. The 0.25 s pulse length is appropriate for our 5 km range runs. The non-SAS ambient noise is a 20 dB increase to the PCSWAT calculated ambient noise. The ambient noise assumes SAS processing but since we need the ability to measure changes from ping to ping, it is not quite appropriate. Note that only at the highest source levels is the bottom reverberation above the non-SAS ambient noise.

SAS Imagery

We simulated the SAS imagery from the Seahawk using the results of a parabolic equation solver for sound propagation. Due to the ranges and the environments, we expected the received data to contain multipath returns. While DTI does have limited experience with multipath filled data that we were able to focus, we additionally desired to simulate the results for the proposed test sites to confirm our experience. We chose a few scenarios in terms of bathymetry and SVPs and then simulated several variations of these. The SAS simulations were of either a single point target or a series of five point targets, as seen in Figure 2-15, to represent an extended target with strong highlights.

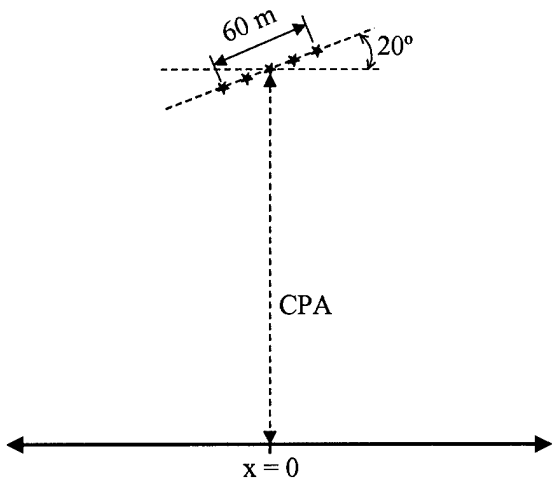

Figure 2-15. Five-point target configuration.

The sound propagation was calculated using the Monterey-Miami Parabolic Equation (MMPE) Model (Smith & Tappert 1999). We used a broadband version of the two-dimensional code from the Ocean Acoustics Library (Smith 1999). The code runs one direction of the propagation, meaning source to target or target to receiver. Thus it must be run twice to calculate the information needed to create a SAS image. The MMPE code allows for a sediment region between the water and the true bottom. We set this region to have the same parameters as the true bottom. The code inputs include the SVP, the acoustic parameters of the sediment and bottom, the bottom bathymetry, the "source" depth (for the source to target runs, this is the depth of the sonar source; for the target to receiver runs this is the depth of the target), and the transmitter and receiver characteristics. We simulated the sound propagation for conditions in both the west coast and east coast sites, Table 2-6 lists the runs and characteristics. For the west coast, we simulated two target locations. Figure 2-16 shows the location of two sunken vessels, one known as "Woody" (a sunken wooden ship) and the other as "sub" (believed to be a sunken submarine), as well as the simulated sonar (ship) heading. Figures 2-17 and 2-18 contains the bathymetry read off the chart and used in the MMPE code for the Woody and sub, respectively. A modified bathymetry is also indicated in these figures and were used in additional runs so we could create images from non-smooth bottoms (see below). Figure 2-19 shows the SVP used for the San Pedro site simulations. Figure 2-20 is the chart for the Salmon region, with the bathymetry in Figure 2-21, and SVP in Figure 2-22.

Table 2-6. MMPE code run parameters. The depths and SVPs can be seen in Figures 2-17, 2-18, 2-19, 2-21, and 2-22.

Run	Target range	"Source" depth	Maximum depth	SVP
Xmitter-to-Woody	1 km	45 m	120 m	San Pedro
Woody-to-receiver	1 km	64 m	120 m	San Pedro
Xmitter-to-Woody	5 km	122 m	350 m	San Pedro
Woody-to-receiver	5 km	64 m	350 m	San Pedro
Xmitter-to-Sub	1 km	122 m	500 m	San Pedro
Sub-to-receiver	1 km	329 m	500 m	San Pedro
Xmitter-to-Sub	5 km	122 m	850 m	San Pedro
Sub-to-receiver	5 km	329 m	850 m	San Pedro
Xmitter-to-Salmon	1 km	56 m	150 m	Salmon & Iso
Salmon-to-receiver	1 km	111 m	150 m	Salmon & Iso
Xmitter-to-Salmon	5 km	59 m	150 m	Salmon & Iso
Salmon-to-receiver	5 km	111 m	150 m	Salmon & Iso

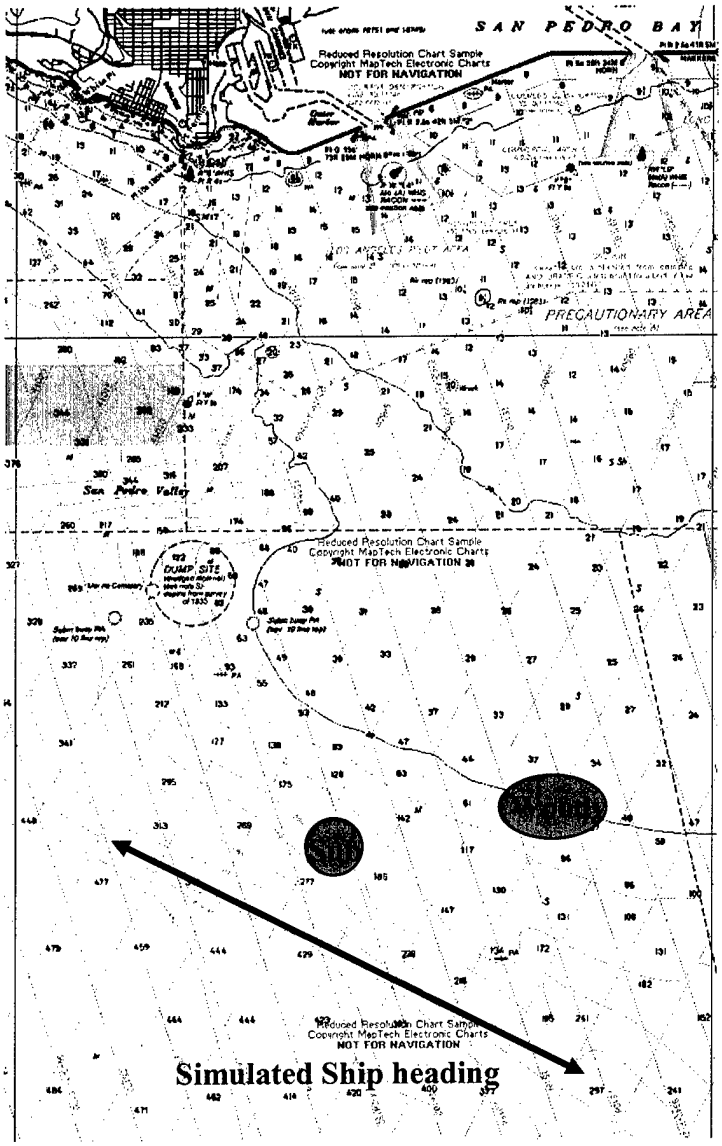

Figure 2-16. Portion of San Pedro Channel Chart. The locations of the Woody and Sub targets are marked as well as the simulated ship heading. Bathymetry for the simulations were read off the chart which is marked in fathoms.

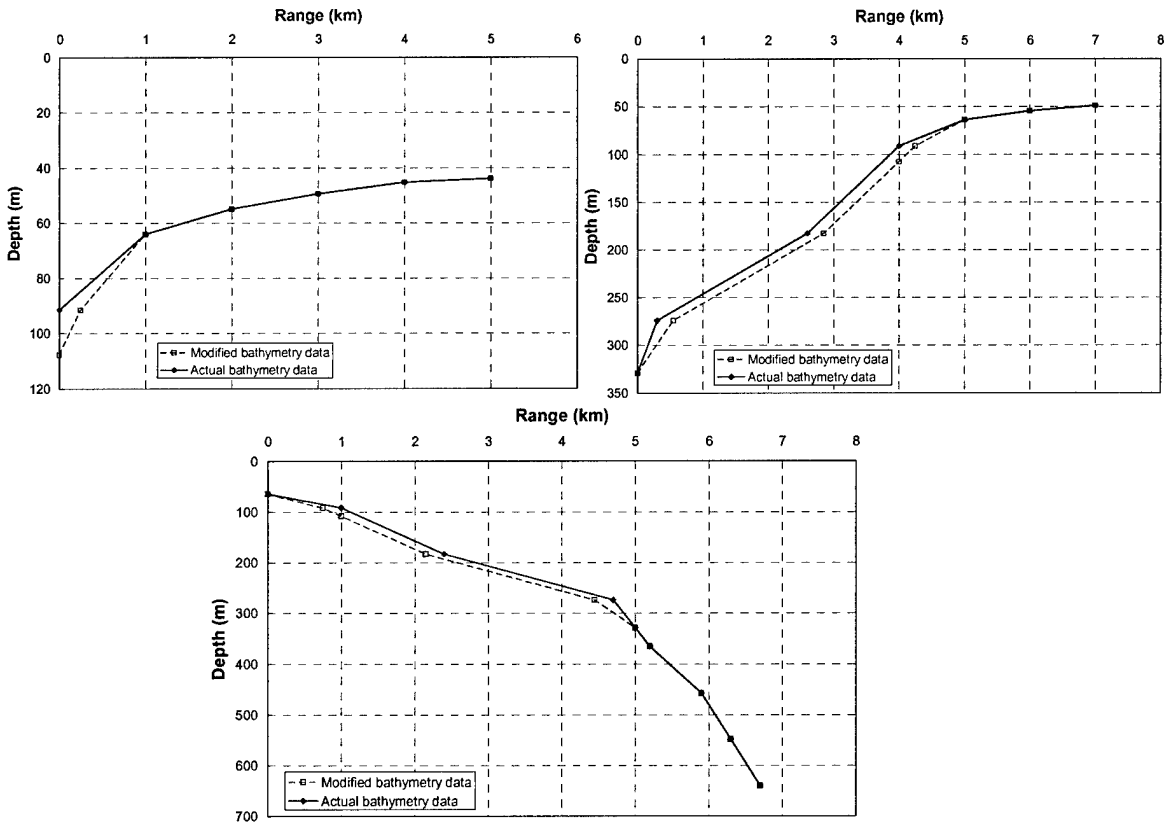

Figure 2-17. The water/bottom interface used in Woody PE runs. Upper left panel is transmitter-to-Woody for 1 km distance. Upper right panel is the same but for 5 km distance. Lower panel is the Woody-to-receiver interface and useable for both runs.

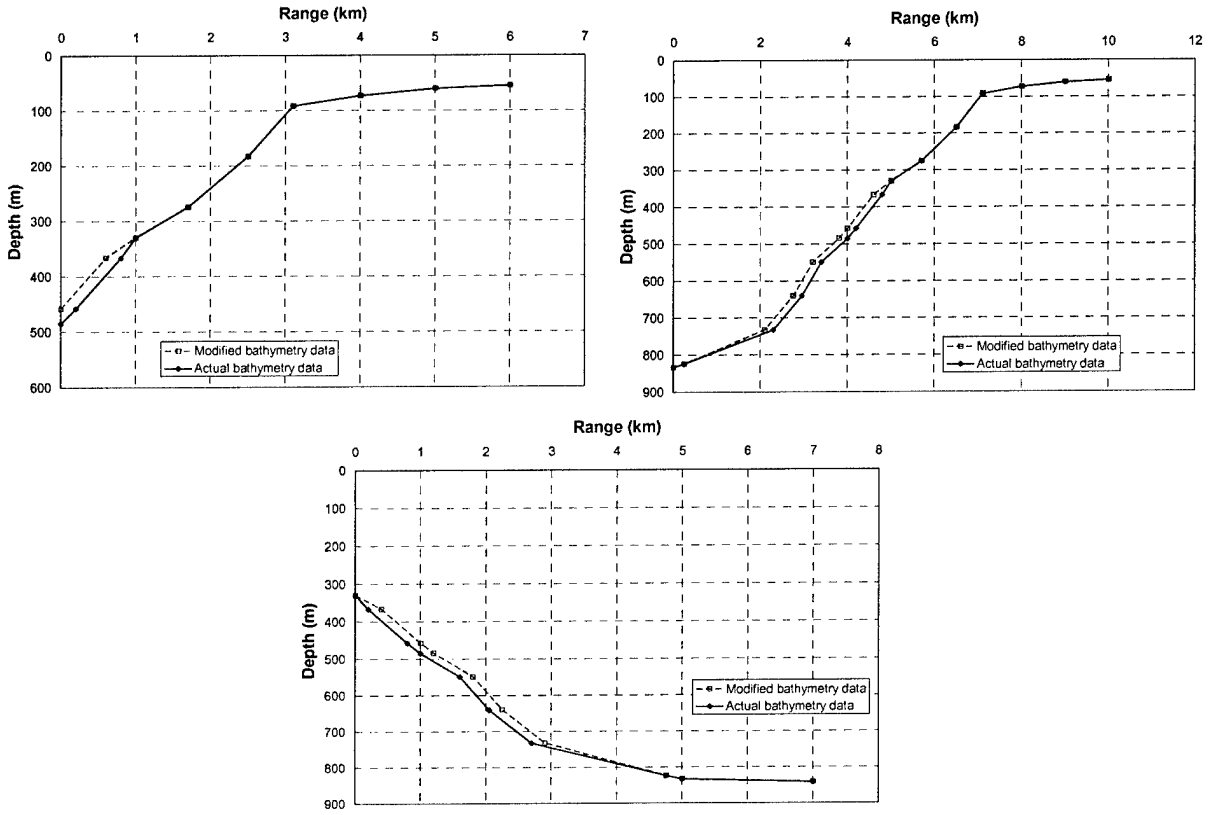

Figure 2-18. The water/bottom interface used in sub PE runs. Upper left panel is transmitter-to-sub for 1 km distance. Upper right panel is the same but for 5 km distance. Lower panel is the sub-to-receiver interface and useable for both runs.

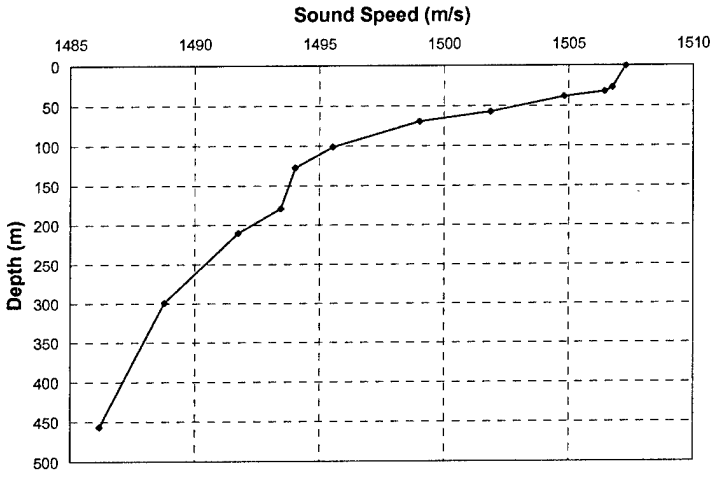

Figure 2-19. Sound velocity profile for San Pedro site.

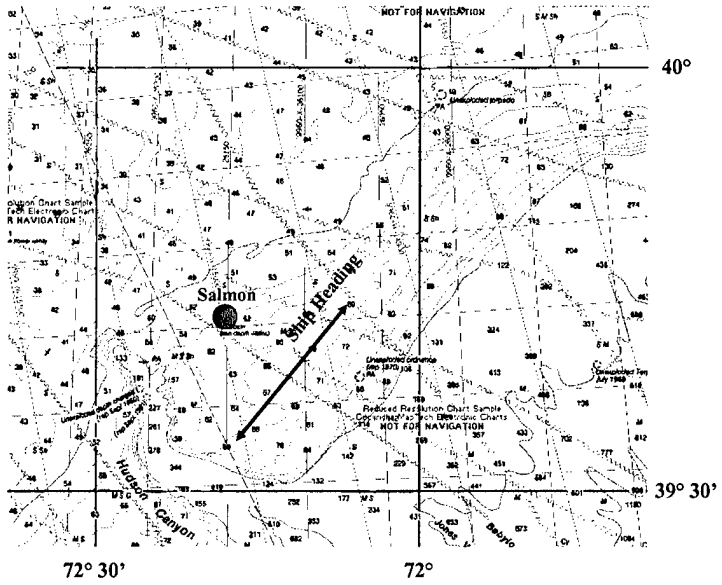

Figure 2-20. Chart of Salmon site. Salmon location is marked. Ship heading for simulations is indicated. All depths are in fathoms.

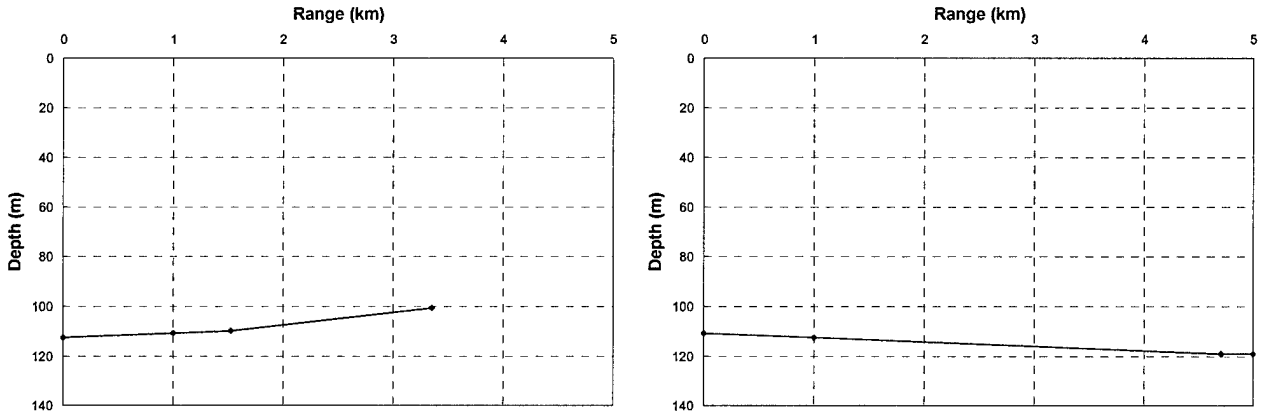

Figure 2-21. The water/bottom interface used in 1-km Salmon PE runs. Left panel is transmitter to Salmon. Right panel is Salmon to receiver.

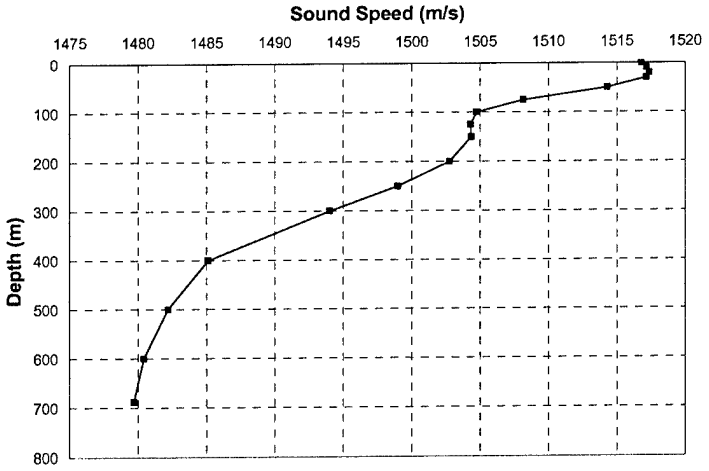

Figure 2-22. Sound velocity profile for Salmon site.

With the MMPE results, we created a variety of SAS images. For each pair of MMPE runs, we created a single point and a five point SAS image. For the San Pedro runs, the modified bathymetry runs allowed us to simulate the effects of bottom variations over a synthetic aperture (the bathymetry has to remain the same within a ping, but can change between pings in this simple arrangement). We created three bottom types which varied along-track, as shown in Figure 2-23. Type A is simply one bathymetry for half of the image along-track and the modified bathymetry for the second half. Type B alternates bathymetry every ping. Type C alternates bathymetry every 10 pings. The San Pedro site simulations demonstrated that there would be multiple images of each point and each image can be focused. For the Salmon site, we only simulated the one and five point targets at 1 and 5 km ranges. These simulations demonstrated the same basic results, so further simulations were deemed unnecessary. Table 2-7 lists all the SAS simulations created.

Table 2-7. Summary of SAS simulations run. The majority of the images can be found in Appendix B.

Run	Target	Number of Points	Range	Target depth	Sonar depth	Notes
1	Woody	1	1 km	64 m	45 m	Actual bathymetry
2	Woody	5	1 km	64 m	45 m	Actual bathymetry
3	Woody	1	5 km	64 m	122 m	Actual bathymetry
4	Woody	5	5 km	64 m	122 m	Actual bathymetry
5	Woody	1	1 km	64 m	45 m	Modified bathymetry
6	Woody	5	1 km	64 m	45 m	Modified bathymetry
7	Woody	1	5 km	64 m	122 m	Modified bathymetry
8	Woody	5	5 km	64 m	122 m	Modified bathymetry
9	Woody	5	1 km	64 m	45 m	Type A bathymetry
10	Woody	5	5 km	64 m	122 m	Type A bathymetry
11	Woody	5	1 km	64 m	45 m	Type B bathymetry

Run	Target	Number of Points	Range	Target depth	Sonar depth	Notes
12	Woody	5	5 km	64 m	122 m	Type B bathymetry
13	Woody	5	1 km	64 m	45 m	Type C bathymetry
14	Woody	5	5 km	64 m	122 m	Type C bathymetry
15	Sub	1	1 km	329 m	122 m	Actual bathymetry
16	Sub	5	1 km	329 m	122 m	Actual bathymetry
17	Sub	1	5 km	329 m	122 m	Actual bathymetry
18	Sub	5	5 km	329 m	122 m	Actual bathymetry
19	Sub	1	1 km	329 m	122 m	Modified bathymetry
20	Sub	5	1 km	329 m	122 m	Modified bathymetry
21	Sub	1	5 km	329 m	122 m	Modified bathymetry
22	Sub	5	5 km	329 m	122 m	Modified bathymetry
23	Sub	5	1 km	329 m	122 m	Type A bathymetry
24	Sub	5	5 km	329 m	122 m	Type A bathymetry
25	Sub	5	1 km	329 m	122 m	Type B bathymetry
26	Sub	5	5 km	329 m	122 m	Type B bathymetry
27	Sub	5	1 km	329 m	122 m	Type C bathymetry
28	Sub	5	5 km	329 m	122 m	Type C bathymetry
29	Salmon	1	1 km	111 m	56 m	
30	Salmon	5	1 km	111 m	56 m	
31	Salmon	1	5 km	111 m	59 m	Flat bottom
32	Salmon	1	5 km	111 m	59 m	Flat bottom, isovelocity SVP

Due to the large number of images created, only a few are shown here along with the related transmission loss images created by the MMPE code. All images focused to 2 m resolution. For the San Pedro site, only the sub at 5 km is shown here: Figure 2-24 are the transmission losses; Figure 2-25 are the one and five point images with the original bathymetry; and Figure 2-26 are the three mixed bathymetry images. Appendix B has the remaining simulated SAS images and related transmission losses for the San Pedro site. All the Salmon site calculations are shown here: Figures 2-27 and 2-28 are the transmission losses for the 1 km and 5 km ranges (note that a flat bottom was used for the 5 km calculations). Figures 2-29 and 2-30 are, respectively, the 1 and 5 km SAS images. These images contain many more multipath images of the points than the San Pedro images, but all are focused to 2 m resolution. From these simulations we concluded that we would be able to produce focus SAS images from data collected at either location.

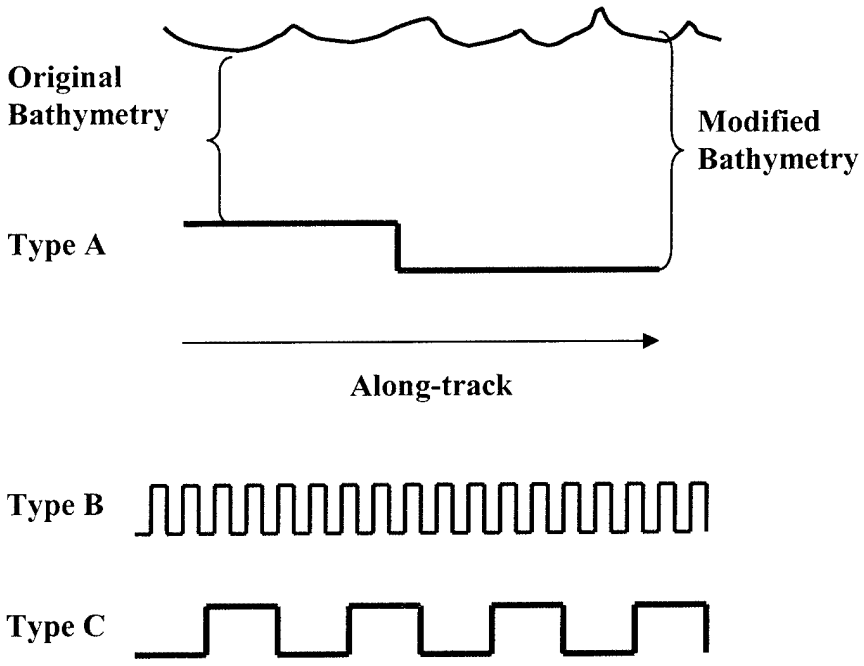

Figure 2-23. Schematic representation of the three bottom variations simulated.

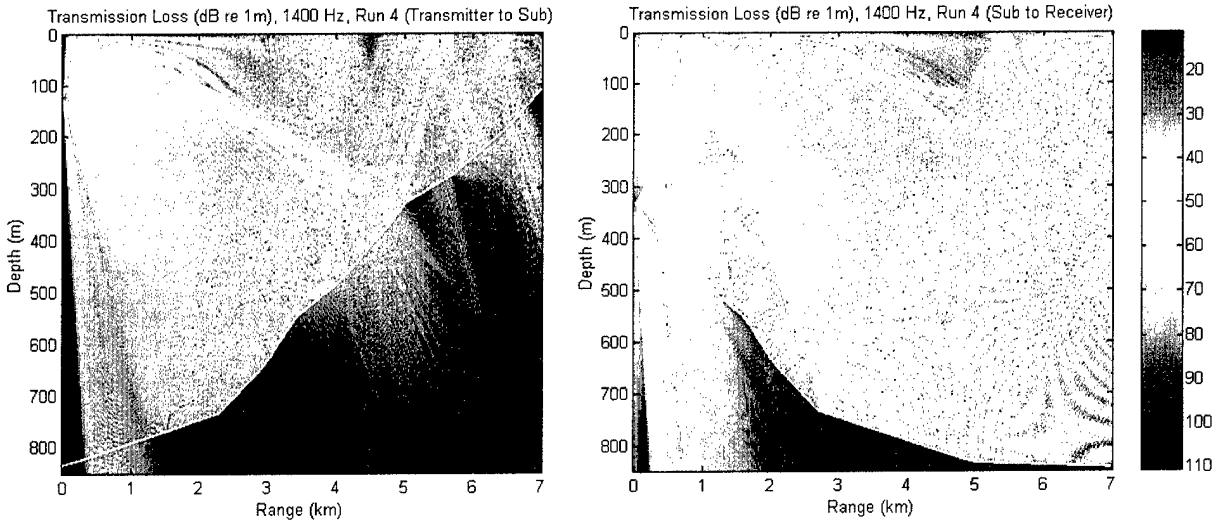

Figure 2-24. Far-range transmission loss for sub location. Left panel transmitter to Sub. Right panel sub to receiver.

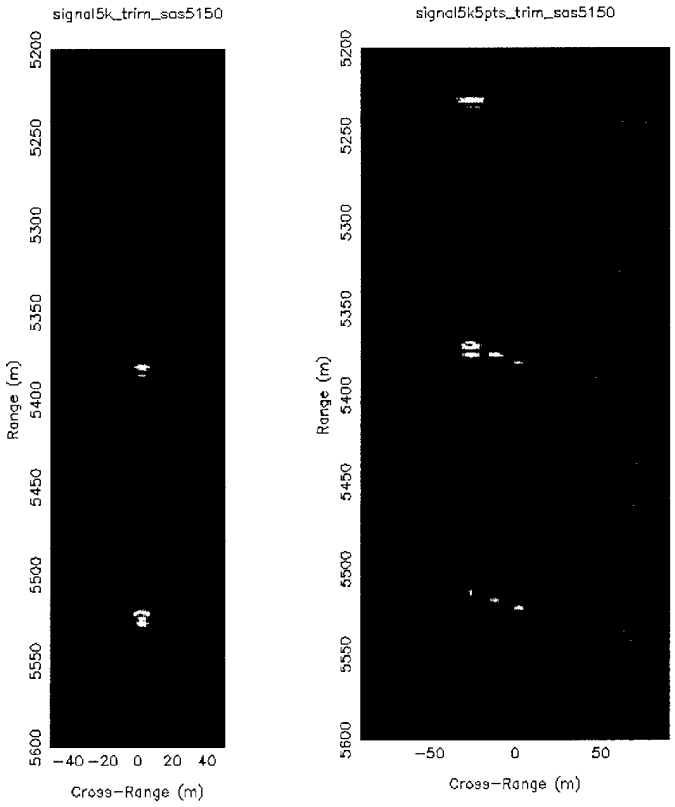

Figure 2-25. Sub at 5 km. Left panel is single point, right panel is 5 points. The color scale used only clearly shows three of the five points. The bathymetry and the way the sound interacts with caused the fading of the other points.

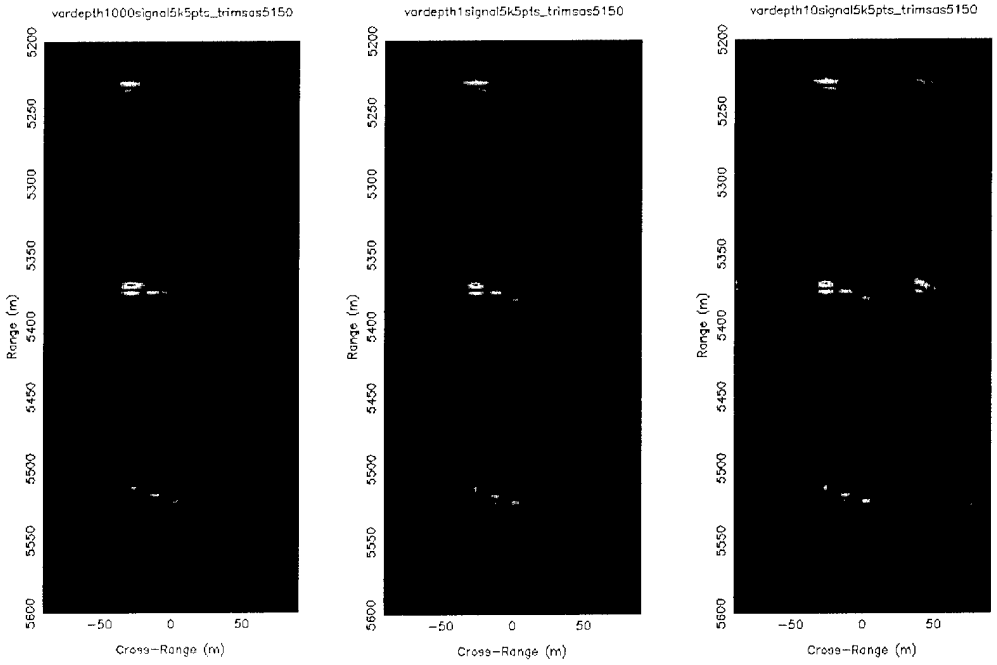

Figure 2-26. Sub at 5 km with three different bottom variation schemes. Type A is left, type B is the middle, and type C is the right panel. Again only three of the five points are visible with this color scale. Additionally the type C bathymetry appears to have induced strong sidelobes.

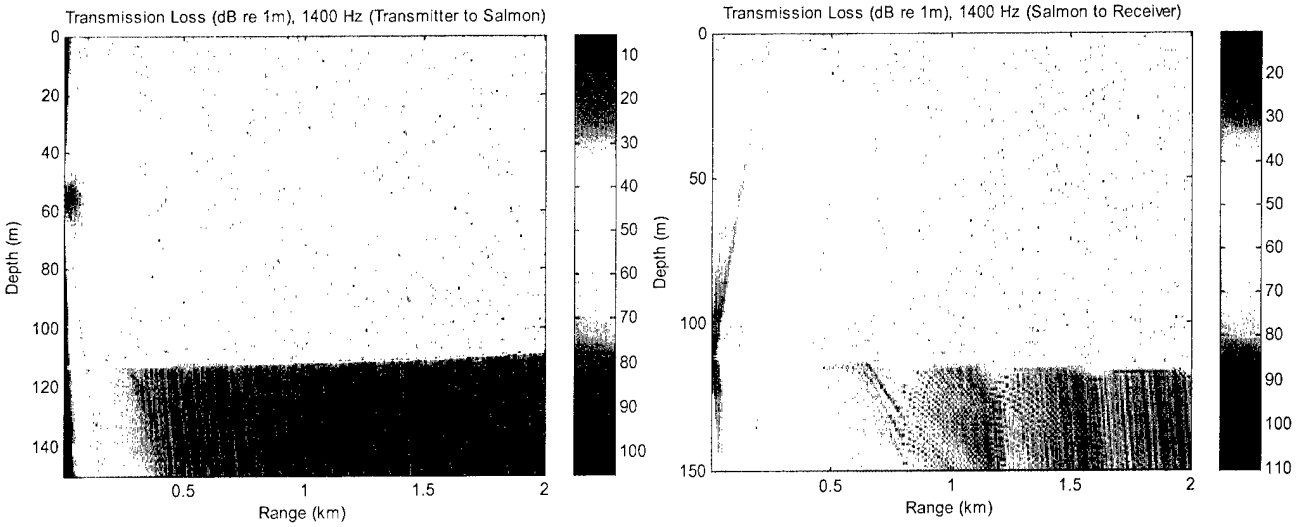

Figure 2-27. Transmission loss for 1 km at Salmon. Left panel is transmitter to Salmon. Right panel is Salmon to receiver.

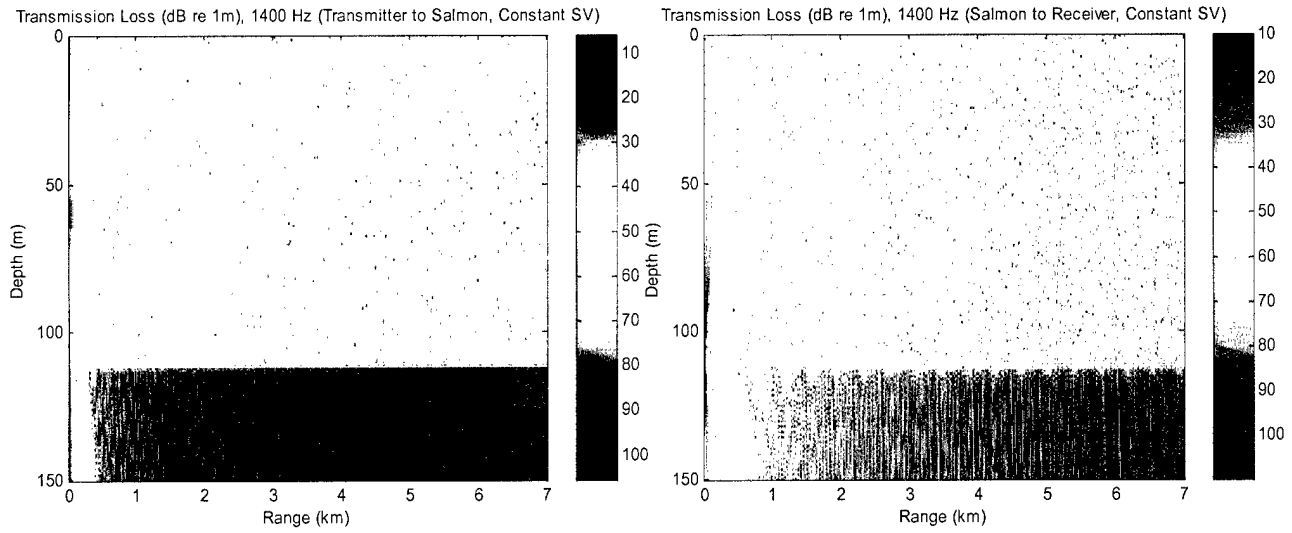

Figure 2-28. Transmission loss at Salmon site for 5 km with constant SVP. Left panel is transmitter to Salmon. Right panel is Salmon to receiver. Note that these results are generally the same as those in Figure 2-27, even though the bottom and SVP are different.

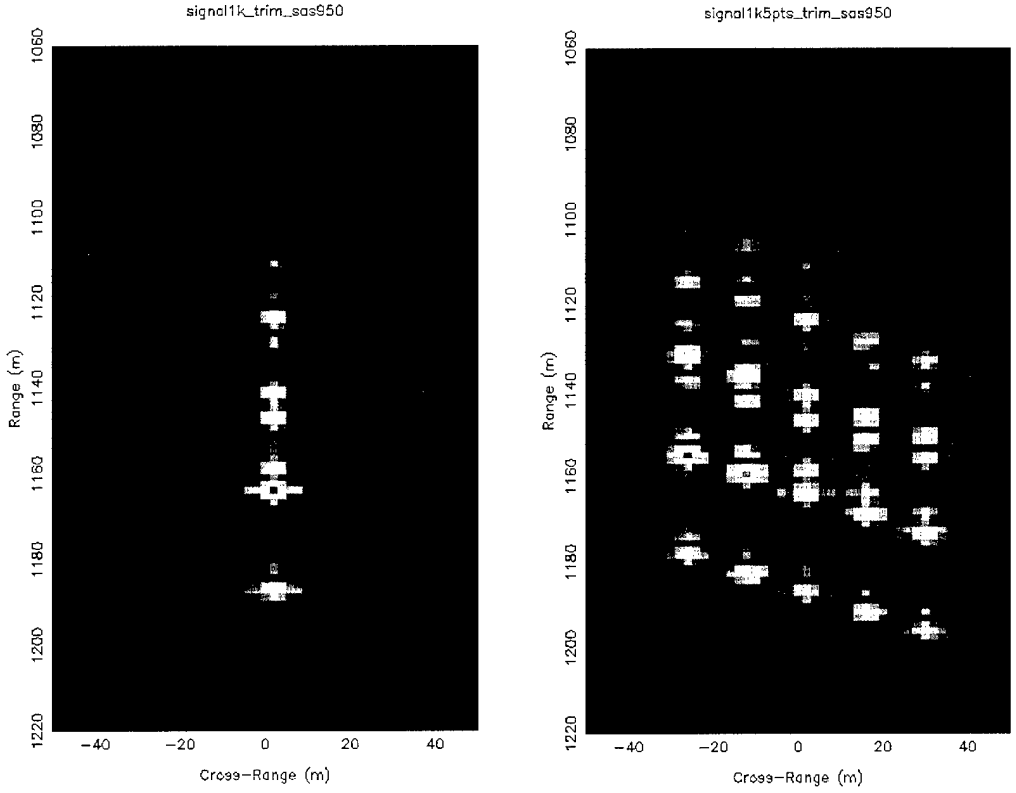

Figure 2-29. Short range Salmon images. Left panel is one point target. Right panel is five points.

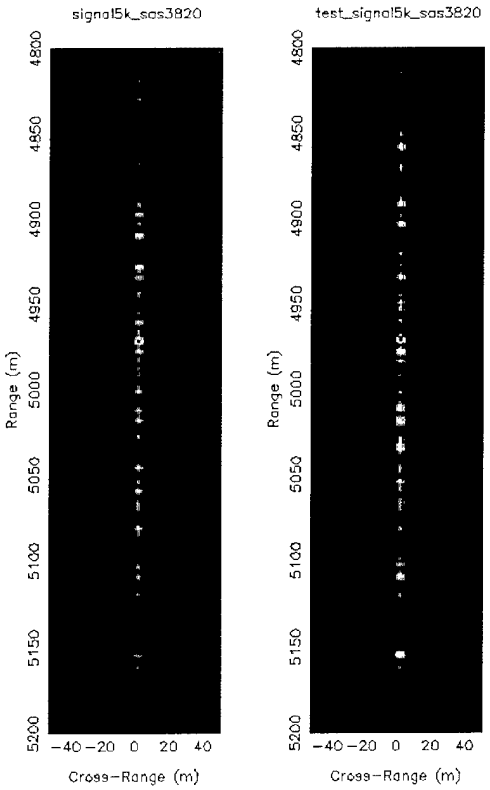

Figure 2-30. Salmon SAS simulation single point at 5 km, flat bottom. Left image uses SVP from Figure 2-22. Right image uses constant SVP.

2.3 Trial Planning

To insure a successful trial, we produced a comprehensive trial plan. This included, among other things: the purpose of the trial; descriptions of the systems used; responsibilities; equipment operation information; daily tasks; and individual data collection runs. The actual trial plan can be found in Appendix A, but in this section we describe the methodology in determining the aspects of the trial plan which were specific to our needs. Section 2.3.1 delineates the requirements and choices for individual data collection runs. Section 2.3.2 describes the need and choice of point targets. Section 2.3.3 describes the on-board data processing. Section 2.3.4 discusses the collection of SVPs during the trail.

2.3.1 Run Requirements

The purpose of the trial is to demonstrate the SAS capability of the Seahawk system through data collection against a variety of targets. There are both generic and specific run requirements, which are described below. Each run, or track, passes a target field once while simultaneously transmitting and receiving data.

The generic requirements are for creating SAS images. All tracks past a target must be a straight line that passes the target, i.e., not headed directly towards the target. The vessel

speed and length of the track are dependent upon the maximum distance and resolution desired for the scene:

$$v_{SAS} = \frac{L_{physical}}{4}\frac{c}{r} = \frac{L_{physical}}{2PRI} \quad (2\text{-}1)$$

$$L = \frac{r\lambda}{\delta_{az}} \quad (2\text{-}2)$$

where v_{SAS} is the vessel speed limit imposed by SAS, $L_{physical}$ is the length of the real receive aperture, c is the speed of sound, r is the maximum range desired, PRI is the pulse repetition interval, L is the length of the synthetic aperture, λ is the wavelength of the transmitted sound, and δ_{az} is the azimuthal, or cross-range, resolution. On the Seahawk, the maximum range allowed and the PRI are intertwined - setting one sets the other and there are only small set of range-PRI pairs available. Because of this, if the desired target field is closer than the maximum range as determined by the PRI, the r in Equation 2-2 may be set to the shorter value and longer ranges in the collected data will not contain a full synthetic aperture of data. The track length of the run is a minimum length of L with L/2 of the track before the closest point of approach (CPA) to the target and L/2 after CPA, see Figure 2-31.

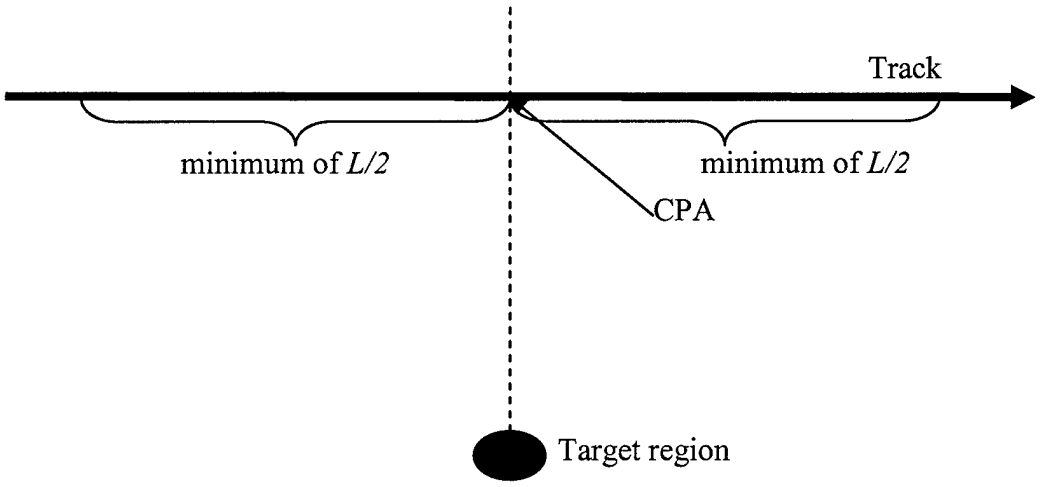

Figure 2-31. Schematic of a generic SAS run.

The specific run requirements are for achieving the goals of the program. The choice of target field, distance from the target, and aspect of the target are the key parameters. Additionally, we added a priority to the runs developed. Thus we could re-arrange the plan while at sea depending upon the circumstances.

As mentioned in Section 2.2.2, our primary target was the Ex-USS Salmon and our secondary targets were the Bidevind and Texas Tower #4. We chose our target field to be a region approximately 400 m long (cross-track) with our target located in the middle of that region. This would give us some clutter surrounding the target as well as allow for the unknown orientation and approximate positions of the targets. In addition to the regions surrounding the targets, we added regions of "pure" clutter, i.e., no known objects in the field. For these, we planned to choose areas while at sea that were convenient and no chance of including our target field in the field of view. Note our processing method for this trial (see Section 2.4) requires an object in the scene as a focusing aid. Due to the possibility of no objects in the field, our ability to process these "pure" clutter data sets would depend upon benign array motion.

The goal of the trial was to image a target at 4-5 km range[8]. The tracks with this range were high priority. However, because our simulations of the area are based on monthly averages of the environment, there is always the chance that the environment on a given day is not conducive for sound propagation to these ranges, especially since several bottom bounces of the sound were expected for these ranges. The average SVPs for the area indicated that direct sound paths existed for ranges out to ~500 m. Thus as a precaution to possible inappropriate environmental conditions, and to verify target location, we made 500 m CPA runs a high priority as well.

We did not have any information about the orientation of any target previous to the trial. To be able to best study the targets we desired to record data from all aspects. Circular tracks are not practical for our application. However, three straight line tracks around the target field, forming a triangle, are practical. From these aspects we are likely to record data from near broadside and near end-on directions. Thus we organized our runs in triangles around a given target (see Figure 2-32) with the mid-point of each leg at CPA.

[8] The nature of SAS requires data from a target from further ranges when not at CPA. For example, a target at 4.5 km will need data that extends to 5 km. Towing the Seahawk at 3 kt with a 6 s PRI cannot receive data much past 4.5 km, thus we could not plan on a target field at 5 km.

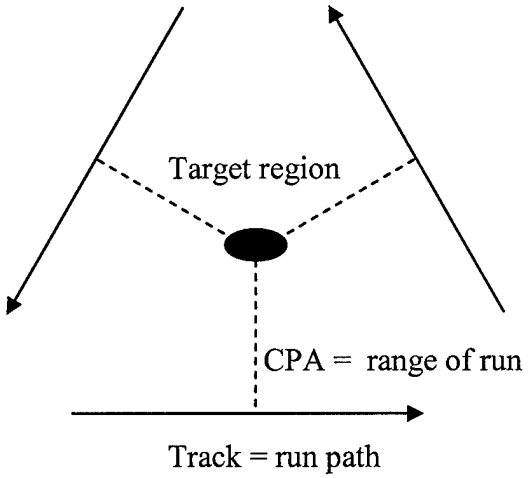

Figure 2-32. Schematic of three legged tracks. The directions of the runs and order of the legs are executed as is most reasonable during the trial.

We designed a few runs outside the standards mentioned in case time permitted us to push the system. Most were not optimal for Seahawk as currently implemented. These fell under a four categories:

1. Longer target ranges (8-10 km).
Tactical ranges for an ASW system are much further than 4-5 km. A SAS demonstration at a near tactical range is warranted; however, the length of the Seahawk arrays will only accommodate further ranges if we exceed the SAS speed limit. Any data collected at 8-10 km ranges would be about a factor of two times undersampled. All images would have strong grating lobes.

2. Omni-direction transmission.
We planned the majority of our transmissions to use the 120° directional beam mode to reduce the left-right ambiguity from the omni-directional receive arrays. The 120° beam allows for some beam steering ("squinting" in radar terminology) and thus multiple aspect processing of the data. Additional runs using the omni-directional transmission mode would allow us to steer beams in any direction and exploit multiple aspect processing even further.

3. Faster tow speed at short range.
We considered the possibility that the slow speed of the vessel would induce more motion in the arrays than desirable for SAS. Thus a faster tow speed, say 5 kt, would demonstrate smoother array motion. These data would be undersampled along-track since the array length dictated a 3 kt tow speed, thus grating lobes would appear in the SAS images.

4. *Intermediate (between 0.5 km and 5 km) ranges.*
The 0.5 km range was chosen to assure us SAS imaging and target location, while the 5 km range was the objective of the trial. Since it is possible that the environment would allow us one and not the other, we desired to add more risk mitigation and attempt runs with the target field in between the two ranges. Thus if 5 km were lost to us, perhaps 3 km would not be. It would also allow us to map out the environmental effects.

The priority for these additional runs are the same order shown. These are reflected in the run plans in Appendix A.

2.3.2 Point Target - a Risk Mitigator

The first trial with a SAS system is best conducted with known point targets. A point target has a well understood sonar magnitude and phase response. Thus motion and environmentally induced errors can be determined and removed for the regions of the scene that contain the point target. Therefore, if the array motion is larger than expected, the environment has larger effects than expected, or there are other unexpected systems problems, e.g., phase offsets in the receivers, we should still be able to form images and demonstrate SAS while tracking down possible improvements for future trials. Since Seahawk had not been used for SAS yet and there were upgrades to it, we decided that a point target was required for risk mitigation.

The ideal point target is a simple geometric shape such as a sphere or a corner reflector. For a strong response, the size of the target should be large compared to wavelength. This is simple for high frequencies, e.g., larger than 50 kHz, since the wavelength is only a few centimeters. For our 1.4 kHz system the wavelength is ~1 m, thus geometric targets would need to be many meters in size. Additionally, the target would need to be able to withstand the pressure at ~100 m depth. This means that a geometric target would be unwieldy and difficult to deploy/recover. We investigated a variety of other options, including both passive and active options. Due to costs, we were limited to being able to deploy and retrieve from the trial vessel. Any active option had to operate within our receiver frequency band. We located an acoustic pinger that could operate at 1.677 kHz, the InterOcean 1090EP Acoustic Pinger. This frequency was within the 3 dB point of the receivers (~1.71 kHz) and outside the transmitter band. The source level of 145 dB would reach the receivers above the background noise levels according to our calculations, yet was not loud enough to disturb mammals.

We planned to deploy this pinger at each target site. To do so we devised a mooring system (see Appendix A). The size (16.5 cm diameter, 48 cm length) and weight (12 kg/26.5 lbs) of the pinger accommodated a simple mooring system and required two people to deploy/retrieve - one to operate the capstan and one to guide it in/out of the water.

2.3.3 On-Vessel Processing

Prior to the October sea trials, the only Seahawk data available to DTI was laboratory test-signal data used to evaluate proper function of the hydrophone channels. These data were used by DTI to verify that our data parsing and pre-processing routines properly ingested the Seahawk telemetry. Because they lacked any target information, the lab data were inappropriate for the development and testing of real-time SAS processing software. This situation was expected during the program planning stages, and motivated DTI to focus our on-vessel processing efforts toward our research tools rather than our real-time processing capabilities.

Despite the absence of data to support real-time software development, our existing real-time SAS processor, PRO*SAS*^{TM}, was installed on DTI's on-board processing workstation, ready to be tested with Seahawk target data. In anticipation of this opportunity, decisions were made early in the test preparations to support these early real-time tests. In particular, when developing the front-end data parser and pre-processing software, we chose the PRO*SAS*^{TM} native data file format for all of our on-board work. This format is quite general, packaging together all information that is required for SAS processing, including all relevant sonar specifications, motion data, acoustic data, and some PRO*SAS*^{TM}-specific configuration information. In addition to allowing early testing of PRO*SAS*^{TM}, tools already existed to convert this data format into our older research-tool formats, so there was no penalty incurred for choosing the new format.

Because the real-time processor was originally designed for use with high-frequency survey-style sonars with rigid-arrays, some adaptations would be necessary to use PRO*SAS*^{TM} with towed-array data. The primary difference between Seahawk and the model used in PRO*SAS*^{TM} is that the towed arrays used by Seahawk have a different set of constraints describing the relative positions of hydrophone elements. Whereas the positions of elements on a rigid array are completely described by the position and attitude of the center of the array, positions of hydrophones on a towed array must be individually specified. In order to use PRO*SAS*^{TM} for Seahawk towed-array data, the hydrophone positions must be specified as if they were described by a rigid array. There are two ways to do this: first, if the motion of the array is quite small and doesn't exhibit high-order bending motions, the array description may be approximated as if it were a long rigid array. This approximation will obviously break down when the sonar experiences significant motion, for example during higher sea state or if the ship's navigation isn't carefully controlled. The second method for describing the array to PRO*SAS*^{TM} is to incorporate array shape estimation into the front-end pre-processor, allowing the exact position and orientation of each hydrophone element in the array to be estimated. Once these locations are determined, the acoustic data could then be sent to PRO*SAS*^{TM} as a series of one-channel data records, i.e., consider each of the 48 channels to be an individual one-channel "rigid array", each sent to PRO*SAS*^{TM} as if it were an independent ping. By deceiving PRO*SAS*^{TM} in this way, the channel positions are accurately retained, and the SAS processing could proceed as usual. This method takes advantage of the fact that PRO*SAS*^{TM} does not care when acoustic data are collected; it is only concerned about the positions of acoustic phase centers as it assembles the synthetic aperture.

During the October sea trials, DTI was prepared to test the first of these methods (the long rigid-array approximation) with PRO*SAS*™. The latter method required additional software development that was beyond the scope of this early processor test. Detailed evaluation of these and other real-time processing methods will be carried out in preparation of future sea tests.

2.3.4 Sound Velocity Profiles

In order to understand the transmission losses and multipath we may find in the sonar data, we planned to measure the SVP several times during the trial. We purchased equipment from Sippican, Inc. to measure temperature and sound velocity profiles. To take these measurements, we dropped probes from a moving vessel while recording the data to a laptop. We used the MK21/USB Bathythermograph Data Acquisition System for the data recording and processing. The Expendable Bathythermograph (XBT) probes measure water temperature as a function of depth. Using a constant salinity, the SVP is calculated from these temperature profiles. The Expendable Sound Velocimeter (XSV) probes measure the SVP directly. We purchased only a small number of the XSVs and we used them to check the XBT results.

2.4 Data Processing

In this section we describe the data processing techniques used to create the images of Section 3.2. The steps are not identical to those used in our MCM, rigid array SAS processing and found in numerous publications, such as Chang, et al. (2000), Chatham, Nelson, & Chang (2000), Marx et al (2000), and Putney et al. (2001). The changes were due to the flexible nature of the receiver array and lack of redundant phase centers[9]. Here we describe the data quality assessment (Section 2.4.1) to assure ourselves that the collected data, both acoustic and non-acoustic, were worthy of processing. We explain the method used to create SLS images, which were an additional data assessment tool, in Section 2.4.2. In Section 2.4.3 we delineate the steps we use to create SAS images from the Seahawk data.

2.4.1 Data Quality Assessment

Because SAS processing is very sensitive to the quality of the raw data, it is important to independently assess data quality as they are collected. During the execution of the sea tests, monitoring the quality of the collected data allows the test director to assess the level of success for various types of runs, and gives her the ability to schedule additional runs if data quality is deemed unacceptable for a particular run of interest. When the data are eventually transferred to scientists for SAS processing, data quality assessments allow

[9] In rigid array SAS processing, DTI uses a technique known as Redundant Phase Center (RPC) processing (sometimes called displaced phase center). In RPC processing the towbody motion is estimated through range-wise correlations on data from overlapping segments of the hydrophone array on successive sonar pings. The complex correlation between the signals received on two repeated looks is sensitive to phase errors on the order of a fraction of a cycle. We desired the presence of these overlapping segments, or redundant phase centers, in the LRSAS data to attempt similar motion estimation techniques for a flexible array.

them to prioritize the runs and focus their attention on data sets that should pose the fewest challenges to the still-in-development towed array SAS processing software.

As soon as data sets were received by DTI on-board the test vessel, analysts performed basic quality assessments of both the acoustic raw data and the limited amount of non-acoustic data (NAD) provided by the system.

The NAD were limited to pitch/roll/heading of the towbody and ship-mounted GPS records. After each run was completed and the data transferred to DVD-R media, the NAD were extracted and plotted as a function of time. This procedure allowed the analyst to quickly identify any sections of data where the NAD were missing or obviously corrupt, and also provided for an initial assessment of the severity of motion that the towbody experienced during the run. Both of these pieces of information are useful when screening runs for those that are likely to result in successful SAS processing.

The acoustic raw data must be of high quality to facilitate SAS image formation. The two factors that generally are of most concern are phase calibration of the hydrophone array, and, to a lesser extent, gain calibration of the channels.

In synthetic aperture processing, the majority of the final image content is contained in the phase information of the raw data. Thus, it is important to calibrate the hydrophone array so that the phase responses of all channels are the same when stimulated by a common source (i.e., "coherent"). This calibration may be accomplished either by designing and tuning the array itself to satisfy this requirement, or by providing carefully measured calibration data. In practice, it is exceedingly difficult to fabricate an array that is naturally coherent, so it is common to employ a combination of the two methods – first design and build the array as carefully as possible, then characterize its response and correct the phase and gain response in software. Unfortunately, there were no phase calibration data available for the Seahawk system, so we had to rely on the natural response of the system.

During the quick-look data quality assessments, it was not possible to characterize the array phase response. Doing so requires analysis of isolated, point-like scatterers in the data, which was beyond the scope of the quick-look assessment. This type of procedure is employed, however, during the actual SAS processing of the data, and a better understanding of the phase calibration of the array can be obtained at that time. Despite the difficulty in measuring phase calibration, however, it was generally accepted that the response of the Seahawk array would likely be sufficiently coherent for our needs. The low frequency signal used by the system results in such a long wavelength that accurately recording its phase is a simple matter for modern digital-to-analog converters. One degree of phase, for example, corresponds to a data collection time of almost 2 μs. Time scales on this order are easy to accurately calibrate, and discussions with L-3OS engineers confirmed that phase response should be adequate for our needs.

The gain response of the array, though less important than phase, is relatively easy to assess. As each data set was collected, DTI analysts extracted the raw hydrophone data for further study. These data were extracted prior to any time offset adjustments, quadrature demodulation or range compression, in order to isolate the raw hydrophone data from the

effects of data pre-processing. Two basic procedures were used to evaluate gain calibration. The simplest computed the average signal magnitude recorded from each array channel over the course of a run. This produces a good estimate of relative overall channel gain. The results of these analyses were generally satisfactory, as shown in Figure 2-33. In order to evaluate any potential non-linearity or other non-standard hydrophone response, the data was also collected into a series of magnitude histograms – one for each array channel. This allowed us to identify any channels with inconsistent hydrophone sensitivity or pre-amplifier gain responses. Representative results from this analysis are shown in Figure 2-34. This procedure confirmed the information from L-3OS engineers regarding dead or weak channels in the system. Aside from those known problematic channels, the array generally exhibited consistent channel response.

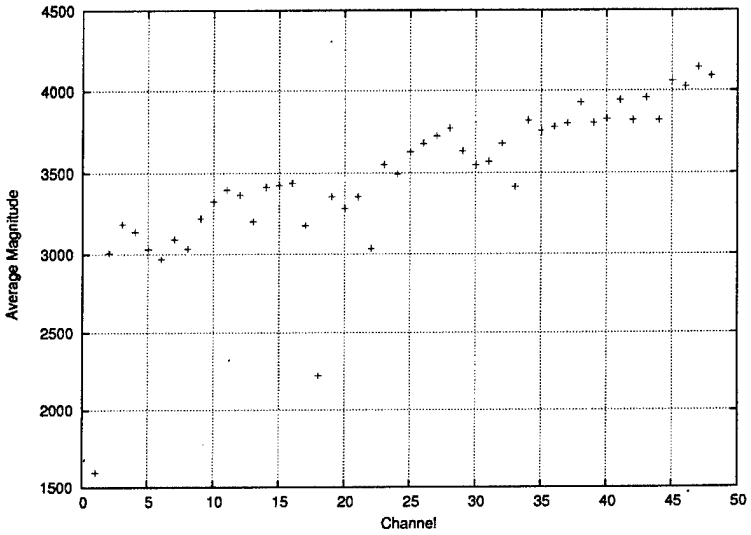

Figure 2-33. Average signal magnitude in each channel for Run S1 (see Section 3.1 for run definition). These result is nearly identical from run to run. This is the port array and channels are labeled backward from those shown in Table 2-3. The channels 1 and 18 (48 and 31 in Table 2-3) are bad channels and this is evident by the weak average magnitude.

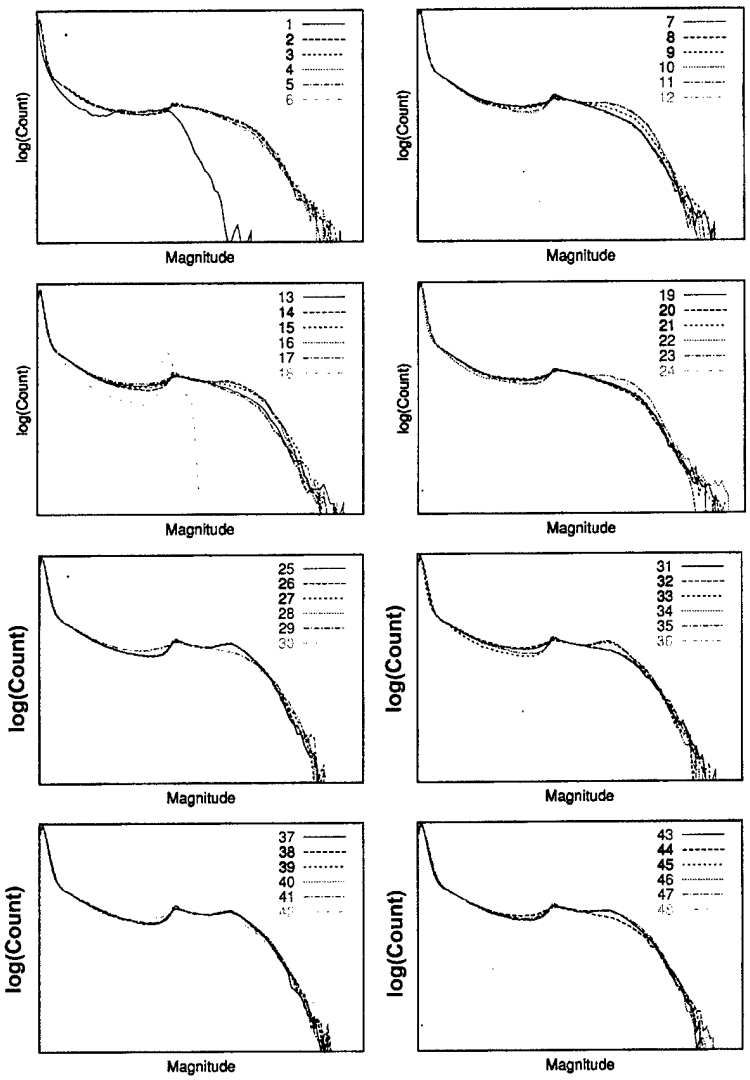

Figure 2-34. Histograms of channel responses for Run S1. The actual magnitudes and count at a given magnitude value are not labeled, but the magnitude increases to the right and log(count) increases to the top. These results are consistent from run to run. This is the port array and channels are labeled backward from those shown in Table 2-3. The channels 1 and 18 (48 and 31 in Table 2-3) are bad channels as is evident by the early fall-off in count with magnitude.

Once these assessments are complete, any obviously bad channels could easily be excluded from subsequent SAS analysis. In addition, it is also possible to utilize these measured gain characteristics to re-calibrate the channel data, although this was not done for the SAS processing results presented in this report.

2.4.2 SLS Processing

Because of the understood difficulties associated with SAS processing, especially in the context of ASW towed array systems, DTI developed a simplified sidescan image processor for the Seahawk data. This processing method is essentially similar to conventional sidescan imaging used in high-frequency imaging sonars, whereby the channel data is coherently summed on each ping to produce a much narrower azimuthal beam width. These beamformed data from each ping are displayed sequentially side-by-side to form an image of the survey area.

DTI's implementation of the sidescan imager is very simple to operate; it reads the data files produced by our front-end preprocessor, coherently sums the channels, and outputs a magnitude-only image file. The resulting file is produced very quickly, and is two orders of magnitude smaller than the original data file, facilitating simple viewing and manipulation.

In order to optimize the image produced by sidescan processing, array deformations should be estimated and compensated for in the raw data. This extra processing step ensures that information from the entire array will contribute to image gain and beampattern sharpening. Because of the significant complexity of incorporating array shape estimation into the image processor, and because the sidescan imagery was to be used only as a qualitative quick-look assessment of the survey area, DTI chose to forgo this step in our sidescan processor. Nevertheless, due to the relatively short array length, long wavelength and calm seas, the simplified processor was able to produce imagery of considerable utility.

2.4.3 SAS Processing

In this section we describe the data processing required to create the SAS images presented in Section 3.2. Due to the combination of a lack of overlapping phase centers in consecutive pings and the flexible receive arrays of Seahawk (redundant phase centers and rigid arrays are assumed in the standard usage of PRO*SAS*^{TM} for MCM), this methodology is different than found in the majority of DTI SAS publications.

Available motion sensors alone were not sufficient to estimate array motion, thus we were forced to rely on algorithms which operate on an object of interest in the scene in order to estimate and compensate motion. The returns from the object must contain sufficient energy to permit tracking of the object from ping to ping with a real aperture beamformer. Such objects are often visible in phase history plots as "smiles," due to their hyperbolic shape. After motion compensation has been applied, a SAS image of the object is formed using a beamforming technique similar to the conventional delay-and-sum technique. Phase Gradient Autofocus (PGA) is applied to compensate residual motion error. The result is a SAS image of the object and surrounding area. The motion corrections derived from the object can then be applied to the full range extent of the acoustic data to produce a full-swath image. Figure 2-35 schematically lays out the process. We proceed with a brief description of the processing steps.

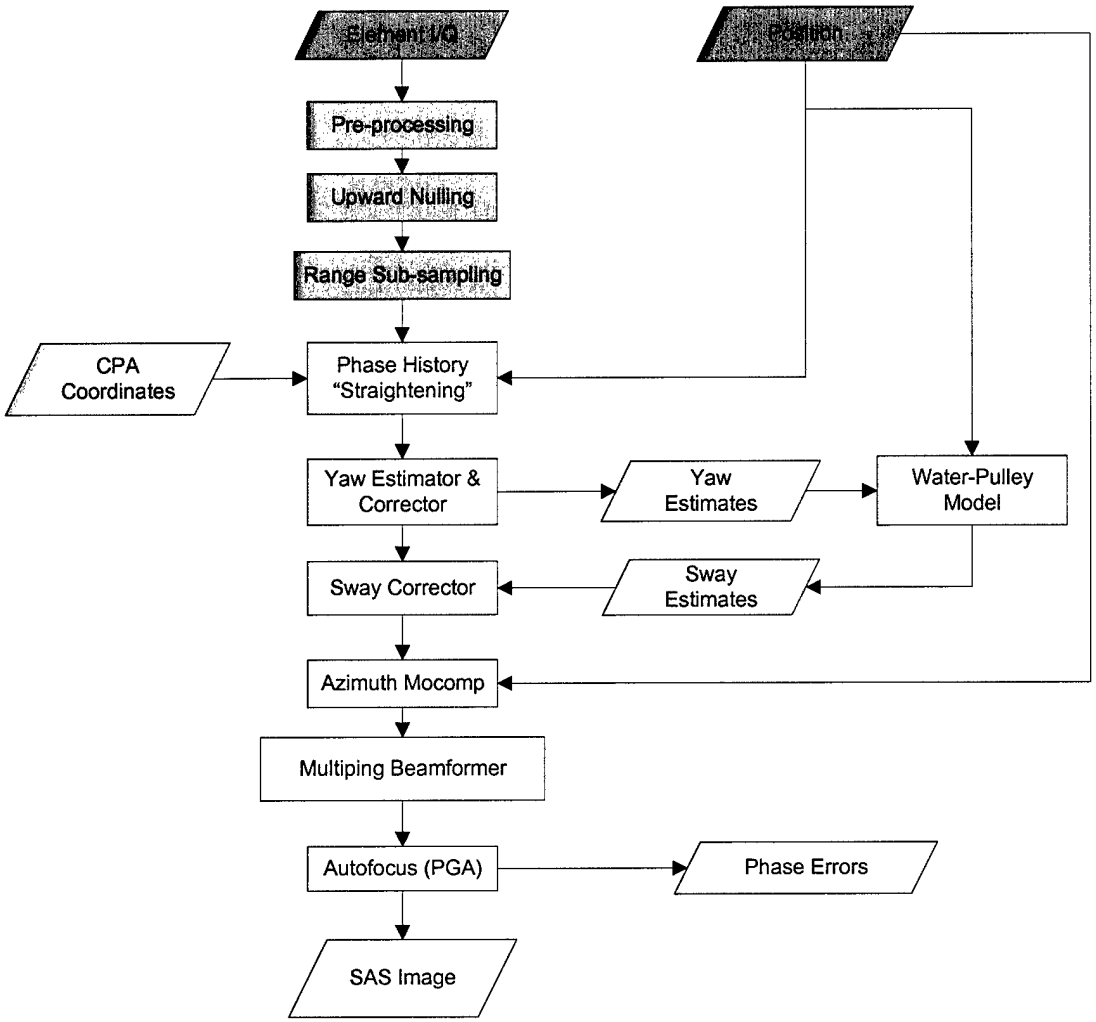

Figure 2-45. Schematic diagram of SAS processing for LRSAS.

Input Data

Input to the SAS processing routines consists of element-level in-phase and quadrature (I/Q) acoustic data and array position data. The array position data are taken to be the most recent 1 Hz GPS position at ping time. These positions are fitted to a line, and the along-track position of each ping is computed as the distance along the line relative to the position of the first ping.

Data Pre-Processing

Data from the Seahawk system were provided to DTI on recordable DVD disks and stored in the native format used by the L-3OS data acquisition system. This format is arranged so that specific types of data are stored in their own record types, each with synchronization words and appropriate identification information. Records available during these sea trials included:

1) Raw telemetry records containing the hydrophone channel data, NAD, and timestamp. NAD fields include heading, pitch and roll readings that are necessary for the SAS navigation processor;

2) GPS records with ship's position information, and both computer and GPS timestamps. The GPS records are the primary source of speed information for the SAS processor; and

3) Notes records containing miscellaneous embedded notations.

To facilitate the use of the DTI SAS processing software tool suite, these data must be converted into a file format understood by the DTI tools. DTI's "PingRecord" file format was chosen for the high level of versatility it provides; it accommodates all the data fields necessary for SAS processing, a comprehensive set of tools exist to manipulate PingRecord files and convert them to other formats, and it is the preferred format for DTI's real-time SAS processing product, PRO*SAS*™. The file conversion includes several data processing operations in addition to simple data re-formatting.

1. Input data stream is parsed to extract the two record types that are relevant to DTI's processing: raw telemetry (containing both acoustic and navigation data) and GPS records.

2. Heading, pitch, roll, and GPS velocities and positions are combined to produce an initial estimate of the towbody trajectory. Since there are no velocity sensors on the sonar body itself, we initially assume that the tow vehicle's forward speed is the same as that of the ship, and may be represented by the GPS records. This speed is used in conjunction with the towbody heading information to dead-reckon a trajectory of the towbody. This provides initial latitude, longitude, heading, and pitch information that will be logged in the output data file. A more sophisticated Kalman filter is available for post-processing that will produce a more optimal estimate of towbody trajectory from the same inputs.

3. The raw acoustic telemetry is scanned for a 0 to 1 transition in the PingNow bit. When detected, a new "ping" of hydrophone data is initialized. A "one-shot" time-out is implemented in the software to ensure that only the first 0 to 1 transition triggers a new ping, and will be unaffected by any subsequent transient noise in the PingNow indicator.

4. Raw hydrophone data are extracted from the acoustic data records. The raw data are stored in an ordering that is natural for a data recorder, but not for an image processing system, thus the data are re-arranged into an ordering that is more natural for our processing. Acoustic records continue to be parsed and accumulated until the next PingNow indicator is detected, at which point the current ping is declared complete and is submitted for initial signal processing.

5. The acoustic data in the ping undergoes a series of signal processing steps:

i) The magnitude samples provided by Seahawk are Hilbert-transformed to convert them to I/Q complex samples.

ii) The time-series data for each channel are match filtered with a replica of the LFM chirp used by Seahawk's projector. This results in range-compressed data with range resolution consistent with the signal bandwidth ($\delta R = c/(2 \cdot BW)$, where δR is the resolution, c is the speed of sound, and BW is the bandwidth).

iii) The time series for each channel is adjusted by its specific time offset. Due to the way the data are recorded by Seahawk, each channel has a small collection time offset. These offsets are deterministic and have been provided to DTI by L-3OS.

iv) The data for each channel are base-banded, i.e., shifted in frequency from the original carrier frequency down to zero.

v) The data from the two arrays are beamformed. Originally, the software was configured to resolve the left/right ambiguity of the towed arrays by forming port- and starboard-directed beam data, producing two PingRecord data streams (one for each side). Ultimately, however, it was decided to utilize the twin array data to steer a null toward the ocean surface in order to minimize interference from the ship's noise (see below). In this configuration, the output data retains the left/right ambiguity, but without surface noise corruption, and the two PingRecord outputs differ only by an overall sign.

6. When the acoustic data for the ping is ready for output, it is packaged into PingRecord format along with its associated trajectory and attitude values and a variety of static system description fields, and written to disk.

The resulting files may be exploited directly by either PRO*SAS*™ or our sidescan image quick-look tool, or may be converted into simpler formats that are more convenient for manipulation by an analyst.

Twin-Line Use (Upward Nulling)

The Seahawk system is designed with two hydrophone arrays trailing after the towbody. Each array is inherently omni-directional, and therefore is sensitive to energy originating from the towship, and has a natural port/starboard ambiguity for contact locations. By combining the signals from both arrays, however, a null may be directed either to the surface to minimize the impact of towship noise, or to one side or the other if left/right ambiguity resolution is required.

The general expression for the beam formed by an array of N omni-directional receivers is

$$S(\theta, R) \propto \sum_{n=0}^{N-1} A_n e^{\left[i\frac{2\pi}{\lambda}(R + nd\sin\theta) \right]}, \qquad (2\text{-}3)$$

where A_n is the element gain, d is the element separation, R is range, and θ is the angle from the normal to the array. If we ignore the behavior with respect to range, we get

$$S(\theta) \propto \sum_{n=0}^{N-1} A_n e^{\left[i\frac{2\pi}{\lambda} nd \sin\theta\right]}. \tag{2-4}$$

For the case of LRSAS, each along-track position on the twin array system has two omni-directional hydrophone elements, so each of these locations may be treated as a two-element array for beam-forming in the axial direction. The signal from this two element array is

$$S(\theta) \propto A_0 + A_1 e^{\left[i\frac{2\pi}{\lambda} d \sin\theta\right]}. \tag{2-5}$$

Normalizing the gain to that of the first hydrophone, and setting this expression equal to zero will determine the (complex) value of A_1 required to place a null at an axial angle of θ:

$$A_1 = -e^{-i\frac{2\pi}{\lambda} d \sin\theta}. \tag{2-6}$$

Evaluating this expression at $\theta = \pi/2$ gives us the coefficient necessary to steer a null toward the port or starboard sides to resolve the left/right ambiguity, and evaluating it at $\theta = 0$ allows us to steer nulls directly upward and downward. The resulting beam patterns are illustrated in Figure 2-36, assuming $d = \lambda/4$ for optimal null depth.

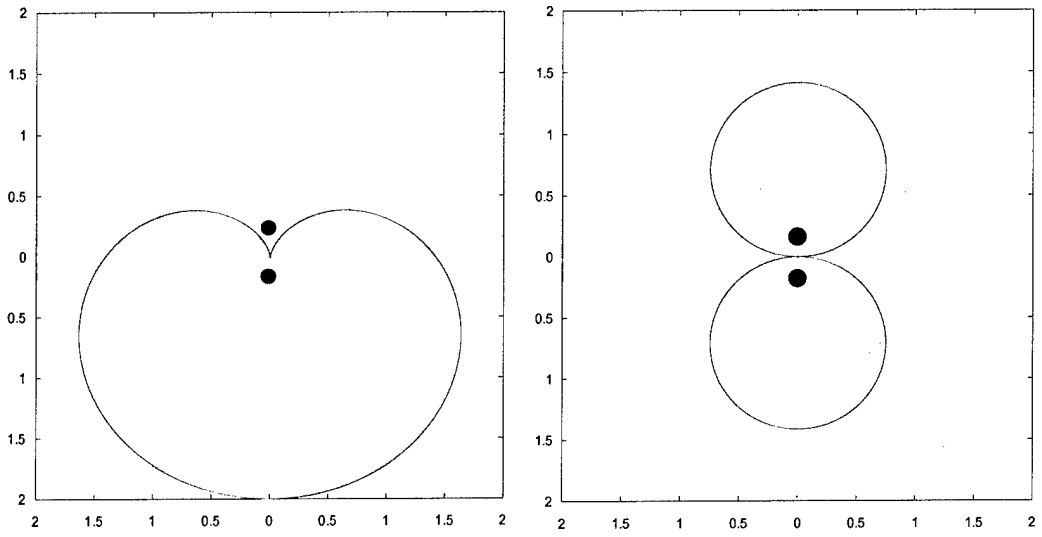

Figure 2-36. Twin-line array beam patterns. Nulls my be directed in either the port or starboard direction, shown left, or simultaneously toward the ocean surface and the seabed directly beneath the array, right. These are horizontal beam patterns.

Upon examining the data collected during the Seahawk tests, there were two striking features observed. First, the test area had remarkably little clutter, obviating the need for left/right ambiguity resolution (additionally, the directional transmit was used for the majority of the runs, which severely lowered the strength of returns from the non-transmit direction). Second, because of the relatively slow tow speeds necessary for proper SAS data collection, the arrays remained directly beneath the tow ship, placing the ship's noise in the main-lobe of the array beam pattern. It was therefore an obvious choice to direct the twin-line null toward the ocean surface to minimize this source of interference.

In practice, data from the two Seahawk arrays were combined by subtracting the signal from each channel of one from that of the corresponding channel from the other. This is what the surface nulling expression above reduces to for $\lambda/4$ array spacing. The resulting data are equivalent to that from a single array with the desired reduced surface sensitivity, and is suitable for use in the DTI SAS processing software. Figure 2-37 is an example of the data before and after surface nulling.

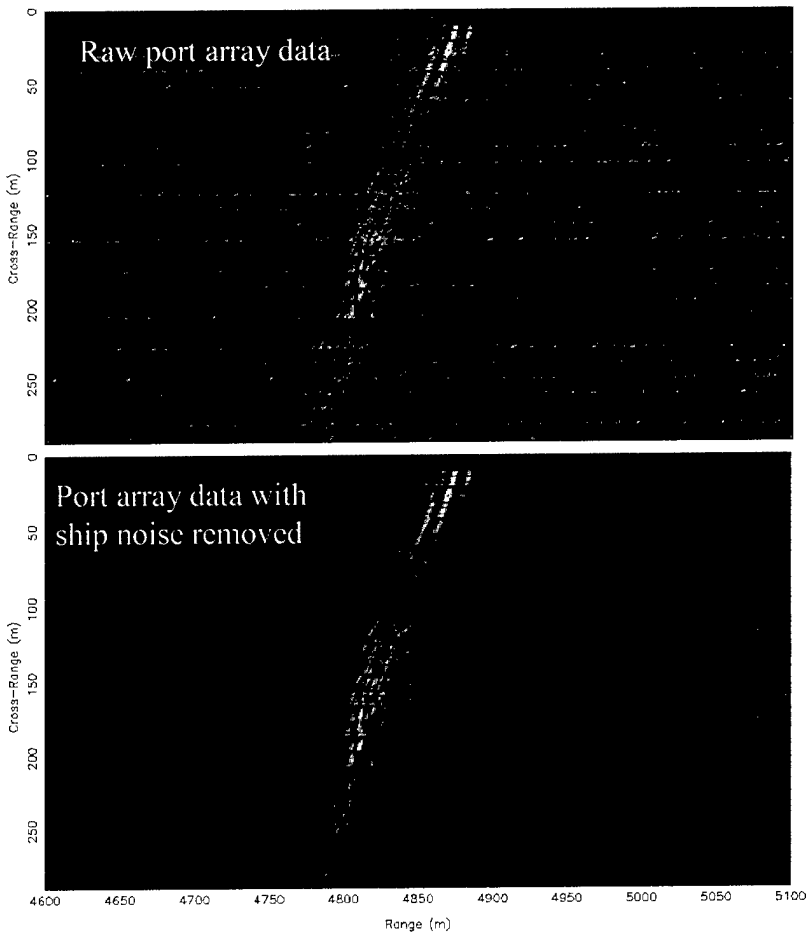

Figure 2-37. Example of surface nulling. Upper panel shows raw data from the port array. Note the high levels of noise away from the signal. Lower panel show the same data after the upward, or surface, nulling has been applied. The noise has been reduced thus enhancing the signal to noise ratio.

In the situation where left/right ambiguity resolution is more critical than the reduction of surface noise, independent port- and starboard-directed data sets could be produced by combining the array data with the appropriate coefficients. Each of the two resulting data sets could then be SAS processed as usual.

Phase History "Straightening"

After the data are conditioned as above, the data are sub-sampled in range to conserve space and decrease processing time before the "straightening" step. The phase history "straightening" is achieved by applying delays, or displacements, to each element signal such that the object is displaced to a constant range, meaning the "smile" is removed, see Figure 2-38. The displacements are computed using array position, the receiver spacing, and CPA. Typically we estimated CPA by eye from the phase histories. In a more formal system, however, the CPA could be determined automatically by utilizing a tracker.

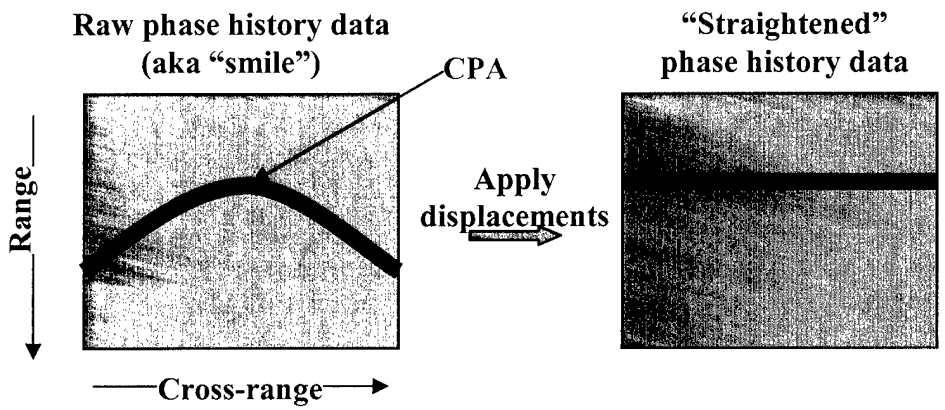

Figure 2-38. Schematic representation of phase history data before and after displacement application. The left panel shows the raw phase history data with the hyperbolic returns from a bright object, often referred to as a "smile." CPA is marked and is the fiducial for the displacements. Right right panel shows the phase history data after the displacements are applied, sometimes referred to as "straightened" data.

Yaw and sway motion estimation techniques

After straightening, the object should appear to be at a constant range and broadside in each ping. Any deviation from this is due to array motion, error in the CPA coordinates, other motion-induced effects, or possibly the environment. In this set of steps, the motion induced deviations are corrected using the signal from the object itself. A previous study (Chang & Campbell 2003) has shown that the ideal point response an array of similar length can be obtained simply by characterizing phase error across the array by a first-order polynomial. We term the 0^{th}- and 1^{st}-order coefficients of this fit as *sway* and *yaw*, respectively, to suggest their motion-based origins. The yaw estimation operates by beamforming a single ping and estimating the Direction of Arrival (DOA) of the object's signal relative to broadside.

The specifics of the yaw algorithm are as follows. The element data are beamformed using fine beam angles with conventional azimuth FFT beamforming. In the resulting beams, the highest amplitude point may be due to either own-ship noise or the object itself, depending on SNR. In order to distinguish the object signal from the noise, we create a normalized azimuth energy profile in four steps:

1. The analyst creates a range gate containing (most of) the signal of the object. This gate is the same for all pings. While it is currently operator-entered, there is no reason that it could not be automatically computed by using a tracker in the future.

2. The energy inside the range gate is divided by the energy outside the range gate for each beam. This removes extraneous noise, such as tow ship noise.

3. The object's relative bearing is roughly determined from the location of the beam of the maximum peak of the normalized energy profile is determined.

4. The peak of the beam (i.e., relative bearing) is refined using the non-normalized energy profile of the object.

This algorithm, as rudimentary as it is, can quickly and accurately determine the object DOA in an automated fashion. In a high-clutter situation, the DOA might be provided by a tracker, in which case this algorithm would be unnecessary. As DOA relative to broadside are determined for each ping, the yaw estimates are recorded for later use and the appropriate phase center displacements are applied in order to correct for the yaw (see Figure 2-35).

Given the propagation conditions and the SNR levels, we found that the object *range*, and therefore sway, cannot be consistently and accurately determined directly from the object signal. Also, the absence of redundant phase centers precludes the use of the redundant phase center (RPC) algorithm[10]. Thus, we decided to simply *derive*, or *infer*, sway from the yaw estimates using an array motion model under the water-pulley assumption, i.e., each point follows the point which precedes it when it reaches the same along-track location. The water-pulley model can be simply written as:

$$\Delta y = \Delta x \tan(\overline{\psi}) \tag{2-7}$$

where

$$\Delta y = y_{new} - y_{old}\,, \tag{2-8a}$$

$$\Delta x = x_{new} - x_{old}\,, \tag{2-8b}$$

$$\overline{\psi} = \frac{\psi_{new} - \psi_{old}}{2}\,, \tag{2-8c}$$

y is the sway, x is the along-track position and ψ is the yaw. The sway estimates are recorded and applied to the phase histories. Due to the integrative nature of the sway derivation process, we limit the extent to about 40 pings. This constrains the compounding of residual sway error. The sway correction process is applied to various along-track sections of the run. Multiple images may be formed off of one of these sway-corrected sections later in the processing. However, images are not formed using data from more than one of these sections.

Image Formation

After yaw and sway corrections have been made to the phase histories, we can form a SAS image. The phase centers need to be resampled to uniform azimuth spacing to allow

[10] DTI typically uses the RPC algorithm (see footnote 9) to estimate the sway of an array between pings.

efficient beamforming operations. The along-track position of each phase center is computed using the recorded ship GPS data[11]. Linear interpolation is used as needed and gaps in positions are filled with zeros. A Hann window is applied to the aperture. The images are then formed using FFTs over a selected aperture (the multi-ping beamformer). Finally, PGA is applied to the scene to correct the image for uncompensated motion and environmental effects.

Full-swath Processing

After a object has been successfully focused, the object-derived motion and phase corrections can be used to create a full-swath image. This process is shown schematically in Figure 2-39 and described as follows:

1. The yaw and sway estimates from the single object processing (above) are applied to the element I/Q data over their full range extent, rather than the "straightened" data. Since these are array motion estimates, this is a valid application of the estimates.

2. The element I/Q data are then partitioned into sub-swaths by range. Typically we created 500 m long sub-swaths. For each sub-swath a synthetic aperture is formed with length given by

$$L_{SS} = L_{OS} \frac{R_{SS}}{R_{OS}}, \tag{2-9}$$

   where L_{SS} is the aperture length of the sub-swath, L_{OS} is the aperture length of the object sub-swath, R_{SS} is the range to the center of the sub-swath, and R_{OS} is the range to the center of the object sub-swath. The sub-swath aperture length is proportional to range of the center of the sub-swath. Thus, the number of phase centers used in a sub-swath decreases proportionally to its mid-range value.

3. Each sub-swath is "straightened" with the assumption that an "object" is at the mid-point of the sub-swath. In order to minimize sensitivity to error, sub-swaths are defined so that the original object (Salmon or Bidevind) itself lies at the center of one of the sub-swaths.

4. The multi-ping beamformer is applied to each sub-swath synthetic aperture with uniform beam spacing. The resolution of each sub-swath image, and the energy therein, is roughly the same due to the scaling of each synthetic aperture length.

5. The sub-swath images are concatenated together to form a full-swath image in range and angle.

6. Azimuth is then interpolated from angle to distance.

[11] The first few images approximated the phase center spacing assuming a constant speed rather than using the GPS coordinates.

7. The phase errors from the object-driven processing autofocus are applied to each azimuth line. This is done rather that running autofocus on each sub-swath since there were no objects in any scene other than the initial object.

This process yields full-swath images that are wedge shaped and with constant resolution. Additionally, this technique can only be effectively applied to form images from the object range and closer, meaning if the object is at 2000 m, the full-swath image is 0-2000 m, even if data were collected from further ranges. This is not an optimal technique and future work with this type of data will include improvements to the processing.

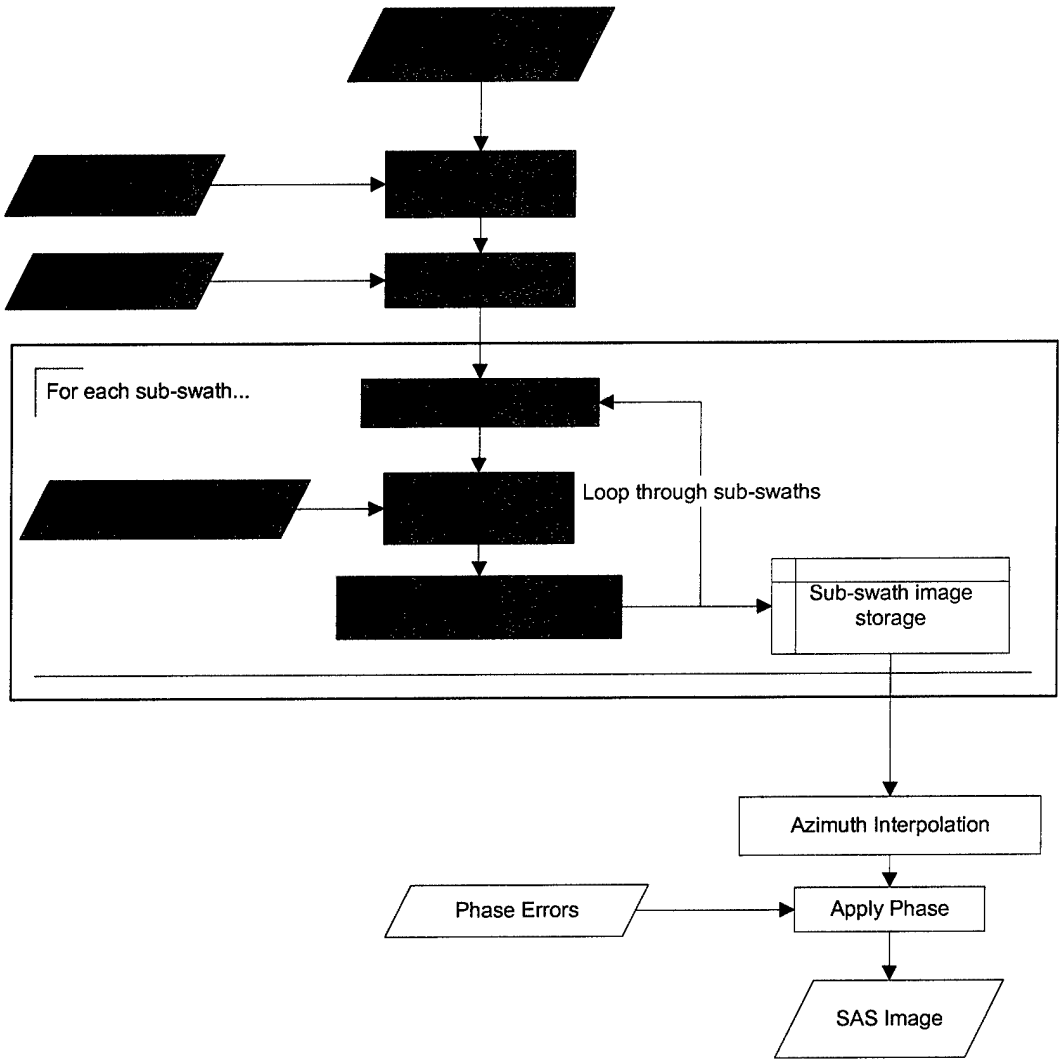

Figure 2-39. Schematic representation of full-swath processing for LRSAS.

Limitation to the Technique

The main limitation to the whole image processing technique described above (as per Figures 2-38 and 2-39) is the use of the ping-to-ping data from one object to estimate individual array element motion. This ping-to-ping limitation is not apparent in a system using a rigid array, such as is typically used in MCM, since the relationship of each receiver element to all the rest is known and therefore the ping-to-ping variations are used to estimate fewer parameters. For the flexible array used here, we would require more information about the array shape than the current system can provide. Such information could be recorded using motion sensors, such as heading and depth sensors, located within the array itself. Additionally, if the acoustic returns change in nature or structure from ping-to-ping, e.g., through environmentally induced fading, the pings become difficult to register. The lack of array element motion and ping-to-ping structure changes have an effect of summing less than the full synthetic aperture planned from the program onset. The initial intention was to form images with at best 2 m resolution and at worst 10 m resolution. In this trial we were unable to sum together as many pings as required to achieve 2 m resolution, although in some cases 10 m resolution was possible (see Section 3). A future system with array motion sensors should not have this problem.

2.5 Advanced Analyses Processing

In order to demonstrate the usefulness of the system, we conducted analyses on the SAS images we created (method in Section 2.2, results in Section 3.2). Some of the analyses required additional processing. This section describes the additional processing required for the clutter analysis (Section 2.5.1) and frequency response analysis (Section 2.5.2).

2.5.1 Clutter Analysis Processing

Clutter is generally defined as anything that is not a target. This can be further divided into geologic clutter (i.e., natural features of the area, such as rocks, ridges, mud, etc.), target-like clutter (i.e., objects that are similar to the target in question), and man-made clutter (may or may not look like the target in question, but is definitely not natural). Our analyses touch upon all of these. Additionally, one object, the Bidevind, is treated as a target, as target-like clutter, and as man-made clutter depending on the circumstance. A portion of our clutter analysis has been separated out as frequency response analysis and is discussed in those sections (2.5.2, and 3.4)

The first analysis is to determine the nature of the data, i.e., have we imaged the sea floor, the sea surface, noise, etc. For this aspect, the processing consisted of simulations. Using PCSWAT, the sonar characteristics, the average depth of the region, and a sound velocity profile we collected while at sea, we calculated the ray trace and the transmission loss for sound in this region.

The other aspects of our clutter analyses required no special processing. The analyses themselves will be discussed in Section 3.3.

2.5.2 Frequency Response Analysis Processing

A potential tool for target classification is the frequency dependence of an object's response, particularly at the lower frequencies where a target structure may resonate. The two objects showed distinct spectral responses over the whole band, indicating the feasibility of this approach. While the Seahawk system is meant to operate at long ranges and at resolutions larger than the average mine, a frequency signature could still be detectable at the near ranges of the system.

A small part of our tasking was to explore the spectral characteristics of clutter with an eye to MCM usage. The frequency band of the Seahawk system is 1.2 - 1.6 kHz. This is a narrow frequency band, thus, unless we were lucky, it will only show the potential of frequency analysis. The processing of the time domain data into frequencies is a straight forward Fourier transform in the range (fast-time) direction for each azimuth position. This is preferably carried out on SAS images, but similar responses exist in standard side-look sonar processed data. Thus we processed both types of data, depending upon which data sets looked promising for clutter.

Ground truth did not exist for any of our data collection sites nor did we collect data against known mine or mine-like target fields, so we cannot be certain that there was any mine-sized object in the data. The Bidevind site, since it is the wreck of a ship carrying cargo and known to be broken in two, is likely to have meter-ish sized objects. The strength of sonar returns of such small objects will likely make only the near range data collection runs useful for mine-like study. An analysis of the frequency response of the Ex-USS Salmon will yield another point on a clutter study, albeit one that was not likely to be mistaken for a mine. Comparisons of the Bidevind and Salmon may also indicate the possibility of using frequency analysis for ASW uses as well. Section 3.4 displays and discusses our results.

3. RESULTS AND DISCUSSION

In this section we display and discuss the results of the sea trial. Section 3.1 summarizes the sea trial and the data collected. Section 3.2 reveals the SAS processed runs (Appendix D contains the SLS imagery for data sets we lacked funding to process) and the run specific details. Analyses of these data are in Sections 3.3 (clutter), 3.4 (frequency response), and 3.5 (target). A discussion of the processing method, results, and possible uses for the system are in Section 3.6.

3.1 Trial Summary

In October 2003 we went to sea to validate with the Seahawk out to 5 km ranges. We have summarized the overall results of this sea trial in this section. In particular, Section 3.1.1 describes the trial and Section 3.1.2 delineates the runs and SVPs collected.

3.1.1 Overall Summary

The mobilization for the sea trial began on 2 October 2003; we left port on 7 October; returned to port 10 October; and all equipment was removed from the vessel on 11 October. We collected a total of 19 full runs and 5 partial runs of acoustic data from two sites. All data were collected during daylight hours to allow for visual marine mammal observations. The weather was clear and wind low from mobilization until 10 October. By mid-day 10 October the wind speed was up to ~20 kt, the water clearly sea state 4 or 5, and all weather forecasts indicated that this weather would continue for several days. Due to the weather conditions and equipment problems described below, we declared the trial completed and returned to shore.

Mobilization

The mobilization went smoothly[12]. The M/V Atlantic Surveyor, owned by Dive Masters, Inc. of Toms River, NJ and docked in Pt. Pleasant, NJ, was our base of operations. This 110 ft (33.53 m) vessel had 56 ft by 24.5 ft (17.1 m by 7.5 m) of deck space available to us (more information about the vessel can be found in the trial plan in Appendix A). Aside from the winch and handling system and a generator, two portable laboratories, 8 ft x 8 ft (2.4 m x 2.4 m) and 8 ft x 20 ft (2.4 m x 6.1 m), were placed on the deck for workspaces. The smaller one housed the Seahawk amplifiers and control units. The larger one was workspace for DTI staff and L-3OS tool storage. It took less than 24 hours of working time for L-3OS personnel to install and test the Seahawk. DTI equipment set-up was less than 8 hours.

During the mobilization at the dock, the sonar could not be tested by actively pinging. On the afternoon of 7 October, L-3OS conducted this testing during transit to the Salmon site when the vessel was further than 15 nm from shore and the mammal observers indicated that the region was clear of mammals. All tests indicated that the sonar system was operating normally.

[12] In fact, the vessel master commented that "this was the easiest mobilization" he had ever done.

At-Sea Days

The full trial began on the morning of 8 October. Two days were spent at the Salmon site. Section 3.1.2 lists the sonar runs and auxiliary data collected. We laid our pinger at 39° 42.32'N, 72° 18.19W (latitude, longitude), which was approximately 0.22 km north of the expected location of the Salmon. The Salmon was detected in the Seahawk passive bearing-time display for all runs against the Salmon. On the first day, eight runs were collected against the Salmon and two of clutter. On the second day, four full runs and four partial runs against the Salmon were collected. Of the partial runs, two were aborted due to marine mammals/sea turtle sightings (marine mammal observation logs can be found in Appendix C), and the other two ceased due to equipment failure, namely the telemetry from the sonar to the topside computers ceased. Each day we collected data from three XBT drops, and on the first day we made an XSV drop.

Upon the end of data collection at the Salmon, we chose our second target to be the Bidevind since it was more likely to be confused with a bottomed submarine and thus of greater interest. On the morning of 10 October, we began work at the Bidevind site[13]. We did not lay down the pinger at this locale since we flooded it during a re-deployment at the Salmon. Additionally, subsequent study of the receiver electronics indicated that the pre-amplifiers cut-off the receiver frequency before the pinger transmit frequency. We completed five runs at this site and aborted several attempts at runs (never turned on the sonar) due to inability to operate vessel at low speeds in the swell. All runs were with the source level set 6 dB down from the maximum (see below). One XBT and one XSV drop were made at this site. The weather began fairly calm in the early morning, but quickly worsened. Our last run completed shortly before 1300, at which time we called an end to the trial. Many of the runs were rough since we were quartering and this required the Atlantic Surveyor to travel a little faster than the planned 3 kt. Thus the sonar and arrays were subjected to more motion for this day than previous days. We were interrupted for approximately two hours on this morning due to the troubles of a small fishing vessel in the area, to whom we eventually supplied fuel.

Hardware Issues

This trial was the first time in several years that the Seahawk system was operated at sea. While most sub-systems could be tested in the lab, not all parts could be tested and some aspects of the sub-systems that could be exercised could not be operated as they would be at sea. Additionally, the improvements made for SAS usage could not be fully tested, e.g., the PingNow circuit could only be operated with a dummy load rather than the actual transmitter. Thus it is not surprising that in this first test of the full system there were some

[13] We wish to note that the latitude and longitude for the Bidevind from numerous wreck databases, including AWOIS, yielded no wreck. Many of the wreck databases additionally give the coordinates for the Bidevind in Loran C. The Loran C coordinate system tends to be used by fisherman who are very much aware of the locale of wrecks due to the presence of fish and thus their livelihood. We found the Bidevind at the Loran C coordinates. It was suggested that the latitude and longitude values were a poor transformation from the Loran C values.

failures in sub-systems. While none of the failures were catastrophic, many did lead to additional post-trial work.

This trial had no requirement to process the data in real time, thus the sonar data were recorded to disk and then to DVD. DTI received the DVDs from L-3OS hours after the data were originally recorded. While the first few data sets could be read, it became clear that there was a problem with several data sets. Before our first run on 9 October, the problem was identified as a lack of a PingNow bit in the acoustic data. We tested the active pinging to confirm this and we concluded that the PingNow circuit had failed. L-3OS suspected that the circuit vibrated loose during the runs. Whether this were the case or not, to repair the PingNow circuit the sonar would need to be brought to shore. It might be repairable there, but this was not certain. L-3OS believed that they could re-insert the PingNow bit after the trial, so we continued with the trial without the PingNow bit placed in the data. This meant that only the first two or three data sets could be truly studied onboard. L-3OS was able to re-insert a PingNow bit after returning to California, albeit at a slightly degraded accuracy.

There were three other problems with the system that became apparent during these two days. The first has been alluded to above in the cause for partial runs. At the end of 9 October, the uplink ceased repeatedly, causing us to terminate runs early. Again vibration was suspected. We reduced the source level by 6 dB; this allowed us to continue operating for the remainder of the trial. Since our SNR simulations (Section 2.2.3) indicated that a 6 dB reduction was allowable for ranges to 5 km and that was as far as we had planned to collect after this stage, this reduction of source level would not stop the trial. The second problem was that the PRI was not stable and was too long (see Figure 3-1). This problem was suspected during the trial because the each ping could be heard through the ship's hull and the time between pings timed by hand was long, however, it was not confirmed until the PingNow bit was replaced in the data and the PRI could be measured. These longer PRIs meant that all the data collected were undersampled in along-track position. All the imagery is affected by this, namely grating lobes will appear in the data. It also meant that we lost any ability to use any redundant phase center algorithms for motion estimation. Third problem was confirmed on the morning of the 9th. There had been miscommunication between L-3OS and DTI before the trial and the frequency of the deployed pinger was just out of the receive band of Seahawk because of a cutoff frequency in the pre-amplifiers of this prototype system, even though the receivers themselves could hear the signal. This meant that we did not have a point target in the field and thus would have to rely upon the main target for SAS focusing. We wish to iterate that the need of the pinger as a focusing aid is for this trial due to the lack of array motion sensors; a deployed system would not need a point target.

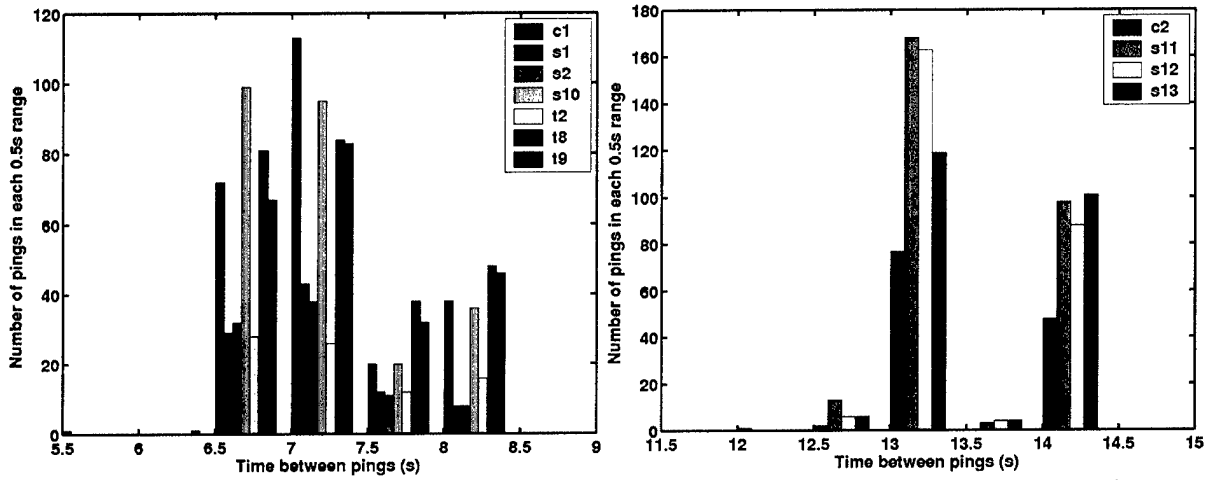

Figure 3-1. *PRI stability.* These histograms show the frequency of the time between pings in 0.5 s bins. The left plot contains data from seven runs with the PRI nominally set to 6 s. Note that the majority of ping intervals are either 6.5-7 s or 7-7.5 s (the position of the bars only denote the half second bin, not a precise value). The right plot contains data from four data sets where the PRI was nominally set to 12 s. These pings tended to be either 13-13.5 s or 14-14.5 s. The lack of stability and long time between pings means that all sonar data were undersampled along-track. The legends refer to the run number as found in Table 3-1.

After the trial, L-3OS assessed the data and system. In addition to the aforementioned problems, they found three others. A switching transient preceded each transmit pulse and the pulses were approximately 80 ms longer than anticipated. These were believed to be due to the differences between the dummy load used to tune the pulses and the actual load. These transmit waveform alterations had little effect on the data. The depth sensor in the towbody exhibited a non-linear error in tracking cable scope from the winch. This did not effect processing and repair is simply recalibration for future trials. The compass in the towbody exhibited an 8.4° error in the east-west direction. This was noted in the passive trial where the error was larger and slowly varied with heading. The error acted like an offset, so the small changes from the mean heading on a given straight track run should be accurate, although the mean heading will be incorrect. If we were to use the towbody heading in the SAS processing, the mean heading would be removed, so this has no effect on SAS processing. Replacing the compass is the easiest fix for future trials.

Since this was the first SAS test with Seahawk and the first use of Seahawk in several years, none of these problems should be considered a showstopper in terms of using SAS with the system. All equipment problems are repairable and the equipment can be made more robust. However, they do have an effect on the post-trial processing in that time was required to compensate for the problems that could have been used to process more data were the problems nonexistent.

3.1.2 Data Collection Summary

As mentioned above, we collected numerous runs at the Salmon and Bidevind sites. Table 3-1 lists these runs with a few pertinent details. Copies of the log sheets are in Appendix C. For the majority of the runs, the ship tracks were recorded. Figure 3-2 shows the recorded ship tracks and location of the Salmon and pinger for the two days at the Salmon site. Figure 3-3 is a similar plot for the Bidevind site.

Table 3-1. Summary of recorded runs. Only a few parameters are shown; the full log sheets are in Appendix C.

Run No.	CPA†	SL gain	PRI	Pulse length	Boat speed*	Xmit direction	Water depth*	Time length	Heading*
8 October 2003									
S1	0.5 km	0 dB	6 s	0.25 s	3.0 kt	Port	350 ft	12 min	227°N
S2	0.5 km	0 dB	6 s	0.25 s	3.0 kt	Port	360 ft	12 min	109°N
S3	0.5 km	0 dB	6 s	0.25 s	3.0 kt	Port	365 ft	11 min	340°N
C1	clutter	0 dB	6 s	0.25 s	3.0 kt	Starboard	360 ft	30 min	210°N
C2	clutter	0 dB	12 s	0.5 s	3.2 kt	Port	375 ft	30 min	20°N
S7	0.5 km	0 dB	6 s	0.25 s	3.1 kt	Omni	360 ft	30 min	105°N
S8	4.5 km	0 dB	6 s	0.25 s	2.9 kt	Port	375 ft	35 min	350°N
S9	4.5 km	0 dB	6 s	0.25 s	3.2 kt	Port	305 ft	35 min	220°N
S10	4.5 km	0 dB	6 s	0.25 s	3.1 kt	Port	375 ft	30 min	101°N
S11	8.0 km	0 dB	12 s	0.5 s	3.0 kt	Starboard	393 ft	62 min	275°N
9 October 2003									
S12	8.0 km	0 dB	12 s	0.5 s	3.0 kt	Port	395 ft	60 min	338°N
S13	8.0 km	0 dB	12 s	0.5 s	3.2 kt	Port	285 ft	55 min	230°N
S14	2.5 km	0 dB	6 s	0.25 s	3.5 kt	Port	378 ft	15 min	114°N
S15	2.5 km	0 dB	6 s	0.25 s	3.5 kt	Port	373 ft	15 min	340°N
S16	2.5 km	0 dB	6 s	0.25 s	3.4 kt	Port	325 ft	8 min	220°N
S16a	2.5 km	0 dB	6 s	0.25 s	3.4 kt	Port	325 ft	1 min	220°N
S16b	2.5 km	–6 dB	6 s	0.25 s	3.5 kt	Starboard	325 ft	23 min	222°N
S17	1.0 km	–6 dB	6 s	0.25 s	5.0 kt	Port	355 ft	6 min	44°N
S15a	2.5 km	–6 dB	6 s	0.25 s	3.3 kt	Port	343 ft	8 min	160°N
10 October 2003									
T1	0.5 km	–6 dB	6 s	0.25 s	3.0 kt	Port	190 ft	10 min	335°N
T2	0.5 km	–6 dB	6 s	0.25 s	3.4 kt	Port	190 ft	10 min	210°N
T8	4.0 km	–6 dB	6 s	0.25 s	3.0 kt	Starboard	210 ft	35 min	39°N
T9	4.0 km	–6 dB	6 s	0.25 s	4.5 kt	Port	190 ft	30 min	275°N
T14	2.5 km	–6 dB	6 s	0.25 s	3.3 kt	Port	190 ft	20 min	260°N

†Nominal distance to target. For fields of no known target, i.e., clutter, this has no meaning.

*These values were recorded in the wheelhouse from the vessel navigation equipment at the beginning of each run.

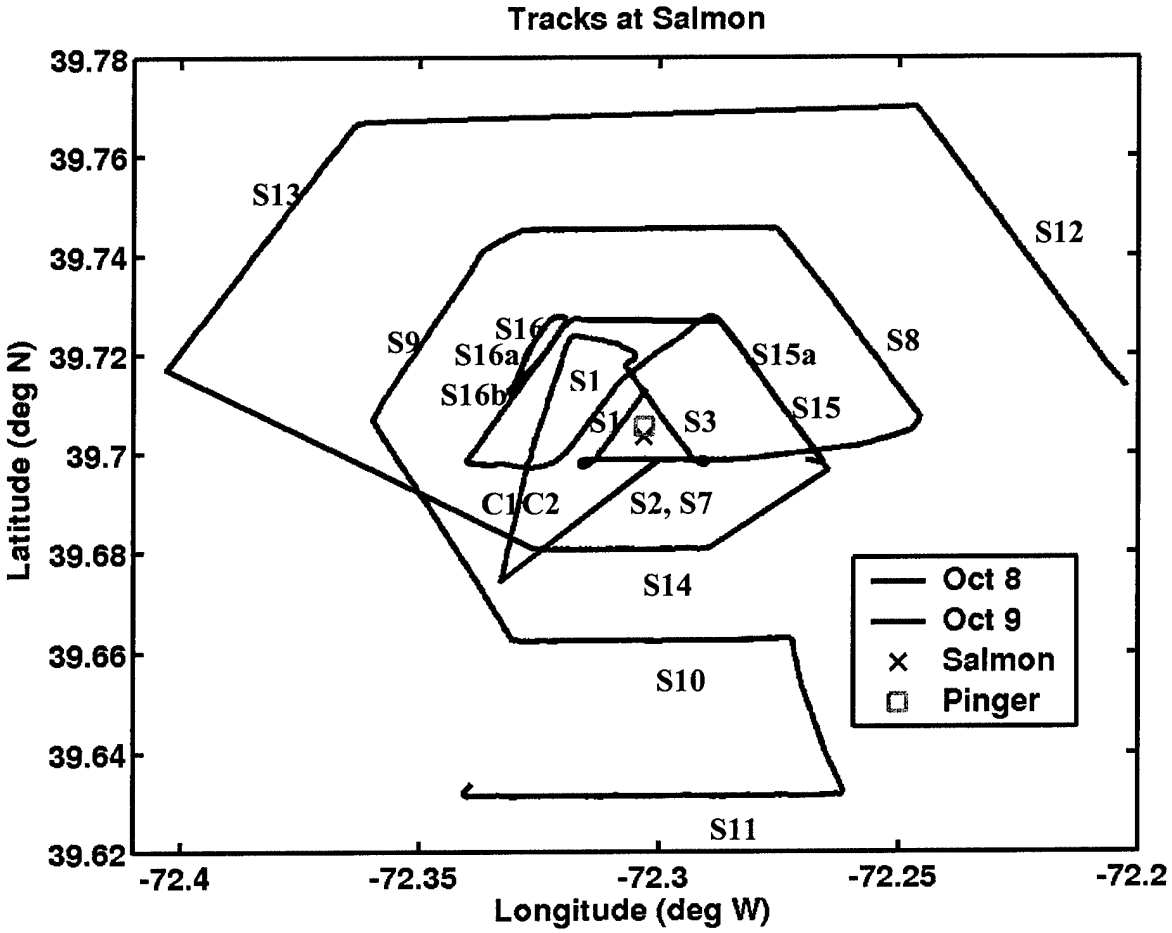

Figure 3-2. Salmon site ship tracks. These are the recorded ship tracks for October 8 and 9. The positions of the Salmon and the pinger are marked. The run numbers are labeled. Parts of Run S7's ship track were not recorded. The recorded track is typically longer than the recorded sonar data.

Early analysis of the data indicated that the PingNow circuit worked during runs S1, S2, and part of S3. L-3OS re-inserted the bit into the data after the trial based upon the direct blast. Any processing of the S1 and S2 data sets used the data with the Seahawk inserted PingNow bit. Processing of all other data sets used the post-trial PingNow bit.

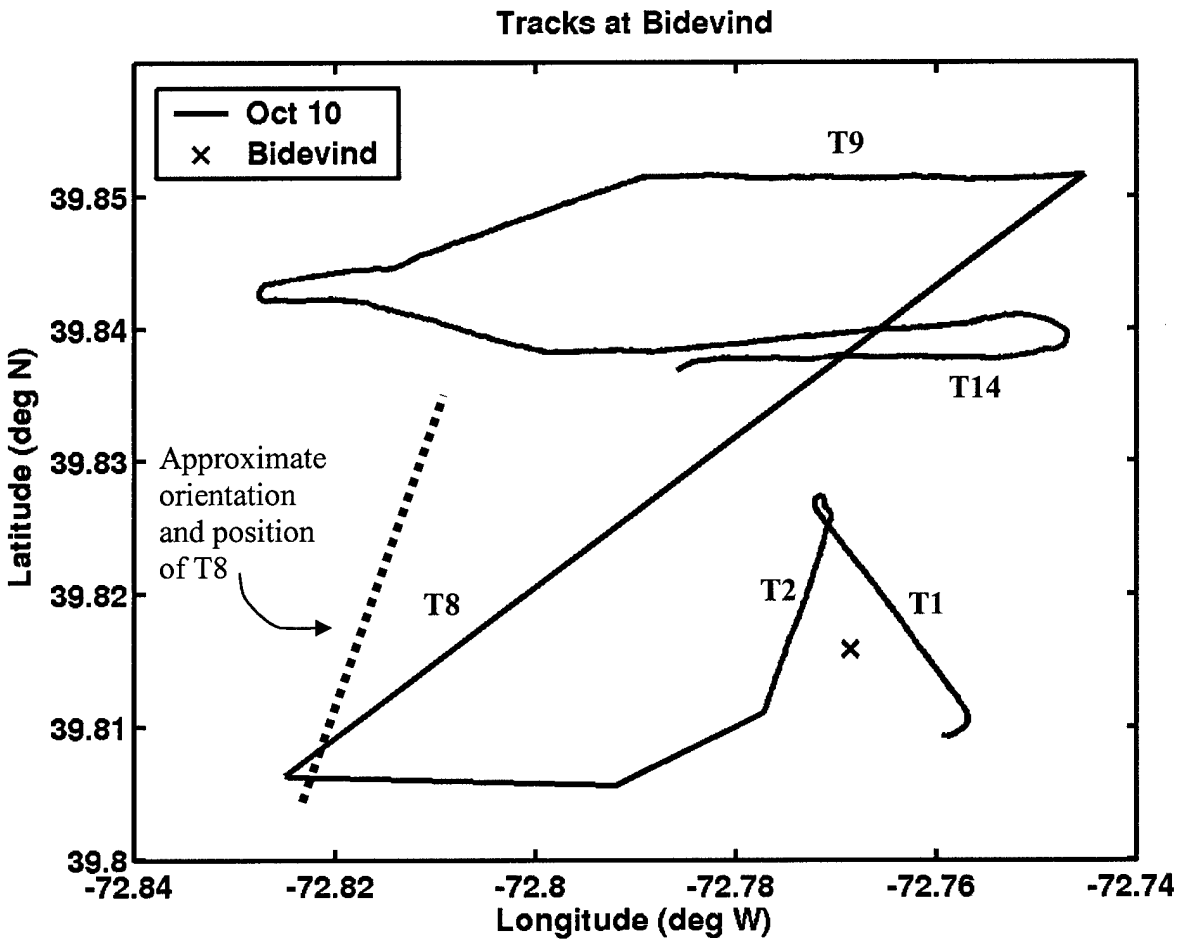

Figure 3-3. Bidevind site ship tracks. These are the recorded ship tracks for October 10. The position of the Bidevind is marked. The run numbers are labeled. The Run T8 ship track was not recorded, but an approximation is shown. The recorded track is typically longer than the recorded sonar data.

Besides the sonar and non-acoustic data collected on Seahawk, we measured the temperature and sound velocity profiles. Table 3-2 lists the XBT and XSV drops made. Figure 3-4 shows the measured (from XSVs) and calculated (from XBTs) SVPs for all three days. The two XSV drops were made immediately after XBT drops and therefore in very similar locations. Variations between these XSV-XBT pairs of SVPs are due to measurement uncertainties and possible non-constant salinity for the SVP derived from the XBT drops. The variations within a day and from day to day are probably due to a combination of time of day and location of the drop. A comparison of our measured SVP and the average SVP for the month of October, which we used in pre-trial simulations, is in Figure 3-5. The measured profile is both faster and slower than the monthly average profile, but they have a similar general shape. The thermal layer at ~40 m depth creates a sound channel from the sea floor to 40 m depth. These measured SVPs were useful for the clutter analysis discussed in Section 3.3.

Table 3-2. XBT and XSV drop summary. The skipped numbers are due to computer reboots between drops.

Drop No.	Drop Type	Serial No.	Time	Date	File name
1	XBT	319723	0820	10/8/03	T6_00001
3	XBT	319727	1230	10/8/03	T6_00003
4	XSV	43011	1232	10/8/03	S2_00004
5	XBT	319731	1703	10/8/03	T6_00005
6	XBT	319732	0915	10/9/03	T6_00006
7	XBT	319728	1215	10/9/03	T6_00007
9	XBT	319724	1741	10/9/03	T6_00009
11	XBT	319733	0747	10/10/03	T6_00011
12	XSV	43012	0748	10/10/03	S2_00012

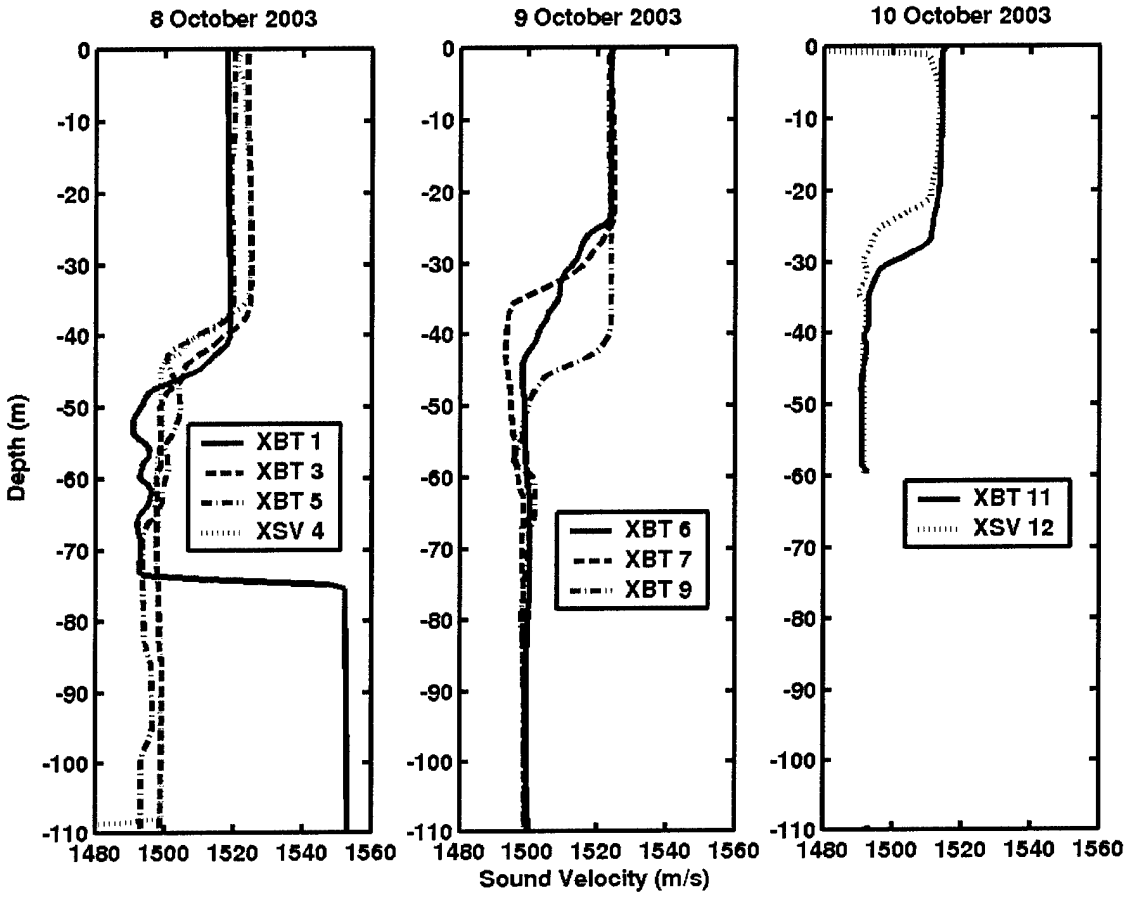

Figure 3-4. Sound velocity profiles. The three days of SVP measurements (from XSVs) and calculations (from XBTs). There was a user error during the first XBT drop causing the apparent increase in the sound velocity at ~75 m depth. In general the variations are due to time of day and location variations, although the assumption of a constant salinity may be incorrect. The third day was in a shallower region.

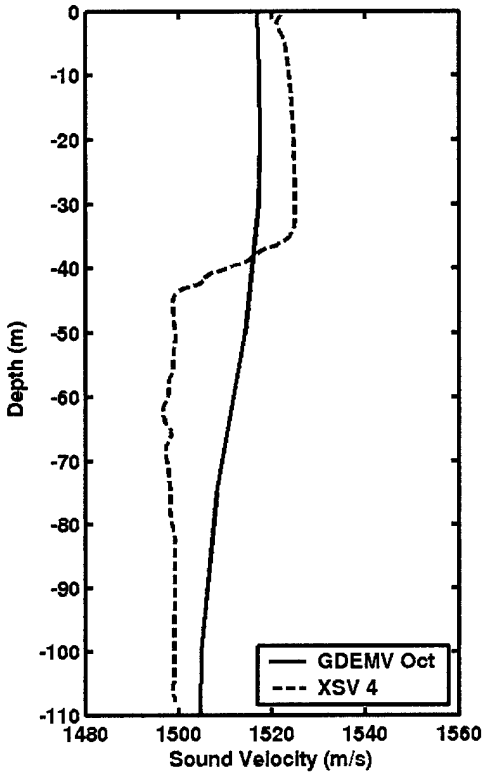

Figure 3-5. Averaged and actual SVPs. The GDEMV database SVP for the month of October for a 0.5° by 0.5° box centered at (39.5°N, 72.5°W) and XSV measurement on 8 October at ~(39.7°N, 72.3°W).

3.2 Imagery

Upon return from sea, we immediately embarked upon processing the collected data into SAS images. As discussed in Section 3.1, there were various issues to contend with (lack of native PingNow bit, undersampled data, etc.) which, combined with issues early in the program meant that we did not have enough funding to process all of the data sets. To insure that the most important runs were processed first, we prioritized the processing order. This priority list began with one image at the short range (500 m) of the Salmon, one long range (4.5 km) Salmon, one short range Bidevind, one long range Bidevind, and one extra-long range (8 km) Salmon. We were not able to process more than these, but these are a very good cross-section of the capabilities of the system. With these images we can demonstrate SAS capability at multiple ranges and indications of classification clues of a submarine versus a sunken freighter.

The data sets which we SAS processed are S2, S9, and S11 of the Salmon and T2 and T9 of the Bidevind (See Table 3-1 for key parameters of each run). These runs were not the only ones at each range. We chose these particular runs because they appeared to be best suited for processing with low funds. This determination was made by evaluating the SLS images and other knowledge we had about the run, e.g., T8 was a rougher ride than T9 so

we expected it to have larger motion and thus the motion estimation would be more difficult. The following sections show the imagery and recorded motion NAD for these five cases. An additional nine data sets were read and SLS images formed. These appear in Appendix D and demonstrate the richness of the collected data. Figure 3-6 is a schematic of the tracks for S2, S9, and S11 to orient the reader. Figure 3-7 is for runs T2 and T9.

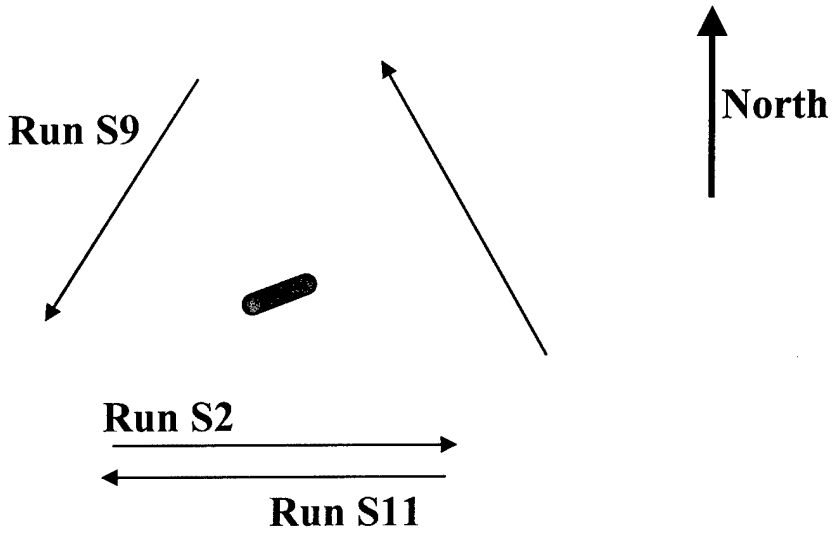

Figure 3-6. Schematic of SAS processed Salmon runs. All three runs were at different ranges. The orientation of the Salmon is approximated by the cylinder as best as we can determine from the collected data.

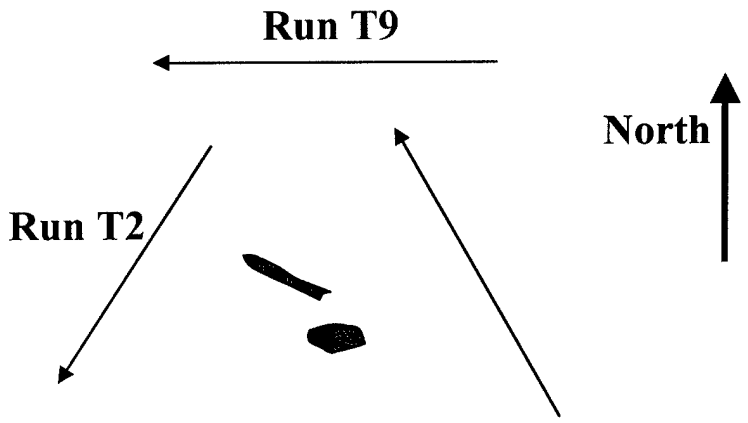

Figure 3-7. Schematic of SAS processed Bidevind runs. The two runs were at different ranges. The orientation and shape of the Bidevind is approximated as best as we can determine from the collected data.

3.2.1 S2: Salmon at 500 m

This was the first data set we SAS processed. Due to the short range, the returns are most likely direct path returns. Thus we did not expect these data to be strongly affected by multipath or other environmental issues. The motion is shown in Figure 3-8. In order to understand the scene, we produced a broadside SLS image, Figure 3-9. The Salmon is at ~500 m range and at 500-600 m along-track. The size and shape of the Salmon indicate that Seahawk did not suffer from excessive yaw during the 90 pings. The bright returns at constant range in the first 100-200 m are the first bottom and surface bounces. There is another object at ~2700 m range. Other clutter issues, such as the bright and dark patches are discussed in Section 3.3.

This data set was benign, motion wise, as seen in Figure 3-8. This was the only SAS processed data set in which the PingNow circuit operated during this run, thus we expect no residual phase errors from the ping finding process. The SAS imagery processing, in this case, did not use the yaw and sway estimations or compensations described in Section 2.4 except for autofocus. We processed this data set at five different aspect angles, 36°, 12°, 0°, –12°, and –24°. Figure 3-10 contains these five SAS images produced from 5 pings each and each image achieved ~6.5 m resolution. However, while the motion was fairly benign, it was large enough (~12° peak to peak deviations in heading) that the motion estimation method available to us at the time (only autofocus since this was the first data set) rendered larger ping sums of no advantage. Proper instrumentation of the array, i.e., motion sensors, would alleviate this problem in the future. In the figure, we can see that the Salmon retains the same basic shape and structure throughout the aspect rotation.

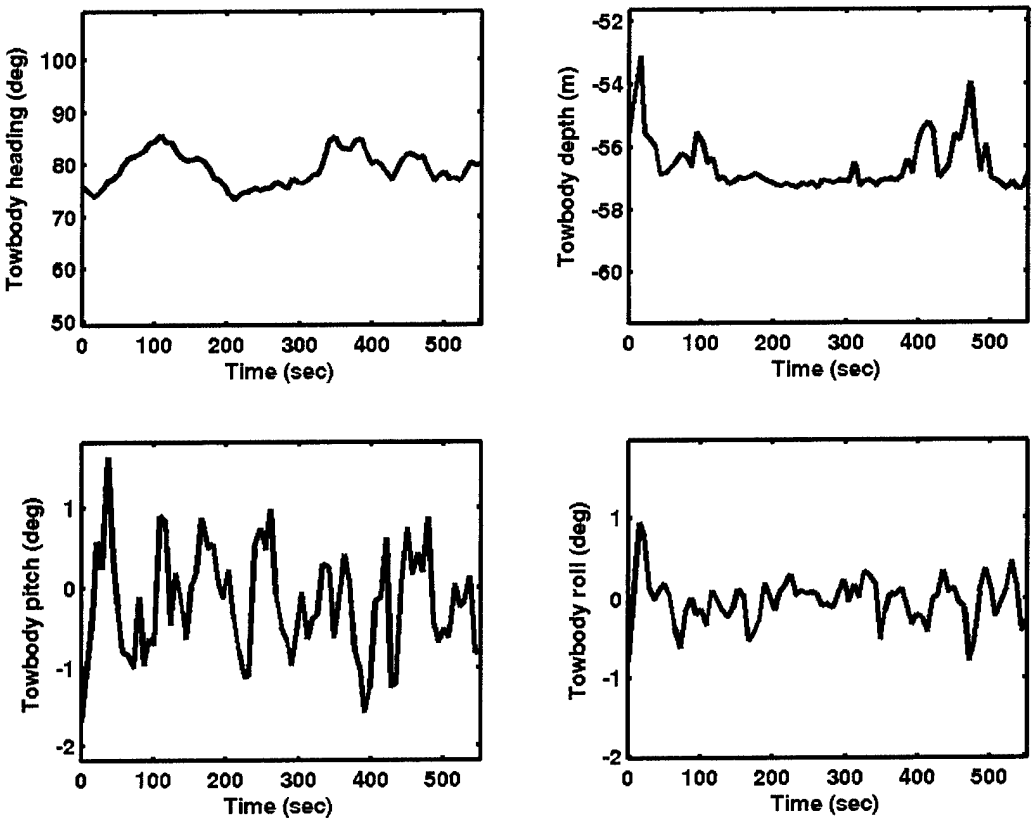

Figure 3-8. Run S2 towbody motion. The heading, upper left, was smoothly varying over ~12°. For the center of the run the depth, upper right, was generally smooth. The pitch, lower left, and roll, lower right, rarely varied ~1° off zero.

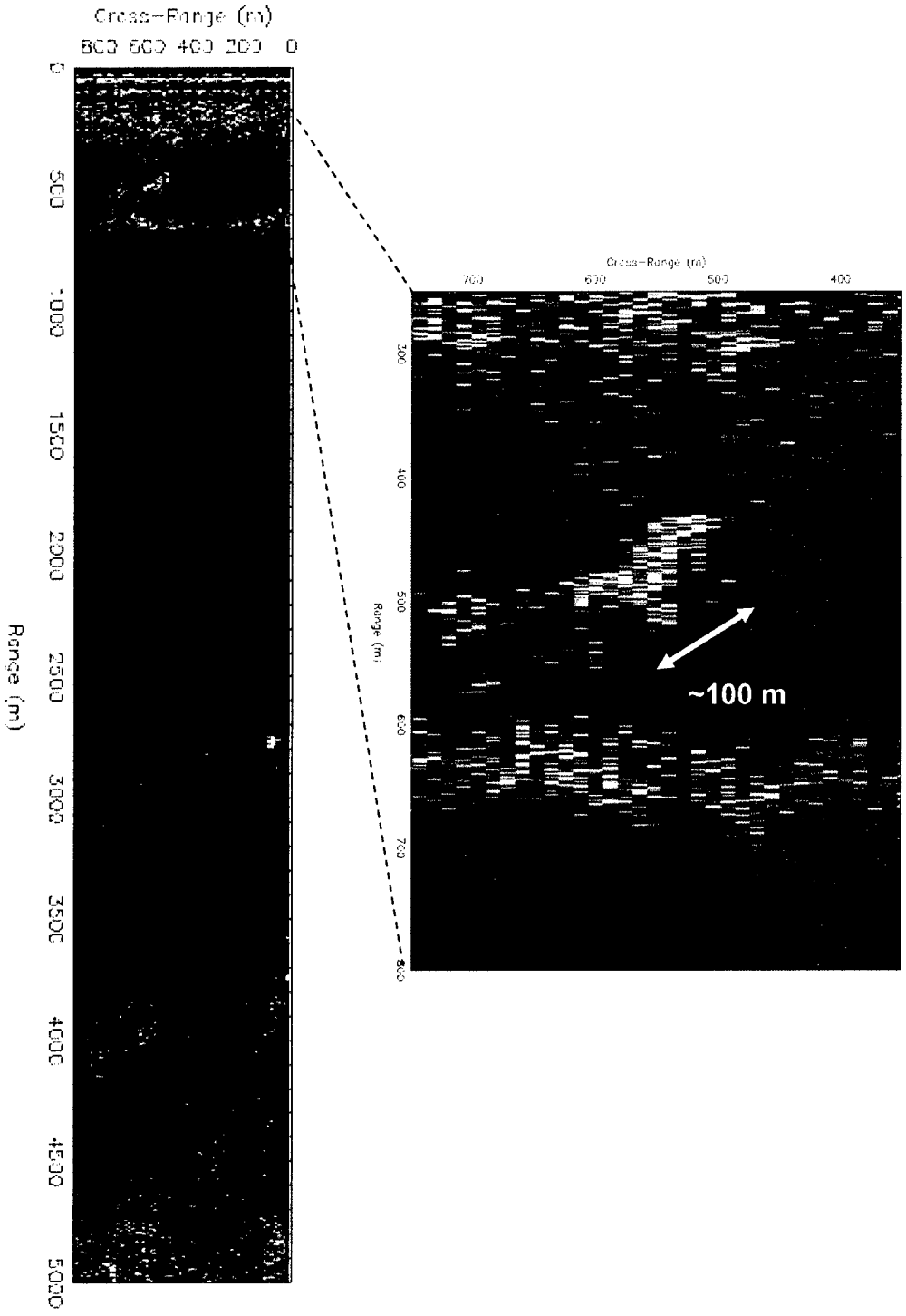

Figure 3-9. Run S2 SLS image. Left panel is full image, right is enlarged region around the Salmon. This range is short enough that the resolution of the SLS image is good enough to resolve the ~100 m long Salmon. The color scale of the image has a range dependent component to enhance the far range data.

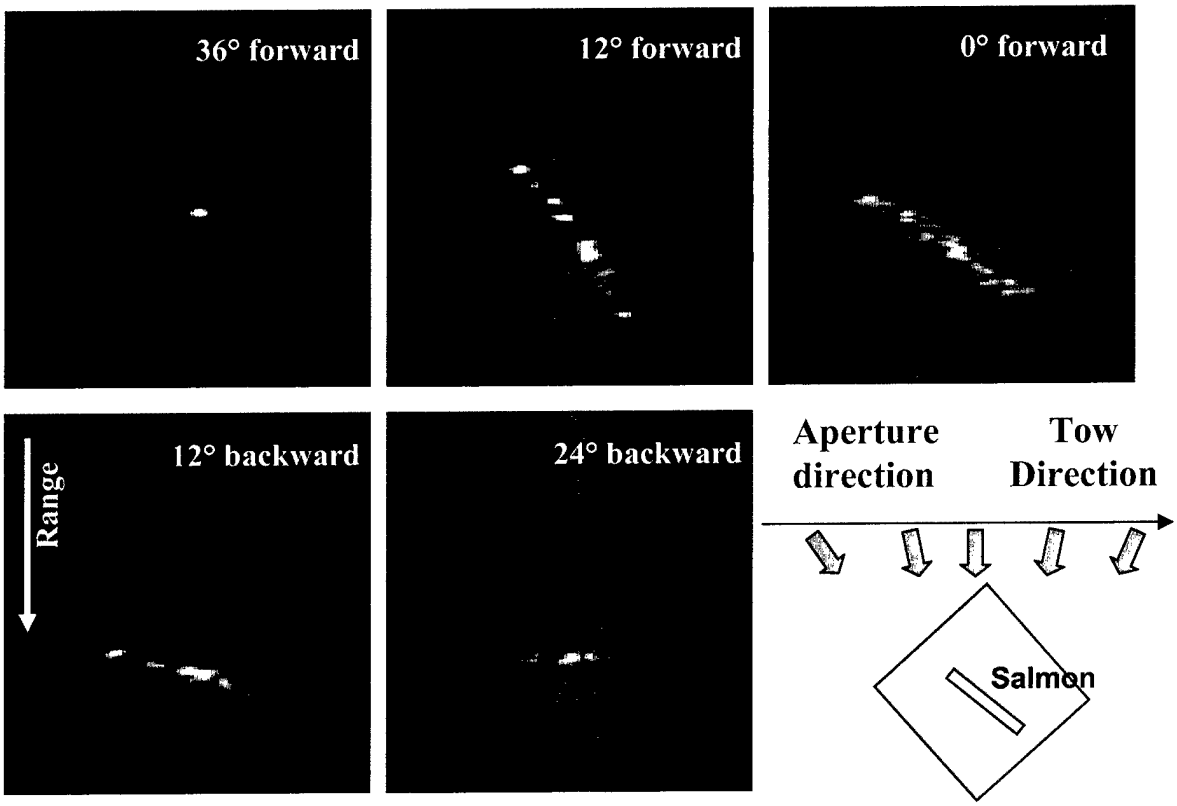

Figure 3-10. Five 5 ping SAS images of the Salmon at 500 m range. Each image is 200 by 200 m in size and from a different aperture angle. The diagram in the lower right schematically demonstrates the scene. The object clearly remains ~100 m long and ~10 m wide throughout the rotation.

3.2.2 S9: Salmon at 4500 m

In this run we viewed the Salmon from another direction. The recorded towbody motion is shown in Figure 3-11. In this case, the towbody clearly suffered from large variations in heading. Figure 3-12 is the broadside SLS image of the scene. The Salmon is the bright object at ~4.5 km. There is a second bright object at ~2.7 km, from which we did not collect a full aperture of data. There do not appear to be any other objects in the field. The on-off nature of the returns in this SLS image imply that the sonar system underwent significant yaw during the run. Due to these variations, only small numbers of pings could be processed at any given time with the motion estimation techniques available to us. At this range, SAS has an advantage over a single ping in terms of resolution. Figure 3-13 shows a single ping image, ~300 m resolution, and a 20 ping SAS image, ~15 m resolution, of the same area. For this range we were able to produce two 20-ping images and one 25 ping image (~12 resolution). Figures 3-14, 3-15, and 3-16 show these images with two different plotting schemes. One is a "top view" and the other a three-dimensional view to clearly demonstrate the dynamic range of the data. The Salmon is clearly far stronger than any background/bottom returns. For this run we produced a full-swath image, Figure 3-17, as described in Section 2.4. The wedge shape is an artifact of the processing

method. The motion estimates were from the 25 ping SAS image. The first pair of grating lobes from being undersampled along-track can be seen in this image. There is a hint of the second object at ~2700 m. The CPA for this second object was not included in the region processed, this it is weak and blurry in this image. There is no other clutter apparent.

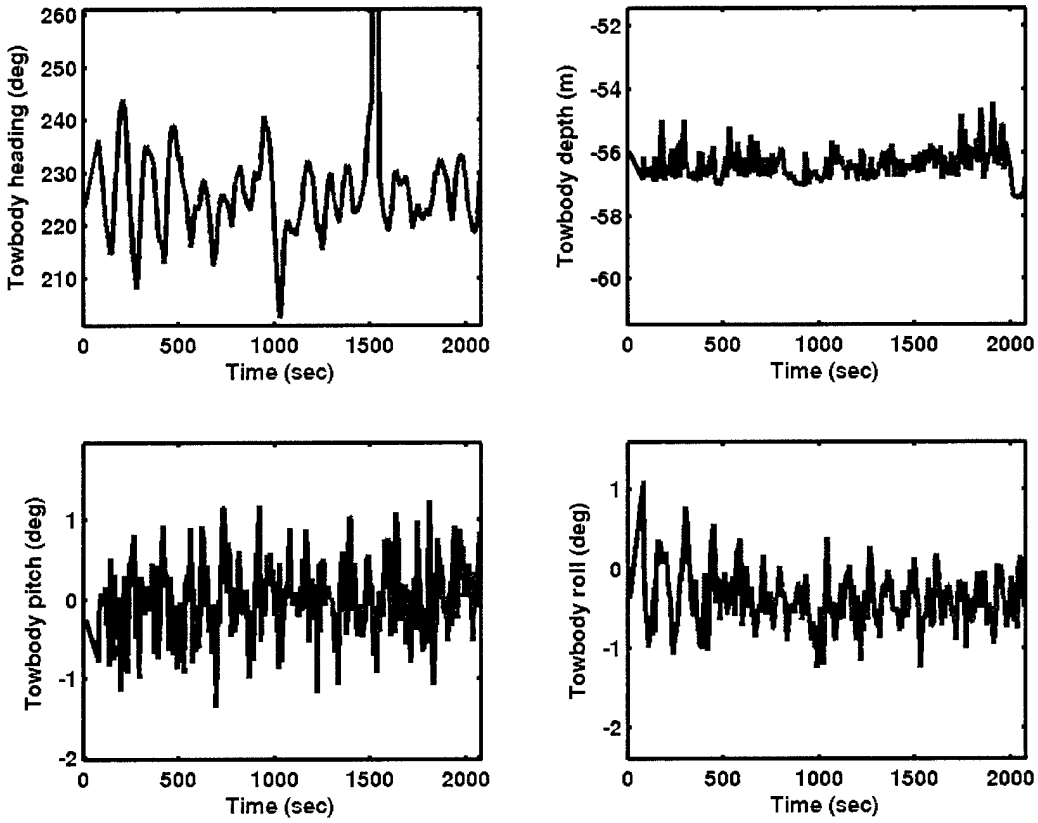

Figure 3-11. Run S9 towbody motion. While the depth, pitch, and roll changes remain relatively small, the heading varies up to 35° within 10s of seconds, aside from the compass glitch at ~1500 s. These large heading changes imply large yaw.

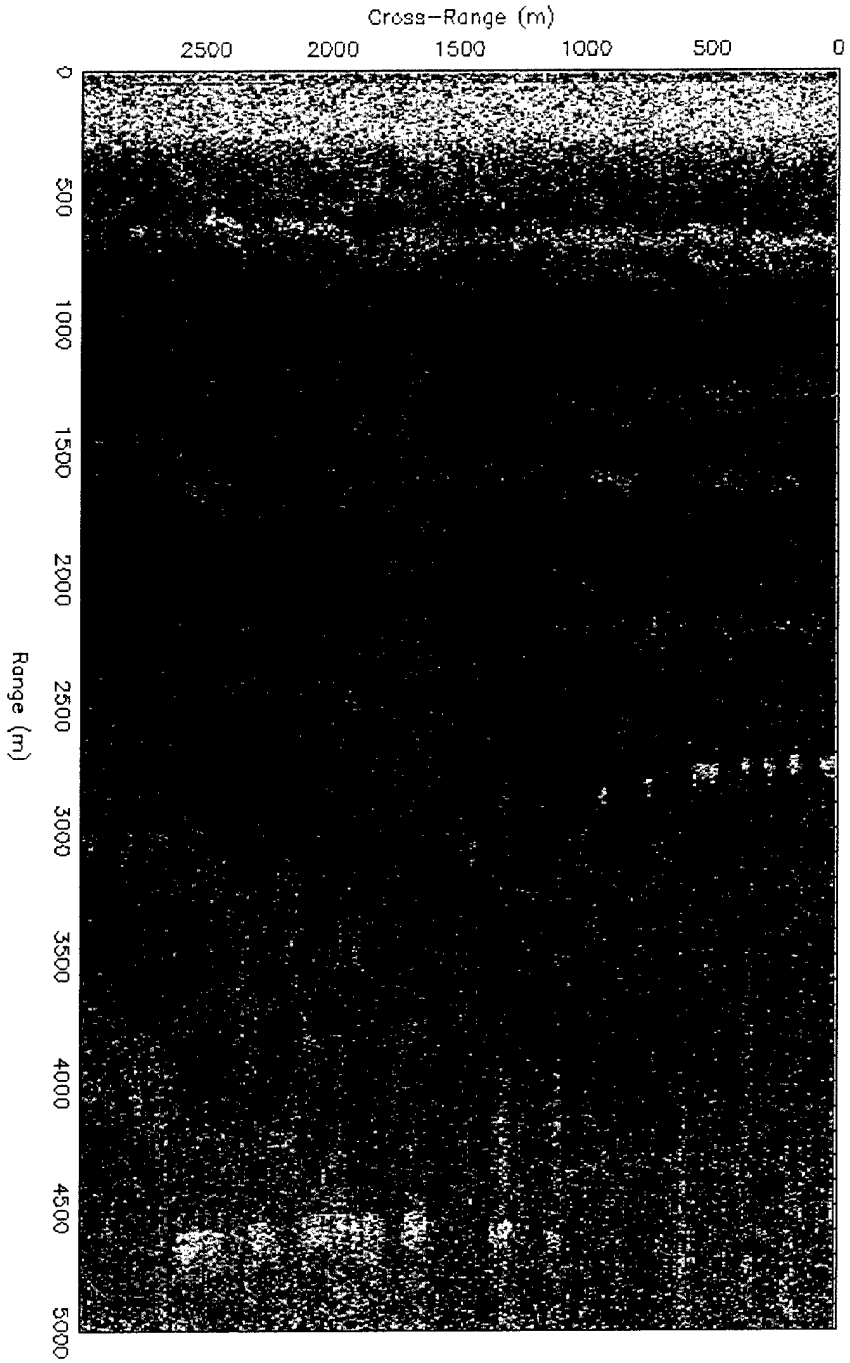

Figure 3-12. Run S9 SLS image. The Salmon is visible as the bright returns at 4500 m range. There is a second object at ~2700 m range in the early part of the run. The on-off nature of the returns, as well as the presence of the majority of the "smile" are effects of the large yaw changes the towbody underwent during the run, as noted in Figure 3-11. The color scale of the image has a range dependent component to enhance the far range data.

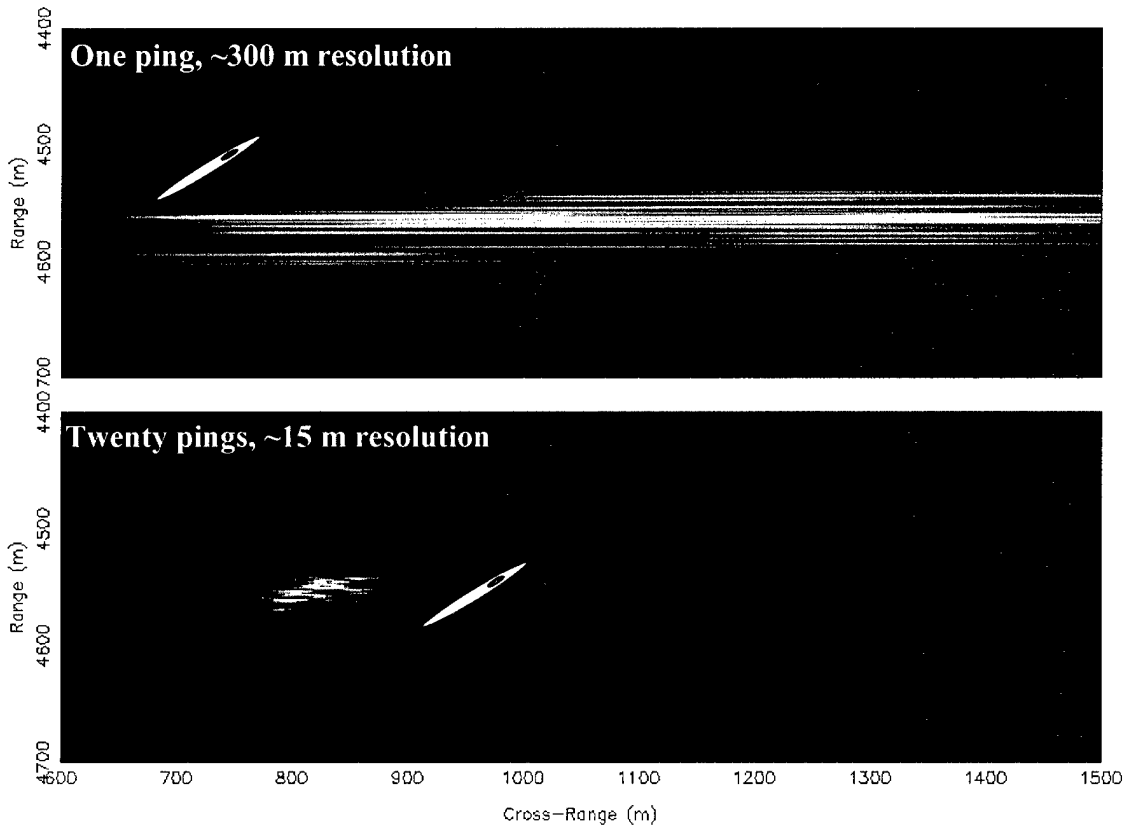

Figure 3-13. Run S9 single ping versus 20 ping SAS image. The upper panel is the single ping image and the lower panel is the 20 ping SAS image. The approximate resolutions are indicated. The cartoon sub, placed for reference, is the same length as the Salmon.

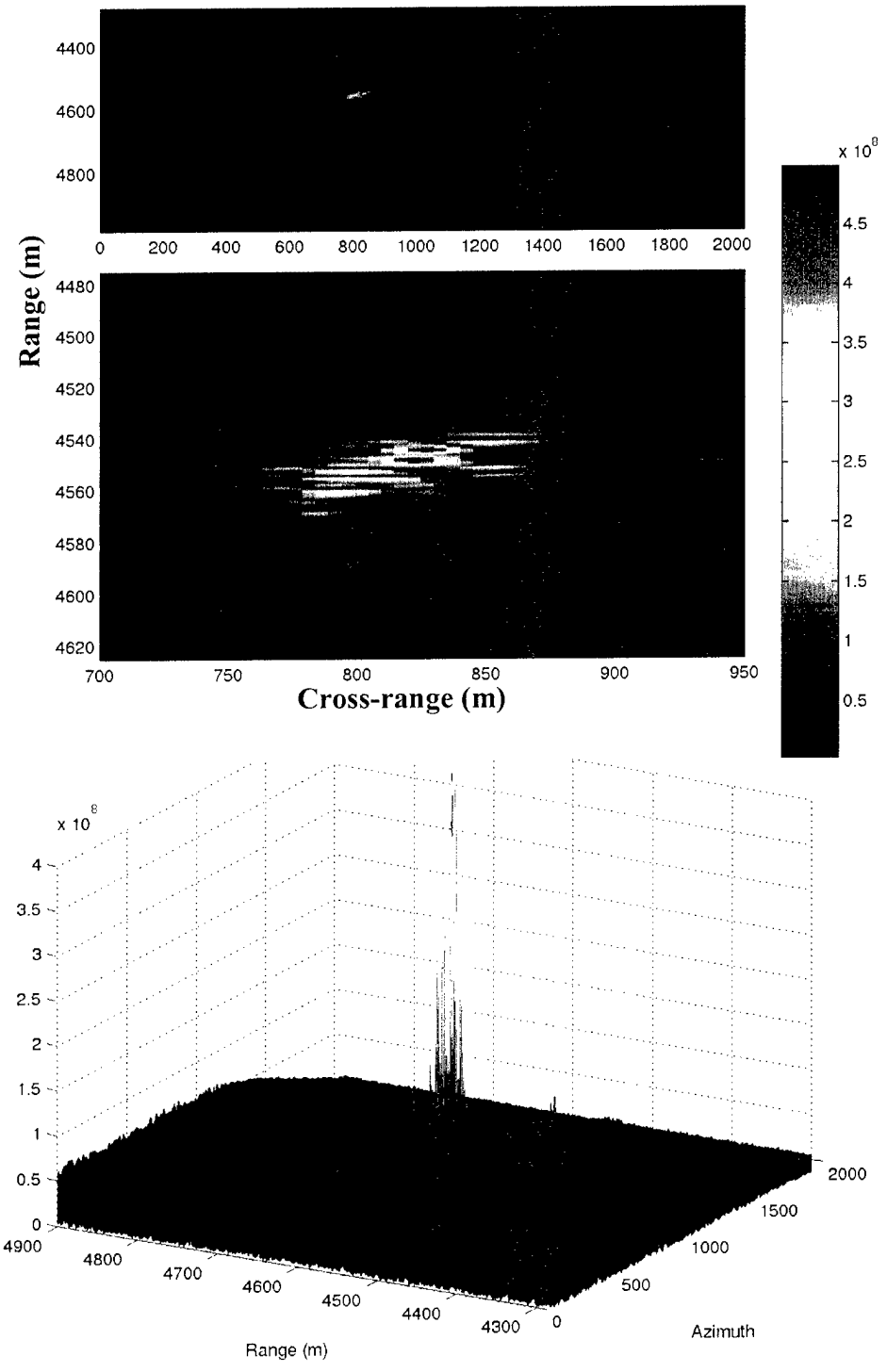

Figure 3-14. Run S9 20 ping SAS image at 11° forward beam. Top panel is a top view, with the center panel zoomed in to see the Salmon more easily. Bottom panel is a 3-D view to demonstrate how much stronger the Salmon returns are as compared to the background.

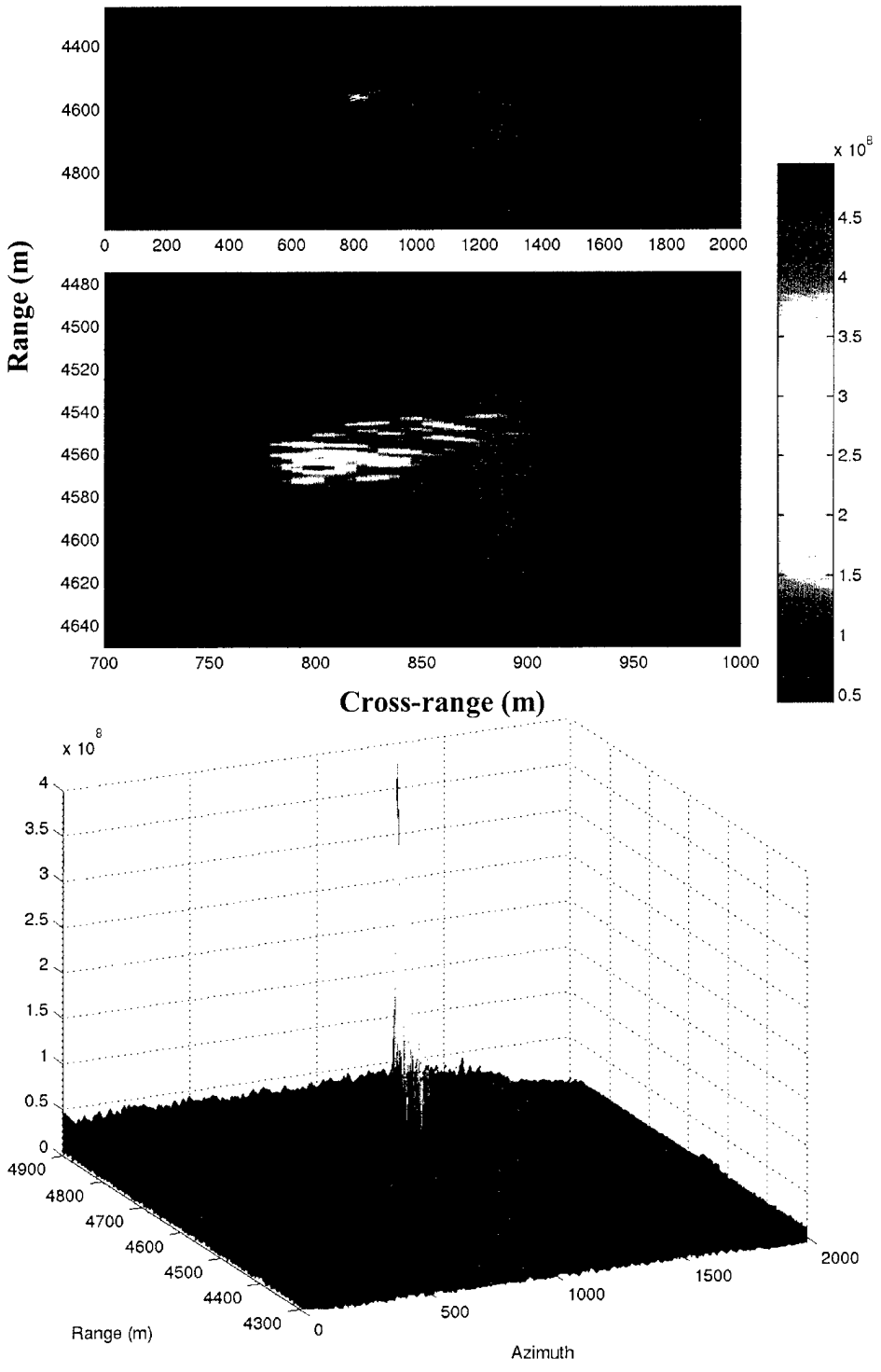

Figure 3-15. Run S9 20 ping SAS image at 9° forward beam. Top panel is a top view, with the center panel zoomed in to see the Salmon more easily. Bottom panel is a 3-D view to demonstrate how much stronger the Salmon returns are as compared to the background.

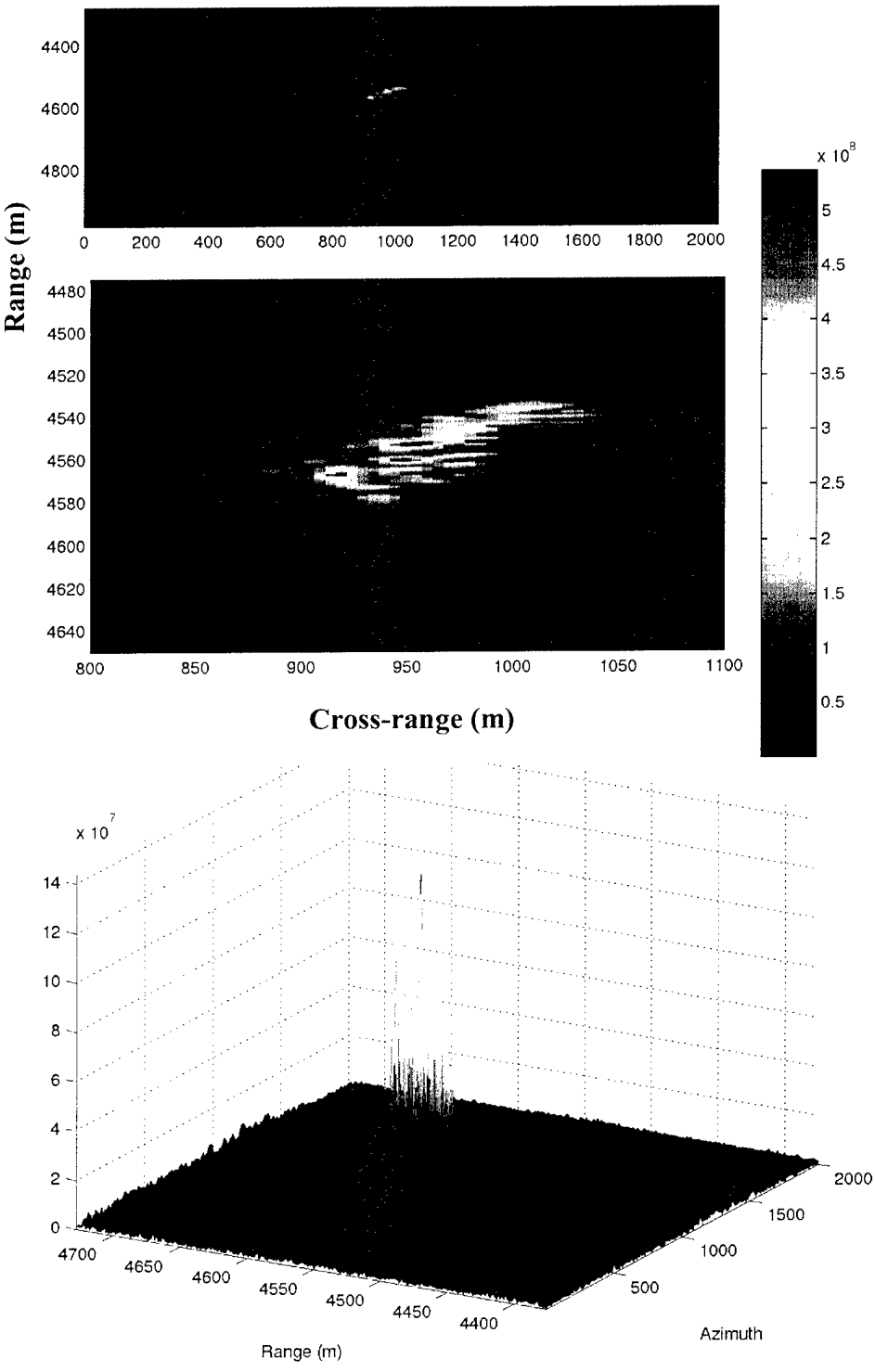

Figure 3-16. Run S9 25 ping SAS image at 8° forward beam. Top panel is a top view, with the center panel zoomed in to see the Salmon more easily. Bottom panel is a 3-D view to demonstrate how much stronger the Salmon returns are as compared to the background.

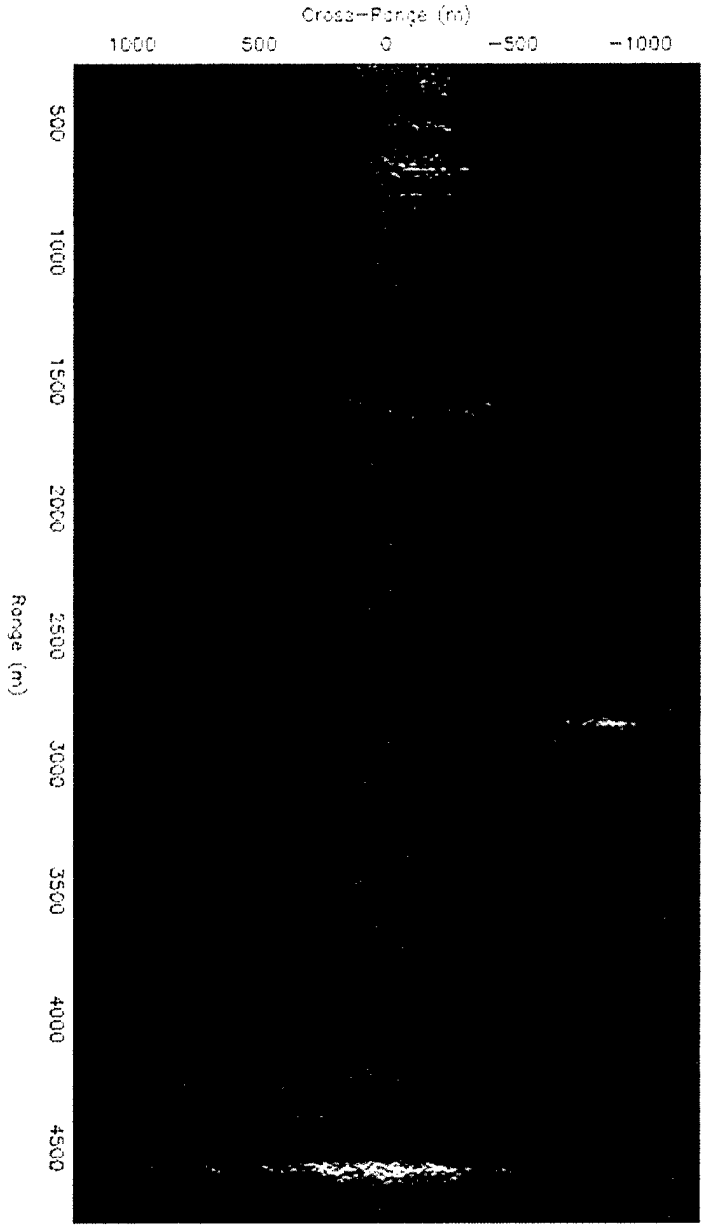

Figure 3-17. Run S9 full-swath SAS image. Motion estimates from 25 ping image, as seen in Figure 3-16. Color scale adjusted to bring out the weak returns, thus the grating lobes (from undersampling) appear stronger than in Figure 3-16.

3.2.3 S11: Salmon at 8000 m

This run was undertaken to demonstrate that 8 km ranges were possible if the array were long enough. To collect these data with the sonar system we took to sea, we traveled at twice the SAS speed limit for the nominal PRI, and more than twice the limit for the actual PRI. Thus all data were undersampled by more than a factor of two and SAS imagery has

strong grating lobes, which would not be present in imagery from a longer array. The towbody motion can be found in Figure 3-18. This motion is not as large as for Run S9, but not as benign as Run S2. In Figure 3-19 we see the Salmon at 8 km and we see that it has the on-off nature seen before which indicates the presence of significant yaw changes in the data. We were able to produce one 15 (~18 m resolution) and one 25 ping (~11 m resolution) image of the Salmon at this range, as seen in Figures 3-20 and 3-21. In these images the same plotting schemes were used as for S9. There are grating lobes of comparable strength to the main lobe ~210 m on either side of the main lobe, as well as weaker grating lobes at further cross-range distances from the Salmon.

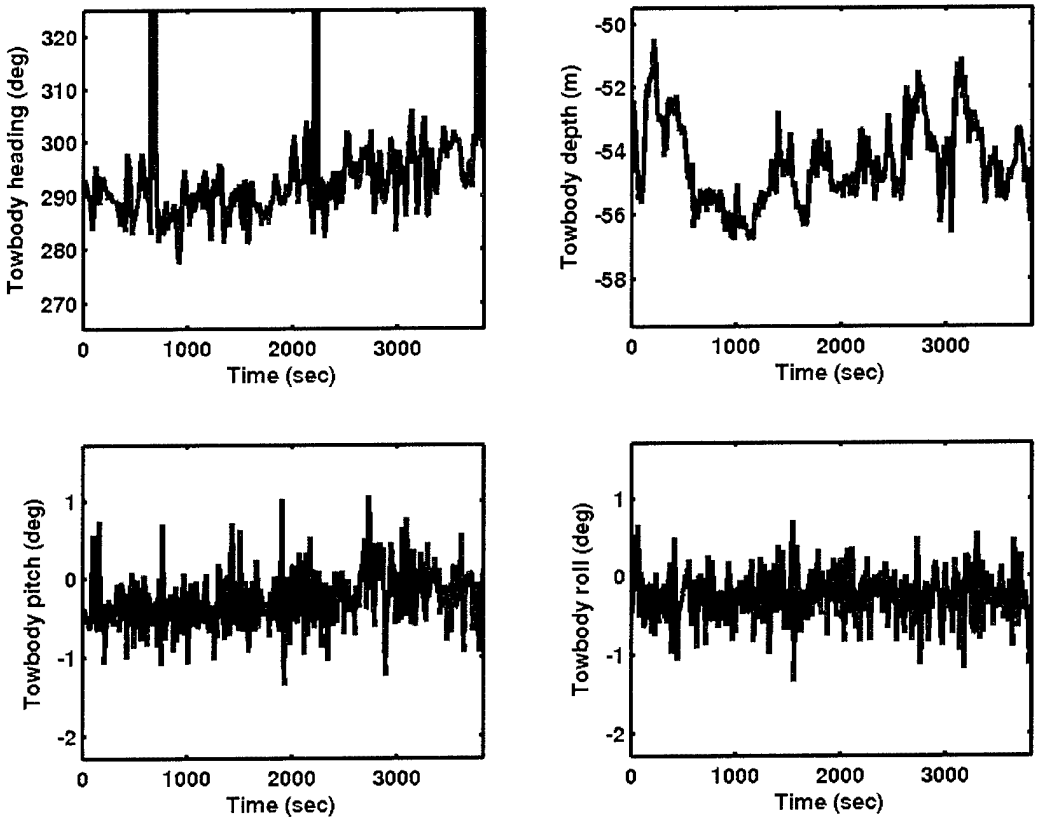

Figure 3-18. Run S11 motion data. There are three obvious compass glitches present in the heading data. The depth changes are larger than earlier runs, although the pitch and roll are comparable.

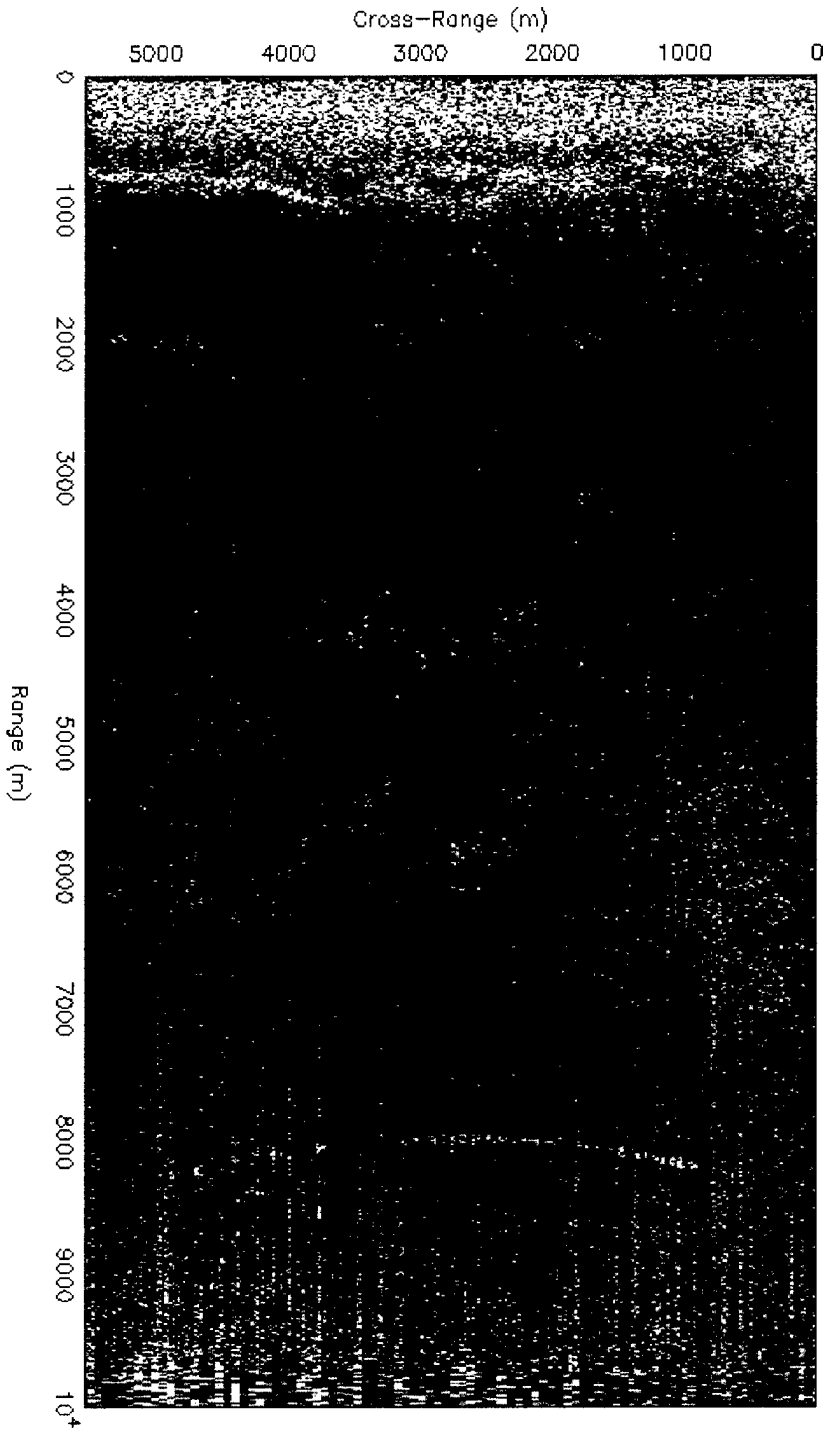

Figure 3-19. Run S11 SLS image. The Salmon is visible as the bright returns at 8000 m range. The on-off nature of the returns, as well as the presence of the majority of the "smile," are effects of the yaw changes the towbody underwent during the run, as noted in Figure 3-18. The color scale of the image has a range dependent component to enhance the far range data. At the furthest ranges the characteristics of the returns have switched to noise.

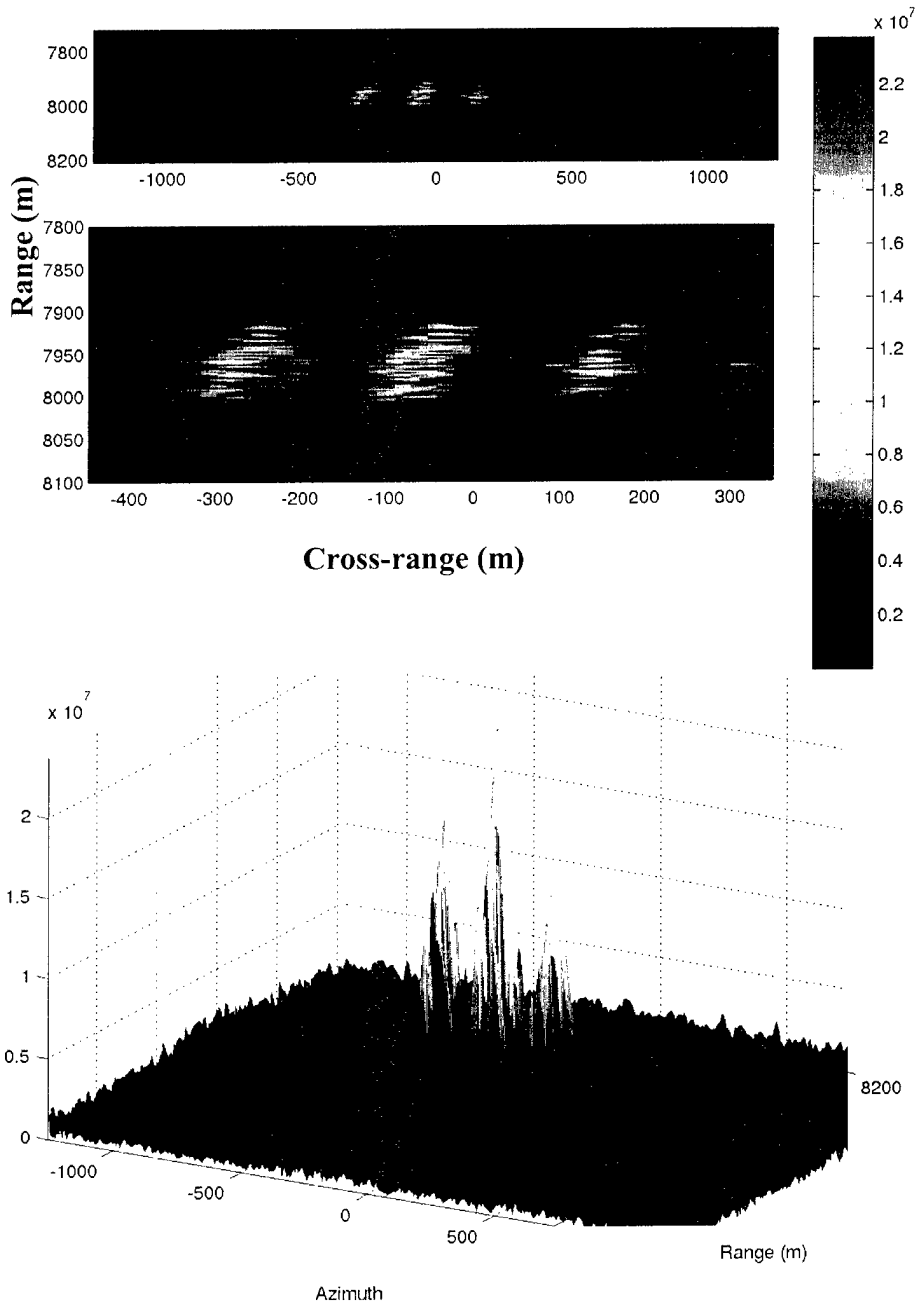

Figure 3-20. Run S11 15 ping SAS image at 17° backward beam. Top panel is a top view, with the center panel zoomed in to see the Salmon more easily. Bottom panel is a 3-D view to demonstrate how much stronger the Salmon returns are as compared to the background. The grating lobes due to more than a factor of two undersampling are present on either side of the main lobe.

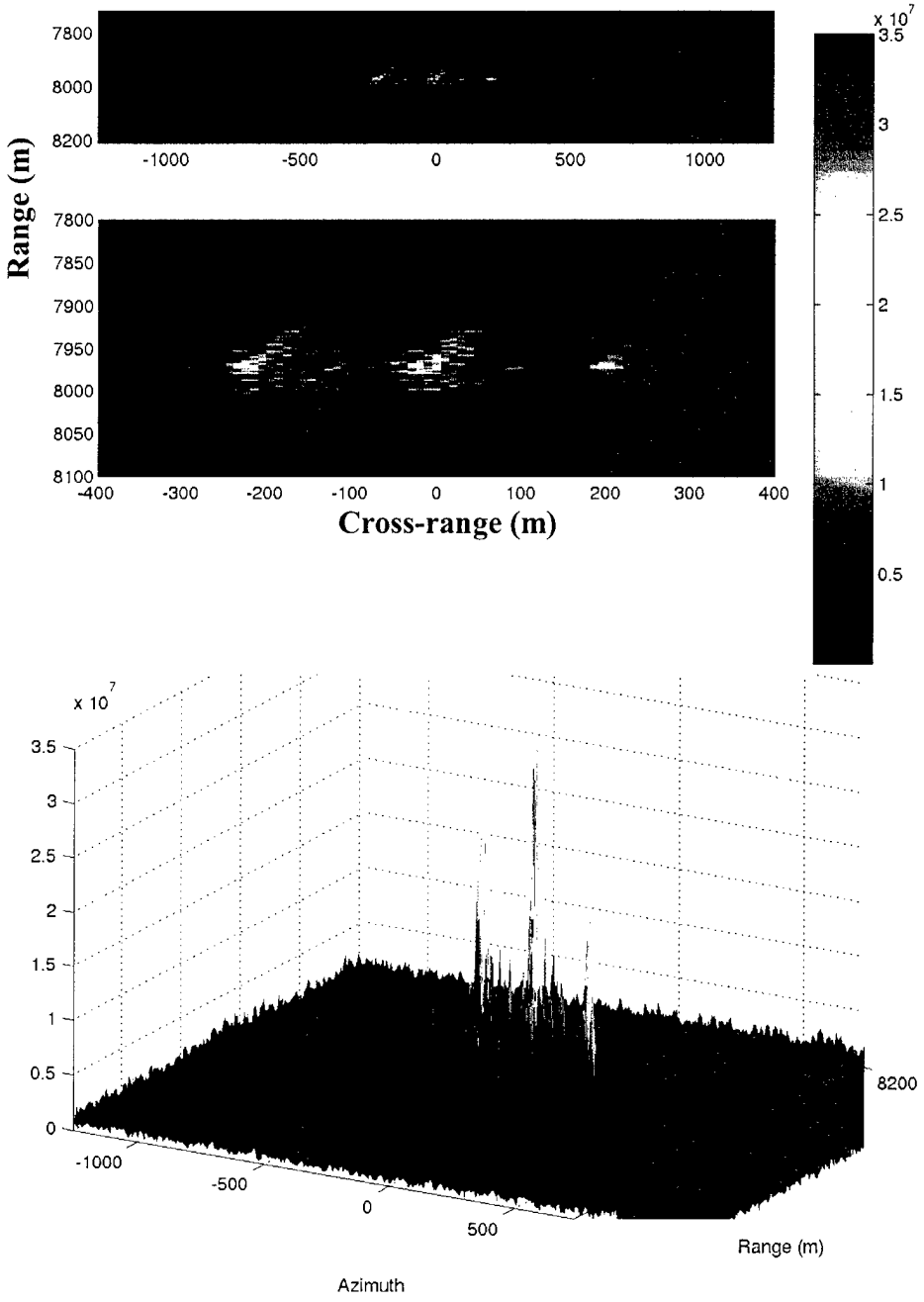

Figure 3-21. Run S11 25 ping SAS image at 12° backward beam. Top panel is a top view, with the middle panel a zoomed in view. Bottom panel is a 3-D view to demonstrate how much stronger the Salmon returns are as compared to the background. The grating lobes due to more than a factor of two undersampling are present on either side of the main lobe.

3.2.4 T2: Bidevind at 500 m

The Bidevind data were collected under a rougher sea state than the Salmon data. However, the towbody motion was not necessarily worse. Figure 3-22 is the motion for Run T2. Figure 3-23 is the broadside SLS image of the Bidevind at 500 m. The Bidevind appears compact, thus the yaw was not excessive. There is the hint of another object at ~4000 m in the early part of the run. We were able to focus 5, 6, and 7 pings at four different points in the run to achieve resolutions of 6.5 m, 5.5 m, and 4.8 m, respectively. Figures 3-24, 3-25, 3-26, and 3-27 show these images. The Bidevind does not have the same appearance from all angles as did the Salmon. Since it is a wreck and a debris field is expected, we do not expect the Bidevind to be as symmetric as the Salmon.

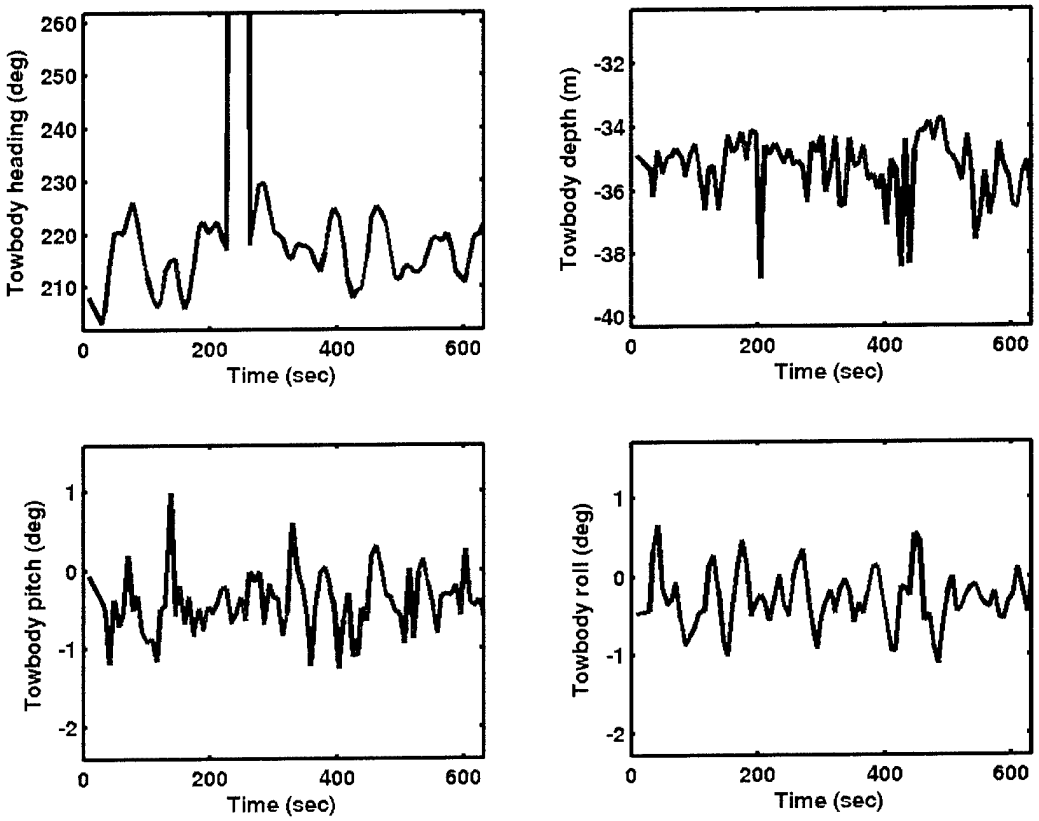

Figure 3-22. Run T2 motion data. There is a compass glitch present in the heading data at a time of ~250 s. There are some moderately large depth changes. The pitch and roll are comparable to Salmon runs.

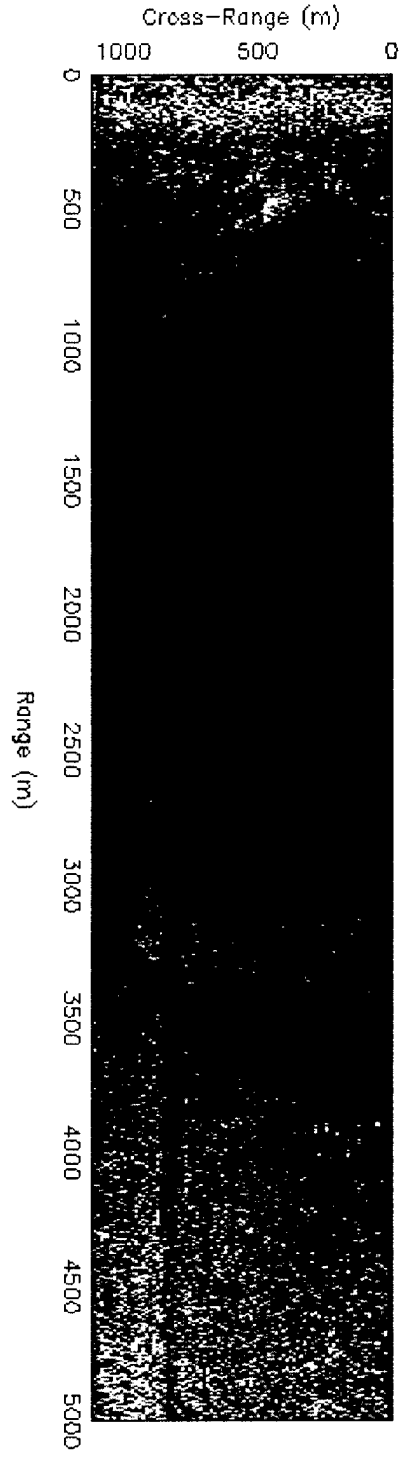

Figure 3-23. Run T2 SLS image. The Bidevind is visible as the bright returns at 500 m range. There is the hint of a second object at ~4000 m. The color scale of the image has a range dependent component to enhance the far range data.

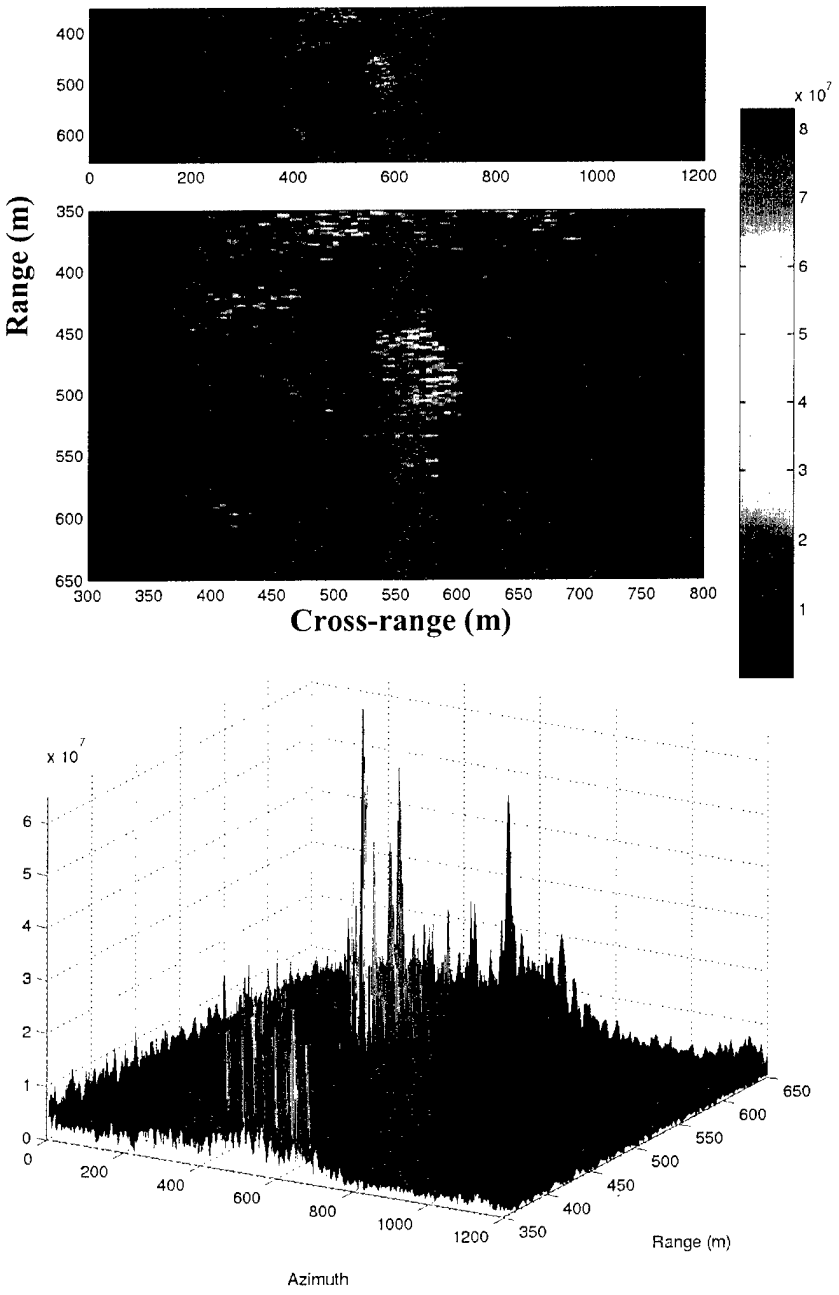

Figure 3-24. Run T2 6 ping SAS image at 35° forward beam. Top panel is a top view, with the center panel zoomed in to see the Bidevind more easily. Bottom panel is a 3-D view to demonstrate how much stronger the Bidevind returns are as compared to the background.

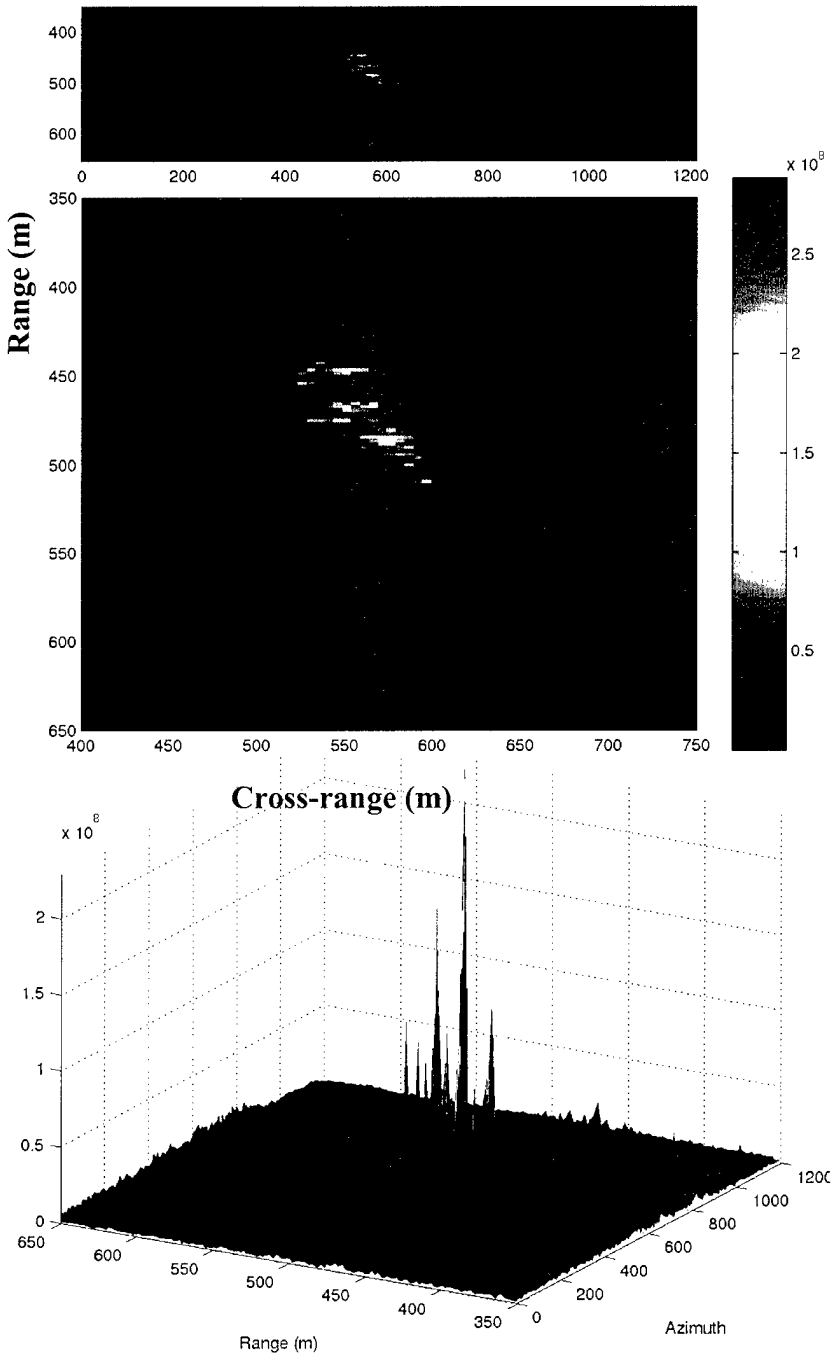

Figure 3-25. Run T2 5 ping SAS image at 5° forward beam. Top panel is a top view, with the center panel zoomed in to see the Bidevind more easily. Bottom panel is a 3-D view to demonstrate how much stronger the Bidevind returns are as compared to the background.

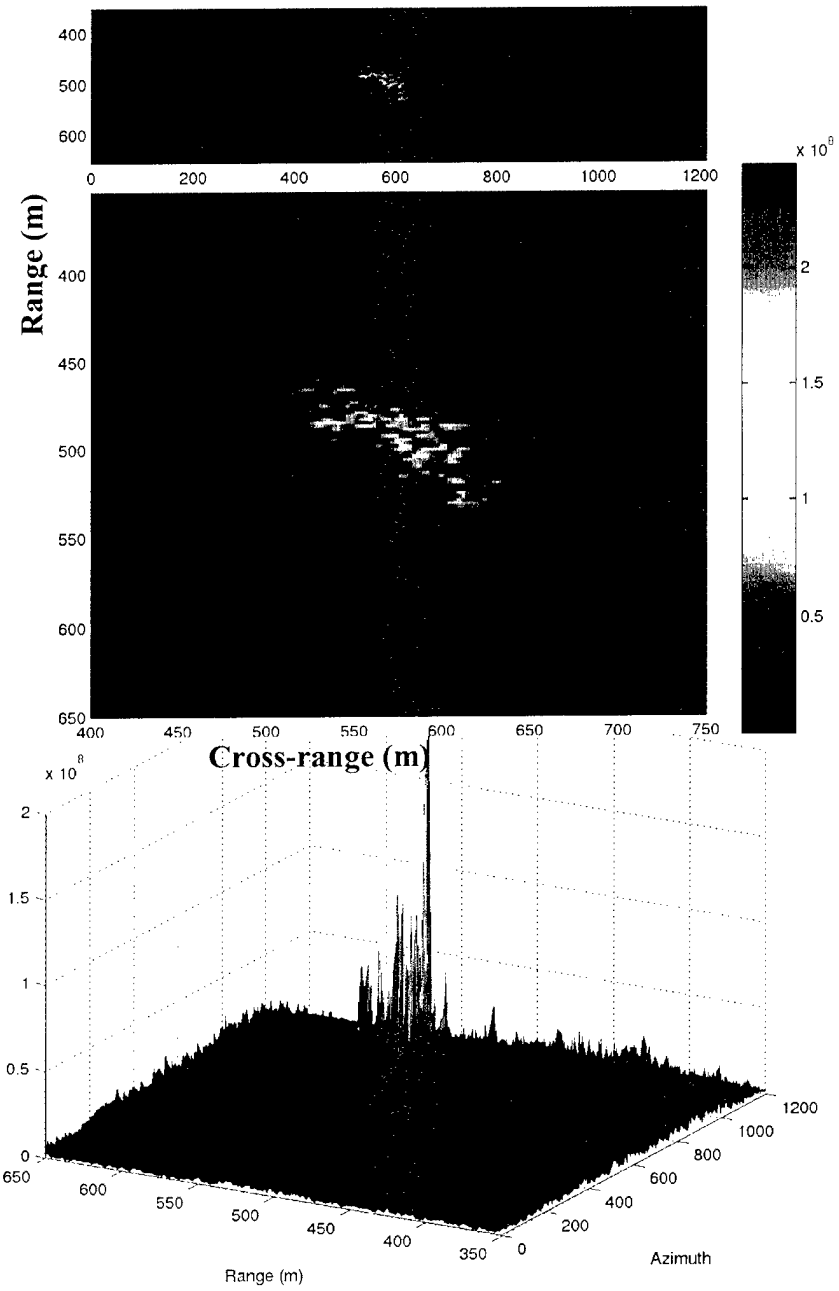

Figure 3-26. Run T2 6 ping SAS image at 15° backward beam. Top panel is a top view, with the center panel zoomed in to see the Bidevind more easily. Bottom panel is a 3-D view to demonstrate how much stronger the Bidevind returns are as compared to the background.

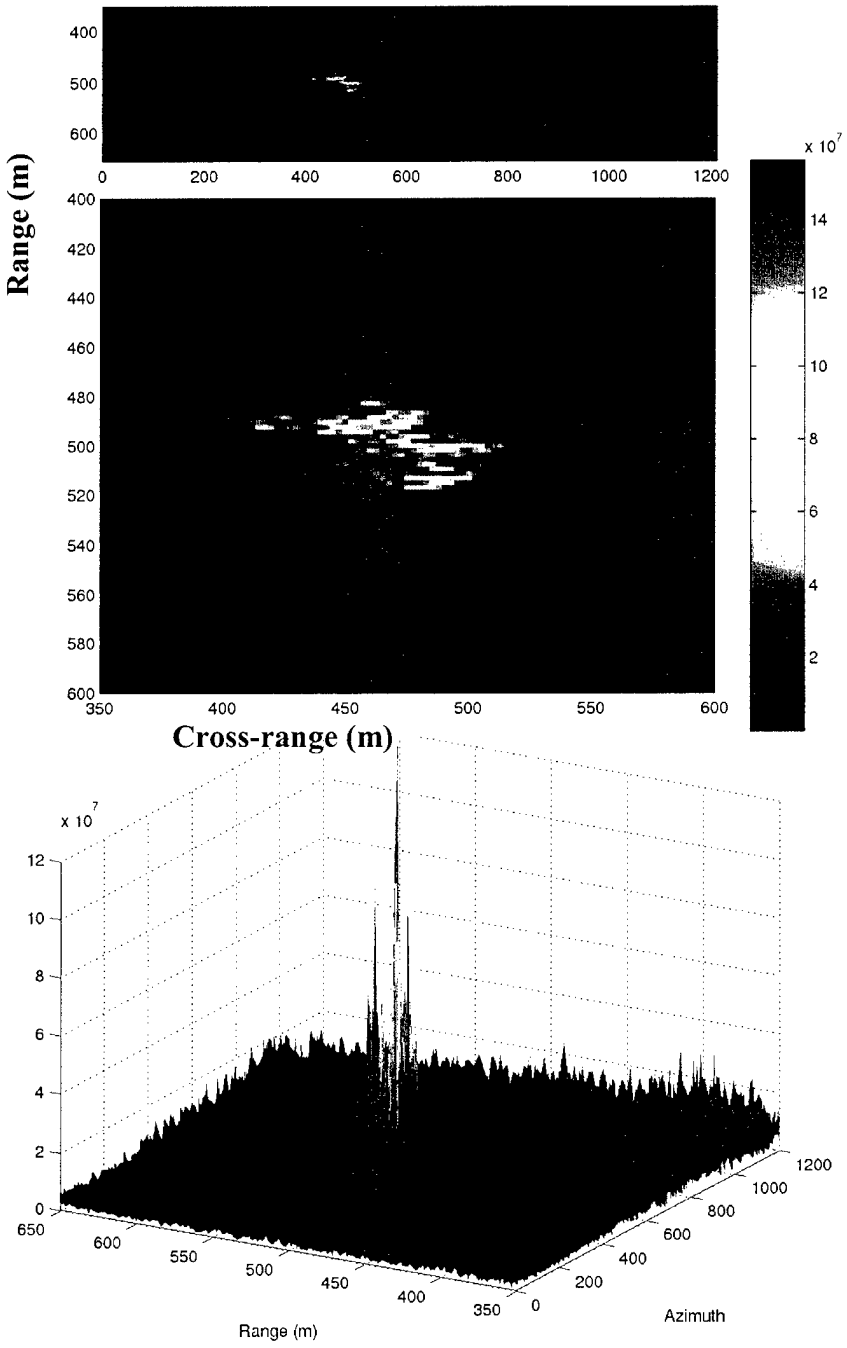

Figure 3-27. Run T2 7 ping SAS image at 40° backward beam. Top panel is a top view, with the center panel zoomed in to see the Bidevind more easily. Bottom panel is a 3-D view to demonstrate how much stronger the Bidevind returns are as compared to the background.

3.2.5 T9: Bidevind at 4000 m

As the day progressed, the sea state worsened. This is more noticeable in the towbody motion data of Figure 3-28. Figure 3-29 is the broadside SLS image of the Bidevind at 4 km. The extended and on-off nature of the Bidevind indicate that the sonar suffered from large yaw for at least a portion of the run. There appears to be a point-like abject at about 2.5 km in the latter portion of the run. The nature of this object in the SLS image indicate that the system motions were reduced for this section of the run. For this run we produced a 20 and a 30 ping image, with resolutions of ~13 m and ~9 m respectively, as seen in Figures 3-30 and 3-31. From the 30 ping region we produced a full-swath image, Figure 3-32. The wedge shape is an artifact of the processing technique we used. This scene is basically featureless outside of the Bidevind.

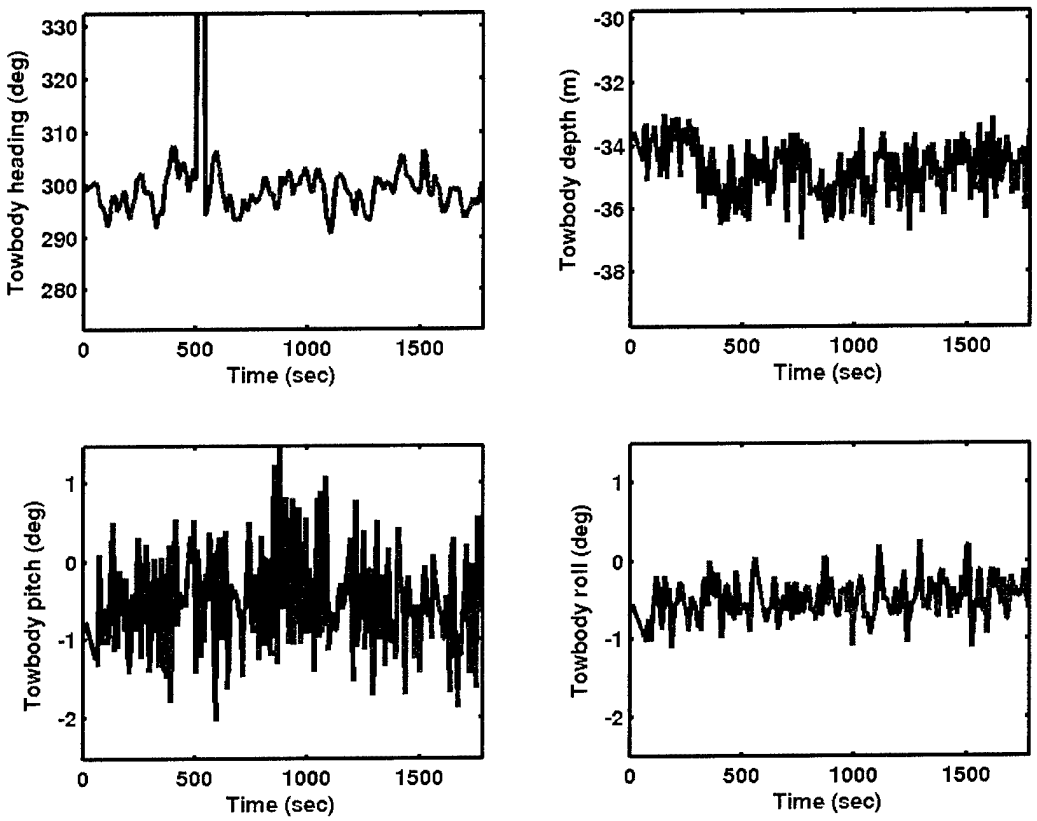

Figure 3-28. Run T9 motion data. There is compass glitch at ~500s in the heading data. The depth and pitch changes have a higher frequency and larger excursions than earlier runs, however, the roll is comparable to Salmon runs.

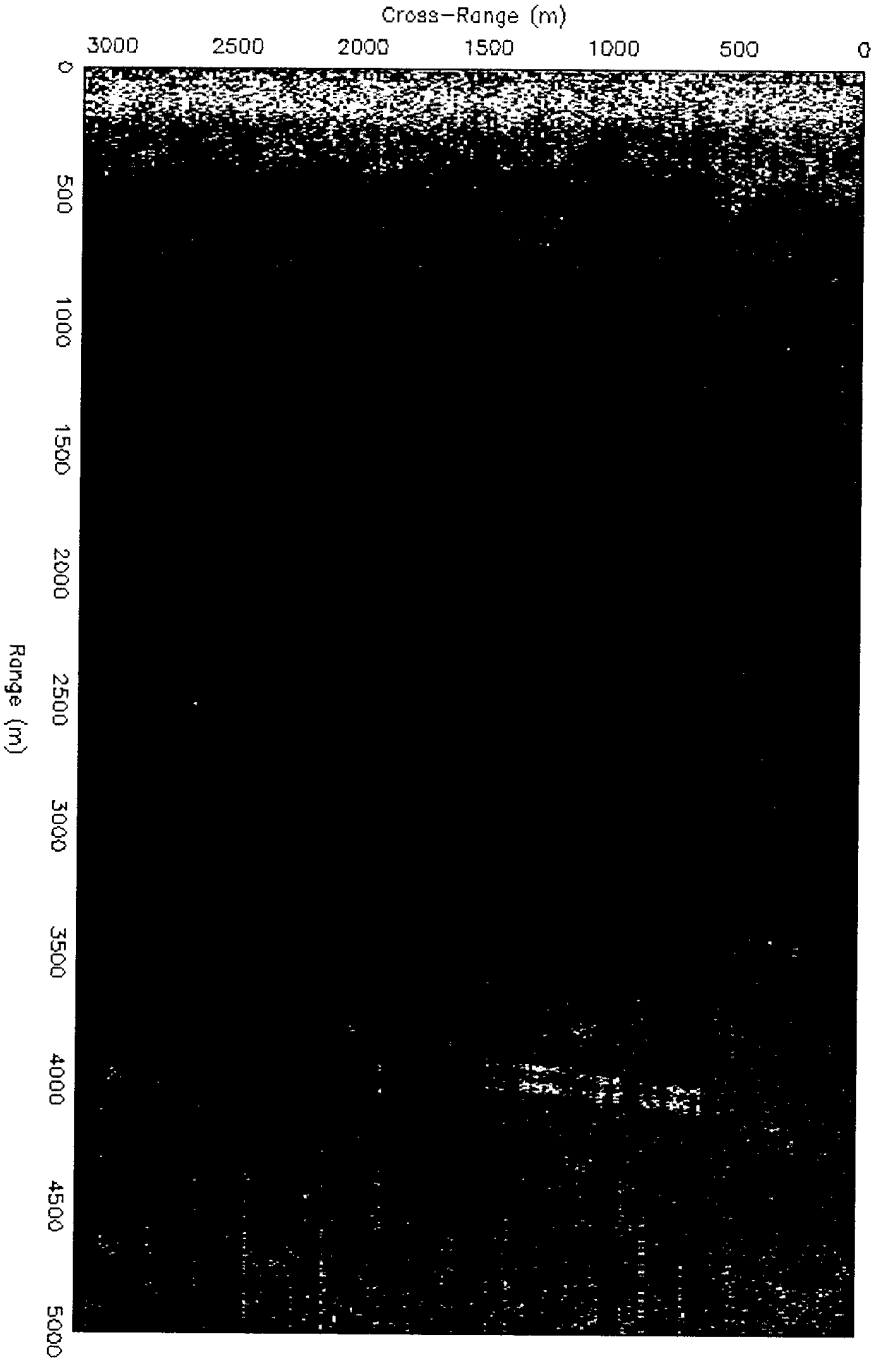

Figure 3-29. Run T9 SLS image. The Bidevind is visible as the bright returns at 4000 m range. The on-off nature of the returns, as well as the presence of a large portion of the "smile," are effects of the yaw changes the towbody underwent during the run. The color scale of the image has a range dependent component to enhance the far range data.

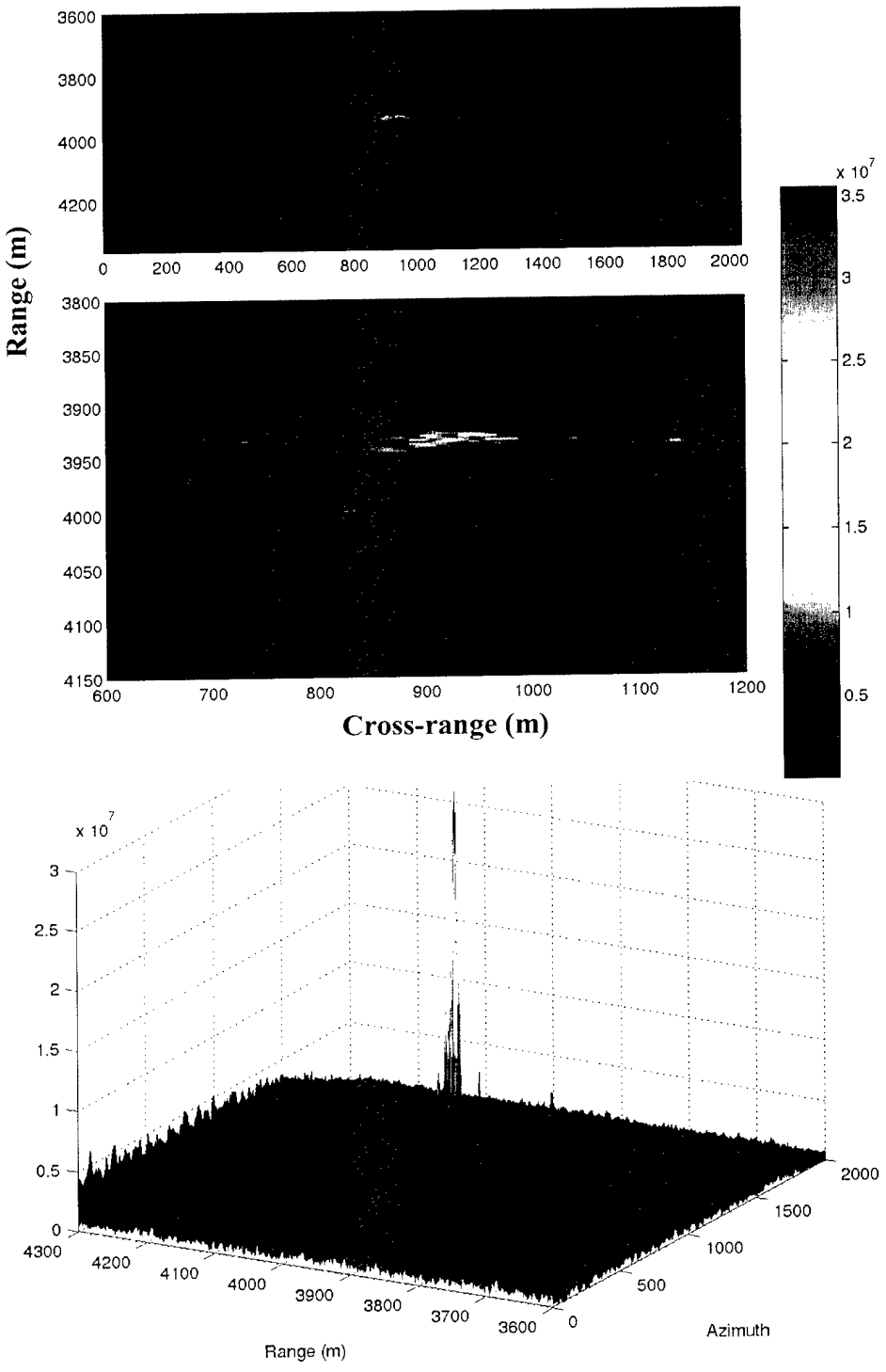

Figure 3-30. Run T9 20 ping SAS image at 12° forward beam. Top and middle panels are a top view, with the middle a close-up of the Bidevind itself. Bottom panel is a 3-D view to demonstrate how much stronger the Bidevind returns are as compared to the background.

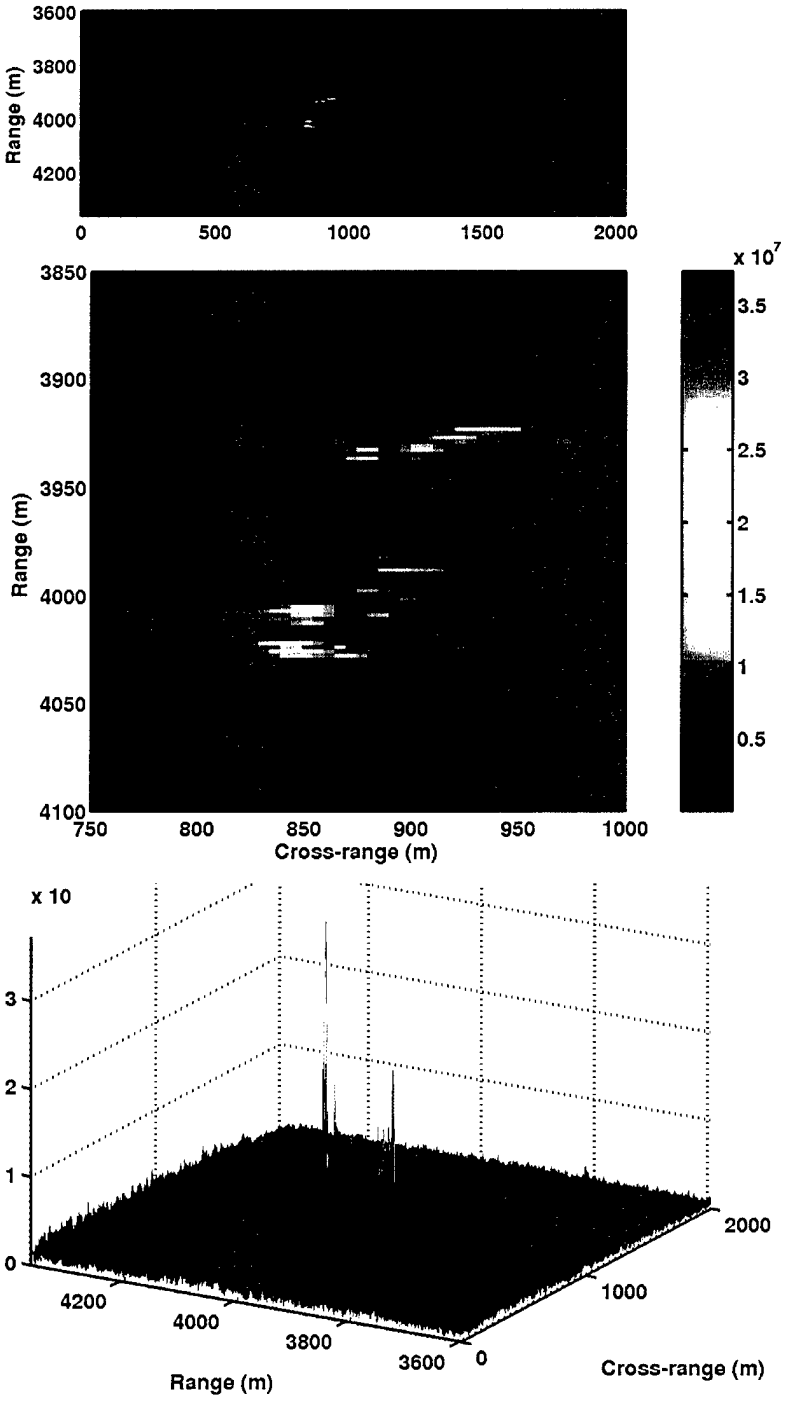

Figure 3-31. Run T9 30 ping SAS image at 1° forward beam. Top and middle panels are a top view, with the middle a close-up of the Bidevind itself, note the two distinct regions of returns. Bottom panel is a 3-D view to demonstrate how much stronger the Bidevind returns are as compared to the background.

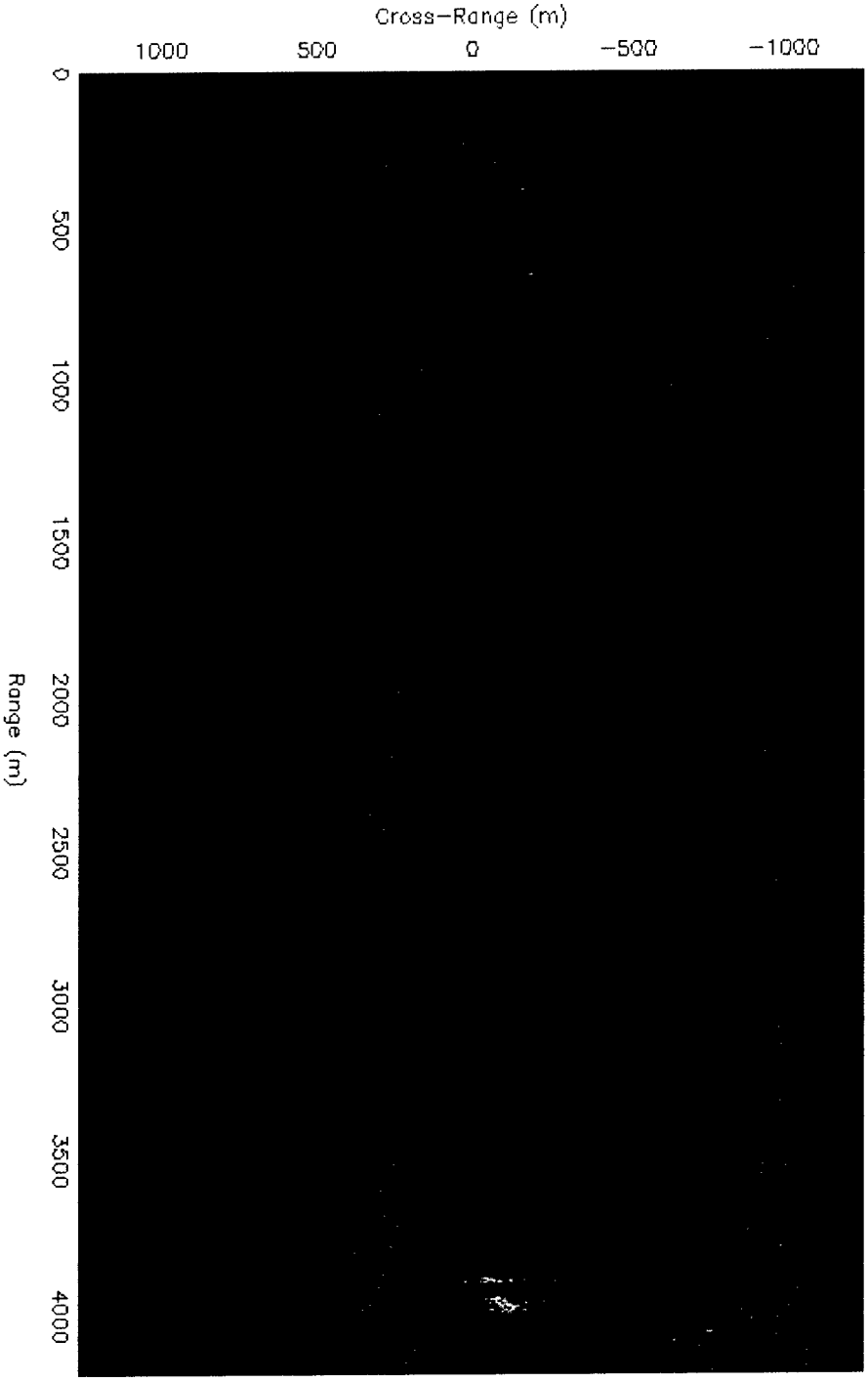

Figure 3-32. Run T9 full-swath SAS image. This image was produced using the motion derived from the 30 ping SAS image seen in Figure 3-31. Color scale was enhanced to view weaker returns.

3.3 Clutter Analysis

A key ability of any detection system is distinguishing targets from clutter. In order to understand the potential of a system with a frequency range similar to Seahawk's, we need to study the clutter at these frequencies along with the targets. In this program we were tasked to collect data against any available clutter found at the sea trial location. There are three basic types of clutter: geologic, man-made non-target-like, and target-like (which is typically man-made). For geologic clutter we collected data on whatever was surrounding our prime man-made objects. For this trial, the target is a bottomed diesel submarine, in particular, the Ex-USS Salmon. We collected target-like clutter in the form of the Bidevind.

In this section we discuss the clutter as found in the images, both SAS and SLS. Any discussion of frequency responses and clutter will appear in Section 3.4. We begin the clutter discussion with what we expect from the data in Section 3.3.1. The geologic clutter analysis is in Section 3.3.2 and man-made clutter in Section 3.3.3.

3.3.1 Limitations on Clutter

Based upon simulations of SNR as a function of range conducted before the trial Section 2.2.3, we expected to be able to image the majority of the sea floor since the bottom reverberation would be larger than other noise sources. Post-trial, we ran PC SWAT using the measured SVPs for the Salmon and Bidevind sites, see Figure 3-33. These simulations assumed a flat bottom to make them approximate for all runs. The bottom for each region is a shallow slope, so the actual transmission losses will be similar to these, but the locations of the low/high loss regions will have shifted slightly from those shown. From these plots, and ray traces not being shown since they repeat the information, we can determine that there are regions of the bottom which we should be able to image. The region out to ~600 m contains direct path returns from the bottom, with the lowest loss (thus expected strongest returns) at the furthest range. Approximately each 1300 m after this direct path region is a region of low loss bottom bounce, again with the strongest returns at the furthest range of each patch. We expect the recorded returns to follow a similar pattern.

We used two different pulse lengths during the trial, 0.25 s and 0.5 s. As was noted in Section 3.1.1, the pulse lengths were approximately 0.08 s longer than intended. All receiver data were recorded, i.e., no "blanking" during the pulse. Thus we expect the first approximately 250 m and 435 m, respectively, of returns to contain the direct blast and be useless in terms of detection of clutter or anything else. This can be seen in the SLS images in Section 3.2 and Appendix D.

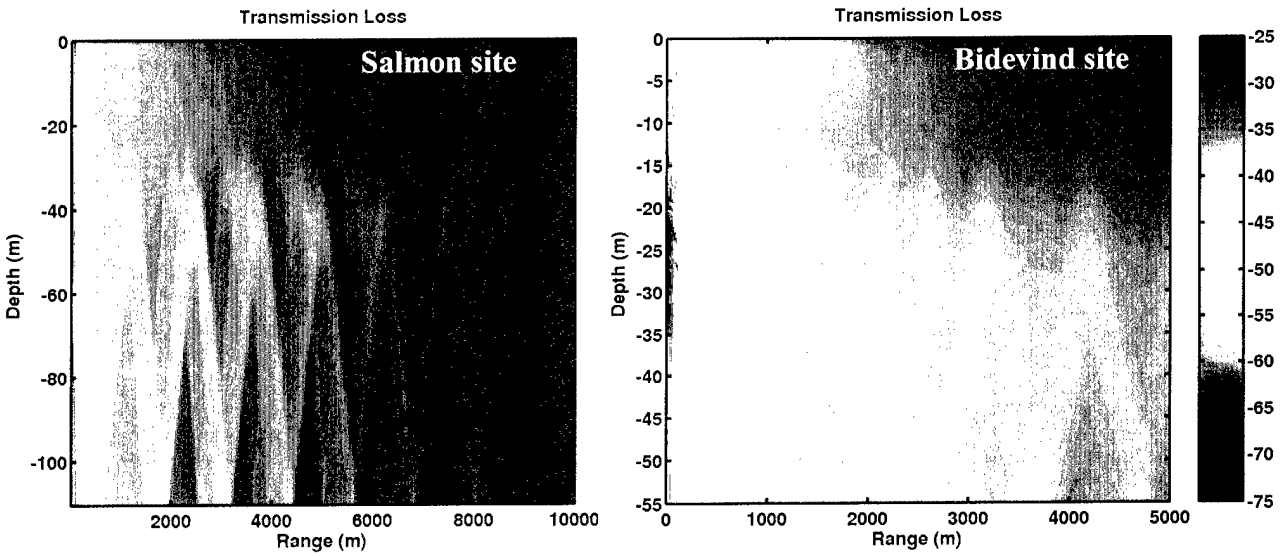

Figure 3-33. Transmission losses for Salmon and Bidevind sites. These transmission losses were calculated using PCSWAT and the SVP from the XSV collected at the respective site. The left image shows the results for the Salmon area and the right for the Bidevind. In both cases a flat bottom was assumed. Note the sound channel in each case and that there are obvious regions where returns from the bottom are likely and regions where such returns are unlikely. Data from the first 500-600 m for both regions are likely to be direct path returns. Beyond that, returns are more and more likely to contain bottom bounces in both directions. In all cases, the last returns of each section appear to be strongest. The range extent shown for each site is roughly the longest range of the sonar data collected at the site.

3.3.2 Geologic Clutter

As seen in the SLS and SAS images in Section 3.2, there does not appear to be a complex bottom. In fact, aside from a few bright objects, the images appear to be speckle[14]-like in both SLS and SAS images. Figure 3-34 shows several characteristics worth explaining. The region of the sonar direct blast is marked. The returns in this region are in the rest frame of the sonar, thus they occur at the same distance (time) in every ping. In Figure 3-33, the further range of each band of low loss has the lowest loss, e.g., the direct path returns at ~600 m have a lower transmission loss than those at 300 m. The bright band at ~600 m in Figure 3-clutterdemo appears to be the last of the direct path returns. Note that the band is not a perfectly straight line. This is probably a combination of array motion, bathymetry, and depth variations. Each ~1300 m after the 600 m band is brighter than the surrounding region. This spacing is consistent with the bands of low transmission

[14] Speckle is a phenomenon in which coherent radiation is scattered by a rough surface and generates a random intensity distribution and thus a granular appearance. Typically the pixel, or resolution cell, contains a large number of scatterers whose response to the radiation (or sound) will constructively or destructively sum together. When the effect is due to stationary objects, it is repeatable in subsequent looks.

loss. Since the returns in these bands underwent multiple bottom bounces, each band contains some information from the preceding band bottom region, which explains some of the similarities seen amongst them. In between these bands the returns are weak, which is consistent with the transmission loss calculation. There are some small bright patches in the weak regions. These may be strong reflectors on the bottom or in the water column. In general, no strong geological features were noted in the data.

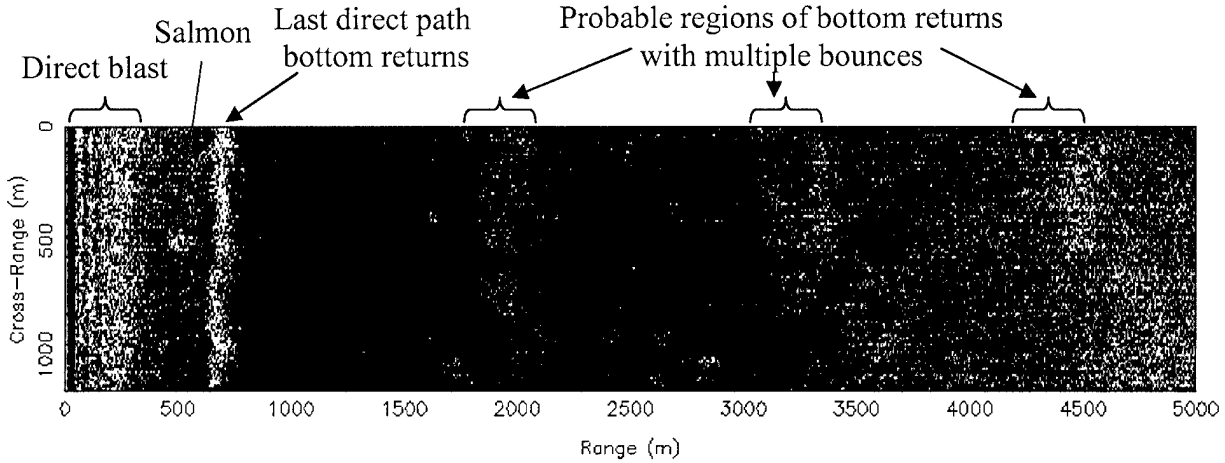

Figure 3-34. SLS image of S3 to demonstrate clutter characteristics. Key features seen in majority of data sets are marked. The image display was created with a range-dependent color scale. The direct blast, as discussed in Section 3.3.1, cannot be used for clutter studies. Direct path returns are noted as are the pattern of regions that are probably bottom returns which underwent multiple bounces between transmit and receive.

If there were structure in the bottom, we would expect to have regions of raw data containing "smiles." These "smiles" would then be focusable into the bottom (Figure 3-35 shows the "smiles" for the Salmon). We have seen this in other data sets, but not in any of the LRSAS data. Figure 3-36 shows a region of raw data without a bright object. These data have a speckle-like appearance, thus it is not surprising that focused regions also appear speckle-like. This implies, unfortunately, that there was no significant geologic clutter in the region. We lack ground truth, but the knowledge of heavy trawling in the area leads us to believe that the bottom may indeed be devoid of anything clutter-like at our frequency. Thus in this region of the Atlantic Ocean, we need only worry about target-like man-made clutter.

3.3.3 Man-made Clutter

We are dubbing anything not obviously geologic clutter as man-made. This may not be strictly accurate, but the few small, strong objects in speckle-like regions can be treated as man-made. Since the Salmon is our chosen target, anything that is not the Salmon is labeled as clutter. There are a couple of non-Salmon bright returns that appear to originate from highly acoustically reflective objects. The Bidevind is the most obvious piece of clutter that satisfies this criterion. Approximately 2,500 m from the Salmon is another bright object (see, e.g., Figures 3-9 & 3-12). Unfortunately, it lies far enough to the side of

the Salmon that it did not fall within our processing region. Of these two bright objects, only the Bidevind was processed to a state for comment and comparison to the Salmon.

The Bidevind is target-like clutter since its size and shape are reminiscent of the Salmon. In some of the views, there are clearly two regions of returns separated of order 50 m. One piece appears in many of the images as an approximately 100 m long, >10 m wide object (Figures 3-27, 3-30, and 3-31). In some views the object appears wider with many weak returns around it, which could be debris or other scatterers (Figures 3-24, 3-25, 3-26, and 3-31). The second piece is not as organized. It is present in the 4 km images and diffusely in the 35° forward beam 500 m image (Figure 3-24). The reports of the torpedo strikes indicate that the ship was hit aft twice, first aft of the engine room and the second time in the crew's quarters and shattering the stern (Lawson 2004). Thus the larger, long portion is probably the majority of the ship and the second piece the stern of the boat and perhaps debris. The discussion on distinguishing the Bidevind from the Salmon can be found in Section 3.5.

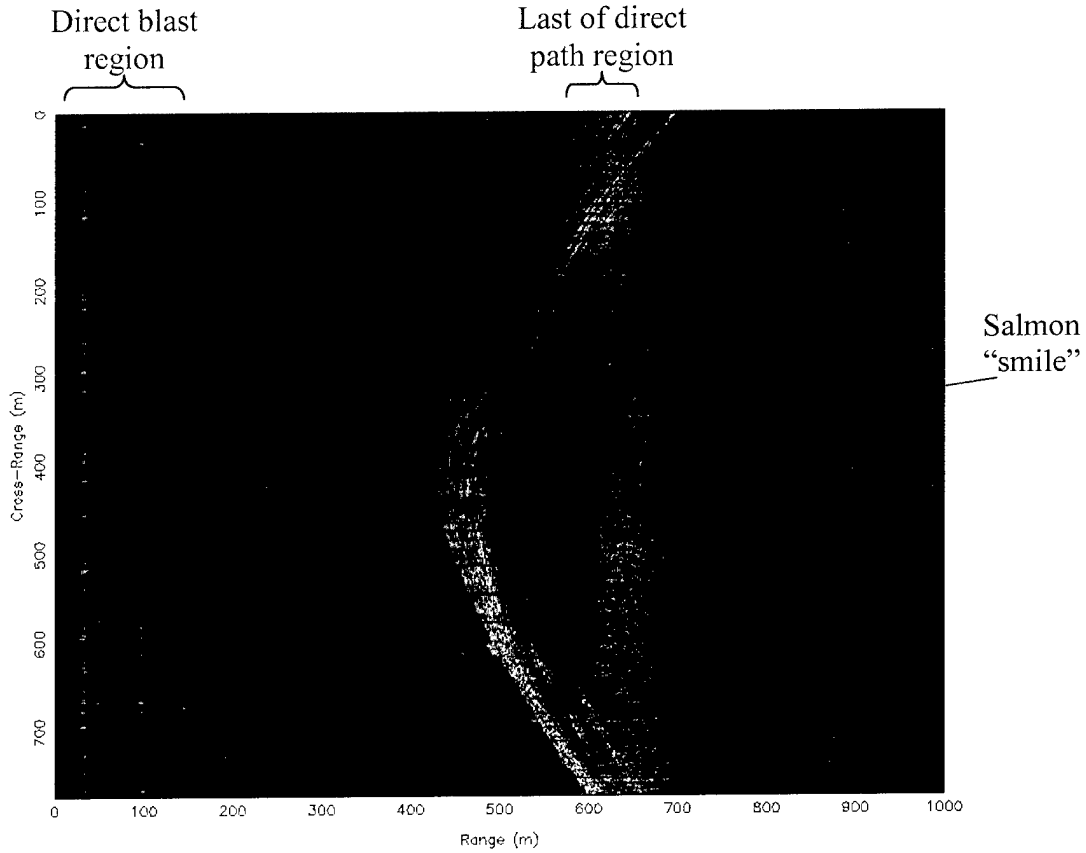

Figure 3-35. Raw phase history data of the Ex-USS Salmon demonstrating a "smile." The direct blast and end of the direct path regions are marked. The hyperbolic shape of the returns from the Salmon are due to the changing range of the target as we approach and then recede from CPA. The wide, diffuse returns early in the run and the narrow width strong returns at the end of the run are due to the changing aspect of the Salmon - nearly end on at the beginning to broadside at the end.

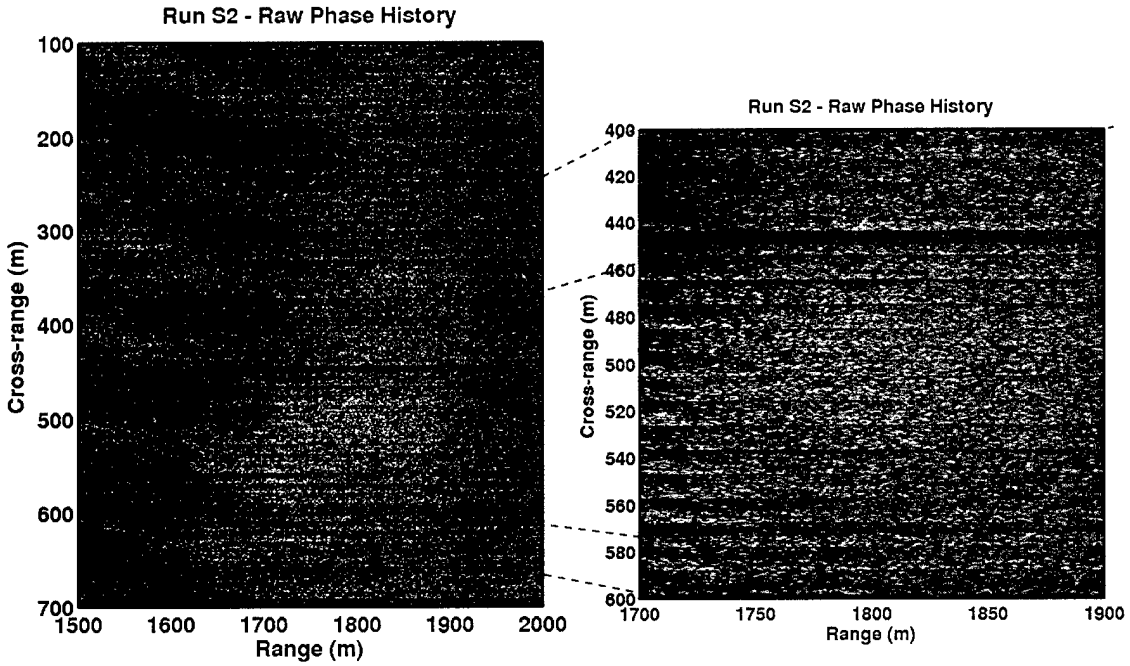

Figure 3-36. Run S2 phase history data in region devoid of bright targets. While there are changes in acoustic strength in the swath, there are no obvious "smiles" in these data. The speckle-like quality of the data is shown in the zoomed in region. Dead channels are also noticeable.

3.4 Frequency Response Analysis

The Seahawk bandwidth of 400 Hz yields a small region to study the frequency dependence of returns from the various targets and clutter. While not a large band, we can investigate the potential for frequency characteristics that could be used for classification. We processed the majority of the SAS images shown in Section 3.2 in the manner described in Section 2.5.3. For the small images around the individual objects (Salmon or Bidevind), we processed the whole scene at once. For the full swath images, we created ~500 m long range swaths for processing. The small swath size allows us to better determine the source of any apparent frequency dependency. Additionally, we processed one SLS image in the same manner.

The general results are that we find differences in the clutter and target responses. The regions without a bright return from a man-made object have a weak, effectively white spectral response. The Salmon and Bidevind yield structured frequency responses which appear to be aspect dependent. The image resolution and sharpness has an effect on appearance of the spectral response; if the energy is not concentrated in the along-track pixels, then the frequency response tend to be whiter and thus harder to discern from the background. Section 3.4.1 contains a few clutter regions; Section 3.4.2 covers the Salmon; Section 3.4.3 the Bidevind; and Section 3.4.4 is a brief discussion of all the data.

3.4.1 Non-strong Target Clutter Frequency Response

The regions of data without a strong object in the scene are discussed first to yield a sense of how the Salmon and Bidevind frequency responses are due to the object, the clutter, and the system. Figure 3-37 shows a region devoid of bright returns from the full swath image of Run T9. The SAS image (upper panel) shows slight variations in strength across the image, but no obvious objects. The frequency response (lower panel) is nearly white. There is a fall-off in strength at the low and high frequencies. This is most likely due to the transmitter and/or receiver beam frequency shape. This is confirmed by the similarity to the frequency response of an SLS image, Figure 3-38. This is an empty region near the Salmon, Run S9. This drop-off in strength is not surprising and may partially explain the lack of very low and very high frequency responses in the Salmon and Bidevind.

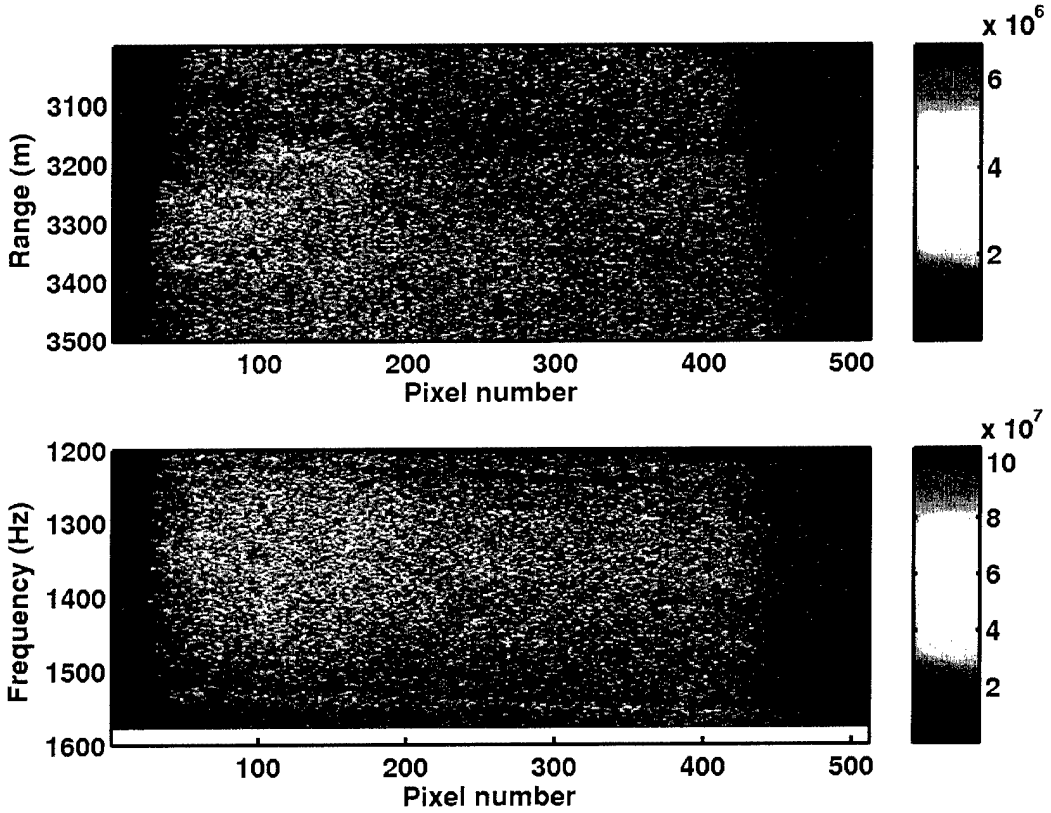

Figure 3-37. Time and frequency domain image of a region devoid of an obvious object. The frequency response is nearly white for this patch of the full swath image from the Bidevind Run T9. The response is stronger where the time domain image is stronger, but there are no obvious returns. The frequency response may possibly be weaker for the low and high frequency ends. This may be due to the shape of the transmit or receive beams.

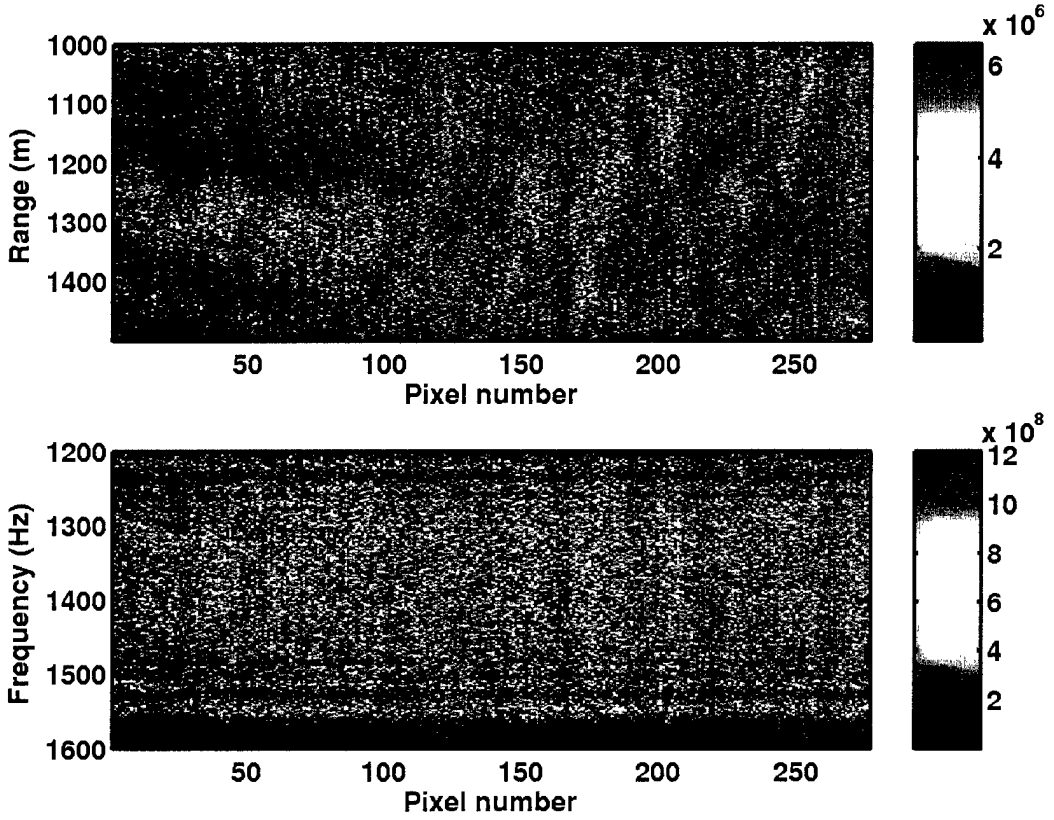

Figure 3-38. Time and frequency domain image of a region devoid of an obvious object in an SLS image. The frequency response is effectively white. The slight diminishment in strength at the low and high frequencies are most likely due to the transmitter/receiver beam responses.

3.4.2 Salmon Frequency Response

All of the Salmon images were created from different aspects. Three are shown here. Two are nearly end-on and one approximately quartering. The frequency responses for the three images are in Figures 3-39, 3-40, and 3-41. In all cases the responses are more structured than the background. Different regions of the submarine yield different frequency responses. These responses may be due to resonances within a cavity or absorption, scattering, or reflection off of different structures in the submarine. Such responses are expected to be aspect dependent.

The small bandwidth of the system may not allow us to measure the multiple responses from a resonance, however, there are hints to the existence of resonances in some of the aspects. All three figures show responses at ~100 Hz intervals starting at ~1260 Hz, although a response at ~1560 Hz is not always discernable, but that may be explained by the frequency response of the system as mentioned in Section 3.4.1. Figure 3-39 may be hinting at a higher frequency resonance in the 1450-75 Hz region. None of these are conclusively resonances and without further ground truth of the submarine (plans,

materials and thicknesses, which cavities are filled with what, etc.) or a larger bandwidth, it isn't possible to know for sure.

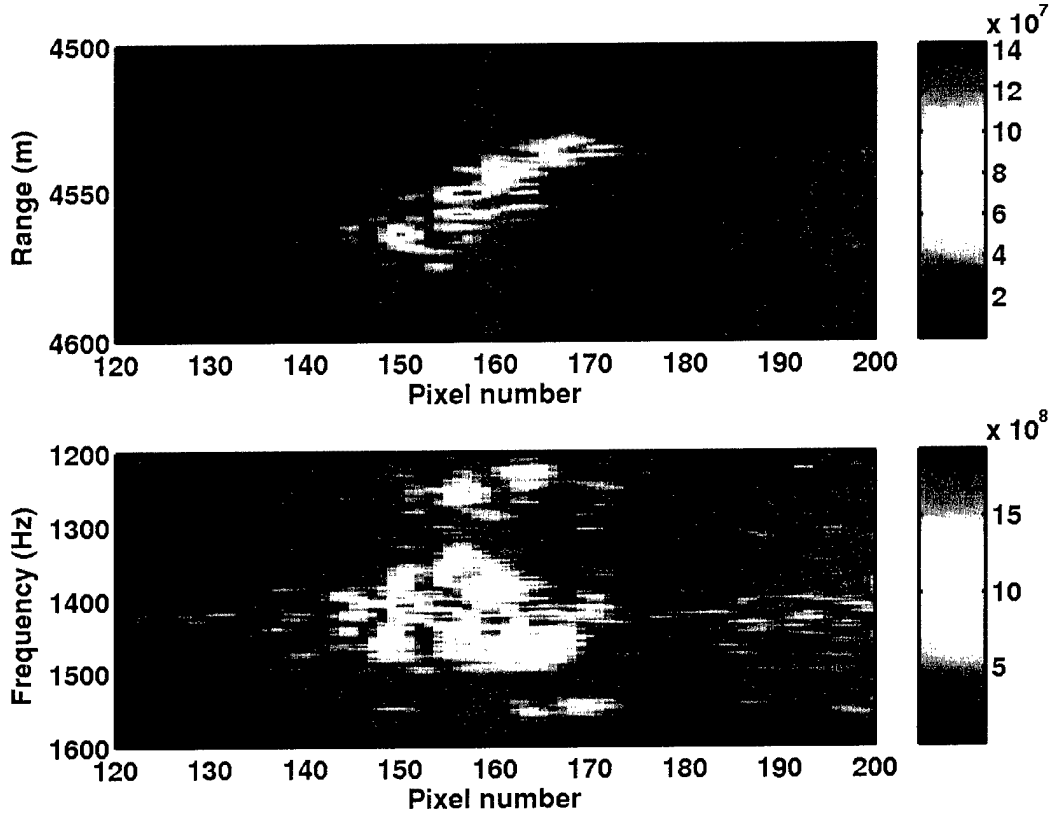

Figure 3-39. Time and frequency domain images of the Salmon at 4.5 km with 25 pings. The frequency response varies as a function along track from this aspect. At pixel 150, the strongest frequency response is at ~1410 Hz, with additional bands around 1440, 1460, 1475, and 1550 Hz. At pixel 157 there are peaks around 1260 and 1365 Hz and many bands at 1420-80 Hz (which are nearly identical in multiple along track locations). At pixel 160 the peaks are at 1420 and 1430 Hz. At pixel 163, there are strong bands at 1220-30, 1450-75, and 1540-65 Hz.

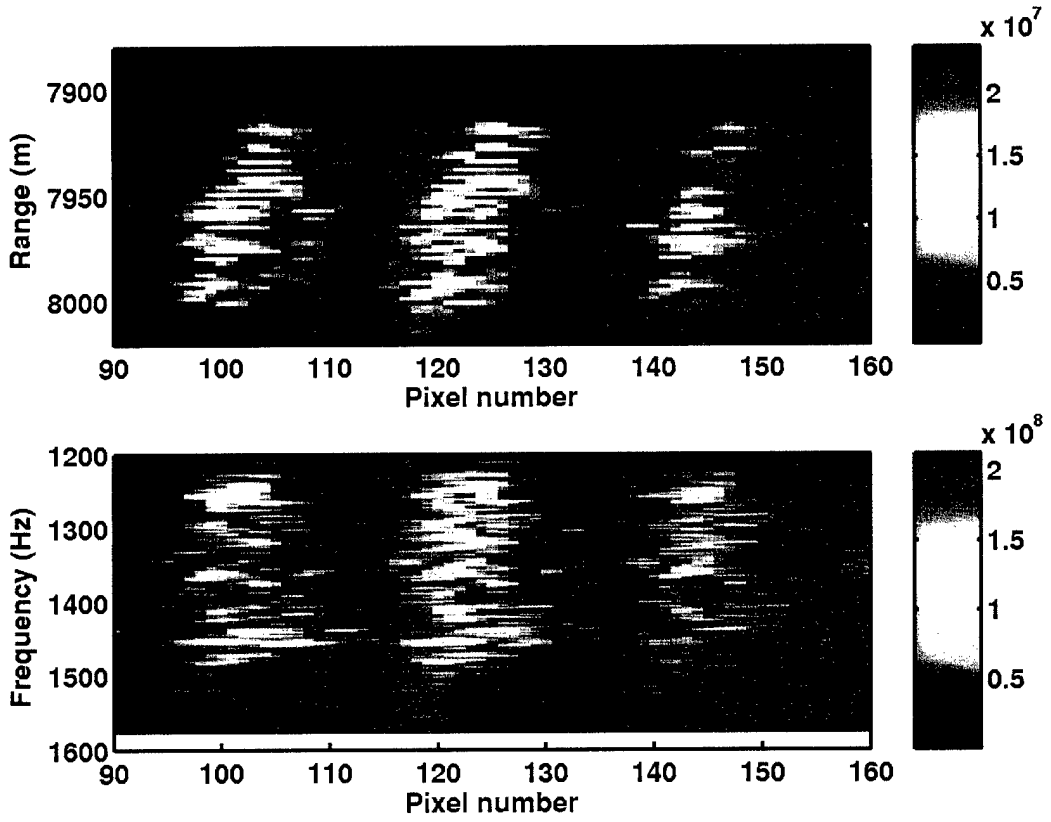

Figure 3-40. Time and frequency domain images of the Salmon at 8 km with 15 pings. The grating lobes repeat in both the time and frequency domain images, but weaker in this non-normalized representation. The largest peaks are at ~1255-1265 Hz and 1355-1370 Hz at pixels 121-122. There are additional peaks at ~1290, 1320, 1410, 1440 Hz and bands near 1455 and 1480 Hz.

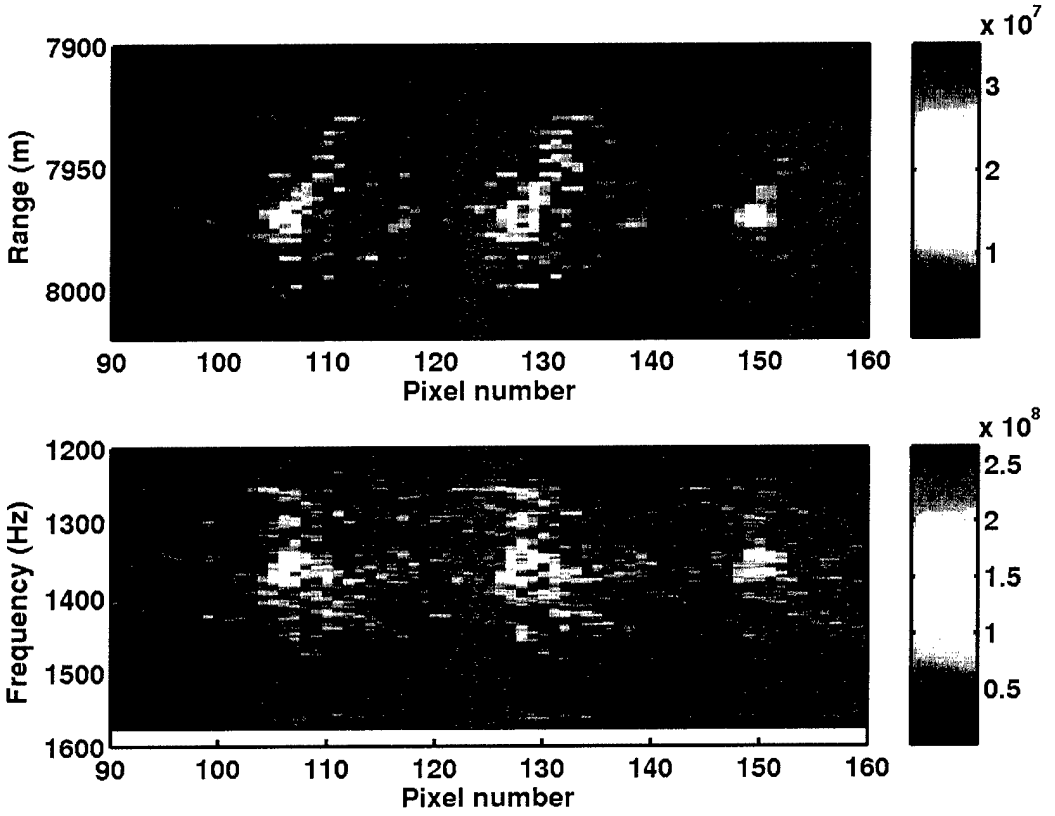

Figure 3-41. Time and frequency domain images of the Salmon at 8 km with 25 pings. The grating lobes show the same responses as the main image, but weaker in this non-normalized representation. The two largest peaks in frequency occur at ~1350 and ~1365 Hz. There are additional peaks at ~1265, ~1300, ~1400, and ~1450 Hz.

3.4.3 Bidevind Frequency Response

The Bidevind responses (Figures 3-42, 3-43, 3-44, 3-45, and 3-46) vary more with aspect than the Salmon responses do. Figure 3-42 shows a frequency response with barely more structure than the white background. This may mean that the SAS image is not well focused or that this is an aspect incompatible with the sonar frequencies. Figure 3-46, like Figure 3-42, shows two well separated pieces of the wreck. The frequency response in Figure 3-46 has a similarly smooth frequency response, although there are a few definite peaks. Figures 3-43, 3-44, and 3-45 all demonstrate more structured frequency responses, although none as distinct as the Salmon. In Figure 3-44, there is a very strong return in the SAS image that does not have a correspondingly narrow frequency peak, in fact, the responses approach white. Perhaps the time domain response is due to a corner reflector which has a frequency independent response.

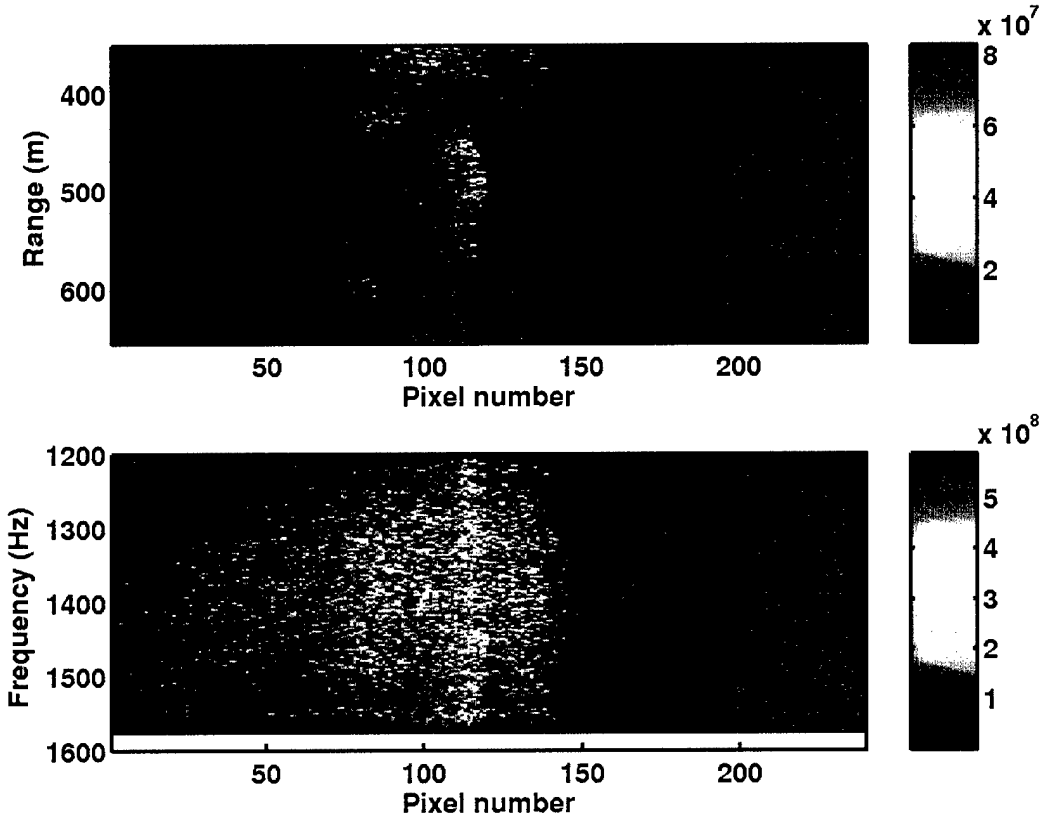

Figure 3-42. Time and frequency domain images of the Bidevind at 500 m with 6 pings and 35° forward look. The Bidevind spans pixels ~80-120. The frequency response is more structured in this region than in the other portions of this small scene. However, there are not the strong, broad peaks that were seen with the Salmon at this approximate aspect. The elongated portion of the Bidevind, at ~pixel 115, demonstrates multiple narrow peaks, but it is difficult to pick out the peaks since they are only one or two frequency and pixel bins in size.

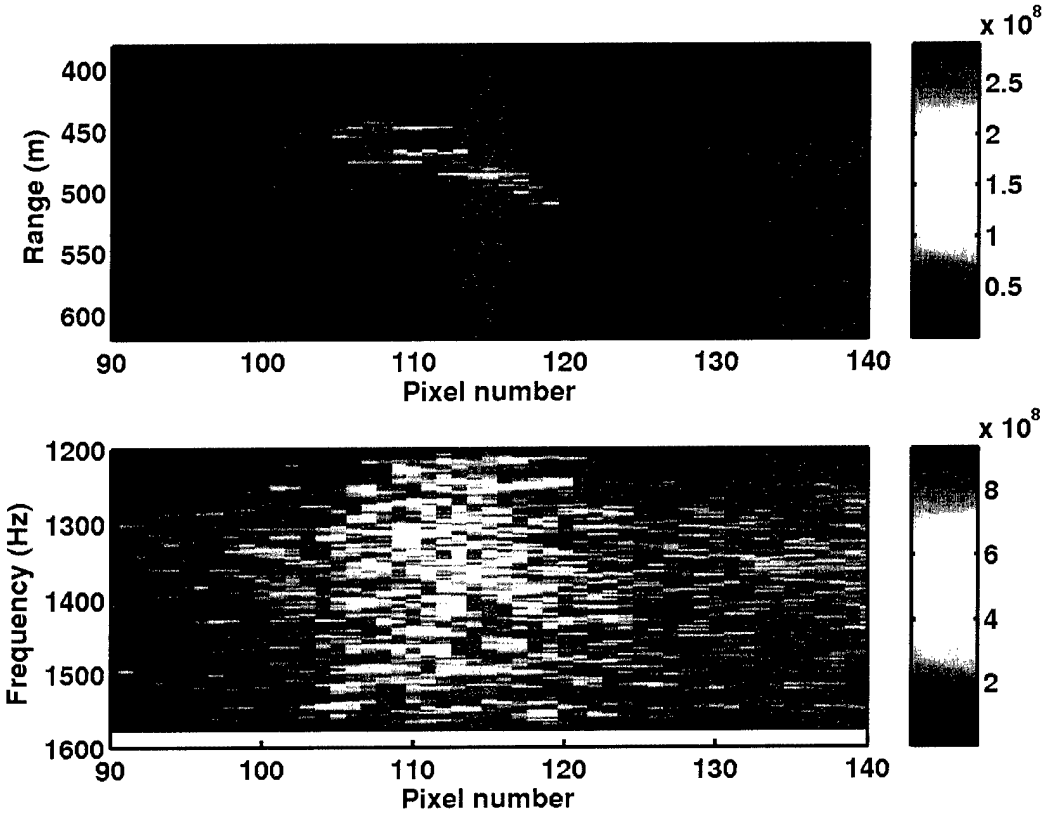

Figure 3-43. Time and frequency domain images of the Bidevind at 500 m with 5 pings and 5° forward look. The Bidevind spans pixels ~105-120. The frequency response contains broader peaks than in the previous figure. The largest peaks correspond to the strongest return in the time domain image at pixel 112. There are peaks at ~1280-95, ~1340, ~1365, and ~1410 Hz. Peaks at these frequencies are found at many other pixels as well. A few pixels have a peak at 1305 Hz.

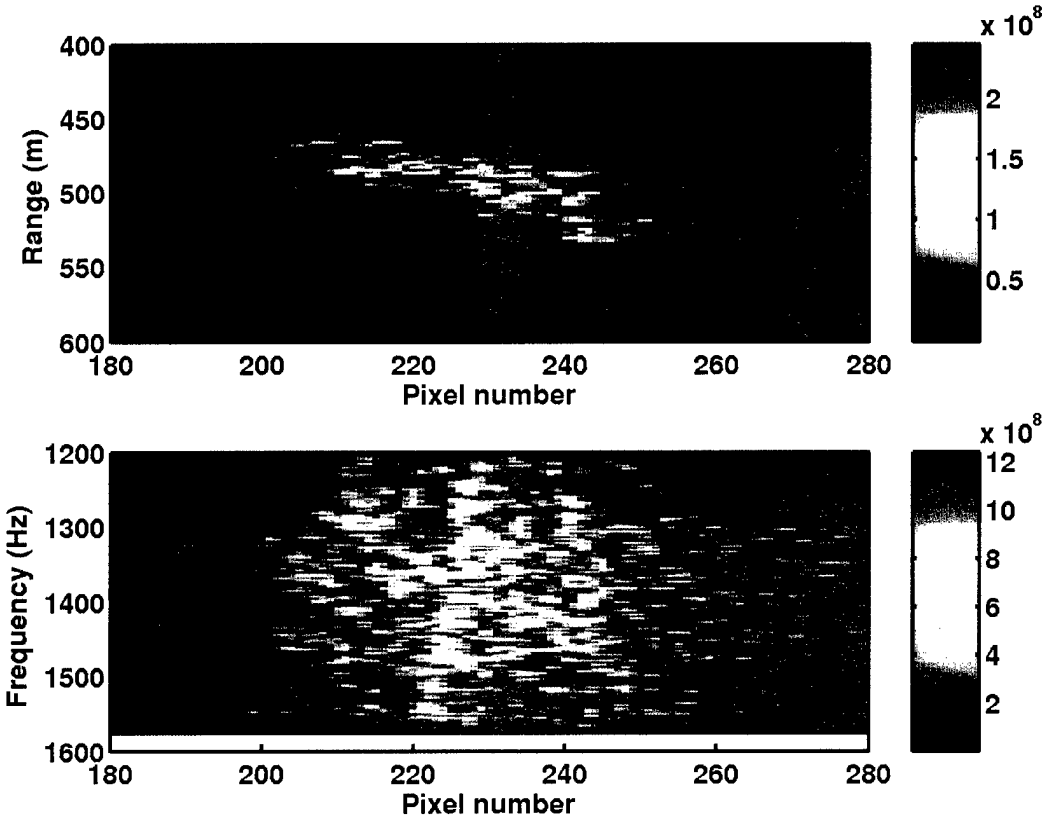

Figure 3-44. Time and frequency domain images of the Bidevind at 500 m with 7 pings and 15° backward look. In this instance, the strongest returns in the time domain image do not produce the largest peak in the frequency domain, although all peaks in frequency correspond with portions of the time domain image. The largest peaks are at pixel 235 and ~1415 Hz and at pixel 242 and ~1375 Hz. There are a batch of responses between pixels 227-30 at ~1315-65 Hz. Frequency structure appears elsewhere, but in no particular pattern.

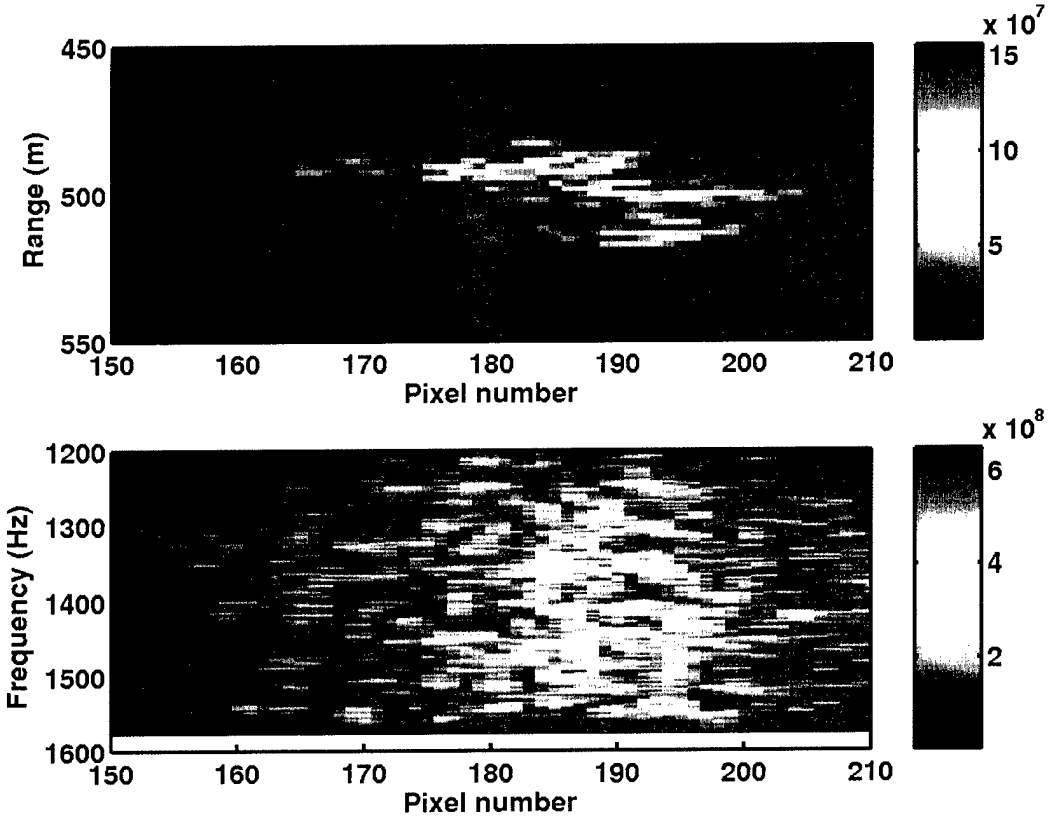

Figure 3-45. Time and frequency domain images of the Bidevind at 500 m with 7 pings and 40° backward look. Complicated frequency structures correspond to the pixels with strong returns in the time domain. Around pixel 187, large peaks are at ~1310, ~1335-40, ~1370, and ~1495 Hz. At pixel 190, there is a strong peak at 1305 Hz. Around pixel 193, there are peaks at ~1360, ~1420, ~1450-60, and ~1540 Hz.

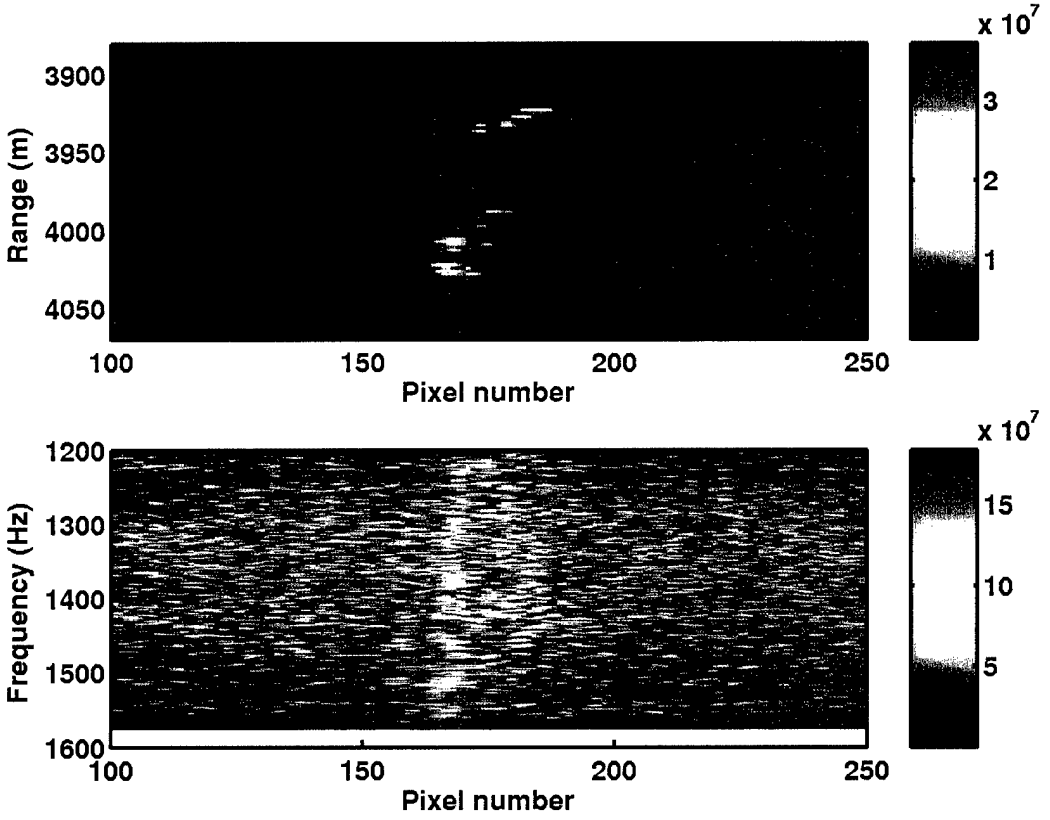

Figure 3-46. Time and frequency domain images of the Bidevind at 4 km. The frequency peaks are not as strong as in some other images, as can be seen by the higher background. The large, broad peaks in frequency correspond to the pixel which contains the strongest time domain response, pixel 168. The responses are strongest around ~1320, ~1365, ~1405, and ~1415 Hz. There are peaks in other pixels, but they are typically only one or two frequency bin/pixels in size so are difficult to resolve.

3.4.4 Frequency Response Discussion

The study of frequency responses was a small portion of this program, mainly due to the narrow bandwidth. The intent was to see what the frequency responses were and if there were any reason for further study. It is clear, and not surprising, that strong, physically structured objects have frequency dependent responses. From the two objects observed, aspect dependent frequency responses were observed as well as object dependent responses. The Salmon is known to be an intact[15] submarine and the Bidevind a wrecked freighter in at least two pieces with scattered cargo, including 7000 tons of manganese ore (Lawson 2004). These data hint at the possibility of using frequency responses for ASW classification. The lack of ground truth for the Bidevind, and thus knowledge of meter-ish

[15] Some reports are that the Salmon now contains large quantities of water, so some form of breach has occurred.

sized clutter, does not allow us to make firm statements about the utility of these frequencies for MCM usage.

3.5 Target Analysis

A fundamental objective of this program is to validate the utility of Long Range SAS for ASW and MCM use. The ability to detect targets and differentiate them from clutter is paramount. For our target detection and classification analysis we use one of the best known processors, the human eye and brain. The small quantity of data and funds require this usage, but for a proof-of-concept it is more than adequate since this study was not intended to extend to development of detectors or classifiers. In Section 3.2 we saw the SAS imagery produced; in Section 3.3 was a clutter discussion; and in Section 3.4 was the frequency response of the processed objects. In this section we tie those results together and analyze the ability to distinguish the Salmon from the Bidevind for ASW (Section 3.5.1) and MCM (Section 3.5.2) uses and a more general discussion of the utility of multi-aspect processing (Section 3.5.3).

3.5.1 Distinguishing Targets from Clutter for ASW

As intended, the trial location was dictated by the ASW target requirements. The Ex-USS Salmon was the prime target since it is, in fact, a bottomed diesel submarine. The Bidevind was chosen as the secondary target because it would represent target-like clutter in that there would be a long boat shaped piece. Each object was observed from multiple ranges and aspects. There are several characteristics to investigate to demonstrate the improvements in detection and classification that SAS could provide over standard active sonar processing. They are discussed below.

Size and location of an object are the most obvious improvement SAS can give to long range systems. We did not process data in the standard acoustic ASW manner, e.g., the passive time-bearing or the active range-bearing display, nor is a direct comparison to SAS possible from such data displays. However, raw phase history and SLS imagery are reasonable representations of these standard acoustic ASW processing methods. The raw phase history data is a time-range plot, but for a stationary target (which we have) the "smile" is the bearing to the object – the object appears in the side of the beam moving to CPA (broadside) and back out the other side. The SLS image is a time-broadside bearing or time-broadside range display. For Seahawk, the full aperture yields ~3° beamwidth, thus at 500 m the beamwidth is ~26 m, at 5000 m it is ~260 m, and at 15000 m it is ~800 m.

Standard acoustic ASW receivers have a constant angular extent, thus the contact dot in a range-bearing display will enlarge as the range increases. This effect is seen in the SLS imagery (compare, e.g., Figure 3-9 with Figures 3-12 and 3-19). SAS removes this increasing size with range problem since resolution is not a function of range. Figure 3-47 shows the Salmon at 4.5 km. The upper panel is an SLS image where all that can be seen is a bright return at ~4.55 km that extends 100 m in range and ~1000 m cross-range (it would be ~200 m in length without array motion). The right panel contains the same data processed with SAS and it is clear that there is an object of ~50 m range extent and ~100 m cross-range extent. This improvement in object size immediately yields a classification

advantage. Had the SAS image revealed a 500 m long object, then it could clearly be ignored. If the SAS image revealed an object much smaller than the known acoustic response size of the submarine, then it could probably be ignored as well. This size-knowledge improvement increases with object range for a given system, for the Salmon at 8 km, the non-SAS resolution would be about two times larger than in the SLS image shown here but the SAS image would have the same resolution as in the figure. Clearly not only is the size of the object more distinguishable, but the position of the object is as well. Thus once classified, its location is also well known.

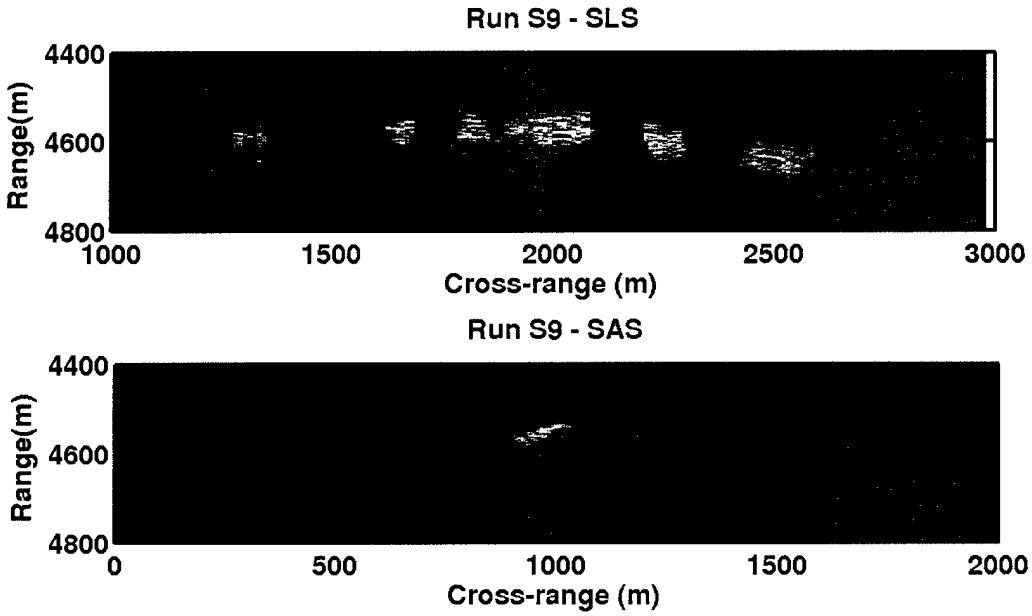

Figure 3-47. Comparison of SLS and SAS images of the Salmon at 4.5 km. The upper panel is the SLS image of the Salmon. Note that the bright returns are visible over 1 km cross-range. This is partially due to array motion, but the center 200 m in cross-range and ~100 m in range would show bright returns even in perfectly straight motion. The lower panel is the SAS image of the Salmon for 25 pings. Note the bright cigar shape in the center. The cigar shape is ~100 m in cross-range and 45 m in range. There are grating lobes in this image due to the along-track undersampling.

Once a detection can be ruled a possible target via general size considerations, there is additional information in the SAS image that can be used to distinguish targets from clutter. Detailed responses of the detected objects, such as shape and location of highlights, can be used for classification. This is a standard technique in MCM where the shape of an object and its shadow are used for classification. From Figures 3-10, 3-14, 3-15, 3-16, 3-10, and 3-21 and Figures 3-24, 3-25, 3-26, 3-27, 3-30, and 3-31, we can study a few of the differences between a submarine and a ship wreck. All the Salmon images show an elongated object about 100 m in length and <20 m width (typically the resolution of the image). The Bidevind images vary from a similar shape and size to something different, depending upon aspect.

We have also investigated the potential of using frequency response as a classification tool. As discussed in Section 3.4, we have neither proven nor disproven this as a possible technique. Further data collection on targets and clutter would be required to make such a decision. However, even if it can be used to rule out a few sources of clutter, it would be worthwhile to pursue. Its greatest potential would be using a combination, i.e., fusing, of an image-based classifier and a frequency-based classifier to reduce false alarms. This sort of work is in the research stages in MCM.

3.5.2 Distinguishing Targets from Clutter for MCM

The intent of the MCM portion of the trials was to collect data on whatever was available in the region as clutter and target, i.e., we were not to lay targets or target-like clutter. Unfortunately, there was very little in the way of targets or clutter for MCM usage at the Salmon site. The Bidevind quite probably contains mine-sized debris (i.e., 1-2 m in size) which would be clutter since the ship was not known to include mines in its cargo. The lack of ground truth makes determination of such debris nearly impossible. The array motion rendered few-meter sized resolution infeasible for this trial, thus a true study of the SAS imagery for MCM usage is not possible. The frequency response analysis indicated that there were frequency peaks from the Bidevind that were not present in the white response of the background. In Figure 3-46, the largest peaks are from the smaller piece of the boat. Thus it is not ruled out that mine-sized debris frequency responses can be detected from 4 km range. Ground truth is required to confirm or deny this. On the other hand, there is nothing that indicates that this type of system would not be useful for MCM.

3.5.3 Distinguishing Targets Using Multi-aspect Processing

In Section 3.5.1 we discussed the differences between the Salmon and Bidevind images, noting the changes with target aspect. Some of these aspect changes were due to different runs, thus ship/sonar headings, past the object, but most were within a given run. The processing for this latter reason is multi-aspect processing. This holds the strongest promise in terms of a classification tool. If, for example, the two images seen in Figure 3-48 were produced as broadside SAS images (the typical processed image in MCM) as seen in Figure 3-49. These would be a tough call for many classifiers to distinguish with a high confidence. The fleet would not necessarily have a chance to take a second pass to confirm the classification and would thus have to prosecute both objects. If, instead, all the S2 and T2 images (Figures 3-10, 3-24, 3-25, 3-26, and 3-27) were produced, the classifier would probably declare S2 a submarine with high confidence and rule out the other object. The broadbeam of the transmitter and the individual receivers permit such processing and we recommend it.

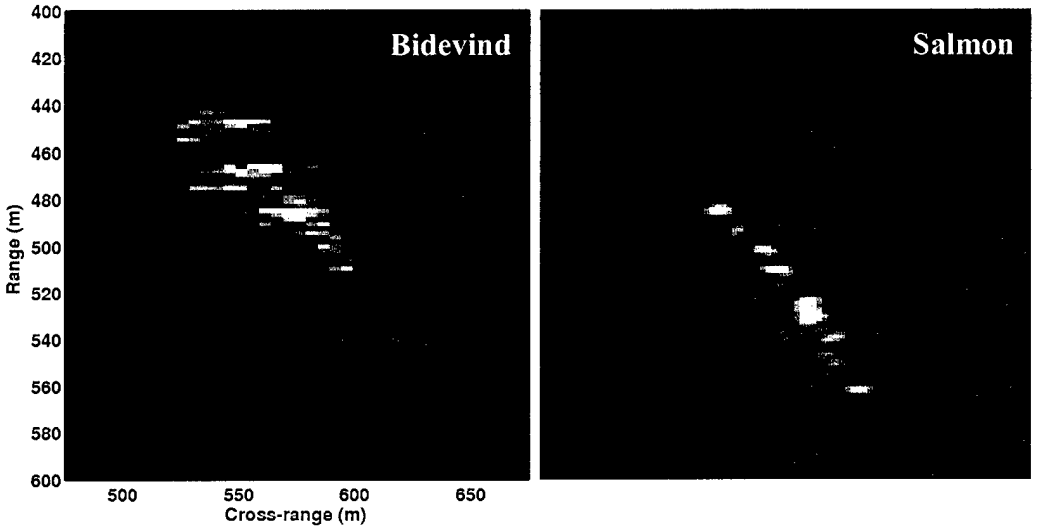

Figure 3-48. SAS images of the Salmon and Bidevind at 500 m range. In these two images, the objects look very similar. The differences could easily be due to array motion or the environment of the day rather than the object.

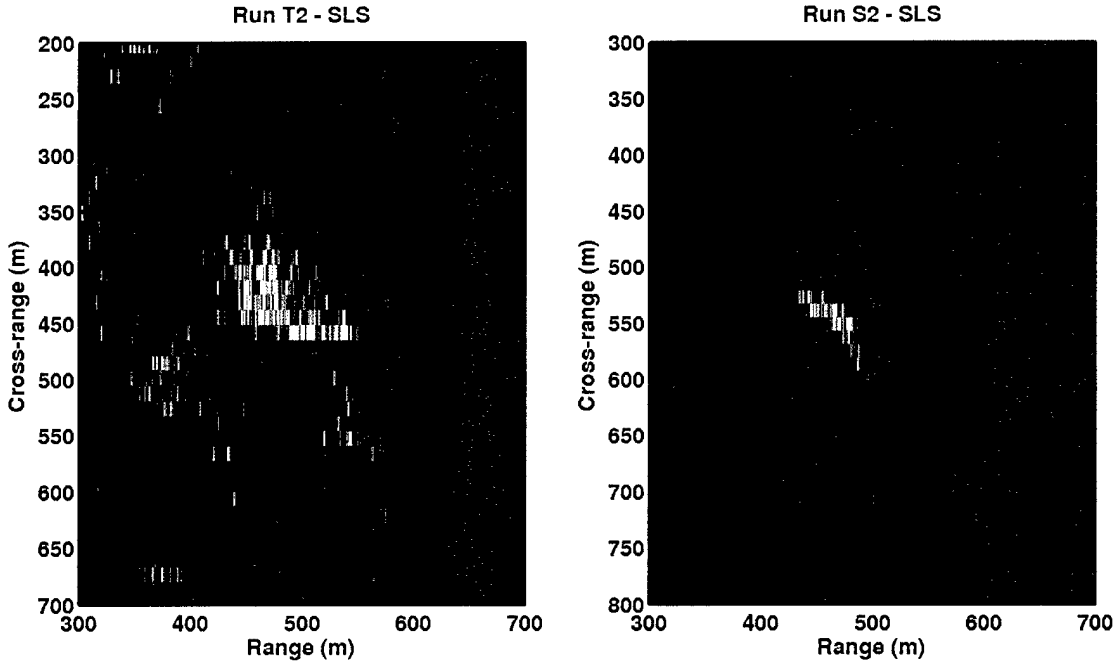

Figure 3-49. SLS images of the Salmon and Bidevind at 500 m range. These near range SLS images demonstrate that a submarine and a shipwreck can look very similar. Both are of similar length extent. The Salmon, on the right, is narrower than the Bidevind, on the left. However, there is more clutter in the Bidevind image and a lower transmit source level, which could conceivable be concealing a similar object.

3.6 Discussion

Overall this program was a success. However, not unexpected technical, environmental, and operational issues arose that required constant re-evaluation of the plan. Additionally, there were several unexpected problems, namely long and variable PRI, which disallowed any redundant phase centers and introduced grating lobes into the SAS images, and an uncluttered environment, which removed the possibility of using bright points for processing. Despite these problems, we focused the Ex-USS Salmon and the Bidevind into objects recognizable for what they were – namely a submarine shaped object and a ship wreck-like region.

In Section 3.6.1 we discuss the focusing issues, while in Section 3.6.2 we discuss multi-aspect processing. A discussion of ASW SAS with the Seahawk and its ilk is contained in the recommendations, Section 5.

3.6.1 Focusing Issues

The SAS processing we did to the data was not our standard processing, mostly due to the aforementioned problems. In other ASW SAS programs, we applied similar processing techniques to the techniques used here, although those systems were not designed for SAS. This technique was also similar to the prominent point processing of earlier MCM DARPA programs (e.g., Nelson et al. 2002) in that a bright object was forced to focus by compensating for the non-perfect phase histories in whichever way necessary. In the MCM SAS development chain, this "snippet" processing was a first stage, so we are not dismayed by this requirement for these data collected on our first ASW SAS trial.

This method proves that SAS is possible with a Seahawk-like system. However, it was very analyst intensive. From the SLS imagery, the towbody motion, and the motion applied to the data for correction, it was clear that the system suffered from a large amount of yaw and sway. Due to the flexible nature of the array, this was not as easy to estimate as it is from the data recorded by a rigid array where the position of each receiver is know with respect to each other, the transmitter, and the towbody. It is possible to know this information, to some level, with the use of motion sensors in the array. Heading and depth sensors placed at the front, middle, and end of the array in conjunction with the sensors in the towbody and models of how the arrays move would yield the relational position information required. As part of an earlier DARPA program (Nelson et al. 2002), using array motion simulations, we simulated SAS imagery from a 50 ft long towed array with perfect array motion knowledge, estimated array motion knowledge, and no array motion knowledge. We did not apply our motion estimation techniques, such as RPC, to the data but only used the simulated motion sensor data and PGA. The images where no motion corrections were made was not focused but the images with the estimated motion compensated were reasonably focused, see Figure 3-50 (note that this simulation was at a higher frequency than Seahawk and at shorter wavelengths smaller motions have a larger effect. The study was over several frequencies and as the frequency was decreased the focusing improved, so we expect this to work well for Seahawk frequencies). We expect that this sort of processing, along with sonar data derived motion estimates, would allow us to focus data over a whole scene without the being so analyst intensive.

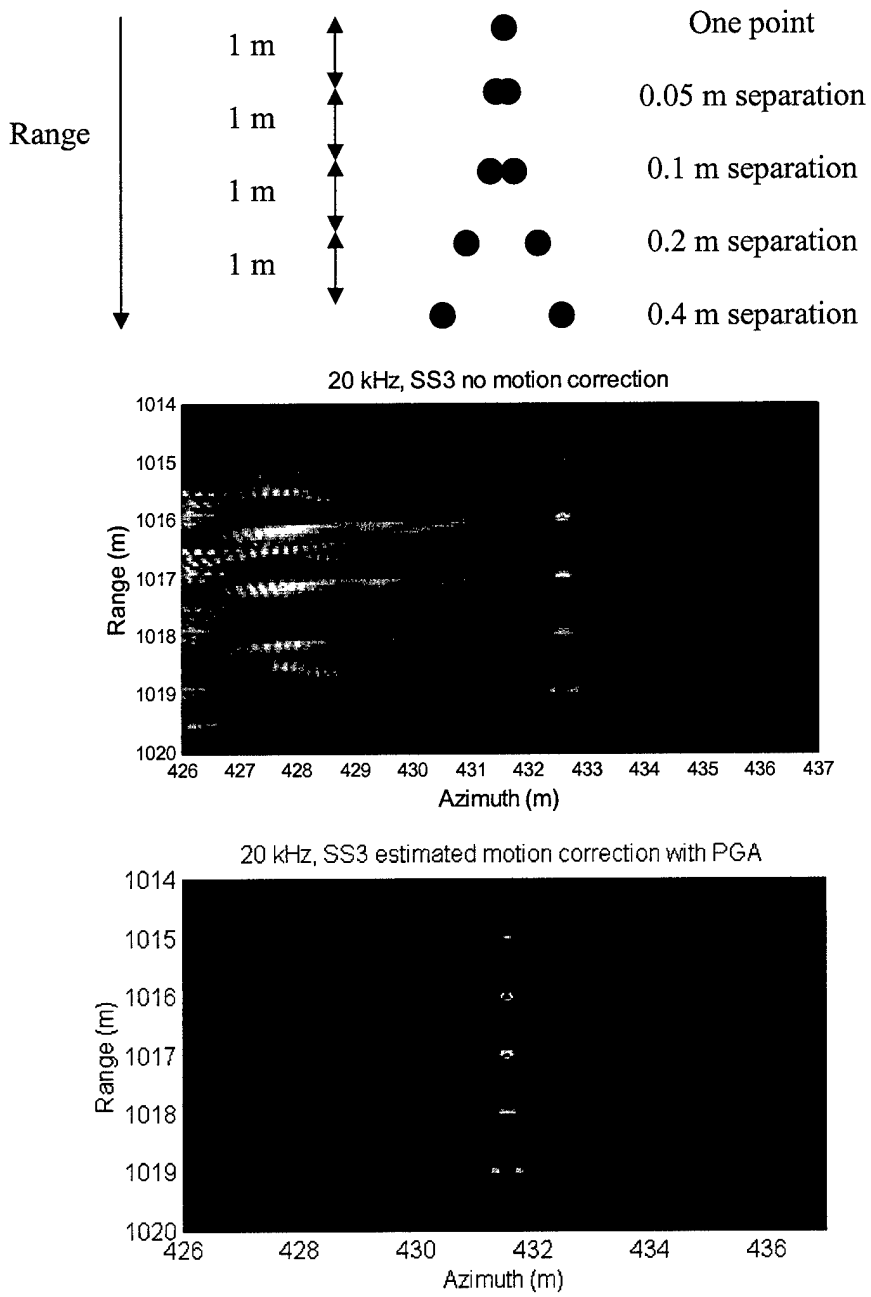

Figure 3-50. Simulated towed array SAS data of nine point objects to show resolution. 15 m array, 5 cm elements, 20 kHz, 5 kt tow speed, sea state 3. Upper panel is schematic of organization of point targets. Middle panel contains the image with no motion correction applied. Bottom panel is the simulation corrected with array motion from a Kalman estimator and PGA.

When embarking upon this program, the intention was to create SAS images with resolutions between 2 m and 10 m. While we never achieved 2 m resolution, better than 10 m resolution was achieved in Runs S2, T2, and T9 with S9 and S11 achieving only

slightly worse resolutions at 12 m and 11 m, respectively. All indications were that the processing method required for these data combined with the array motion of the system, that was not measured, precluded achieving higher resolutions. Meaning there was no ocean physics reason for not achieving the desired resolutions, only an engineering issue of non-estimated and uncompensated motion which could be alleviated through motion sensors in the array.

3.6.2 Multi-Aspect Processing

The standard MCM SAS processing is of a broadside image only. This lack of processing in MCM is typically due to the narrow beams available at the frequencies, usually >50 kHz, used rather than a fundamental issue of SAS processing. The processing of SAS images in other beams requires wide receiver and transmitter beam. The Seahawk, with its 1.4 kHz, 120° transmit and omni-direction receive beams, afforded us the opportunity to investigate non-broadside beam SAS processing. As shown most dramatically in Figure 3-10, multi-aspect SAS processing has the potential to provide multiple looks at an object from only one pass. This is a time saver in terms of classification. As seen in Figure 3-48, two different objects can look the same from some aspects, so the ability to add more aspects rapidly will reduced false alarm rates and improve probability of correct classification.

The multi-aspect processing achieved in this program was using our non-standard SAS processing techniques. This is not a requirement. Once we have a properly instrumented array, as mentioned in Section 3.6.1, and can produce imagery in a more automated manner, multi-aspect processing would be a relatively simple addition to the processing toolkit. There will be issues in motion compensation and perhaps additional motion estimation techniques would be required, but we expect these to be along the lines of orientation (i.e., processing a different beam) corrections, and thus similar to those needed for ASW SAS processing.

The largest issue in multi-aspect processing will be the increase in processing requirements and image output. If a small number of aspects, e.g., three, were required for classification, a tripling of processing/storage requirements may be acceptable. However, should classification studies prove to require more aspects, the processing required and data produced may swamp computing resources. For a deployable system, the ability to return to a possible detection and then create multi-aspect imagery over a small region may be the preferred method. This is an issue to defer to the future, but to keep in mind during system development.

4. CONCLUSIONS

The purpose of this program was to demonstrate, with an at-sea trial, the concept of collecting and subsequent SAS processing long range data from a mono-static towed array sonar system. Both ASW and MCM capabilities were to be addressed with the demonstration. The data collected during the at-sea trial 7-10 October 2003 of the NY/NJ coast at the Shallow Water Test Facility succeed in this demonstration.

As seen in Section 3.2, we were able to SAS process into imagery the Ex-USS Salmon and the Bidevind at 500 m, 4000-4500 m, and 8000 m (for the Salmon) ranges. At the 500 m ranges, the SAS images are a small improvement in terms of resolution (~5-7 m) over more conventional sonar processing schemes (~25 m), but this is expected for these short ranges which can be achieved with many other systems, especially those at higher frequencies. The 4000-8000 m range images are nearly tactical ranges for ASW systems. In these cases, the imagery produced demonstrates much higher resolution (~10 m) than a standard system would produce (>300 m). SLS imagery is not the standard in the ASW world, however, the standard time-bearing or range-bearing sonar products would never be able to pin-point an object size and position with the same accuracy. More importantly, the increase in resolution and change in format to imagery (such as used in MCM) demonstrate the potential for classification with such a system. We also demonstrated the potential usefulness of multi-aspect processing for classification. This type of processing is only possible with broad transmit and receive beams, which exist in ASW systems.

We chose the trial location knowing that a bottom diesel submarine was present since this type of target is of strong interest to the ASW community. Unfortunately, due to local conditions there was little geologic clutter at our frequency and due to weather/equipment problems, we were only able to collect data against one other known object, the sunken freighter Bidevind. Thus a conclusive or even minor study of distinguishing targets from clutter was not possible. However, this one object has the good fortune of being target-like clutter. As discussed in Sections 3.4 and 3.5, the two objects can be distinguished from one another at certain aspect angles. If images from multiple aspect angles were used for classification purposes, it looks tantalizingly possible to lower false alarm rates. Since multiple aspect angles can be collected and processed from one pass by an object, this is a useful tool to develop and may not add extra time requirements into a CONOPS with such a system.

While the frequency response study discussed in Section 3.4 was initially aimed at MCM concepts, it did demonstrate potential for ASW usage at well. The Salmon and Bidevind had apparently different frequency responses. There is a chance that some data sets were better focused and thus more structured responses would have been detected which would falsely lead to this conclusion. The small bandwidth, 400 Hz, meant that detecting the multiple responses from resonances would be difficult or impossible, but there are some hints of possible resonances from a few aspects. The frequency responses did alter with aspect angle, which is expected, thus these data are probably good. This study was not conclusive, but indicate that there is a possibility for an additional classification clue.

Further work with a larger bandwidth and more objects is desired before an answer can be given, but it is clear that the frequency response of objects could be useful.

This trial only addressed the use of SAS for zero-Doppler targets at 1.4 kHz. There are a two main reasons for this: first, SAS is best suited for zero- and low-Doppler targets; and second, current ASW systems are poor at zero- and low-Doppler targets, so this is a niche SAS would fill with ease. This does not preclude SAS imaging of moving targets. In fact, we have addressed this in other programs. The key need for SAS imaging a moving target is a velocity hypothesis. Current tracking sonars could supply such a clue and the subsequent SAS image could be used for classification purposes. We see a SAS system merging into standard active ASW sonar systems and thus giving these systems a revolutionary increase in capabilities.

The MCM portions of this program had a slightly different focus than the ASW portions. The main thrust was to study clutter at 1.4 kHz in both SAS images and frequency responses. As stated previously, the trial site was apparently devoid of significant clutter. The Salmon was a little large to be mistaken for a mine (although a bottomed diesel submarine can be considered an intelligent mine). The Bidevind, with all its wreckage held the most hope clutter studies. Due to array motions, we were unable to achieve the theoretical 2 m resolution with the system. Thus, it was not possible to definitively identify mine-like clutter in the data. In terms of frequency responses, similar comments as mentioned above with respect to ASW uses of frequency responses apply – different objects appear to have different frequency responses. Nothing in this study indicates that frequency responses cannot be detected from long ranges. It is clear that the Atlantic Ocean and its bottom north and east of the Hudson Canyon has a nearly white frequency response from 1.2–1.6 kHz.

This program has shown the potential usefulness of SAS for ASW use, especially in terms of classification and reducing false alarms. Any reduction in number of detections to prosecute is welcomed by the Navy. In Section 5 we present our recommendations for further work, but in general it is to proceed with this line of work. Additional clutter studies are paramount. ASW uses are clear and MCM uses are possible too. The use of the data collected during the October 2003 trial for classifier development is another point made.

5. RECOMMENDATIONS

This program was originally proposed as the first phase of a three phase program. The first phase as a proof of concept with existing hardware, the second to demonstrate the concept's significance by using more appropriate hardware and more rigorous testing, and the third phase to transition into the fleet. With the success of the trial, we wholeheartedly recommend continuing this work with the next phase.

In Section 5.1 is a more detailed discussion of the concept for the next phase. Section 5.2 describes possible CONOPS to demonstrate the role a fleet-ready system would play in ASW scenarios. Section 5.3 details our suggestions for further processing development to achieve the plans of 5.1 and 5.2. Section 5.4 suggests further work in frequency responses.

5.1 Next Phase Concept

The program described in this report was a proof of concept. We have proven that long range SAS, with all the bottom bounces and other multipath issues, can work. A system such as the Seahawk can be developed into an ASW SAS system and applied to the ASW problem in a tactically valid operational concept. The key to demonstrating this is to show that this technique will be able to enhance an operator's ability to distinguish targets from clutter at reasonable ranges and speeds. By taking the system out to sea and collecting a large quantity of data against clutter we can characterize the clutter. Additional trials including a target will then allow us to demonstrate how the clutter looks different (or not) from targets. However, the L-3OS Seahawk system as it is currently configured will not allow such trials to occur.

To undertake a study of clutter, the Seahawk system requires repairs and upgrades to the configuration used in October 2003. Certain changes were made to the Seahawk for the October trial to make it SAS compatible, however, some of these changes were not robust and anticipating more strenuous at sea trial periods, better versions need to be installed. There is a key upgrade to Seahawk for the future SAS work – the addition of motion sensors to the arrays and extending the length of the arrays. The acoustic data in this program could only be SAS processed around regions containing a strong object in order to derive the positions of the receive array elements. This was an inherent known hardware liability deemed acceptable for the experiment as devised. Motion sensors in the arrays will fix this problem and allow us to image scenes without strong objects in them and to better image scenes with objects. To be able to demonstrate tactical speeds and distances, we require longer arrays to allow proper along-track sampling of the synthetic apertures. By doubling the length of the arrays (which cost-wise is an additional small fraction of the work required to add sensors to the current arrays), we will be able to collect data at 5 km range while traveling 6 kt and data at 10 km while traveling at 3 kt (the minimum speed of the system). Such tests will demonstrate nearly tactical speeds and distances, although in separate runs. For both at once, it is simply an engineering matter of building longer arrays, and the lengths required (>100 m) have already been demonstrated in other systems.

We recommend three trials for a follow-on program to demonstrate the tactical advantages of such a system. The first is an engineering trial to test the new arrays and the hands-off processor. This trial would be in U.S. waters for convenience. A trial off the Southern California coast or back to the Shallow Water Test Facility region near Hudson Canyon in the Atlantic is reasonable. Both locations contain clutter that would be useful to collect data against after the system is proven. Each has its advantages and disadvantages during the year (weather, marine mammals, etc.). The second trial will be solely to collect clutter in a region of interest. The clutter should challenge the system, such as found in many WESTPAC locations. For the third trial we suggest the system to be tested in an ASW exercise where with the opportunity to collect data against a zero-Doppler target as well as clutter. Additional trials may be useful to characterize clutter in different regions of the ocean.

5.2 Concept of Operations

While it is important to know if an ASW SAS system can function (i.e., distinguish targets from clutter), it is also important to know if there exists a method to use the system in the Navy effectively. To illustrate possible uses for an ASW SAS towed array system, DTI examined a set of scenarios developed at the Applied Physics Laboratory (Benedict 2001) and developed a few notional CONOPS for these scenarios (Chang 2004). In particular, we looked at ASW cueing in support of carrier battle group (CVBG) protection, port/theater ballistic missile defense (TBMD) unit/sea lines of communication (SLOC) protection, and choke point control/large area search operations. The SAS system could be placed on a variety of platforms. Four examples examined included (1) a surface combatant using the SQS-53c with an 1800 ft array zig-zagging at 20 kt; (2) a littoral combat ship (LCS) using a 1 kHz VDS with an 1800 ft array at 20 kt; (3) an unmanned surface vehicle (USV) using a 1 kHz VDS with an MTFA-like (600 ft) array up to 15 kt; and (4) an USV using a 1 kHz VDS with a shorter array (~150 ft) up to 10 kt. Platform (4) has a system comparable to our next phase concept (Section 5.1).

Our analysis shows that SAS implemented on even this small variety of assets can fulfill a number of ASW cueing roles in the WESTPAC, even against low/no-Doppler threats. Initial clearance of op areas can be accomplished within 24 hours for large CVBG OPAREAS (200 x 200 nm^2) using 5 - 6 combatant or LCS class SAS platforms and for smaller CVBG OPAREAS (80 x 80 nm^2) using 2 – 8 USV class SAS platforms. One or two SAS-capable combatants or LCSs deployed in front of the CVBG/TBMD unit can protect it or the SLOC. A reasonable number of SAS platforms can protect the OPAREA, although this might be better accomplished with distributed systems. Choke point lane clearance can be accomplished with LCS or USV classes of SAS platforms in a single transit along lane. LAS can be accomplished with combatant or LCS SAS within reasonable amount of time.

Thus an ASW SAS system could have an operational use in the fleet. The aforementioned is but one possible CONOPS. We recommend continuing with the development of the ASW SAS system. Additional CONOPS should be developed as well, preferably in consultation with the fleet to best satisfy their needs.

5.3 Further Processing Development

There are four key processing developments we recommend as a part of continuing this program: multi-aspect SAS processing; real-time towed array processing; moving target SAS processing; and target detection/classification processing. We have at least touched on all of these topics, but will re-iterate our thoughts for those which we only alluded to previously. The multi-aspect SAS processing has been discussed in Section 3.6.2 and would be an asset for classification.

The real-time towed array processing is required for a deployable system since waiting much longer can mean the difference between neutralizing a threat and being hit. This requires the motion sensors described in Section 5.1, codes to incorporate those measurements into SAS processing, additional codes to efficiently process towed array data, and plenty of data for testing. We expect a real-time towed SAS processor to be similar to our rigid body SAS processor, PRO*SAS*^{TM}. In fact, the recommended development parallels the development of PRO*SAS*^{TM}, which has been successful used on a Hugin autonomous underwater vehicle and other towed systems.

We have demonstrated the long range ASW SAS detection and classification concept on a bottomed diesel submarine, which is a feat current ASW sonars cannot perform as easily. However, current active and passive sonar systems can locate and track a moving submarine very well. SAS has the potential to enhance detection and classification of moving targets. With a velocity hypothesis, which could be provided by a tracker using more standard sonar processing of the data, we can change the reference frame of the data and focus an image of a moving target. This requires development starting from simulations and SAS data, preferably in an analyst intensive mode. Once a processor is created, it could be merged with a tracking system to enhance the detection and classification capabilities.

The multi-aspect processing and the moving target processing have the potential to reduce probability of false alarms and increase probability of correct classification. However, the manner in which they would be used, namely in an imaging mode, is different from current ASW classification schemes. Thus developing a classifier is required, though this need not be from scratch since MCM classifiers operate similarly.

We recommend further work on all of these processing topics. All will benefit ASW SAS and the Navy's ability to protect its ships from lurking non-friendly submarines.

5.4 Frequency Responses

The work on object and clutter frequency responses in this program was of lower priority than the long-range SAS aspects. However, that is not to say that it is of low importance. Frequency responses of an object can be a distinctive signature. Spectroscopy is often the only tool available to positively identify an object that cannot be touched and poked in a lab, be it a particular type of star, the components of a Mars rock, or an object on the bottom of ocean. Sound frequency responses, or spectra, can probe the structure of an object in an analogous manner. The berths, torpedo tubes, etc. of a submarine will produce

a different set of responses from a sunken boat or coral reef. A mine will respond differently from the scattered remains of a destroyed boat or garbage dump.

The frequency responses of the EX-USS Salmon and the Bidevind were different enough to be suggestive of the potential classification uses of this technique. While an appropriately chosen 400 Hz band might be effective, i.e., there may be a frequency regime where the target of interest responds every time and clutter very rarely does, it was too narrow to make definite statements from a survey point of view in this program. We do recommend future studies of the frequency responses of both ASW and MCM targets and clutter. A study should be done with a larger frequency band initially. If key frequency ranges are identified, smaller bands could be used in a deployed system.

5.5 Automatic Target Recognition (Classification)

Whether for autonomous operations or to aid humans, an automated target recognition (ATR) system will be needed in ASW. Such a system will detect and classify objects and report this information to those deciding to prosecute or not. A major component of such a system, in terms of effort and difficulty in development, is the classifier. Developing a classifier requires large quantities of target and clutter data for development and testing.

The data collected against the Ex-USS Salmon was from all around the submarine, i.e., multiple aspects, and multiple ranges. There was no clutter in the area and the ocean conditions were favorable on the data collection days. The LRSAS data set is the most comprehensive set collected against an actual submarine, albeit over a small frequency range. Due to all of these conditions, it is comparable to the data sets collected on platters for mine countermeasures work. The LRSAS data set does contain a slightly less comprehensive set of clutter data in the Bidevind runs.

Thus we also recommend using the LRSAS data set for developing the target models of an ATR system (classifier) for ASW. This will require additional processing of the data, in particular the initial processing of most of the data. It is a rich data set and should be used to the fullest extent possible.

REFERENCES

Benedict, J. 2001, "Illustrative U.S. Military Operation in a Contested Area Scenario & Associated ASW Objectives/Missions/Metrics," APL/JHU Presentation, 8 May 2001.

Chang, E. 2004, "Synthetic Aperture Sonar (SAS) for ASW CONOPS and Recent Results," presented at the NDIA 2004 Undersea Warfare Technology Spring Conference, 17 March 2004.

Chang, E. & Campbell, J.D., 2003, "Synthetic Aperture Processing for Tactical Active Sonar," presentation at 2003 ONR Active Signal Processing Review, DT-PRW-0370-03001.

Chang, E., Marx, D.S., Nelson, M.A., Gillespie, W.D., Putney, A., Warman, L.K., Chatham, R.E., & Barrett, B.N., 2000, "Long Range Active Synthetic Aperture Sonar Results," IEEE Oceans 2000 Conference Proceedings.

Chatham, R.E., Nelson, M.A., & Chang, E., 2000, "Results from the DARPA and ONR Synthetic Aperture Sonar Programs," AeroSense 2000 Conference Proceedings.

Lawson, S. 2004, "M/S Bidevind - Norwegian Merchant Fleet 1939-1945," web page at http://www.warsailors.com/singleships/bidevind.html, last accessed 28 July 2004.

Marx, D., Nelson, M., Chang, E., Gillespie, W., Putney, A., & Warman, K, 2000,"An Introduction to Synthetic Aperture Sonar," IEEE SSAP 2000 Conference Proceedings.

Nelson, M., Warman, L.K., Marx, D., Chang, E., Putney, A., & Tinkle, M. 2002, "The DARPA Synthetic Aperture Sonar Technology Demonstration, Phase 3 Final Report," DTW-9803-02001.

New Jersey Scuba Diver, 2004a, "Deep Sea Wrecks 2: Bidevind," http://njscuba.net/sites/list_deep_sea_2.html, last accessed 23 August 2004.

New Jersey Scuba Diver, 2004b, "Texas Tower #4," http://njscuba.net/sites/wreck_texas_tower.html, last accessed 23 August 2004.

NUWC Division, Newport 2003, "Narragansett Bay Shallow water Test Facility," http://www.npt.nuwc.navy.mil/Ranges, click on "Ex-Salmon Site," last accessed 23 August 2004.

Putney, A., Chang, E., Chatham, R, Marx, D, Nelson, M, & Warman, L.K., 2001, "Synthetic Aperture Sonar – the Modern Method of Underwater Remote Sensing," IEEE Aerospace 2001 Conference Proceedings.

Smith, K.B. 1999, "Parabolic Equation Models," http://oalib.saic.com/PE, last accessed 19 August 2004.

Smith, K.B. & Tappert, F.D. 1999, "Monterey-Miami Parabolic Equation," http://oalib.saic.com/PE/mmpeintro.html, last accessed 19 August 2004.

Tamul, J. 2001, "GDEM Variable Extraction - Web Version 1.0," https://128.160.23.42/gdemv/gdemv.html, last accessed 23 August 2004.

APPDENDIX A: SEA TRIAL I PLAN FOR ASW/MCM SAS VALIDATION EXPERIMENT WITH THE SEAHAWK

Originally: DTW-0223-03010

Sea Trial I Plan for ASW/MCM SAS Validation Experiment with the Seahawk

September 2003

Prepared By:

Angela Putney

TABLE OF CONTENTS

1. INTRODUCTION

The "Long-Range, High Coverage Rate Synthetic Aperture Sonar for ASW and MCM Phase I: SAS Validation Experiments" project (hereafter LRSAS) requires several sea trials for the validation of the concept. This document describes the motivation, pre-trial in-lab and in-water tests, the planned trials, operational procedures, and responsibilities for the first of the sea trials planned as part of the validation of long-range, high coverage rate SAS for ASW and MCM.

The goal of the trial is to collect sonar data suitable for SAS processing on bottom objects of sizes similar to submarines and to mines and general clutter at the system frequency out to 5 km. The objects are those that already lie on the sea floor, i.e., they are not placed there by this program. If all goes well, the data, to be processed after the trials, should show the feasibility of using the Seahawk or similar systems for detection and classification of objects underwater at long ranges. The specific goals of this trial will be to collect data appropriate for imaging from at least one known object from at least three ranges and to collect data against at least one region of unknown but expected clutter from the same ranges. We expect to be able to collect data for multiple targets and clutter regions during the course of the trial. The location of the trials is approximately 80 nmi south of Long Island and east of New Jersey, see Figure 1-1. There are numerous man-made targets of opportunity as well as geophysical clutter available in the general area that is marked with a red line. Details on the targets are in Section 5.

There are two corporations involved in the trials, Dynamics Technology, Inc. (DTI) and L-3 Communications Ocean Systems (L-3OS). The general responsibilities are the overall project and SAS processing for DTI and the sonar system (the Seahawk) and vessel for L-3OS. Detailed responsibilities are described in Section 3, along with permit, data rights and safety information.

Aside from the aforementioned sections, this document contains descriptions of systems and procedures. Section 2 describes the systems to be use on the trial. Section 4 explains the checks to these systems. Section 5 describes the basic trail overview, i.e., the components of an individual run. Section 6 describes the mammal mitigation measures to be conducted on this trial. Section 7 is the day to day plans, i.e., which runs will be conducted on which day.

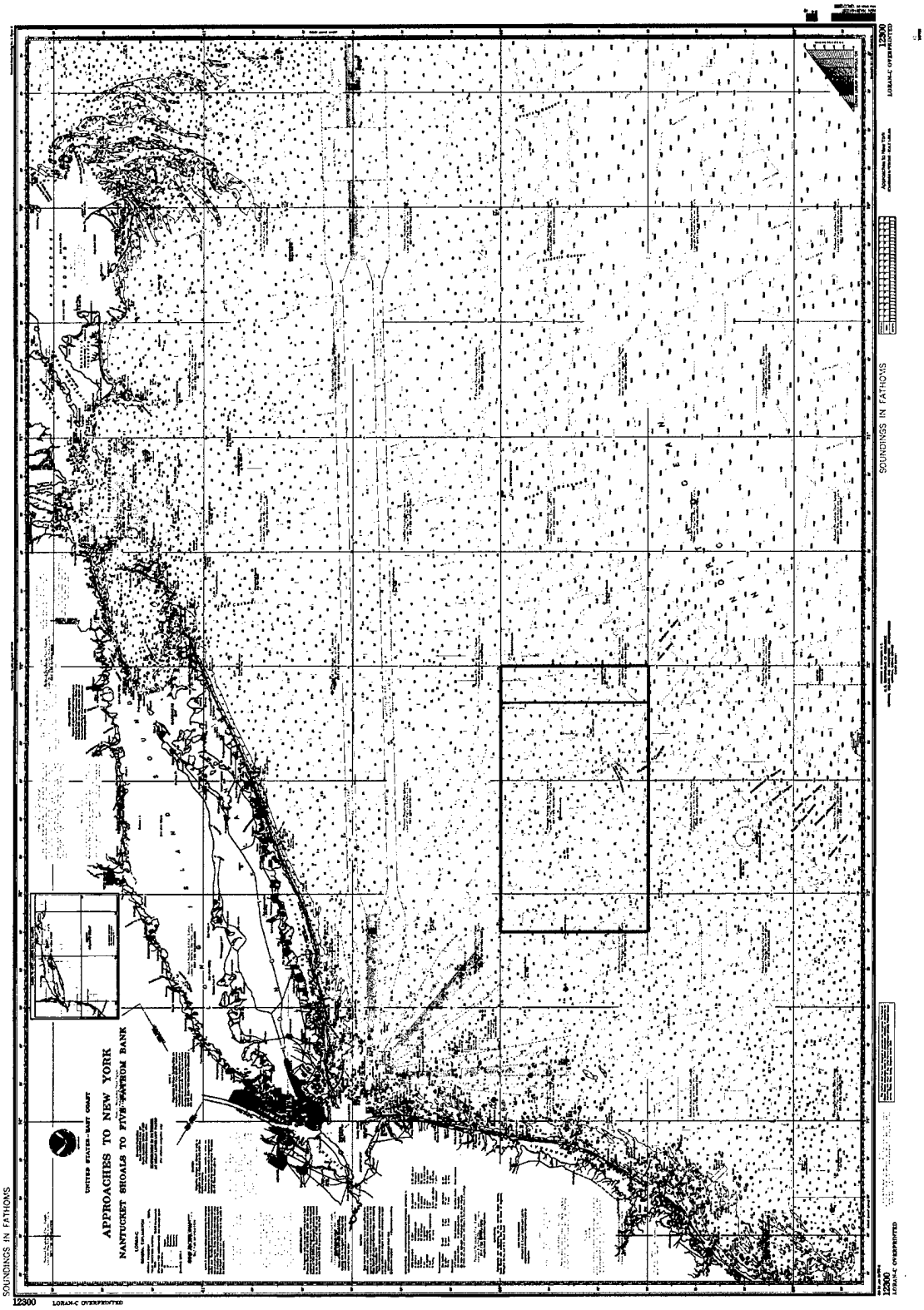

Figure 1-1. Chart showing general test area for LRSAS trials. Red box on the right marks the planned trial region.

2. SYSTEMS DESCRIPTIONS

This section contains the basic descriptions of the different pieces of equipment needed for the sea trials, in particular, the sonar, data recording, data processing, and vessel. The descriptions will contain some key constraints, e.g. minimum and maximum vessel speeds. Equipment operating manuals are to be found elsewhere.

2.1 Sonar equipment

The L-3OS Seahawk system consists of a variable depth sonar with a twin-line array trailing behind a towed body. The array comprises 96 acoustic channels, and forms narrow beams (4½° wide in azimuth when steered to broadside) with no port-starboard directional ambiguity. The arrays are housed in two acoustic modules, each approximately 21 meters long, with a five centimeter diameter. They are towed behind a compact, stabilized tow body. The tow body and acoustic modules are designed to provide stable, low-noise operation at speeds from 3 to 20 knots.

The array data can be processed to provide passive or active acoustic analysis. Active mode operation in achieved with the aid of an array of 16 compact, high-efficiency transmitters which extend from the tow body. Active operation is centered around 1400 Hz. At this frequency, the transmitters in the tow body provide up to 219 dB re μPa of omnidirectional acoustic power. The tow body transmit array can also provide directional acoustic transmission, achieving up to 221 dB re μPa directed to any one of four quadrants. A variety of continuous wave (CW) or frequency modulated (FM) waveforms can be broadcast. These waveforms are chosen by the operator, and can be optimized according to water depth, target speed, and other environmental and operating conditions.

A single tow cable supports the tow body. It is partially faired, and allows operation down to 265 meters' depth at 3 knots tow speed. Transmit power is supplied to the tow body through conductors in the cable. A fiber optic transmission line in the tow cable provides data and command communication between the operator console and the tow body.

The sonar and arrays are deployed using a winch and handling system (WHS) from the vessel. The WHS has a footprint less than 80 square feet, providing versatile installation options on a variety of vessels. Power can be provided to the WHS from the ship, or from a self-contained generation system.

The dry end of the system comprises an operator console, as well as two cabinets which contain transmit power amplifiers and a power amplifier controller. The operator console provides two monitors for sonar and status displays that can be selected by the operator. The sonar data can be selected to highlight, for example, high-resolution range information or target Doppler information, in individual beams or across all azimuths. It is anticipated that the most heavily-used display mode during the proposed Sea Trial will show the raw acoustic output from the individual array channels, allowing monitoring of noise levels and signal strengths across the array. The operator can also monitor non-acoustic sensor data and system status and health reports during sonar operation. The system also allows off-

line system tests of the transmit power system and the acoustic receive arrays. The operator console also contains an RS232 port that will collect data from an L-3OS GPS system. This will provide time and position reference with which to stamp the sonar data.

2.2 Data recording equipment

Data acquired by the Seahawk is initially stored on the internal processor hard drive(s) in a continuous manner, along with time markers and status information. At the start of a data collection run, the time marker corresponding to the desired start of recorded data acquisition is noted by the operator. At the end of the run, recording is halted by notification of the operator or by predetermined signal or event. The operator will then prepare the stored data for recording on DVD disc.

An information header or text file will be created containing information on the acquired data, such as times, locations, conditions, course, speed, unusual events, etc. The format of this information is described elsewhere. The stored data file is then checked for size to be sure it will not exceed the approx. 4.7Gbyte limit of the DVD disc. If the data exceeds 4.7Gbytes, the file will be distributed among multiple DVD discs. A commercial software package is then used to select the header file and the data file from the processor and physically write the files to the DVD as a standard MS Windows formatted disk. Upon successful recording of the information, the operator removes the disk and affixes a predetermined identification number and title on the disc or discs. The process will then be repeated to create a backup set of the data.

The quality of the DVD stored data is then checked by reading the files back into a PC computer to insure interchangeability and playback integrity. Data recording is considered complete upon successful reading of all data files by the computer.

2.3 Data processing equipment

For this trial, the Seahawk processing will be available to allow us to determine if the sonar is operating properly and if we are receiving returns where expected. However, due to the need to pull the data out of the processing stream early, it will not be possible to play back the native Seahawk processing at a later time. Note that active display has not yet been tested in current mode.

Proper operation of the Seahawk sonar is monitored during the trial by the L-3OS system operator. System power, transmit power amplifier power, and tow body power will be monitored before and after each run to ensure correct operation of the Seahawk. During towing operations, towing characteristics are monitored to insure stability of the receive arrays. This data will include tow body roll, pitch, yaw, depth (via pressure), temperature, and heading. Tow cable tension and angle are also monitored from the winch and handling system. Limits will be predetermined for all predefined trial run characteristics, but may be modified or adjusted as needed by the L-3 Test Director to account for actual operating conditions such as wind speed, ship speed, and sea state.

During the trial, DTI will conducting SAS-quality checks of the data. The results of these checks will determine if alterations need to be made to any test procedures or equipment. Additionally, an off-line streaming SAS processor will be operable during the trials. This streaming processor will allow a first attempt at SAS data processing. We expect to require additionally algorithms to process the flexible array data, thus the full SAS processing be done off-line at DTI.

Acoustic data from each of the 96 channels in the acoustic array are monitored continuously during operation. This raw data can be displayed for operator inspection. Additionally, standard sonar processing of the active sonar data can be performed to provide access to characteristics of the data that are more familiar to sonar operators. The raw channel data will be formed into directional beams so that target locations can be displayed in range and bearing. Ship motion is compensated, so that target data from CW pulses can be separated into Doppler bins to display target motion. Time-resolved correlation data of FM echoes pulses are also generated. This allows the operator to examine target extent and gain some resolution of target features.

2.4 Vessel

The vessel to be used for the sea trial is the M/V Atlantic Surveyor, owned by Divemasters, Inc. of Toms River, NJ. The vessel is docked in Pt. Pleasant, NJ. Figure 2-1 is a photograph of the Atlantic Surveyor. Table 2-1 contains a few details of the vessel.

Figure 2-1. Photograph of *M/V Atlantic Surveyor*.

Table 2-1. Some information on the *M/V Atlantic Surveyor*.

Length	110.0' (33.53 m)
Beam	26.0' (7.93 m)
Depth	11.5' (3.51 m)
Draft (light)	6.0' (1.90 m)
Draft (operational)	9.0' (2.75 m)
Displacement	68 net tons
Deck load	65 long tons
Clear deck space	56.0' x 24.5'
Crew	4
Guests	12 (in 3 staterooms)

3. SUPPORT INFORMATION

This section contains descriptions of the support people and functions and related items. It includes the personnel and their responsibilities, permits we need/have, safety information, and data rights.

3.1 Personnel and responsibilities

Personnel on the vessel represent different organizations and each has different responsibilities. Table 3-1 lists the attendees and basic responsibilities.

Table 3-1. Trail attendees and basic responsibilites.

Person	Organization	Responsibilites
Dr. Angela Putney	DTI	Czar
Dr. Matt Nelson	DTI	Senior Scientist
James Campbell	DTI	Scientist, processing software
Bill Knaack	L-3OS	Seahawk test director
Rainer Farsch	L-3OS	Seahawk software
Norm Windman	L-3OS	Seahawk electronics
Power Han	L-3OS	Seahawk mechanics
Tim Landis	L-3OS	Seahawk winch & handling system
Capt. F. Kurt Perl	Atlantic Surveyor	Boat Captain
Three additional crew	Atlantic Surveyor	Boat crew
Keith Cooper	Navy, SUPSALV	Lead mammal observer
Ridgely Albaugh	Phoenix Inter'l	Mammal observer
Charlie Kapica	Phoenix Inter'l	Mammal observer
Frank Johnston	Phoenix Inter'l	Mammal observer

3.2 Overseas Environmental Assessment

This trial will occur more than 12 miles from any coast thus an Overseas Environmental Assessment (OEA) is required by the Navy. An OEA was prepared for this trial by Marine Acoustics, Inc. (MAI) and given to the Navy to determine the requirements for the trial. Section 6 describes the mitigation activities.

3.3 Safety

The ATLANTIC SURVEYOR is U.S. Coast Guard Inspected and Certified, and fully equipped with all approved fire-fighting and safety equipment. In April 2003 the vessel passed a complete Coast Guard drydock inspection with no deficiencies. Captain Perl will inform all passengers of safety issues.

3.4 Data rights

The collected raw sonar data is the property of L-3OS and considered proprietary information as defined by the PIEA between DTI and L-3OS. However, upon delivery of the data, during the trial and afterwards DTI will have the right to use said data and to process it within the bounds of the contract and PIEA. The processed data is the property of DTI, but L-3OS has certain rights as described in the contract and PIEA.

4. SYSTEM CHECKOUT PROCEDURES AND RESULTS

This section lists the checks of the sonar-related system prior to and during the test. The initial in-lab checks were completed Jan. 2003 and results are available in other documentation. Further testing of the equipment occurred in September 2003, including in-water passive testing of the system. A description of the on ship checkout, the week prior to the trial is included herein with places for results to be added at trial's beginning. The procedures for the daily checks are described here along with check-off sheets.

4.1 In-lab pre-trial system check

The Seahawk system and its subsystems will be subject to operational inspections to insure that all Sea Trial requirements are supported. These inspections culminate in pre-trial operation that exercises all features used during the proposed Sea Trial at sea. This shipboard integrated system check will include:

- Built-in-test (BIT) interrogation of the transmit power amplifiers, sonar processor, tow body electronics, and acoustic arrays;
- Towing and operation at the Seahawk system maximum operational depth of depth of 265 meters;
- Display of sonar signal processing results from targets of opportunity, with an assessment of beamformed sonar target signal-to-noise ratio and sidelobe level;
- Recording of data from the 96 array acoustic channels, the tow-body non-acoustic data, and data from the GPS unit through the RS232 interface;
- Transfer of this data to storage computers and analysis of all channels' acoustic self-noise under tow conditions;
- Monitoring of forward- and aft-directed acoustic power transmitted in all directional and omnidirectional transmit modes; and
- Operation of the winch and handling system.

Individual subsystems have gone through extensive checkout under laboratory conditions. Recent tests have included:

- Measurement of electronic self noise and acoustic response (gain and phase) of acoustic channels on the laboratory bench;
- Vibration testing and thermal cycling of the acoustic modules; and
- Reeling of the array modules under tension.

Further tests that will be carried out on the Seahawk system immediately prior to its operation at sea will include the following:

- Recording and retrieval of acoustic data, tow body non-acoustic sensor data and GPS data, in the format appropriate for the proposed Sea Trial;
- Inspection of seals, hydraulics, and individual transmit elements in the tow body,;and
- Inspection of seals, hydraulics, bearings, and operating pressures and temperatures of the winch and handling system.

4.2 On-ship pre-trial system check

Upon arrival at the test facility, the Seahawk system will be assembled and subject to an end-to-end test to ensure its safe arrival. The acoustic modules will be connected to the tow body, and a comparison of acoustic noise among all channels will be done to identify any degraded sensors. Calibration tones will be injected into the array electronics to quantitatively assess the channels' electronic sensitivities, and a channel-by-channel "tap test" may be done if it is desired to isolate any irregularities in the acoustic noise and electronic calibration tests.

These data will be recorded, together with the data from the ship's GPS navigation system, to ensure that all necessary data interfaces can be synchronized and recorded properly. Other system BIT checks will be carried out to verify the health of the sonar console, the power amplifier system, and the towed body electronics. The winch and handling system will be installed on the vessel, powered up, and inspected.

4.3 Daily system check

A daily system check will be made with the arrays in their stowed condition, not attached to the towed body. This will allow observation of the health of the telemetry to and from the tow body, as well as BIT checks of the console, power amplifiers, and tow body electronics. A readout of fresh GPS data will be obtained.

5. BASIC TRIAL OVERVIEW

5.1 Purpose

The purpose of this trial is to collect sonar data suitable for SAS processing. SAS data is collected a little differently than standard side look sonar (SLS) data and these differences are important. In addition to the sonar data collection, we need to collect environmental data and to process all data well enough to ascertain its quality.

The intent of this section is to describe the standard procedures for the trial. This section should be well understood by all before the first run is ever conducted. Section 7 contains the day to day details of each run (target, vessel speed, sonar settings, etc.) and is expected to be the most used section while the trial is underway. The sonar and environmental data collection procedures are explained in 5.2. A brief description of the targets is in Section 5.3. The data processing procedures are in Section 5.4.

5.2 Data Collection Procedures

Every data collection run will follow the same basic procedure, regardless of differences in the distance from the target, the length of the run, the ping repetition interval (PRI), and possibly the source level. This section describes the elements of run; Section 7 will fill in the details of individual runs along with planned order and importance. The Appendix is filled with log sheets for the different tasks and to record the environment. These sheets will be completed as the data are taken.

5.2.1 Vessel operations

The vessel must keep the array on a smooth straight path for the duration of a run. To do this, the vessel needs to follow a straight path past the target. Figure 5.1 schematically demonstrates the arrangement. The straight path must begin a set distance (determined by the details of the particular run; see Sections 5.2.2 and 7) before the closest point of approach (CPA) of the target and continue to a similar distance after CPA. The vessel needs to be on the track early enough to allow the towed array to fully exit any turn and be on a straight path before it reaches the position where sonar transmission will begin.

Keeping a vessel on a perfectly straight path is not always simple. Sharp coarse corrections to place the vessel back on the planned track are not acceptable. *IF* course corrections are absolutely necessary, they should be executed *very slowly* and *very smoothly*.

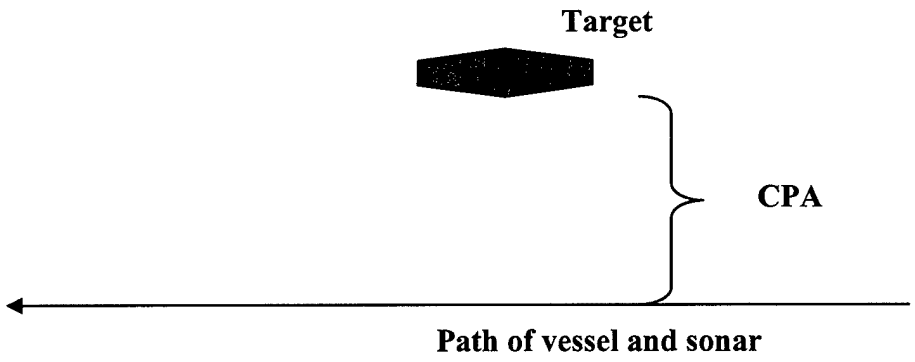

Figure 5–1. Schematic of vessel operations during a run.

5.2.2 Sonar operations

As mentioned above, the path of the sonar is a straight line past the target. CPA will occur in the middle of the path. However, the sonar will be on path before the required start position (see Figure 5–2). The steps taken can be described as follows:

1. Sonar settled on path: Receivers operating, start recording ambient noise
2. Sonar crosses start point: Turn on transmitter
3. Sonar crossed end point: Turn off transmitter
4. Approximately 10 s later: Turn off recording

There are several details of the sonar operation that change from run to run. The CPA distance from the target dictates the sonar transmission requirements of PRI, pulse length, and source level. Table 5–1 gives some examples of these values and Section 7 will detail the values require for the individual runs.

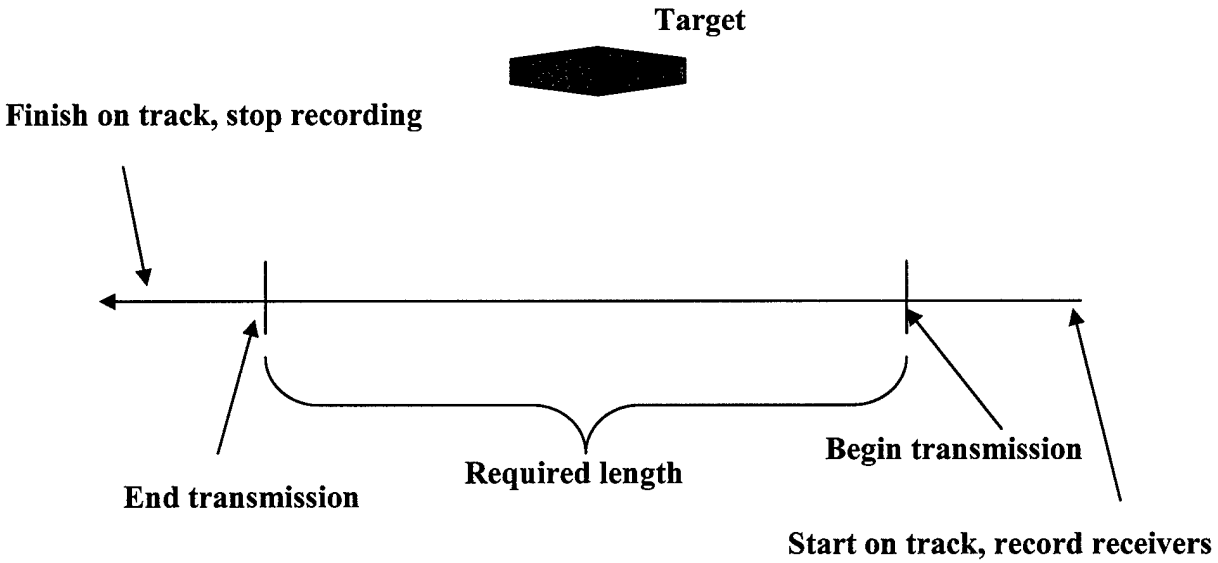

Figure 5–2. Schematic showing transmitter and receiver operations during run.

Table 5–1. Example sonar system parameters for different target ranges.

CPA/ max range	PRI	Pulse length	Boat speed	Duration of run	Length of run	Number of pings per run
0.5 km / 0.7 km	6 s	0.25 s	3 kts	>= 9 min	~0.8 km	~90
1.0 km / 1.2 km	6 s	0.25 s	3 kts	>= 11 min	~1.0 km	~110
3.0 km / 3.2 km	6 s	0.25 s	3 kts	>= 25 min	~2.1 km	~250
4.0 km / 5.0 km	6 s	0.25 s	3 kts	>= 35 min	~3.1 km	~350

5.2.3 Environmental parameter measurements

We will measure weather conditions (to include wind speed and direction, visibility) with a frequency dependent upon the measurement device(s). If weather can be machine recorded regularly, ~0.5 hr averages; if human recordable, of order once an hour beginning at least half an hour before first transmission of the day and continuing through the last transmission. This is useful for determining ability to conduct test and to conduct marine mammal observations.

We will record sea state with a frequency dependent upon method used, but preferably of order once per hour. This may be a by eye measurement or a conversion from the average wind speed. This is useful for determining ability to conduct sea trial, for later processing of the data in regards to understanding the expected level of heave. Note, NOAA has a series of wave buoys with daily data available that can be downloaded from the web upon return (or on board if we had web access) for any post-trial processing needs. Unfortunately none of the buoys are exactly at our locale, Figure 5–5 shows the location of the Salmon with respect to the buoys (blue squares).

We desire to measure sound velocity profiles once or twice a day. Actual measurement depends upon device used to do this. This is useful for post-processing comparisons of imagery with conditions (measurements from the tow body can be used to approximated the sound speed for SAS processing). At present we have no device to do this. We shall see if we can acquire one in time.

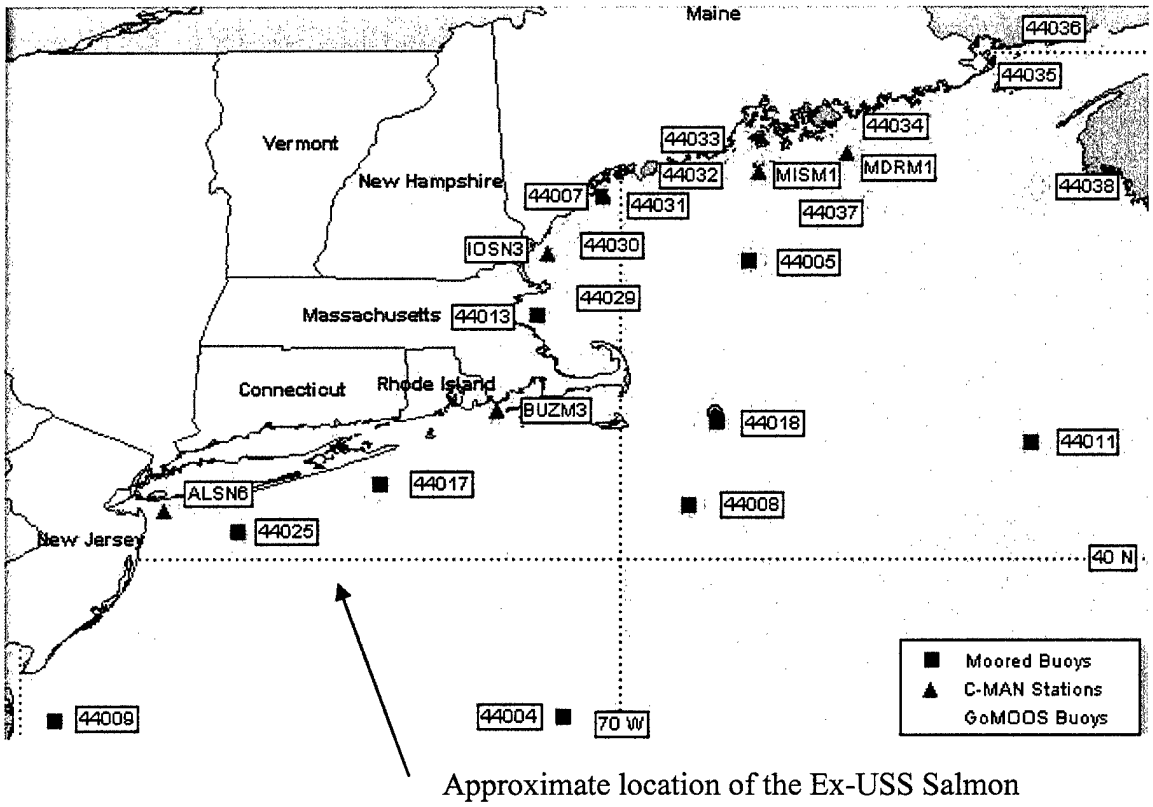

Figure 5–5. Location of the Salmon with respect to the NOAA buoys. The wave buoys are the blue squares.

5.3 Target descriptions

In order to test the system we need to collect data against "targets." Since there are multiple objectives for these trials, there are multiple types of targets. The ASW portion of the trial requires large, boat sized, targets and clutter. The MCM portion requires clutter and, if possible, small, ~2 m, sized targets. Since this is a first SAS trial with this system, there is an additional requirement of placing known point targets into fields. Thus for this document, the term "target" will refer to actual objects, like a sunken boat or a point source we lay down, as well as to regions lacking known objects that we will .

The general region of the trial contains many targets of opportunity, i.e., wrecks and the like, as well as purposely placed targets. The main target of interest is the ex-USS Salmon (SS-573), a decommissioned submarine that was purposely sunken with filled air to act as a "clean, environmentally safe, and realistic target." It is anchored to the bottom at 356 ft below the sea surface and composes a portion of the Shallow Water Diesel Submarine Test Facility (SWDSTF) operated by NUWC (see Figure 5–3). Some other possible targets include the Texas Tower #4 (Figure 5–4), an offshore radar installation that collapsed in a storm in 1961 and the Bidevind (Figure 5–5), a steel Norwegian tanker sunk by torpedo in 1942. Section 7 contains the location of the targets and the planned runs against them.

The point target we will be laying down is a lower power pinger. The pinger is 155 dB source with a frequency of 1.677 kHz and 1 s PRI. It takes 6 D cell batteries and should last 4 days per set of batteries. Figure 5–6 shows the planned mooring for the pinger. We plan to place it in each scene to assure a point target.

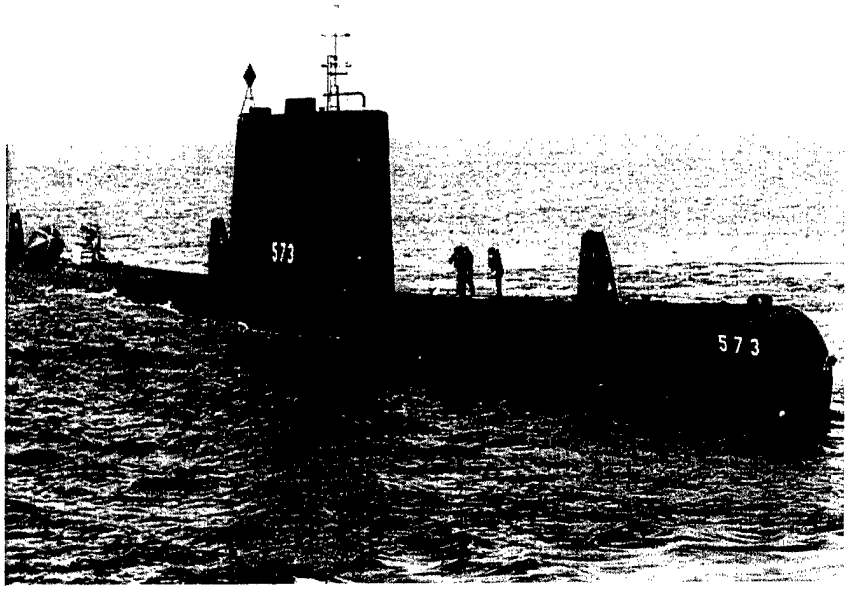

Figure 5–3. Ex-USS Salmon before sinking. (From SWDSTF web page)

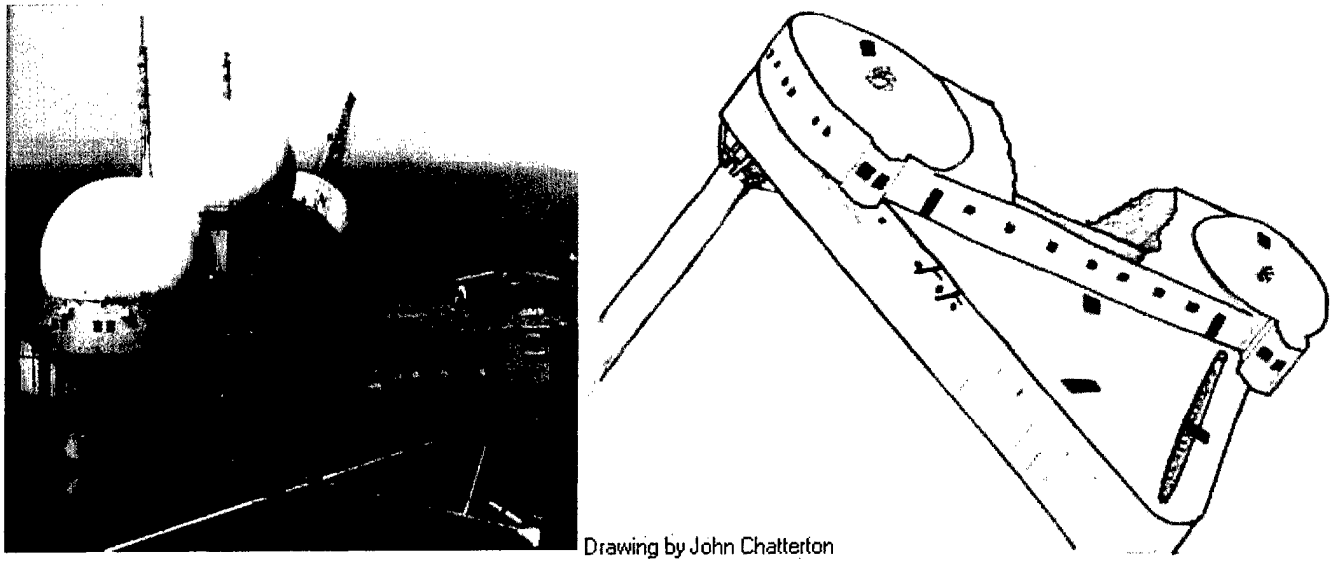

Figure 5–4. Texas Tower #4. Before sinking on the left, and what it looks like now, approximately, on right. (From http://njscuba.com/shipwrecks/texas_tower.html)

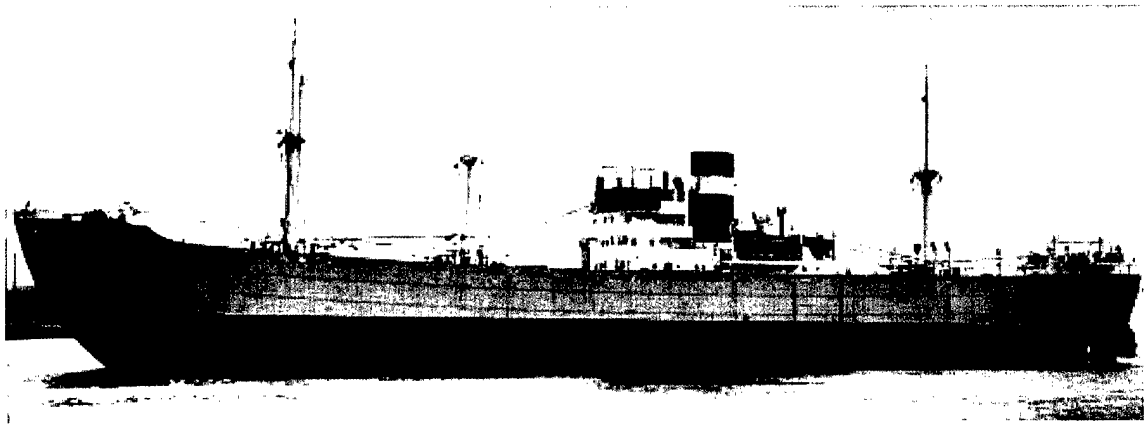

Figure 5–5. Bidevind, Norwegian tanker. (From http://njscuba.net/sites/list_deep_sea_2.html)

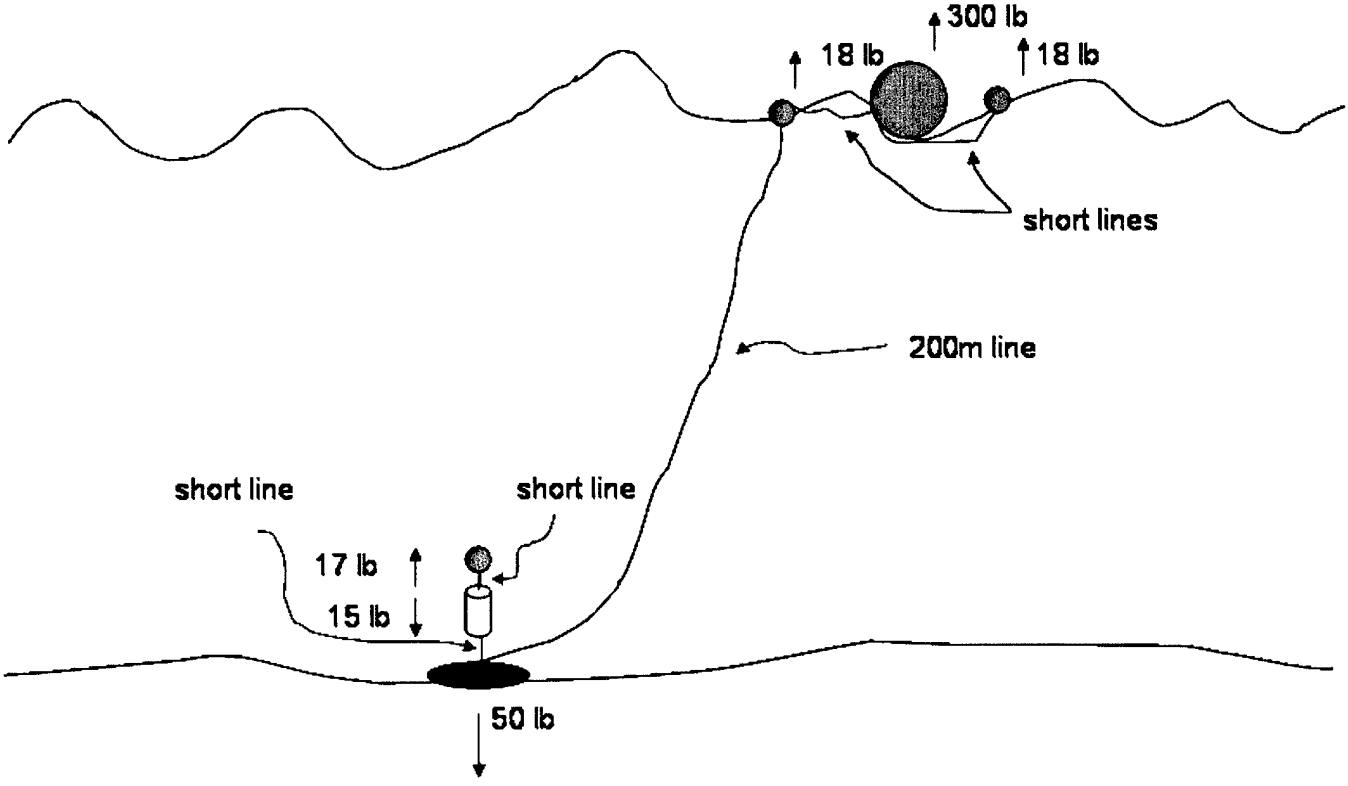

Figure 5–6. Mooring concept.

5.4 Processing operations

5.4.1 Seahawk processing

The sonar data will be viewed with the Seahawk system as it is collected to check for integrity. This will be done primarily by monitoring a sonar display that graphically presents the electronic level emanating from each channel. Saturated, degraded, or dead channels will be evident by comparison among channel outputs. When clear targets are present, the operator can choose a more traditional sonar display. Beamformed SNR and sidelobe observations will help to verify that data is free from obvious contamination by phase errors or other distortion.

The operator console's second monitor will allow concurrent observation of non-acoustic data that will allow the operator to verify stable towing behavior of the tow body, and monitor other detectors for the onset of faults concerning temperature, moisture intrusion, etc.

5.4.2 SAS processing

After data is collected and recorded onto a DVD by L-3OS, the DVD will be read by DTI. During the days and evenings DTI will check the quality in terms of SAS processing and attempt to process it. We expect to be able to create a SAS image while on the boat, albeit not a well focused image. We also expect there to be algorithm improvements required to work with flexible arrays that will enhance the quality of the SAS imagery, i.e., focus it better. These algorithm improvements will occur after the trial rather than during it, but as much processing as possible will occur during the trial.

The data quality checks will include beamforming each ping, comparing consecutive pings to determine type and strength of array motion between pings. A series of codes and plotting routines will allow us to do this processing. From these checks we hope to determine if runs need to be altered or not (e.g., travel only into the wind direction to reduce motion). Additionally checks of the motion data quality will be conducted. The checks are described in more detail in Section 7.4.2. If data passes the quality checks, DTI will begin SAS processing to the best of the attendees' abilities.

6. MITIGATION REQUIREMENTS

6.1 Mitigation measures

In order to be compliant with the Navy's guidelines, there are several mitigation measures that must be followed for this trial (these are not intended to establish precedents for future operational employment of similar or other systems).

1. The participating vessel will maneuver, as feasible, to avoid closing within 0.5 km (547 yds) of any marine mammal or sea turtle.

2. All mitigation measures will be employed for the in-transit engineering test as well as the actual SAS At-Sea Test. The in-transit engineering test will be of one to two hours of active transmissions after transiting beyond 13 nm from land.

3. Starting 30 min before the commencement of a transmission event, a visual survey of marine animals will be conducted from the bridge of the participating source vessel out to the range of the appropriate EZOIs (effective zone of influence). This watch will be maintained throughout each transmission event and continue 30 minutes after the completion of the event. The lookouts will be equipped with binoculars and a log of sighted animals will be maintained. If a marine mammal surfaces within the appropriate EZOI, or a sea turtle is sighted within 91 m (100 yards), transmissions will be suspended until the animal is a greater distance from the ship than two times the applicable EZOI. If no additional sightings of the animal are made within the next fifteen minutes, transmissions may be resumed.

4. The participating vessel will minimize passages through sargassum floats and ocean frontal lines to preclude the potential of collision with sea turtles or marine mammals that are known to frequent these conditions.

5. Active transmissions will be suspended or will not be commenced if meteorological conditions are less than 500 m of horizontal visibility or the sea conditions exceed Beaufort 5 (sustained winds > 21 knots and whitecaps everywhere).

The optical observations will require two trained people on station at a given time. There will be four observers total divided into pairs. One pair will observe for an hour and then rest an hour while the second observers are on station. The observers will be trained by MAI before the trial.

6.2 Sunrise, sunset, and twilight times

Since we are allowed to operate in daylight only, Table 6–1 lists the sunrise, sunset, and start and end twilight times for +39°45' –72°30'. All times are listed in Eastern Standard Time. The marine mammal observers will have the final say on when it is bright enough to see, but both civil and nautical twilights are listed for guidance.

Table 6–1. Times of twilight beginning and ending, sunrise and sunset. All times in **EST.**

October day	Nautical Twilight begins	Civil Twilight begins	Sunrise	Sunset	Civil Twilight ends	Nautical Twilight ends
7	0454	0525	0552	1723	1750	1822
8	0454	0526	0553	1722	1749	1820
9	0455	0527	0554	1720	1747	1818
10	0456	0528	0555	1719	1746	1817
11	0457	0529	0556	1717	1744	1815
12	0458	0530	0557	1716	1743	1814
13	0459	0531	0558	1714	1741	1813
14	0500	0532	0559	1713	1740	1811
15	0501	0533	0600	1711	1738	1810
16	0502	0534	0601	1710	1737	1808
17	0503	0535	0602	1708	1736	1807

7. DAILY DATA ACQUISITION AND ANALYSIS

This section describes the procedures for collecting the data and on-boat processing. The daily plans are described along with run priorities. The criteria for acceptable data and moving onto a new target are explained. The planned test fields are shown. The criteria for stopping or pausing a day's tests are enumerated. A description the log sheets for the trial is given.

7.1 Test fields

There will be an engineering test further than 13 nmi from shore on our way to the Salmon site. This is a 1-2 hour test of the transmitter to reassure all that it is working fine before we motor out to the site. The exact location will be determined at the time.

The OEA limits us to 39°30'N/73°10'W, 40°00'N/73°10'W, 40°00'N/72°00'W, and 39°30'N/72°00'W, as is marked in Figure 7–1 as the large red box. Our permission to use the site actually limits us on the eastern border to 72°10'W, and this is shown as the smaller box in fig. 7–1. Table 7–1 lists the coordinates for the three targets.

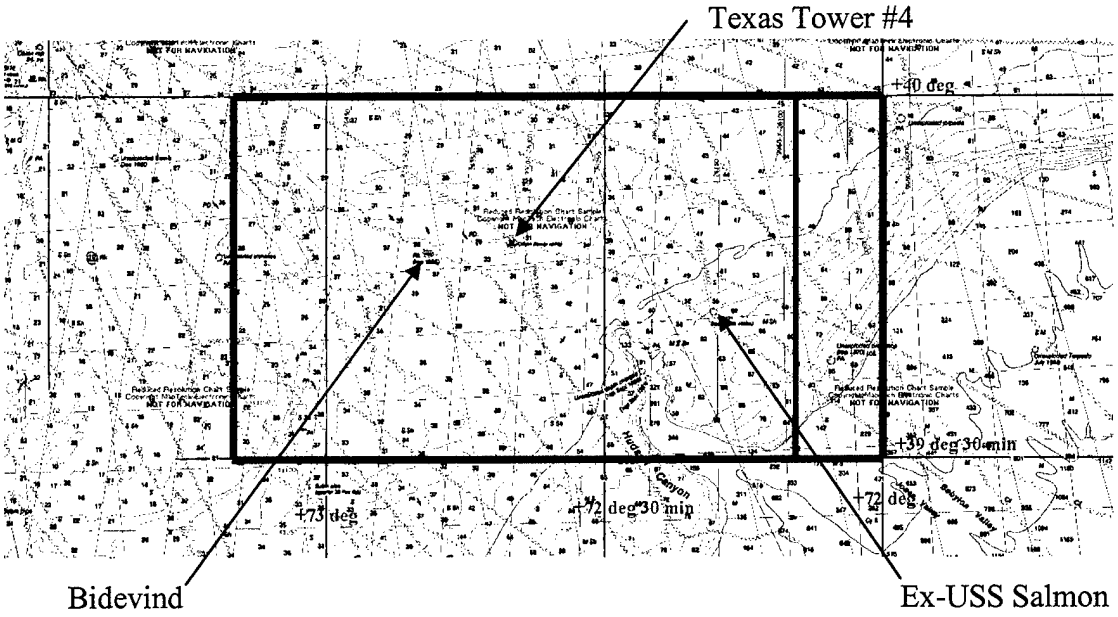

Figure 7–1. Test region with approximate locations of three targets marked.

Table 7–1. Coordinates for the targets.

Target	Latitude	Longitude	Depth
Ex-USS SALMON	39° 42.2'	072° 18.2'	360 ft
Texas Tower #4	39° 47' 56.43"	072° 40' 08.00"	70-180 ft
Bidevind[1]	39° 48' 57"	072° 46' 07"	190 ft

[1] The coordinates usually listed for the Bidevind appear to be a bad conversion from Loran C coordinates. These are the corrected coordinates after we found the wreck based upon Loran C coordinates.

7.2 Daily test plans

This sub-section lists the plans for each day and the priority of a given set of runs. For example, a series of runs will be planned to occur in a patch of ocean with the early part of the day being against an important target and the latter part against something else in the area to avoid long transits during prime test hours. The earlier runs will be marked with a "1" for priority and the latter with a "3" since they are opportunity only. If we get delayed and the early runs finish at the end of the working day, the priority 3 runs may be completely jettisoned from the schedule.

The general plan for the week is as follows:

Tuesday	Wednesday	Thursday	Friday	Saturday	Sunday	Monday
Depart mid-day. Beyond 13nmi from shore test xmitter. Transit to Salmon if OK	Lay pinger, take data	Take data, retreive pinger at day's end Begin transit to new locale	Lay pinger, take data, retreive pinger, begin transit to new locale	Lay pinger, take data, retreive pinger	Contingency day, begin transit home late in day	

The next table contains the run plans in order of priority. In general, we will run triangular tracks around the target (see Figure 7–2). For each target we will determine the orientation of the triangle we desire for the rest of the runs. While we are determining the orientation, we will collect some clutter data (i.e., not containing the target) in simple straight line runs.

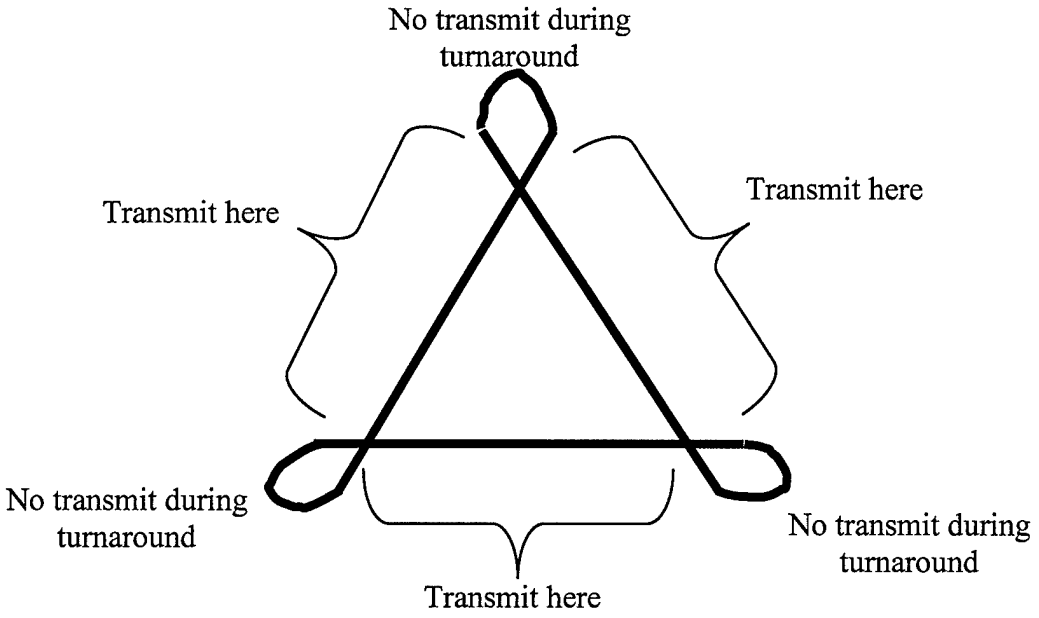

Figure 7–2. Schematic of triangular runs.

Run number[2]	Priority	Run type	Gain setting	PRI	pulse length	Distance to target	boat speed	length/direction of run[3]	comments
S1	1	right	221 dB	6 s	0.25 s	0.5 km	3.0 kts	1 km/ 12 min/ N	Target to right; search orien.
S2	1	right	221 dB	6 s	0.25 s	0.5 km	3.0 kts	1 km/ 12 min/ SE	Target to right; search orien.
S3	1	right	221 dB	6 s	0.25 s	0.5 km	3.0 kts	1 km/ 12 min/ SW	Target to right; search orien.
C1	2	right	221 dB	6 s	0.25 s	0.5 km	3.0 kts	2.8 km/ 30 min/ O	Clutter to right
C2	2	right	221 dB	12 s	0.5 s	1.0 km	3.0 kts	2.8 km/ 30 min/O	clutter to right
S4	1[4]	right	221 dB	6 s	0.25 s	0.5 km	3.0 kts	1 km/ 12 min/ O1	Target to right; 1st triangle leg
S5	1[3]	right	221 dB	6 s	0.25 s	0.5 km	3.0 kts	1 km/ 12 min/ O2	Target to right; 2nd triangle leg
S6	1[3]	right	221 dB	6 s	0.25 s	0.5 km	3.0 kts	1 km/ 12 min/ O3	Target to right; 3rd triangle leg
S7	1	omni	219 dB	6 s	0.25 s	0.5 km	3.0 kts	2.8 km/ 30 min/ O	Testing omni mode/squinting
S8	1	right	221 dB	6 s	0.25 s	4.0 km	3.0 kts	3.1 km/ 35min/O	target to right; 1st leg; far range
S9	1	right	221 dB	6 s	0.25 s	4.0 km	3.0 kts	3.1 km /35 min/ O	target to right 2nd leg
S10	1	right	221 dB	6 s	0.25 s	4.0 km	3.0 kts	3.1 km/ 35 min/O	target to right; 3rd leg
S11	1	right	221 dB	12 s	0.5 s	8.0 km	3.0 kts	5.8 km / 65min/O	undersampling; 1st leg; Xfar rng
S12	1	right	221 dB	12 s	0.5 s	8.0 km	3.0 kts	5.8 km / 65min/ O	undersampling; 2nd leg; Xfar rng
S13	1	right	221 dB	12 s	0.5 s	8.0 km	3.0 kts	5.8 km / 65min/O	undersampling; 3rd leg; Xfar rng
S14	2	right	221 dB	6 s	0.25 s	2.5 km	3.0 kts	2.1 km/ 25 min/ O	target to right; 1st leg; int. range
S15	2	right	221 dB	6 s	0.25 s	2.5 km	3.0 kts	2.1 km/ 25 min/O	target to right; 2nd leg; int.

[2] S = Salmon; T = target that is not Salmon; C = clutter.
[3] N=head North; E,S,W = East, South, West; O=orientation direction, i.e., the one we determine at the test. These all assume directional to right transmission, could use directional to left and go in the opposite direction.
[4] These runs are ONLY if the orientation of the runs must be changed.

									range
S16	2	right	221 dB	6 s	0.25 s	2.5 km	3.0 kts	2.1 km/ 25 min/O	target to right; 3rd leg; int. range
S17	2	right	221 dB	6 s	0.25 s	1.0 km	5.0 kts	1.0 km/ 8 min/O	undersampling data (fast), 1st leg
S18	2	right	221 dB	6 s	0.25 s	1.0 km	5.0 kts	1.0 km/ 8 min/O	undersampling data (fast), 2nd leg
S19	2	right	221 dB	6 s	0.25 s	1.0 km	5.0 kts	1.0 km/ 8 min/O	undersampling data (fast), 3rd leg
T1	1	right	221 dB	6 s	0.25 s	0.5 km	3.0 kts	1 km/ 12 min/ N	Target to right; search orien.
T2	1	right	221 dB	6 s	0.25 s	0.5 km	3.0 kts	1 km/ 12 min/ SE	Target to right; search orien.
T3	1	right	221 dB	6 s	0.25 s	0.5 km	3.0 kts	1 km/ 12 min/ SW	Target to right; search orien.
C3	2	right	221 dB	6 s	0.25 s	0.5 km	3.0 kts	2.8 km/ 30 min/ O	Clutter to right
C4	2	right	221 dB	12 s	0.5 s	1.0 km	3.0 kts	2.8 km/ 30 min/O	clutter to right
T4	1[3]	right	221 dB	6 s	0.25 s	0.5 km	3.0 kts	1 km/ 12 min/ O1	Target to right; 1st triangle leg
T5	1[3]	right	221 dB	6 s	0.25 s	0.5 km	3.0 kts	1 km/ 12 min/ O2	Target to right; 2nd triangle leg
T6	1[3]	right	221 dB	6 s	0.25 s	0.5 km	3.0 kts	1 km/ 12 min/ O3	Target to right; 3rd triangle leg
T7	1	omni	219 dB	6 s	0.25 s	0.5 km	3.0 kts	2.8 km/ 30 min/ O	Testing omni mode/squinting
T8	1	right	221 dB	6 s	0.25 s	4.0 km	3.0 kts	3.1 km/ 35min/O	target to right; 1st leg; far range
T9	1	right	221 dB	6 s	0.25 s	4.0 km	3.0 kts	3.1 km /35 min/ O	target to right 2nd leg
T10	1	right	221 dB	6 s	0.25 s	4.0 km	3.0 kts	3.1 km/ 35 min/O	target to right; 3rd leg
T11	1	right	221 dB	12 s	0.5 s	8.0 km	3.0 kts	5.8 km / 65min/O	undersampling; 1st leg; Xfar rng
T12	1	right	221 dB	12 s	0.5 s	8.0 km	3.0 kts	5.8 km / 65min/ O	undersampling; 2nd leg; Xfar rng
T13	1	right	221 dB	12 s	0.5 s	8.0 km	3.0 kts	5.8 km / 65min/O	undersampling; 3rd leg; Xfar

									rng
T14	2	right	221 dB	6 s	0.25 s	2.5 km	3.0 kts	2.1 km/ 25 min/ O	target to right; 1st leg; int. range
T15	2	right	221 dB	6 s	0.25 s	2.5 km	3.0 kts	2.1 km/ 25 min/O	target to right; 2nd leg; int. range
T16	2	right	221 dB	6 s	0.25 s	2.5 km	3.0 kts	2.1 km/ 25 min/O	target to right; 3rd leg; int. range
T17	2	right	221 dB	6 s	0.25 s	1.0 km	5.0 kts	1.0 km/ 8 min/O	undersampling data (fast), 1st leg
T18	2	right	221 dB	6 s	0.25 s	1.0 km	5.0 kts	1.0 km/ 8 min/O	undersampling data (fast), 2nd leg
T19	2	right	221 dB	6 s	0.25 s	1.0 km	5.0 kts	1.0 km/ 8 min/O	undersampling data (fast), 3rd leg

7.3 Criteria for determining an early end or pause

So that the Czar does not keep people operating in a hurricane, here is a list of who has the authority to end the day's tests, cause a long (several hour) break, or require return to port.

1. Captain Perl has declared that it is unsafe for us to remain at our location. Work will cease and Capt. Perl will take us to another location or port as necessary.

2. Bill Knaack has declared that Seahawk cannot be operated in the current conditions, causing us to stop work until conditions have improved.

3. Bill Knaack has declared that Seahawk cannot be repaired at sea and we must return to port.

4. Marine mammal observers (MMOs) declare seeing conditions too bad for observations. This will cease transmissions until the weather has improved.

5. MMOs sight a mammal and command us to stop transmissions immediately; transmissions will resume when given clearance from MMOs.

7.4 Daily analysis plans

We will be looking at some data sets to check quality. This will help determine the next day's trials. Some checks will conducted during data collection, namely those done with the native Seahawk processing system. The SAS checks will be conducted after data has been written to DVD.

7.4.1 Definition of a "good" data set during data collection

Records of single channels amplitude vs. time will be displayed for time records of interest at the end of each day. These records should show no obviously discrepant channel amplitudes. The stability of target amplitudes and positions, and the absence of "ghosts" or intermittent sidelobe responses, will be examined as an indication of reasonable phase fidelity.

7.4.2 Data analysis to occur after data collection

During the LRSAS sea trials, a number of data processing steps will be undertaken as soon as data is transferred to DTI on DVD. These analyses will evaluate the overall quality of the data and will assess its utility for SAS imaging. The checks may be broken down into two broad categories: those for acoustic data, and those for motion and navigation data.

An outline of the specific analyses follows:

1. Evaluate Acoustic Data

    1.1. Time-series Sanity - may wish to downsample based on bandwidth and sample rate

1.1.1. Plot time-series – NO range compression
1.1.1.1. Look at each channel to verify proper function - include checking spectra and alias searches
1.1.1.2. Look at staves to ensure that channel-combining software has not corrupted data in any way - may wish to squint when combining elements
1.1.2. Repeat with range-compressed data
1.1.2.1. Examine cuts in range to assess effectiveness of matched filter
1.1.2.1.1. Quantify side-lobe levels, peak width, etc.

1.2. Channel statistics
1.2.1. Generate histogram of magnitude for each channel
1.2.2. Calculate statistics for each channel

1.3. Evaluate Channel-to-Channel Phase
1.3.1. Form image laying multiple pings side-by-side
1.3.1.1. Check if phase varies smoothly on bright scatterer
1.3.1.2. Could also be done w/ single ping if necessary
1.3.1.3. Check phase variations for the direct blast
1.3.1.4. Check amplitude delays for the direct blast
1.3.1.5. Check delay of direct blast vs. recorded ping time – delay should be identical on each ping

1.4. Beam-form individual pings
1.4.1. Form many beams per ping, typically one beam per stave – pad raw data to ~10 times the number of channels
1.4.2. Try to identify a distinct return from an object
1.4.3. Check that object moves as expected from ping-to-ping based on ship motion, etc.
1.4.3.1. Sum multipath via intensity addition of range bins around target region to find peak
1.4.3.2. Compare target bearing per ping with navigation change in heading
1.4.4. Estimate sway with edge detection and compare to navigation estimates

1.5. Projector coherency
1.5.1. Evaluate stability of range compression from ping-to-ping using strong point or direct blast

1.6. Projector SL stability
1.6.1. Evaluate apparent energy from ping-to-ping
1.6.1.1. Use time series histograms and statistics
1.6.1.2. All channels fluctuating in unison may indicate projector instability
1.6.1.3. Use direct blast if possible

2. Evaluate Platform Motion

2.1. Motion Sensors
  2.1.1. Generate plots of all motion sensor data for run
    2.1.1.1. Evaluate for general correctness in both time and frequency domain
  2.1.2. Generate and plot sensor-derived trajectory
    2.1.2.1. Get help from Roy?
    2.1.2.2. Evaluate for general correctness

2.2. Acoustic Data
  2.2.1. From beamformed data, identify a target
    2.2.1.1. Generate plot of bearing vs. time
    2.2.1.2. Correct observed bearing for along-track position
    2.2.1.3. Determine if residual bearing (=yaw) is sane
  2.2.2. Form image of "smiles"
    2.2.2.1. Determine if there are any indications of problematic motions
  2.2.3. Run RPC
    2.2.3.1. Evaluate performance (jumps, correlation, etc)

In order to perform these analysis steps, DTI will have all necessary software tools available on the shipboard processing computers. This software will include utilities to do the following:

1. Convert "PingRecord" formatted acoustic data into flat image files (sdt/.spr format).
   1.1. All subsequent analysis will be conducted on flat image data

2. Band-pass filter the acoustic data to retain either the image data or the pinger data.

3. Combine acoustic channels together to form "staves" of size suitable for our synthetic aperture resolution goals.

4. Beam-form acoustic data from each ping, forming a complete set of directed beams for each ping (typically done via an FFT of the stave data).

5. Generate time-series plots from acoustic data; typically one for each channel (or stave), either from a single ping or an accumulation over a user-specified range of pings.
   5.1. This code will be the natural one for generating statistics (mean, variance, etc) on each channel.

6. Register pinger data together and extract array shape and motion data vs. time

7. Extract navigation information from the raw data stream

8. Generate plots of all navigation sensor data for each run
9. Calculate an optimal trajectory based on all navigation inputs using a Kalman filter
10. Prominent point code with asynchronous pinger
11. Prominent point code with natural scatterer
12. Jim's non-standard processing package

APPENDIX

We need to keep track of all sorts of information for later processing and for labeling imagery. The appendix contains sample log sheets.

Cover Sheet to a day of testing in LRSAS

Date: _____ Location: _____ Start time: _____

Operators:

_____

Weather conditions at start:

_____

Check list before starting:

Seahawk:

__ Transmit OK
__ Receive OK
__ Record OK

General:

__ Ambient noise measurements at beginning
__ Ambient noise measurements at mid-day
__ Ambient noise measurements at day's end
__ SVP measurements at beginning of day
__ SVP measurements at end of day

Comments:

_____
_____
_____
_____
_____
_____
_____
_____
_____
_____

Time end: _____

Run Number	Gain setting	PRI/PL (s)	Time/ Length of run	Boat Speed	Omni or direct.	Heading	Water depth	Wind speed/dir	Time start	Time end	Quick Comments

Run number	Problem or Comment	Time	Detailed Comments

APPENDIX B: ADDITIONAL SIMULATIONS

In Section 2.2.3 we presented a few representative results of the SNR and SAS image simulations undertaken for the trial preparation. This appendix contains the remainder of these results. Table B-1 is similar to Table 2-5 except that the figure references are included. The SNR results figures follow the table. Table B-2 is similar to Table 2-6 but includes the transmission loss figure references and a few additional simulation descriptions. The transmission loss figures follow the table. Table B-3 is similar to Table 2-7 with the figure references added. The referenced figures follow the table.

Table B-1. Summary of most of the PCSWAT calculations made. Figure numbers that begin with a "2-" are in Section 2 of the main report.

Run	Source Level	Pulse length	Water depth	Sonar depth	Target strength	Bottom type	SVP	Mode	Figure number
1	219 dB	0.25 s	400 m	100 m	–10 dB	Coarse sand	Iso	D	B-1
2	219 dB	0.25 s	400 m	100 m	–10 dB	Coarse sand	Iso	O	B-2
3	219 dB	2.00 s	400 m	100 m	–10 dB	Coarse sand	Iso	D	B-3
4	219 dB	0.25 s	400 m	100 m	–10 dB	Fine sand	Iso	D	B-4
5	219 dB	0.25 s	100 m	50 m	–10 dB	Coarse sand	Iso	D	B-5
6	160 dB	0.25 s	100 m	50 m	0 dB	Sandy silt	Iso	D	2-13
7	170 dB	0.25 s	100 m	50 m	0 dB	Sandy silt	Iso	D	2-13
8	180 dB	0.25 s	100 m	50 m	0 dB	Sandy silt	Iso	D	2-13
9	190 dB	0.25 s	100 m	50 m	0 dB	Sandy silt	Iso	D	2-13
10	200 dB	0.25 s	100 m	50 m	0 dB	Sandy silt	Iso	D	2-13
11	210 dB	0.25 s	100 m	50 m	0 dB	Sandy silt	Iso	D	2-13
12	220 dB	0.25 s	100 m	50 m	0 dB	Sandy silt	Iso	D	2-13
13	203 dB	0.25 s	100 m	50 m	0 dB	Sandy silt	Iso	D	B-6
14	203 dB	0.50 s	100 m	50 m	0 dB	Sandy silt	Iso	D	B-6
15	203 dB	1.00 s	100 m	50 m	0 dB	Sandy silt	Iso	D	B-6
16	203 dB	2.00 s	100 m	50 m	0 dB	Sandy silt	Iso	D	B-6
17	209 dB	0.25 s	100 m	50 m	0 dB	Sandy silt	Iso	D	B-7
18	209 dB	0.50 s	100 m	50 m	0 dB	Sandy silt	Iso	D	B-7
19	209 dB	1.00 s	100 m	50 m	0 dB	Sandy silt	Iso	D	B-7
20	209 dB	2.00 s	100 m	50 m	0 dB	Sandy silt	Iso	D	B-7
21	212 dB	0.25 s	100 m	50 m	0 dB	Sandy silt	Iso	D	B-8
22	212 dB	0.50 s	100 m	50 m	0 dB	Sandy silt	Iso	D	B-8
23	212 dB	1.00 s	100 m	50 m	0 dB	Sandy silt	Iso	D	B-8
24	212 dB	2.00 s	100 m	50 m	0 dB	Sandy silt	Iso	D	B-8
25	215 dB	0.25 s	100 m	50 m	0 dB	Sandy silt	Iso	D	B-9
26	215 dB	0.50 s	100 m	50 m	0 dB	Sandy silt	Iso	D	B-9
27	215 dB	1.00 s	100 m	50 m	0 dB	Sandy silt	Iso	D	B-9

Run	Source Level	Pulse length	Water depth	Sonar depth	Target strength	Bottom type	SVP	Mode	Figure number
28	215 dB	2.00 s	100 m	50 m	0 dB	Sandy silt	Iso	D	B-9
29	218 dB	0.25 s	100 m	50 m	0 dB	Sandy silt	Iso	D	B-10
30	218 dB	0.50 s	100 m	50 m	0 dB	Sandy silt	Iso	D	B-10
31	218 dB	1.00 s	100 m	50 m	0 dB	Sandy silt	Iso	D	B-10
32	218 dB	2.00 s	100 m	50 m	0 dB	Sandy silt	Iso	D	B-10
33	221 dB	0.25 s	100 m	50 m	0 dB	Sandy silt	Iso	D	B-11
34	221 dB	0.50 s	100 m	50 m	0 dB	Sandy silt	Iso	D	B-11
35	221 dB	1.00 s	100 m	50 m	0 dB	Sandy silt	Iso	D	B-11
36	221 dB	2.00 s	100 m	50 m	0 dB	Sandy silt	Iso	D	B-11
37	203 dB	0.25 s	110 m	55 m	0 dB	Medium sand	Salmon	D	2-14
38	209 dB	0.25 s	110 m	55 m	0 dB	Medium sand	Salmon	D	2-14
39	212 dB	0.25 s	110 m	55 m	0 dB	Medium sand	Salmon	D	2-14
40	215 dB	0.25 s	110 m	55 m	0 dB	Medium sand	Salmon	D	2-14
41	218 dB	0.25 s	110 m	55 m	0 dB	Medium sand	Salmon	D	2-14
42	221 dB	0.25 s	110 m	55 m	0 dB	Medium sand	Salmon	D	2-14

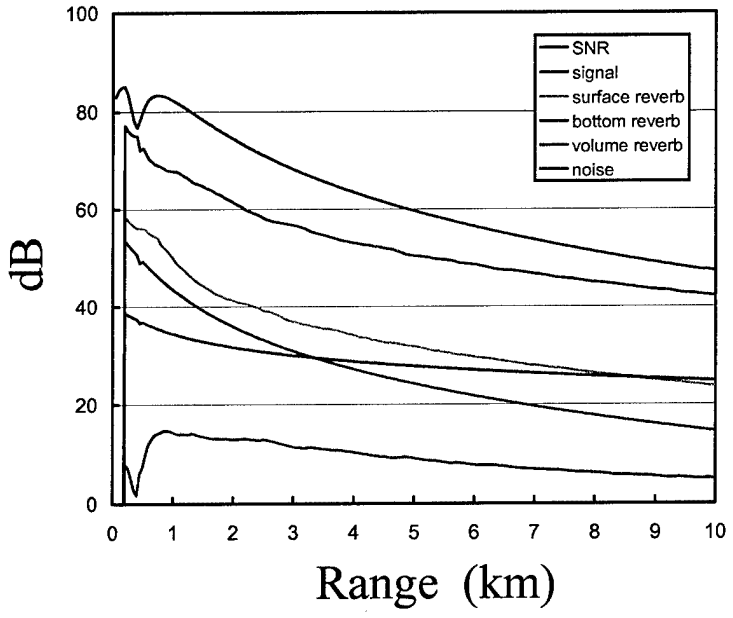

Figure B-1. Simulation results: deep water, coarse sand bottom, directional transmission mode, 0.25 second chirp.

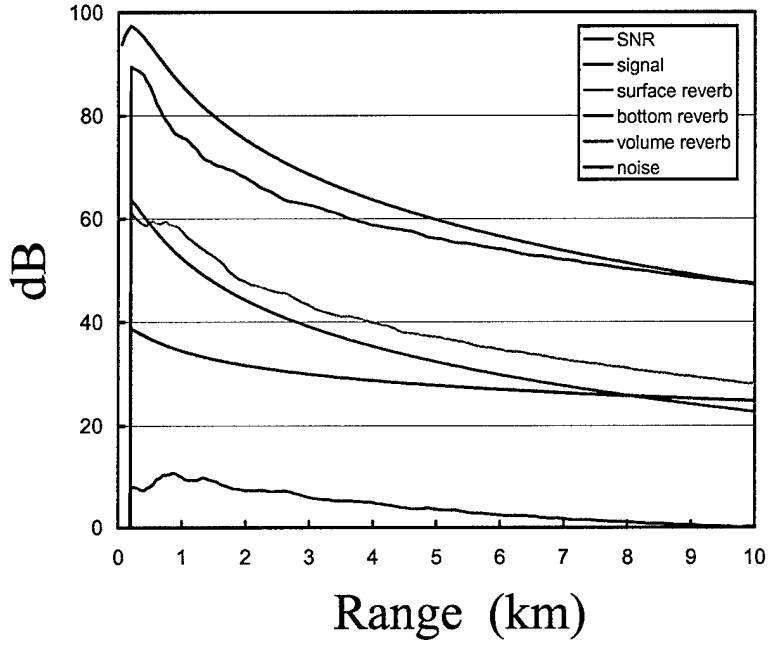

Figure B-2. Simulation results: deep water, coarse sand bottom, omni-directional transmission mode, 0.25 second chirp.

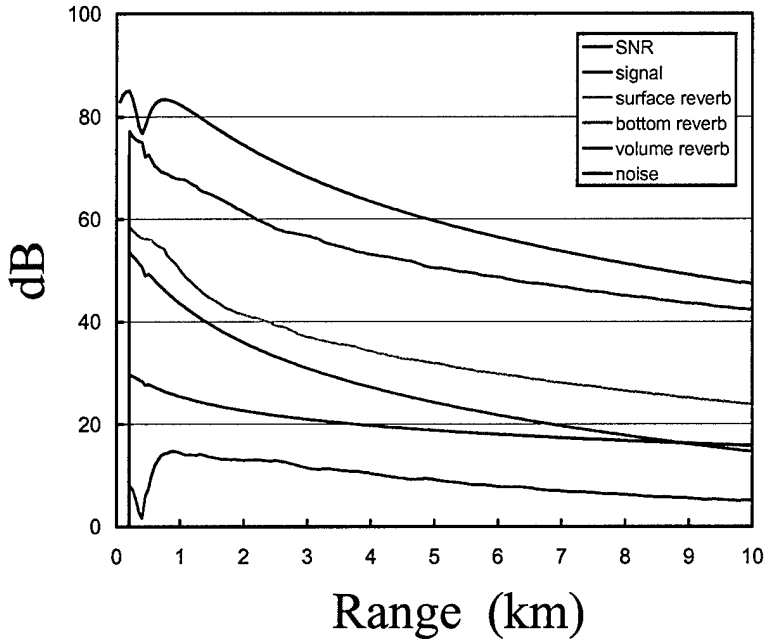

Figure B-3. Simulation results: deep water, coarse sand bottom, directional transmission mode, 2 second chirp.

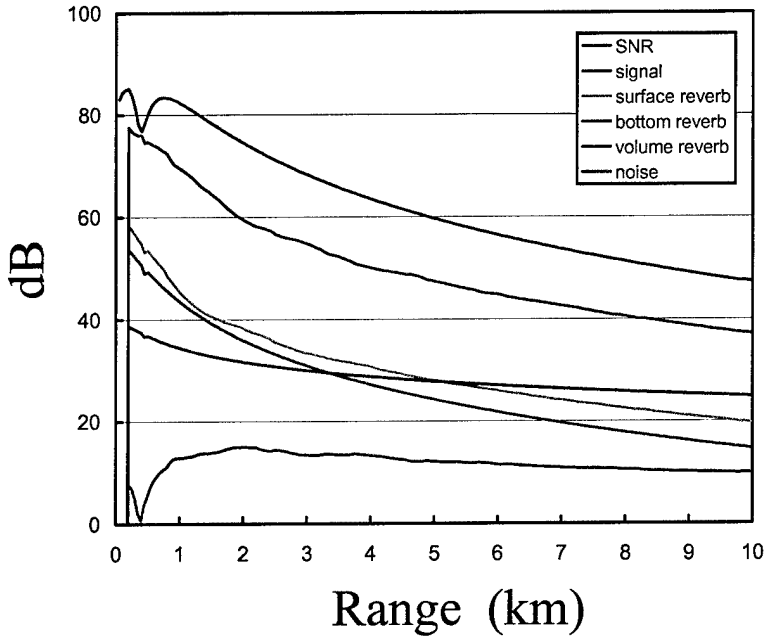

Figure B-4. Simulation results: deep water, fine sand bottom, directional transmission mode, 0.25 second chirp.

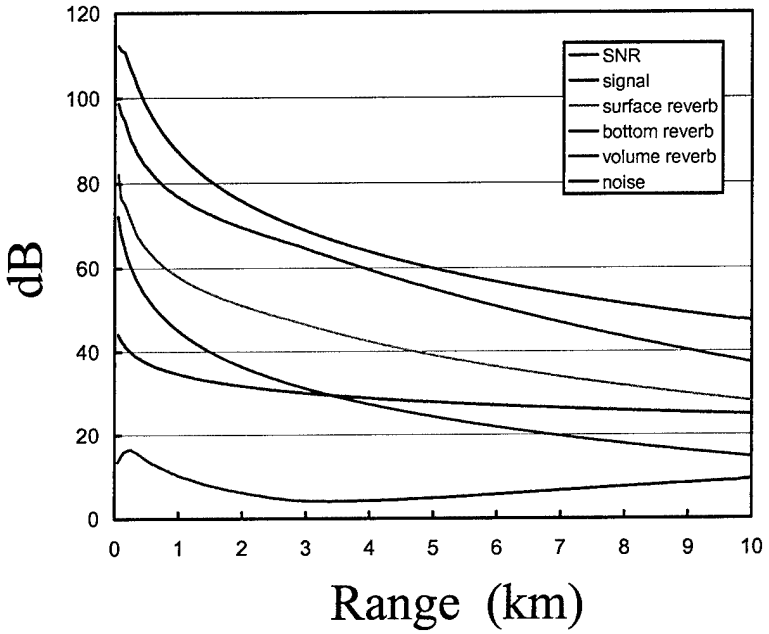

Figure B-5. Simulation results: shallow water, coarse sand bottom, directional transmission mode, 0.25 second chirp.

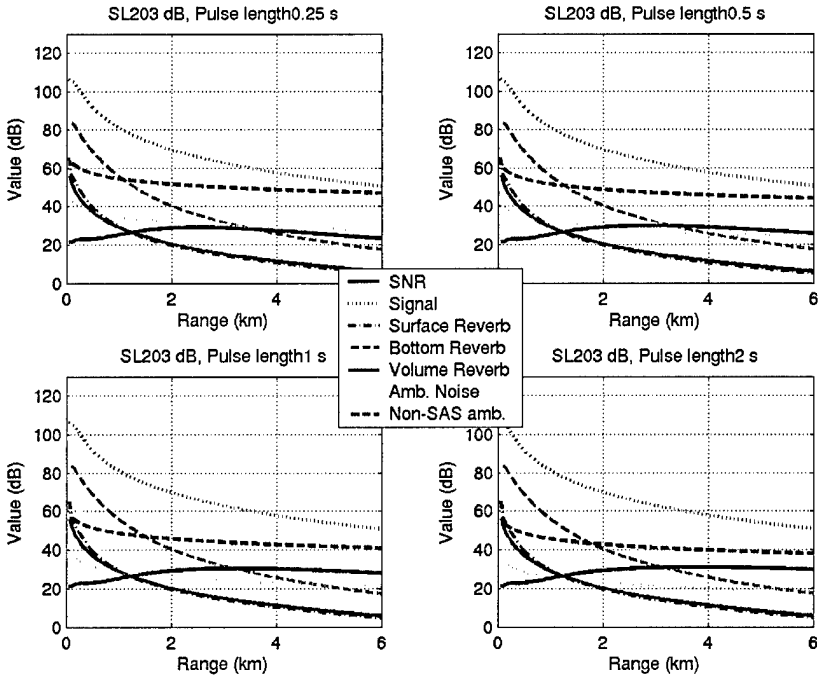

Figure B-6. Pulse length study at 203 dB source level. Directional mode, 100 m water depth, 50 m sonar depth, sandy silt bottom, 0 dB target strength, and isovelocity SVP.

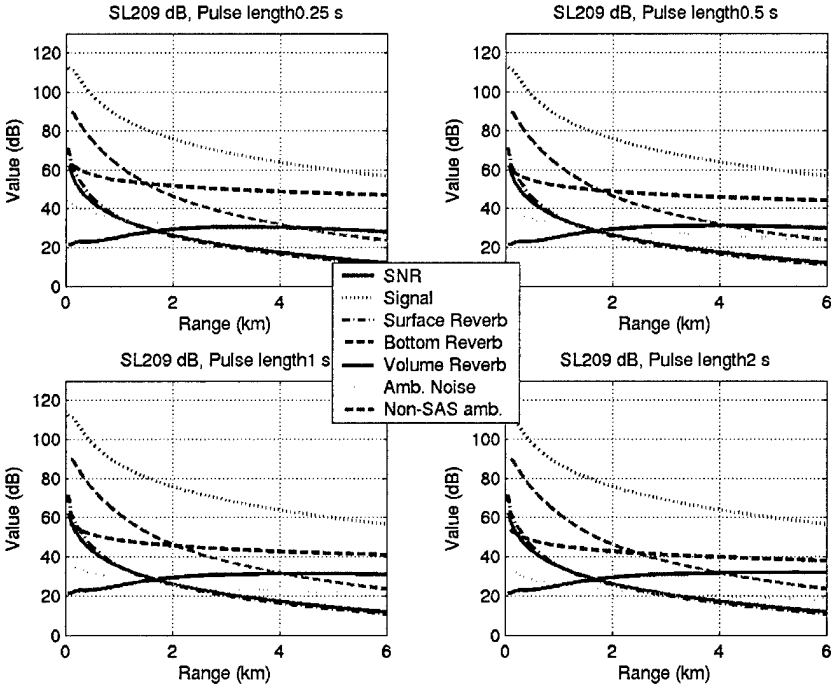

Figure B-7. Pulse length study at 209 dB source level. Directional mode, 100 m water depth, 50 m sonar depth, sandy silt bottom, 0 dB target strength, and isovelocity SVP.

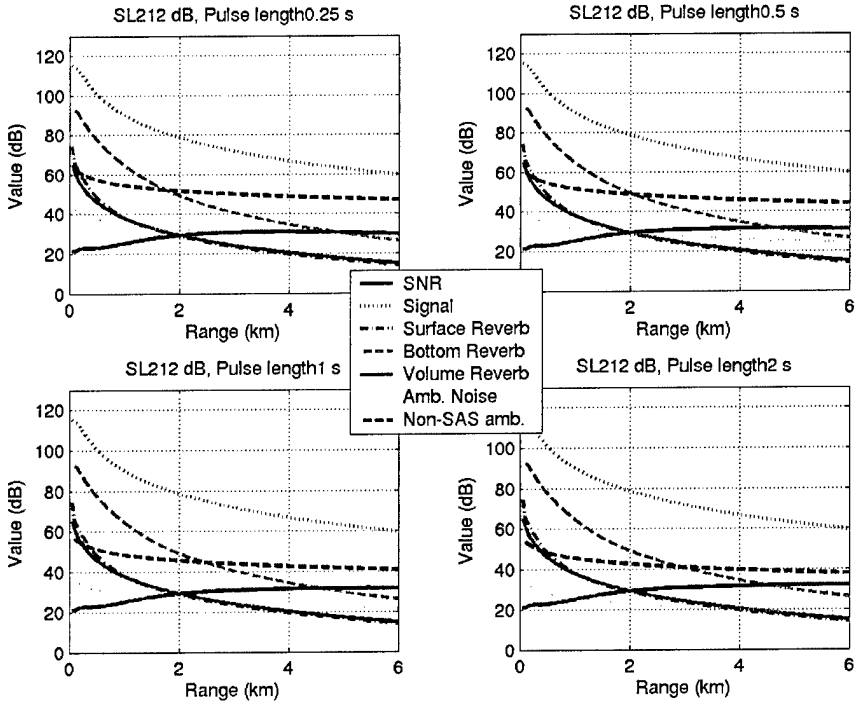

Figure B-8. Pulse length study at 212 dB source level. Directional mode, 100 m water depth, 50 m sonar depth, sandy silt bottom, 0 dB target strength, and isovelocity SVP.

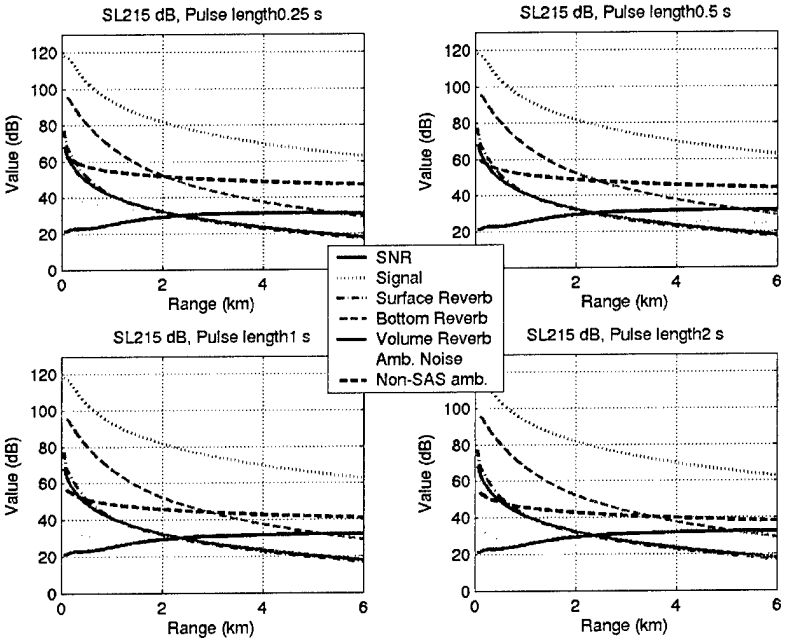

Figure B-9. Pulse length study at 215 dB source level. Directional mode, 100 m water depth, 50 m sonar depth, sandy silt bottom, 0 dB target strength, and isovelocity SVP.

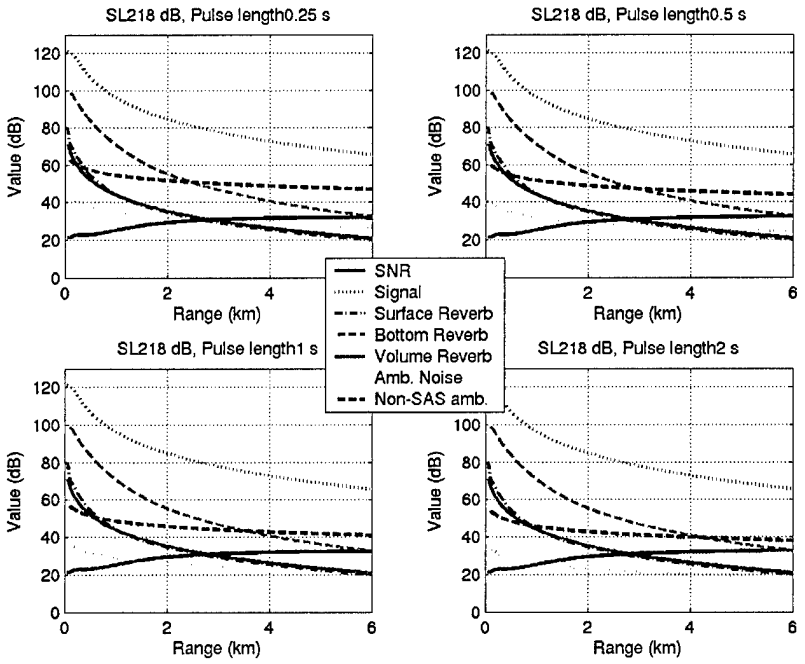

Figure B-10. Pulse length study at 218 dB source level. Directional mode, 100 m water depth, 50 m sonar depth, sandy silt bottom, 0 dB target strength, and isovelocity SVP.

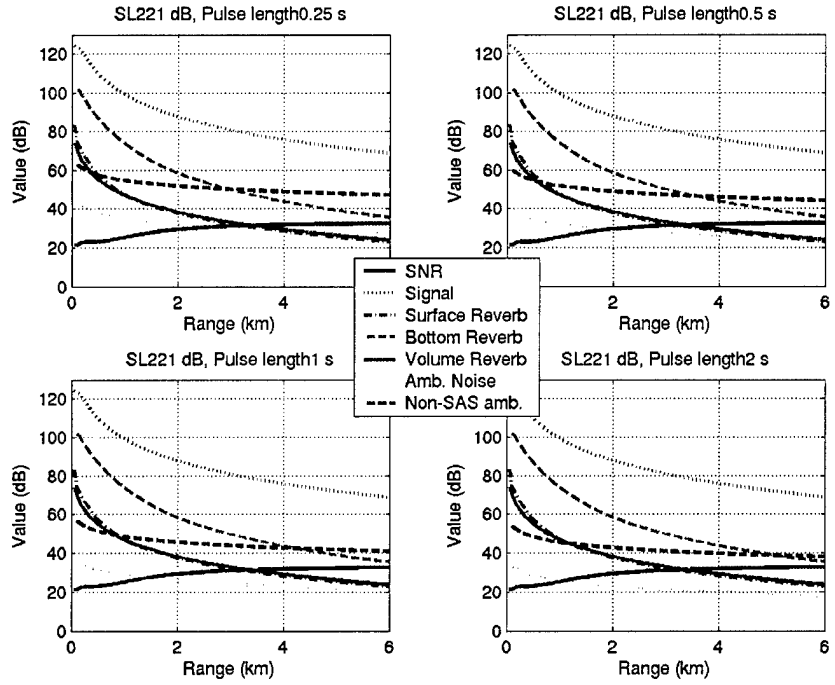

Figure B-11. Pulse length study at 221 dB source level. Directional mode, 100 m water depth, 50 m sonar depth, sandy silt bottom, 0 dB target strength, and isovelocity SVP.

Table B-2. MMPE code run parameters with figure locations. Figure numbers that begin with a "2-" are in Section 2 of the main report.

Run	Target range	"Source" depth	Maximum depth	SVP	Bathymetry	Figure
Xmitter-to-Woody	1 km	45 m	120 m	San Pedro	Original	B-12
Woody-to-receiver	1 km	64 m	120 m	San Pedro	Original	B-12
Xmitter-to-Woody	1 km	45 m	120 m	San Pedro	Modified	B-13
Woody-to-receiver	1 km	64 m	120 m	San Pedro	Modified	B-13
Xmitter-to-Woody	5 km	122 m	350 m	San Pedro	Original	B-14
Woody-to-receiver	5 km	64 m	350 m	San Pedro	Original	B-14
Xmitter-to-Woody	5 km	122 m	350 m	San Pedro	Modified	B-15
Woody-to-receiver	5 km	64 m	350 m	San Pedro	Modified	B-15
Xmitter-to-Sub	1 km	122 m	500 m	San Pedro	Original	B-16
Sub-to-receiver	1 km	329 m	500 m	San Pedro	Original	B-16
Xmitter-to-Sub	1 km	122 m	500 m	San Pedro	Modified	B-17
Sub-to-receiver	1 km	329 m	500 m	San Pedro	Modified	B-17
Xmitter-to-Sub	5 km	122 m	850 m	San Pedro	Original	2-24
Sub-to-receiver	5 km	329 m	850 m	San Pedro	Original	2-24
Xmitter-to-Sub	5 km	122 m	850 m	San Pedro	Modified	B-18
Sub-to-receiver	5 km	329 m	850 m	San Pedro	Modified	B-18
Xmitter-to-Salmon	1 km	56 m	150 m	Salmon	Original	2-27
Salmon-to-receiver	1 km	111 m	150 m	Salmon	Original	2-27
Xmitter-to-Salmon	5 km	59 m	150 m	Salmon	Original	2-28
Salmon-to-receiver	5 km	111 m	150 m	Salmon	Original	2-28

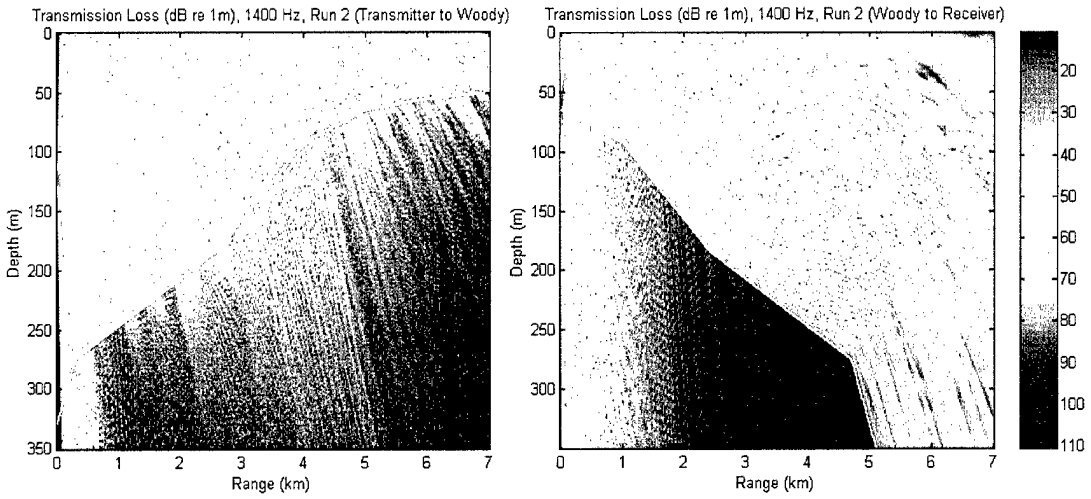

Figure B-12. Close-range (1km) transmission loss for Woody location. Left panel is transmitter to Woody. Right panel is Woody to receiver.

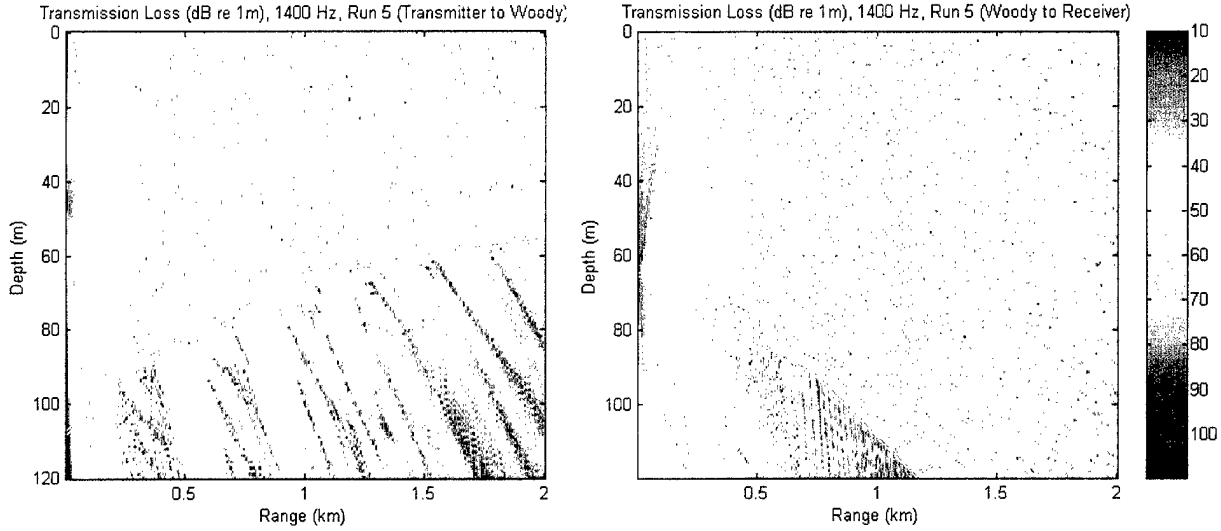

Figure B-13. Close-range transmission loss for Woody location with modified bathymetry. Left panel is transmitter to Woody. Right panel is Woody to receiver.

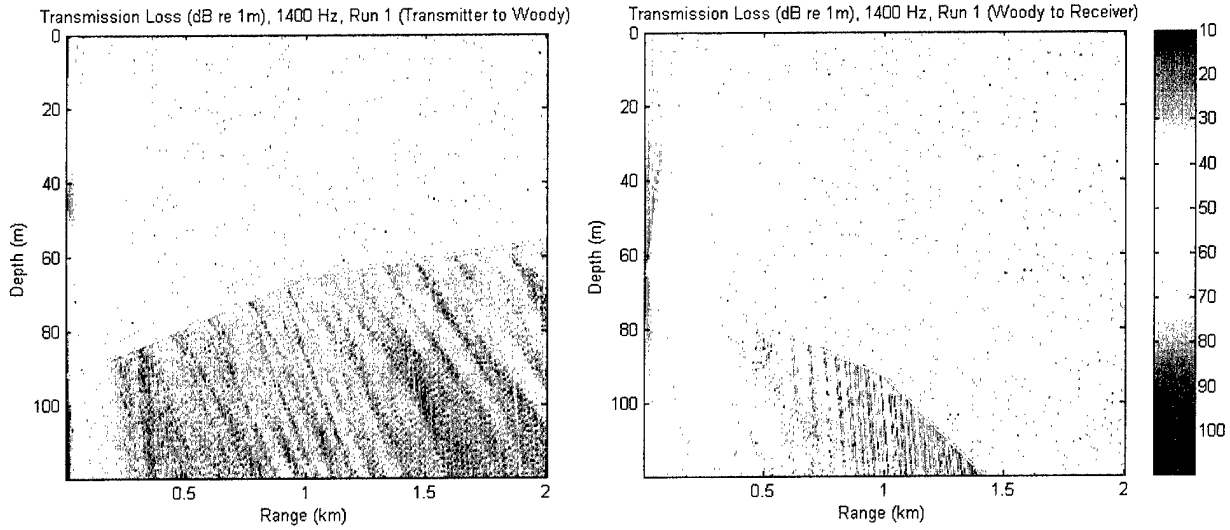

Figure B-14. Far-range (5 km) transmission loss for Woody location. Left panel is transmitter to Woody. Right panel is Woody to receiver.

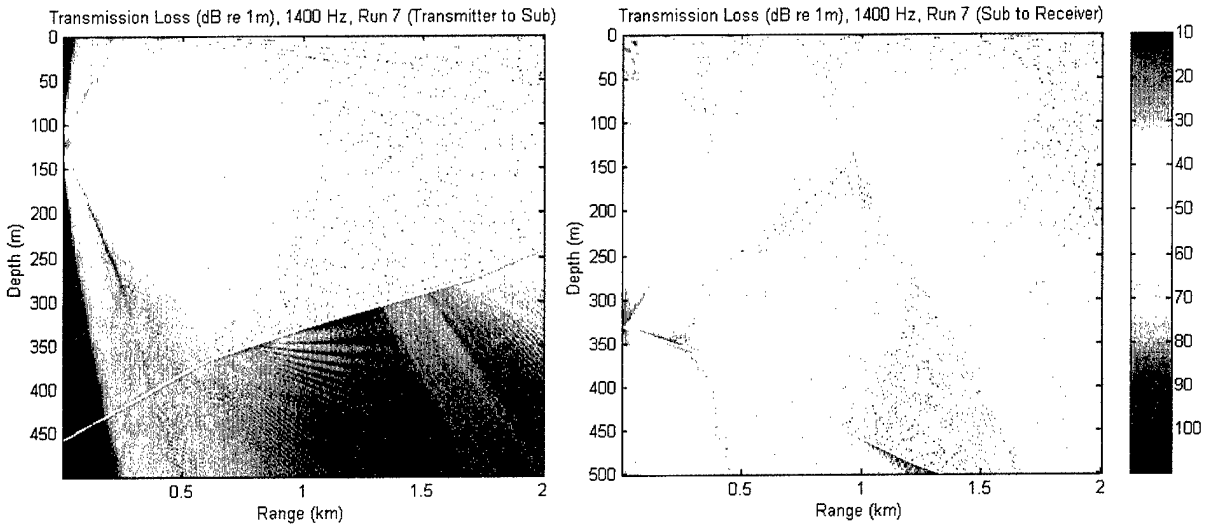

Figure B-15. Far-range transmission loss at Woody location with modified bathymetry. Left panel is transmitter to Woody. Right panel is Woody to receiver.

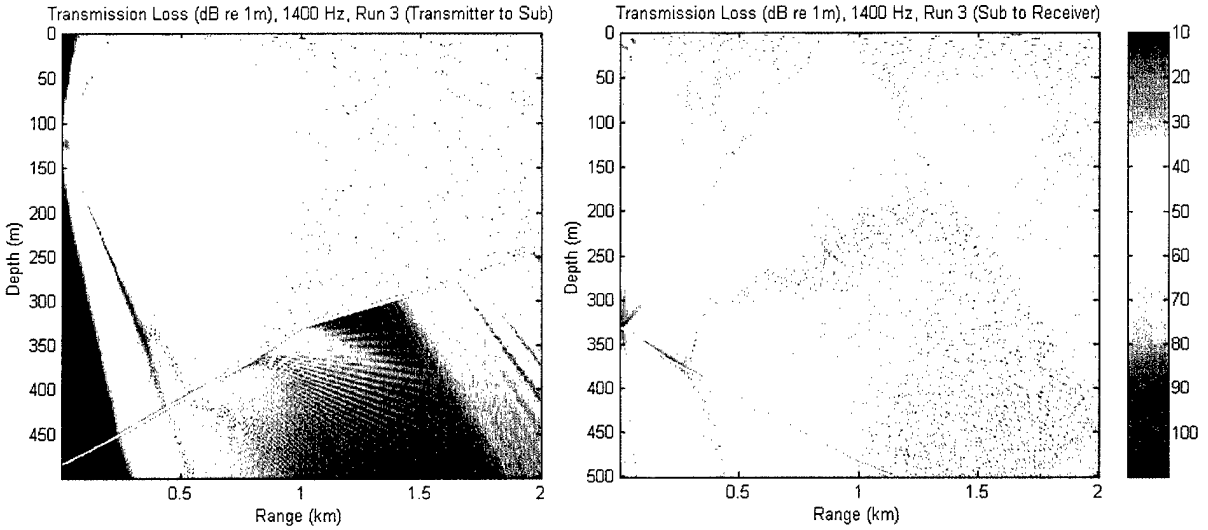

Figure B-16. Close-range transmission loss for sub location. Left panel is transmitter to sub. Right panel is sub to receiver.

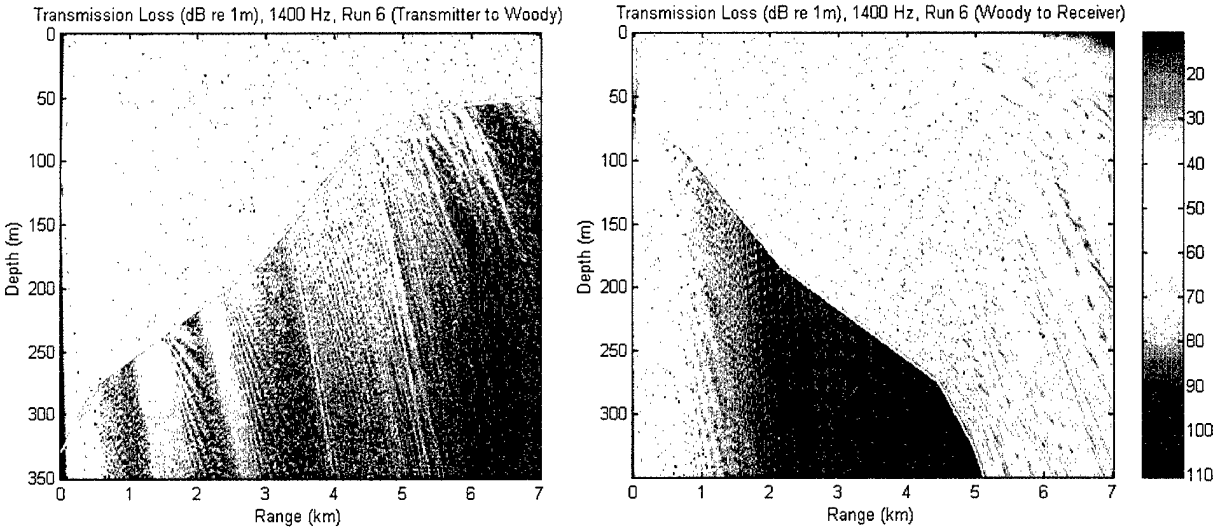

Figure B-17. Close-range transmission loss for sub location with modified bathymetry. Left panel is transmitter to Sub. Right panel is sub to receiver.

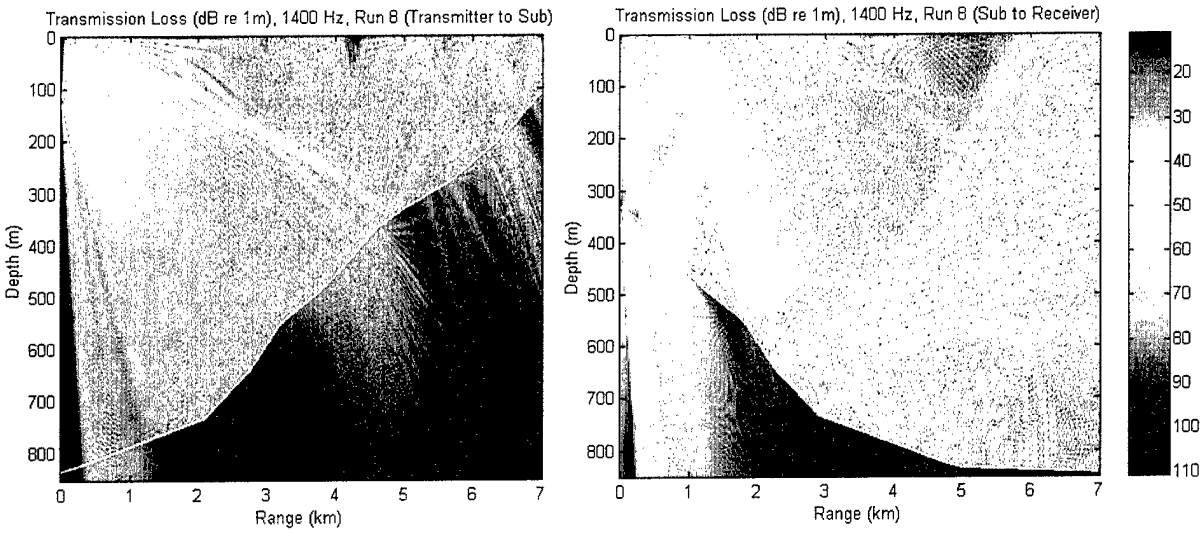

Figure B-18. Far-range transmission loss plot for sub location with modified bathymetry. Left panel is transmitter to Sub. Right panel is sub to receiver.

Table B-3. Summary of SAS simulations run with figure locations. Figure numbers that begin with a "2-" are in Section 2 of the main report.

Run	Target	Number of Points	Range	Target depth	Sonar depth	Notes	Figure
1	Woody	1	1 km	64 m	45 m	Actual bathymetry	B-19
2	Woody	5	1 km	64 m	45 m	Actual bathymetry	B-19
3	Woody	1	5 km	64 m	122 m	Actual bathymetry	B-20
4	Woody	5	5 km	64 m	122 m	Actual bathymetry	B-20
5	Woody	1	1 km	64 m	45 m	Modified bathymetry	B-21
6	Woody	5	1 km	64 m	45 m	Modified bathymetry	B-21
7	Woody	1	5 km	64 m	122 m	Modified bathymetry	B-22
8	Woody	5	5 km	64 m	122 m	Modified bathymetry	B-22
9	Woody	5	1 km	64 m	45 m	Type A bathymetry	B-23
10	Woody	5	5 km	64 m	122 m	Type A bathymetry	B-24
11	Woody	5	1 km	64 m	45 m	Type B bathymetry	B-23
12	Woody	5	5 km	64 m	122 m	Type B bathymetry	B-24
13	Woody	5	1 km	64 m	45 m	Type C bathymetry	B-23
14	Woody	5	5 km	64 m	122 m	Type C bathymetry	B-24
15	Sub	1	1 km	329 m	122 m	Actual bathymetry	B-25
16	Sub	5	1 km	329 m	122 m	Actual bathymetry	B-25
17	Sub	1	5 km	329 m	122 m	Actual bathymetry	2-25
18	Sub	5	5 km	329 m	122 m	Actual bathymetry	2-25
19	Sub	1	1 km	329 m	122 m	Modified bathymetry	B-26
20	Sub	5	1 km	329 m	122 m	Modified bathymetry	B-26
21	Sub	1	5 km	329 m	122 m	Modified bathymetry	B-27

Run	Target	Number of Points	Range	Target depth	Sonar depth	Notes	Figure
22	Sub	5	5 km	329 m	122 m	Modified bathymetry	B-27
23	Sub	5	1 km	329 m	122 m	Type A bathymetry	B-28
24	Sub	5	5 km	329 m	122 m	Type A bathymetry	2-26
25	Sub	5	1 km	329 m	122 m	Type B bathymetry	B-28
26	Sub	5	5 km	329 m	122 m	Type B bathymetry	2-26
27	Sub	5	1 km	329 m	122 m	Type C bathymetry	B-28
28	Sub	5	5 km	329 m	122 m	Type C bathymetry	2-26
29	Salmon	1	1 km	111 m	56 m		2-29
30	Salmon	5	1 km	111 m	56 m		2-29
31	Salmon	1	5 km	111 m	59 m	Flat bottom	2-30
32	Salmon	1	5 km	111 m	59 m	Flat bottom, isovelocity SVP	2-30

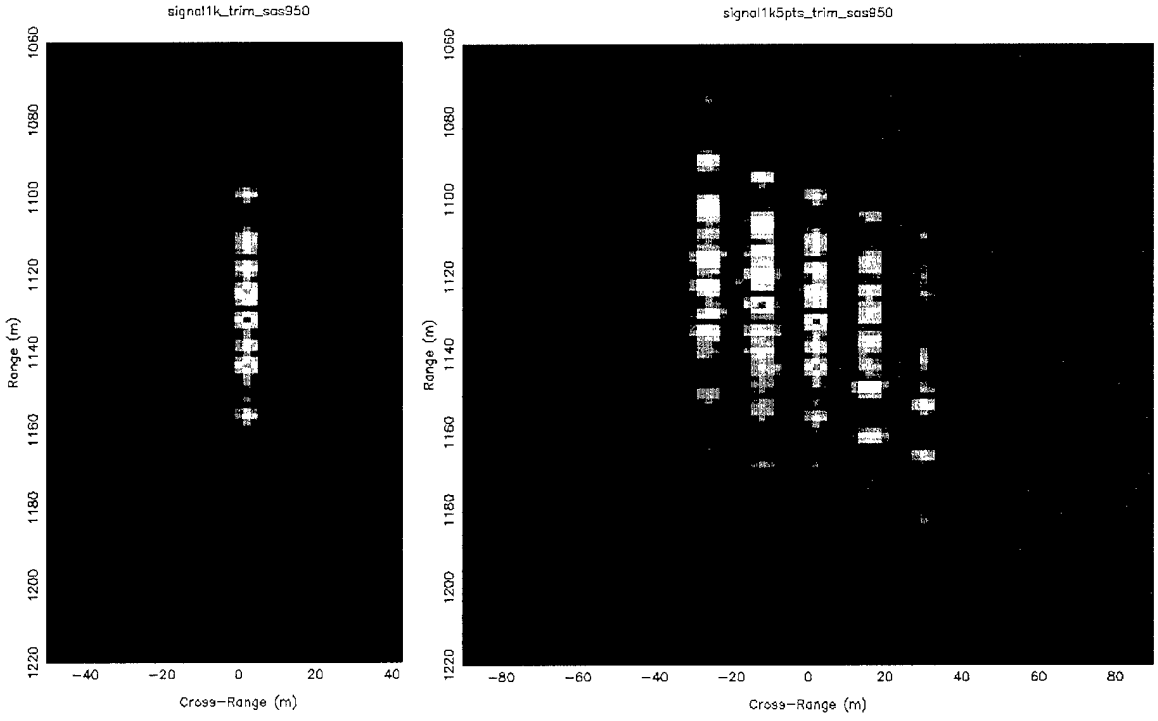

Figure B-19. Woody at 1 km. Left panel is single point, right panel is 5 points.

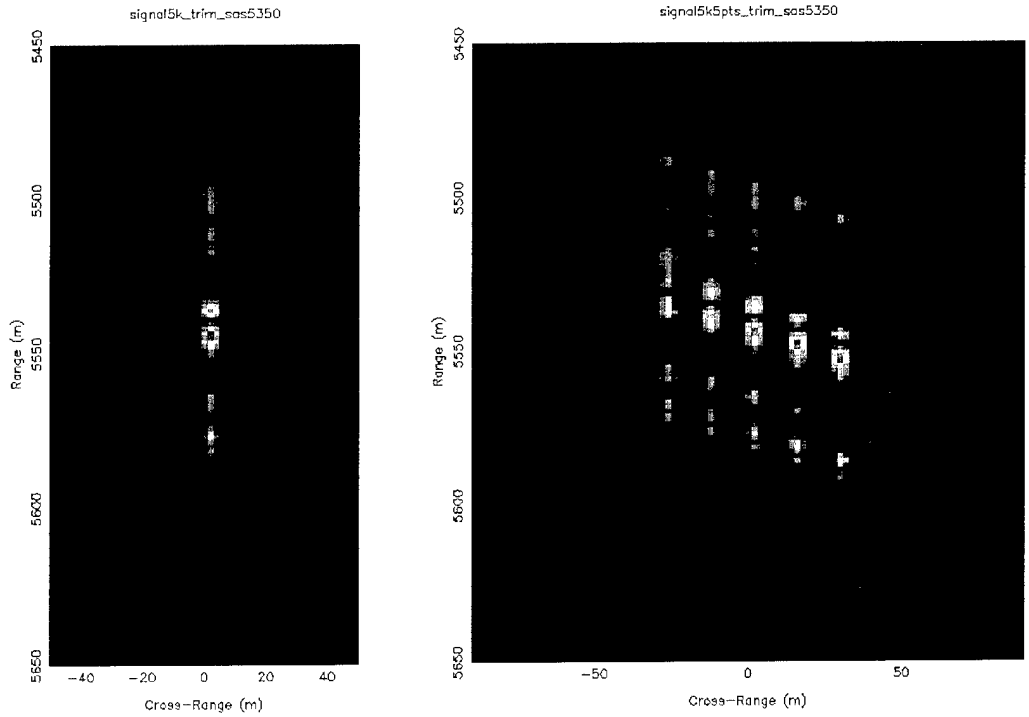

Figure B-20. Woody at 5 km. Left panel is single point, right panel is 5 points.

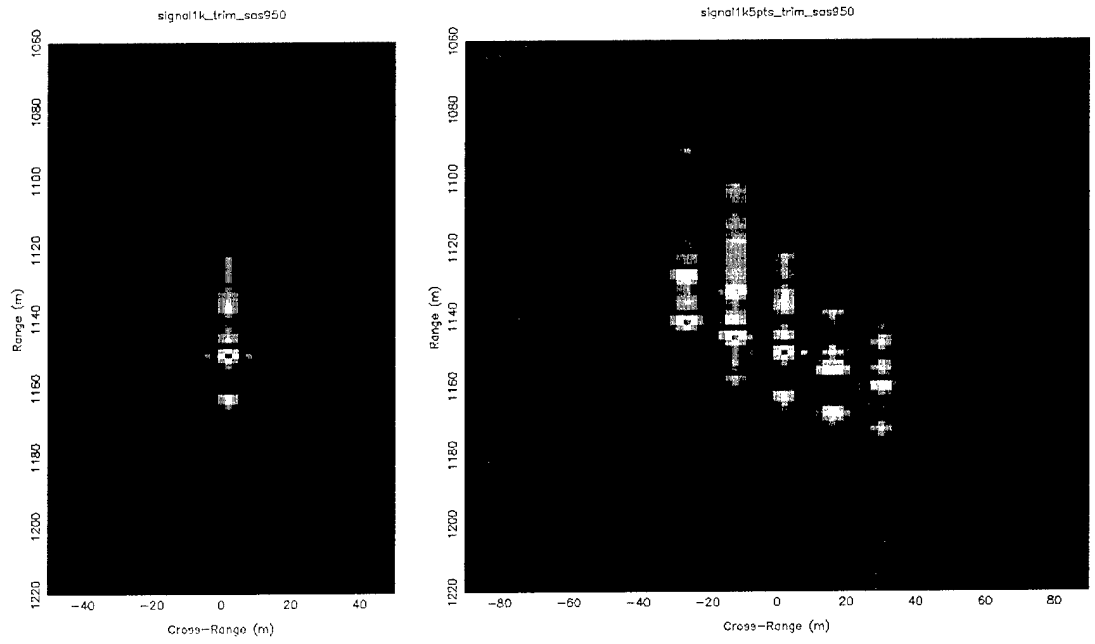

Figure B-21. Woody at 1 km, modified bathymetry. Left panel is single point, right panel is 5 points.

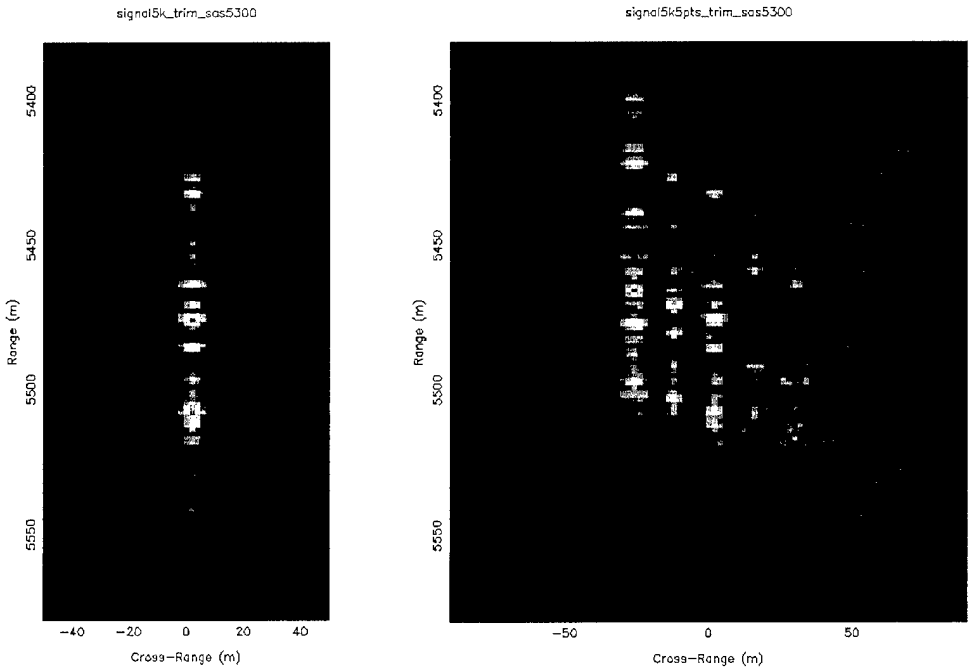

Figure B-22. Woody at 5 km, modified bathymetry. Left panel is single point, right panel is 5 points.

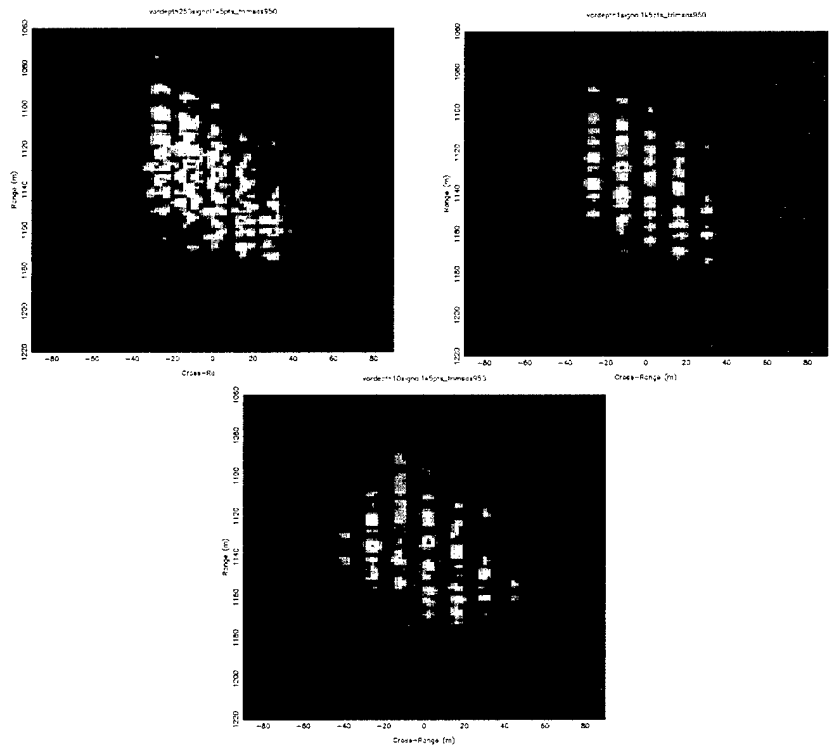

Figure B-23. Woody at 1 km with three different bottom variation schemes Top left is type A, top right is B, bottom is C.

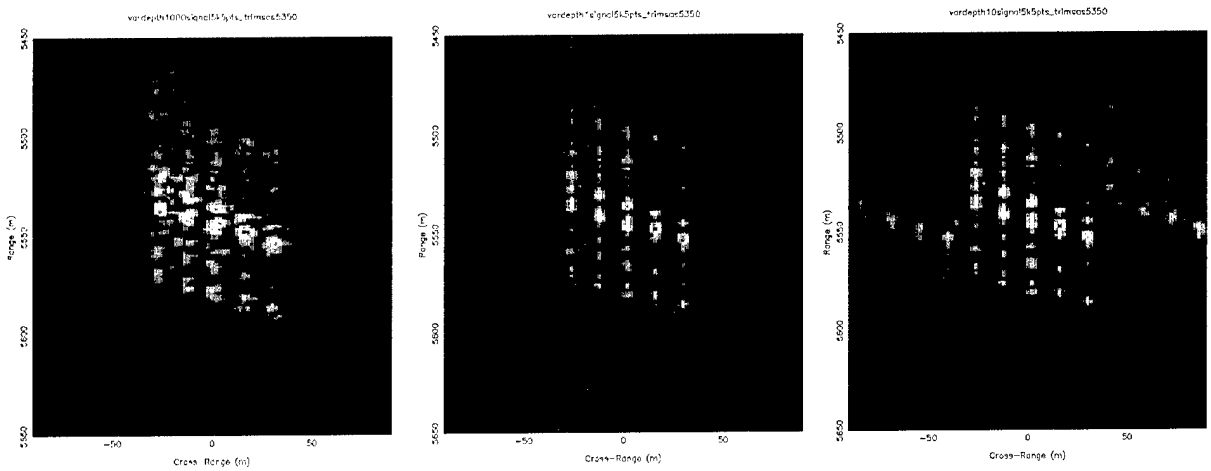

Figure B-24. Woody at 5 km with three different bottom variation schemes. Type A is the left panel, type B is the middle, and type C is the right panel.

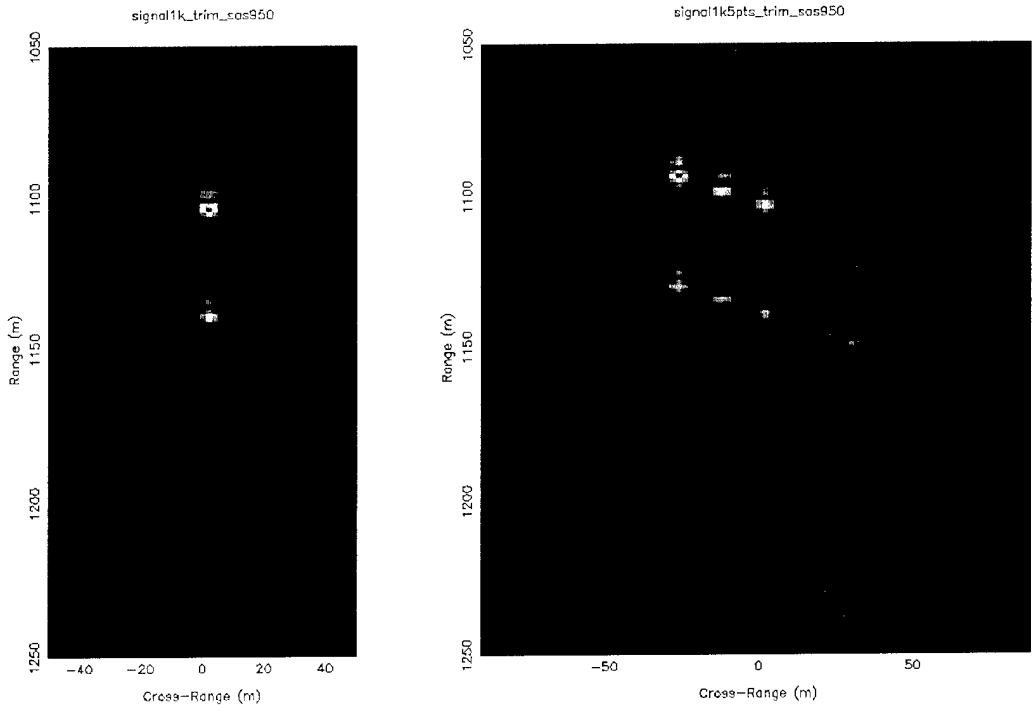

Figure B-25. Sub at 1 km. Left panel is single point, right panel is 5 points.

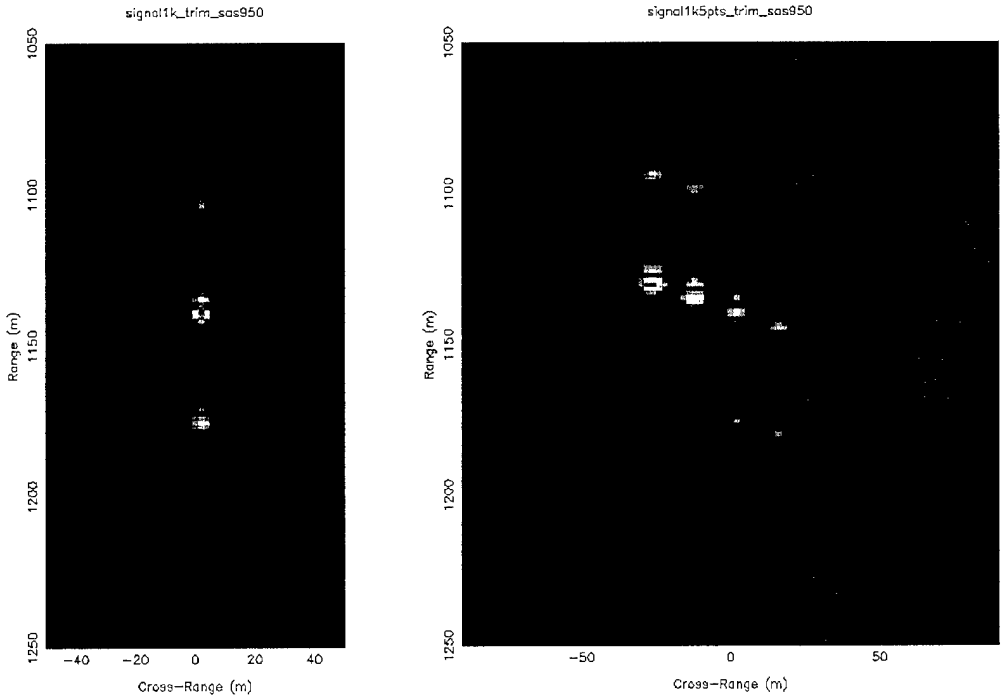

Figure B-26. Sub at 1 km with modified bathymetry. Left panel is single point, right panel is 5 points.

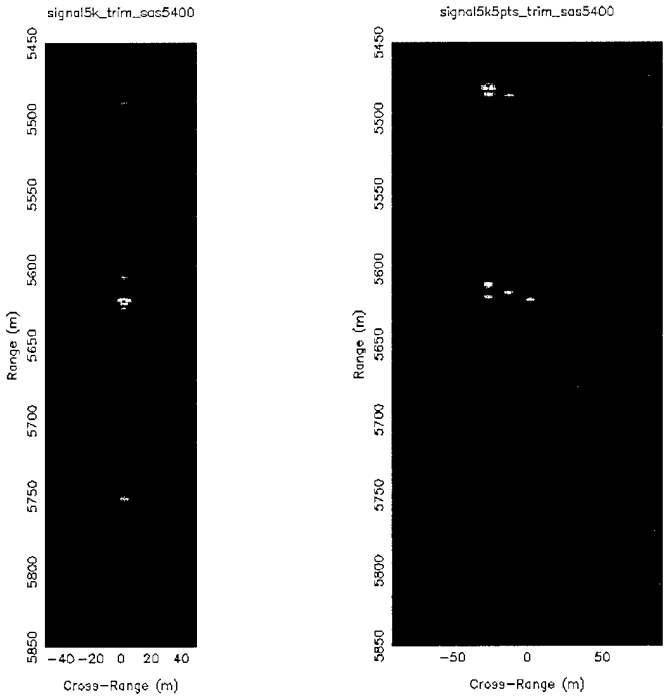

Figure B-27. Sub at 5 km with modified bathymetry. Left panel is single point, right panel is 5 points.

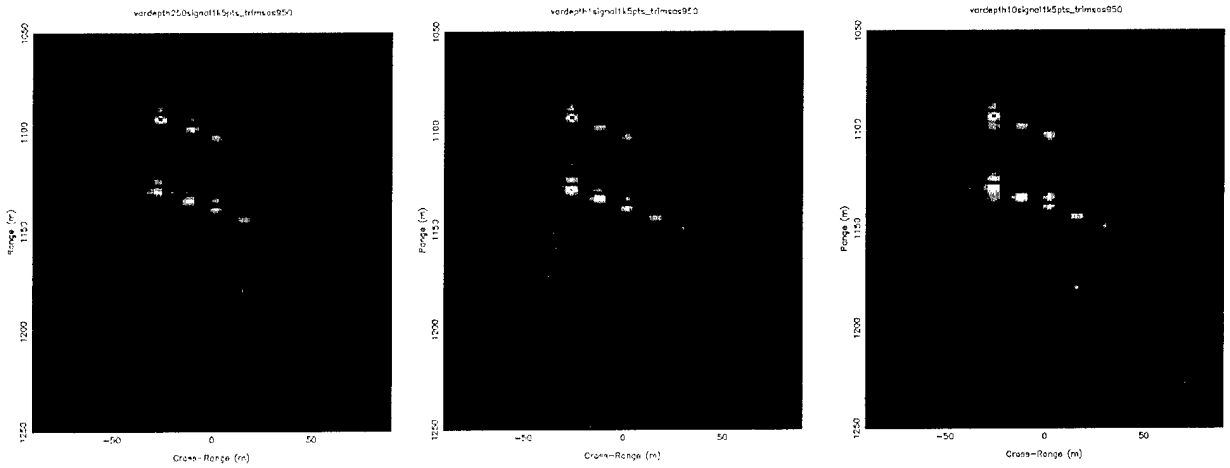

Figure B-28. Sub at 1 km with three different bottom variation schemes. Left is type A, middle is B, and right panel is C.

APPENDIX C: TRIAL LOG SHEETS

This appendix contains copies of the three sets of log sheets recorded during the trial. The XBT/XSV log sheet is on page C-2. The Seahawk runs are listed on pages C-3 to C-5. The marine mammal observation logs are on pages C-6 to C-9.

XBT LOG SHEET

Drop number	Type of drop	Serial number	Time	Date	Lat	Long	Filename	Who	Comments
1	XBT	319723	820	10/8/03	39°43.885	072°16.866	T6-00001	AXP	ok
3	XBT	319727	1230	"			T6-00003	AXP	ok
4	XSV	43011	1232	"			S2-00004	AXP	ok
5	XBT	319731	503	"	39 37.888	72 16.181	T6-00005	AXP	ok — weight deep for this drop
6	XBT	319732	915	10/9/03	39 42.609	72 11.980	T6-00006	AXP	had to reboot far too many times
7	XBT	319728	1215	10/9/03	3944.9	7227.68	T6-00007	AXP	
8 9	XBT	319724	1741	10/9/03			T6-00009	AXP	
11	XBT	319733	747	10/10/03	39 48.6	72 46.2	T6-00011	AXP	many reboots
12	XSV	43012	747	10/10/03	"	"	S2-00012	AXP	ok

2

fryer depth 360-380 ft

DTW-02-020XX

Run Number	Gain setting	PRI/PL (s)	Time/ Length of run	Boat Speed	Omni or direct.	Heading	Water depth	Wind speed/dir (rel to ship motion)	Time start	Time end	Quick Comments
S1	0dB	6 6.25	2m	3.4	port	277	~~350~~ 360 ft	14~~15~~/22°	9:00	9:12	235° ± 12 off ship 228 ship
S2	0dB	6 6.25	~2m	3	port	109	~~360~~ 362 ft	12 162	9:~~36~~	9:37	contact 325/109 ship
S3	0dB	6 6.25	11m	3	port	340	365	11 -45	9:50	10:01	320 contact rough leg - tide/current
C1	0dB	6 0.25	30min	3	stb	210	360	13 +45	1051	11:20	fish boat 2 nm std beacon just broke surface
C2	0dB	12 0.5	30min	3.2	port	20	375	6 -90	1139	1209	several surface contacts
S7	0dB	6 0.25	30min	3.1	Omni	105	360	12 +135	1226	~~1352~~ 1256	
S8	0dB	6 0.25	35min	2.9	port	350	375	7 ~~+45~~	1:25	157	contact w/ salmon early
S9	0dB	6 0.25	35min	3.2	port	220	305	19 +45	~~2~~46	320	
S10	0dB	6 0.25	30m	3.1	port	101	375	7 0	405	435	a little rough (tide/current) speed up
S11	0dB	12 0.5	~2min	3.0	stb	225	393	15 0	510	612	
S12	0dB	12 0.5	60min	3	port	338	395	7 -22	1001	1100	
S13	0dB	12 0.5	55min	3.2	port	230	285	10 +22	1205	1257	
S14	0dB	6 0.25	~45	3.5	port	114	~~378~~	6 +135	1349	1402	14:02 turtle spotted
		Abort above									ceased transmissions
S15	0dB	6 0.25	~15	3.5	port	340	373	7 -22	14~~33~~	1455	uplink ceased
											after ~15min
S16	0dB	6 0.25	~8mn	3.4	port	220	325	6 +45	1520	1528	uplink ceased, power
			returned to beginning								zapped.
S16a	0dB	6 0.25		3.4	port	220	325	10 +45	1550	1550	uplink ceased

DTW-02-020XX

Run Number	Gain setting	PRI/PL (s)	Time/ Length of run	Boat Speed	Omni or direct.	Heading	Water depth	Wind speed/dir	Time start	Time end	Quick Comments
S16b	-6dB	6/0.25	23min	3.5	port	222	325	7 +45	~~1625~~ 1627	1650	forgot to begin powerramps Began 2min late
S17	-6dB	6/0.25	6min	5	stb	44	355	0 +45	1706	1712	okay
S15a	-6dB	6/0.25	8min	3.3	stb	160	343	0 +45	1731	1738	Stopped due to dolphins
	Last spotted around 6,50					not enough time to do more before daylight end					

H:\vas\LR SAS\seatrial1plans\seatrialplans.doc

Run Number	Gain setting	PRI/PL (s)	Time/ Length of run	Boat Speed	Omni or direct.	Heading	Water depth	Wind speed/dir	Time start	Time end	Quick Comments
T1	-6dB	6/0.25	10min	3	port	335	190	17 0	740	750	fan target in 2 pcces
T2	-6dB	6/0.25	10min	3.4	port	210	190	9 -90/68	~~7~~806	816	rough ride
T8	-6dB	6/0.25	35min	3	s+b	39	210	6 +68	850	925	rough ride, no boat data recorded
T9	-6dB	6/0.25	30min	4.5	~~s~~ port	275	190	15 +135	~~10~~40	1110	calmer direction
T14	-6dB	6/0.25	20min	3.2	~~port~~	260	190	17 188	1231	1250	getting too rough to run

H:\ens\LR SAS\ecatrial1plans\ecatrialplans.doc

STBD JUST AFT OF BRIDGE

Marine Mammal Datasheet

Date	Time (Z) Local	Detection Method (eye/7x/25x/ acoustic)	Species	Group Size			Acoustic Trans.? (Y/N)	Comment/Weather Conditions	Angle (from bow)	Distance			Obs. Position	Direction of travel
				Best	Low	High				meters (est.)	7x rets	25x rets	(e.g. bridge)	(compass bearing)
10/07/02	15:40	BEGIN	N/A				N	5-6' SWELL SCATTERED WHITE CAPS						126°
	16:45	STOP-TRANSIT TO DEEPER SITE												
	17:40	START OBSERVING AGAIN												126°
10/7	1836	SECURED OPS / PINGING						5-10K, 3' SWELLS, CLEAR						130°
10/07/02	1850	SUNSET LOSS OF VISIBILITY												
10/08/02	0645	BEGIN OBSERVATION	N/A					5-10K WIND, 2-3' SWELLS, CLEAR						
10/08	0815	EYE 7/50	N/A	-	-	-		5-8K, 2-3 SWELL, CLEAR	START LAUNCH				(OK)	042
	0858	EYE 7/50	N/A					5-10K, 2-5 SWELL, CLEAR	BEGIN XMITTING				STBD AFT RANGE	225°
		"	"	STOP XMITTING - GOING TO NEW LINE										
10/08	0924	EYE 7/50	N/A	BEGIN XMITTING				SAME						
	1025	EYE	??		SINGLE			SINGLE ANIMAL BREACHED ONCE	90° STBD	250	N/A		STBD AFT-RANGE	210°
	1220	EYE 7/50	N/A	ALL	CLEAR		Y	5-10K, 3' SWELL, CLEAR						105°
	1302	EYE	ATLANTIC SPOTTED DOLPHIN	3			N	5-10K, SWAM TO-FRM BOW QUICK USE TO 2-3 SWELL, SCATTERED WHITE CAPS RIDE					STBD AFT-RANGE	105°
10/8	1322	EYE 7/50	N/A	ALL	CLEAR		Y START	"					"	338°
	1450	SOL	N/A	ALL	CLEAR		Y	"					"	209°
	1606	SOL S-10	N/A	ALL	CLEAR		Y	10-15K					"	260
	1720	SOL S-11	N/A	ALL	CLEAR		Y	10-15K						
10/8	1815	EOL	N/A	ALL	CLEAR		Y	10-15K (LAST LINE TODAY)						
10/9	—	decided to check out pinger -												
	0830	confirmed proper operation												
	0900	on scene to resume tests launching buoy												
~~SOL~~	0930	Clear to Xmit												
SOL	1000		"		"			SOL S-12						340

Marine Mammal Datasheet

Date	Time (Z)	Detection Method (eye/7x/25x/ acoustic)	Species	Group Size			Acoustic Trans.? (Y/N)	Comment/Weather Conditions	Angle (from bow)	Distance			Obs. Position	Direction of travel
				Best	Low	High				meters (est.)	7x rets	25x rets	(e.g. bridge)	(compass bearing)
10/09	1100	EOL						5-12 - NO MAMMALS						
	1105	TRANSITTING TO SOL OF NEXT LINE												
	1120	BEGIN OBSERVATIONS AGAIN	N/A EYE 7/50					SLIGHT RIPPLING NO WHITE CAPS 5-10KTS, 3-4' SWELL LONG PERIOD					STBD AFT BRIDGE	
	1205	SOL 16	ALL CLEAR				Y	"					"	250
	1257	EOL 16	ALL CLEAR				STOPPED	"					"	230
	1348	SOL 17	ALL CLEAR					"					"	105
	1400	STOPPED	TRANSMISSION	DUE TO SIGHTING OF SEATURTLE - SEE FORM						OBSERVER'S COG				105
	1433	SOL S-15	ALL CLEAR				Y	5-10K 2-3' SWELL, SLIGHT RIPPLE, NO WHITE CAPS						340°
	1455	EOL	ALL CLEAR				STOP	"						215°
	1519	SOL S-16	ALL CLEAR				Y	"						215°
	1549	SOL S16A	ALL CLEAR				Y	"						215°
	1551	STOPPED	SONAR SYSTEM HAVING PROBLEMS					"						215°
	1626	RESTART 16B	XMITTING					"						215°
	1646	EOL S16B	ALL CLEAR					~5 KTS, SLIGHT GENTLE SWELL w/ ripples						215°
	1710	SOL S-17	ALL CLEAR					"						051°
	1712	EOL S17	"	"				"						"
	1730	SOL S-15A	ALL CLEAR				Y	"						160°
	1738	EYE 7/50	COMMON DOLPHIN		15-	20	STOPPED	PORPOISE XING BOW @ 500yd STBD-toport						
	1752	EYE 7/50	"		15-	20	N	FADED AWAY BEHIND STERN						165
	1808	SONAR TOWFISH ON BOARD												
10/10/03	0645	BEGIN OBSERVATIONS						<5K, Slight Swell w ripple						
10/10/03	0720	SONAR IN WATER						10-15K, 2-3' WAVES RANDOM WHITE CAPS						265°
10/10/03	0739	SOL T-1	ALL CLEAR					"						330°
10/10/03	0749	EOL T-1	ALL CLEAR					10-15 GUST TO 20K, 2-4' SCATTERED WHITE CAPS						220°

Marine Mammal Datasheet

Date	Time (Z)	Detection Method (eye/7x/25x/ acoustic)	Species	Group Size			Acoustic Trans.? (Y/N)	Comment/Weather Conditions	Angle (from bow)	Distance			Obs. Position	Direction of travel
				Best	Low	High				meters (est.)	7x rets	25x rets	(e.g. bridge)	(compass bearing)
10/10/01	0804	EYE/7x50	SOL T-2				Y	10-15 GUST-20K, 2-4' SCATTERED WHITE CAPS	N/A				STBD AFT-BRIDGE	205°
	0815	EOL T-2					N	"	"				"	205°
	0849	SOL T-8					Y	"	"				"	048°
	0904	EOL T-8					N	"	"				"	"
	1039	SOL T-9					Y	15-20K, 3-6' SEAS, MANY WHITE CAPS	"				"	277°
	1108	EOL T-9					STOP	"	"				"	277°
	1230	SOL T-14					Y	"	"				"	295°
	1249	EOL T-14					STOP	" CONDITIONS WORSENING	"				"	291°
	1250	WORSENING WEATHER CAUSING STOP TO OPERATIONS.												

Car

Marine Mammal Datasheet PORT

Date	Time (Z)	Detection Method (eye/7x/25x/ acoustic)	Species	Group Size			Acoustic Trans.? (Y/N)	Comment/Weather Conditions	Angle (from bow)	Distance			Obs. Position	Direction of travel
				Best	Low	High				meters (est.)	7x rets	25x rets	(e.g. bridge)	(compass bearing)
10/07/03	15:40							START OBSERVATION						
	1645							NO MAMMALS TRANSIT TO NEW SITE						
	17:40							START OBSERVATION						
	18:50							SUNSET LOSS OF VISIBILITY						
10/08/03	06:45							START OBSERVATION						
	18:25							SECURE OBSERVATION						
10/09/03	06:00							START OBSERVATION						
SOL	1205							S 12 340°						
13	8K	from tgt						226°						
	1400							TURTLE SEEN GREEN	90°P	15m			PORT Wing	106°
								SPOTTED OFF BOW 200m SECURE						
								TRANSMITTING WHILE						
								SHIP PASSED.						
	1406							MOVE TO NEW LOCATION						
	1435	VISUAL	DOLPHIN CAMERA		15	20		SIGHTED ACTIVE	090P	400m				
	1456							DOLPHINS DEPART		1m				
	1430							SECURE OBSERVATIONS						
10/10/03	0644							START OBSERVATIONS						
	0950							START T-8 - Clear						
	1252							SECURE OPS DUE TO SEAS						

APPENDIX D: ADDITIONAL SLS IMAGERY

This appendix contains the SLS imagery and vehicle motion for the data sets read, but not SAS processed. Some data sets were never read by DTI. The SLS images here demonstrate the richness of the data set. These data could be processed further, but time and money constraints prohibited the work under this program. Future programs may wish to use these data.

The runs represented in this appendix are listed in Table D-1, along with the figure numbers (SLS image and towbody motion data) for reference. Figure D-1 is the general Salmon site run layout with runs represented in this appendix listed. Figure D-10 is the Bidevind site run layout with runs marked. It should be noted that there were problems in inserting the PingNow bit into T14, so all of the image may not be available. Figure D-15 schematically shows the locations of the clutter runs, only one of which was read. Commentary of some runs has been placed in the figure captions. The color scaling on the SLS imagery has been set to a range dependent scaling to enhance the far ranges. The towbody heading is the most variable from run to run. The pitch, roll, and depth changes (depth may be corrupt, as mentioned in Section 2.1.1) remain at similar levels between runs.

Table D-1. Data sets represented in this appendix.

Run	CPA	PRI	Run length	Figures
S1	500 m	6 s	12 min	D-2, D-3
S3	500 m	6 s	11 min	D-4, D-5
S8	4500 m	6 s	35 min	D-6, D-7
S10	4500 m	6 s	30 min	D-8, D-9
T8	4000 m	6 s	35 min	D-11, D-12
T14	2500 m	6 s	20 min	D-13, D-14
C1	Not applicable	6 s	30 min	D-16, D-17

The remaining 12 runs are not represented in this report. Since they are of similar aspects and/or distances to those which do appear, nothing new is expected to be found in them (although that does not mean to say that they are not worthy of processing). Run T1 was corrupt and could not have a PingNow bit inserted by L-3OS, thus no further processing can be expected.

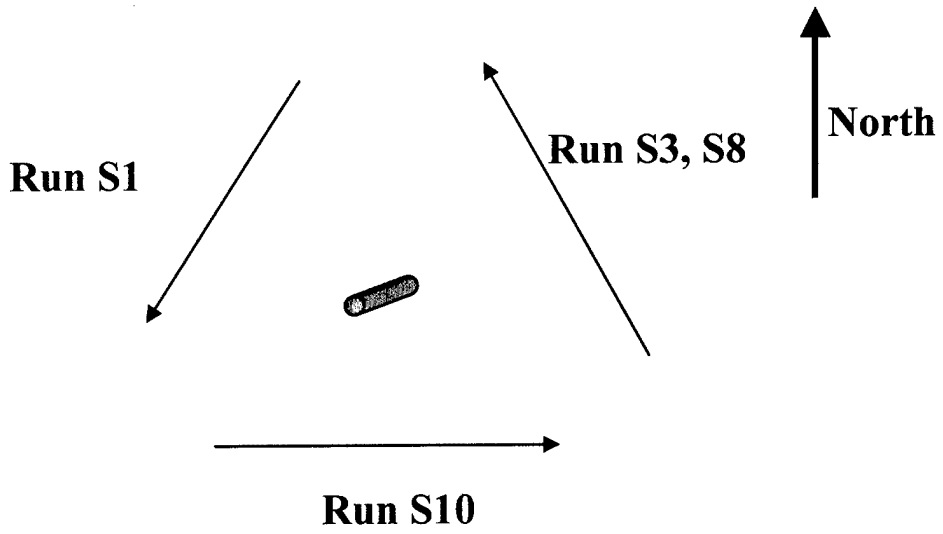

Figure D-1. Schematic of Salmon site runs with SLS imagery in this appendix.

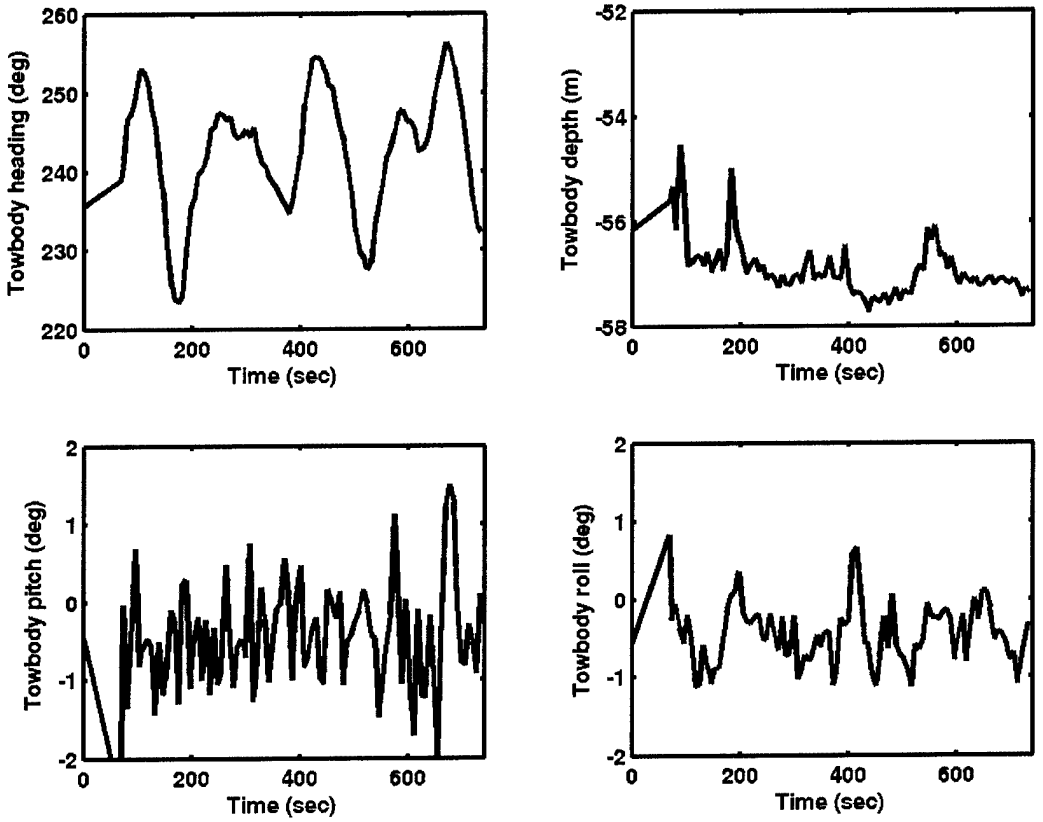

Figure D-2. Towbody motion for run S1. Note the 25° changes in heading when viewing the SLS image.

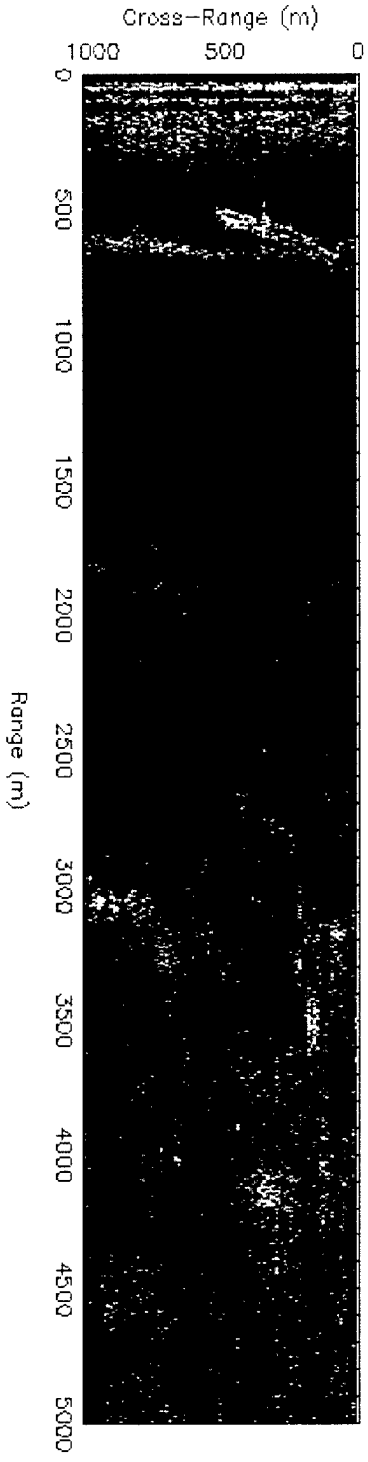

Figure D-3. SLS image for run S1.There is yaw present in the early pings as indicated by the smeared Salmon image. There may be other objects at 3 km and further. The last direct path return at 500 m is evident.

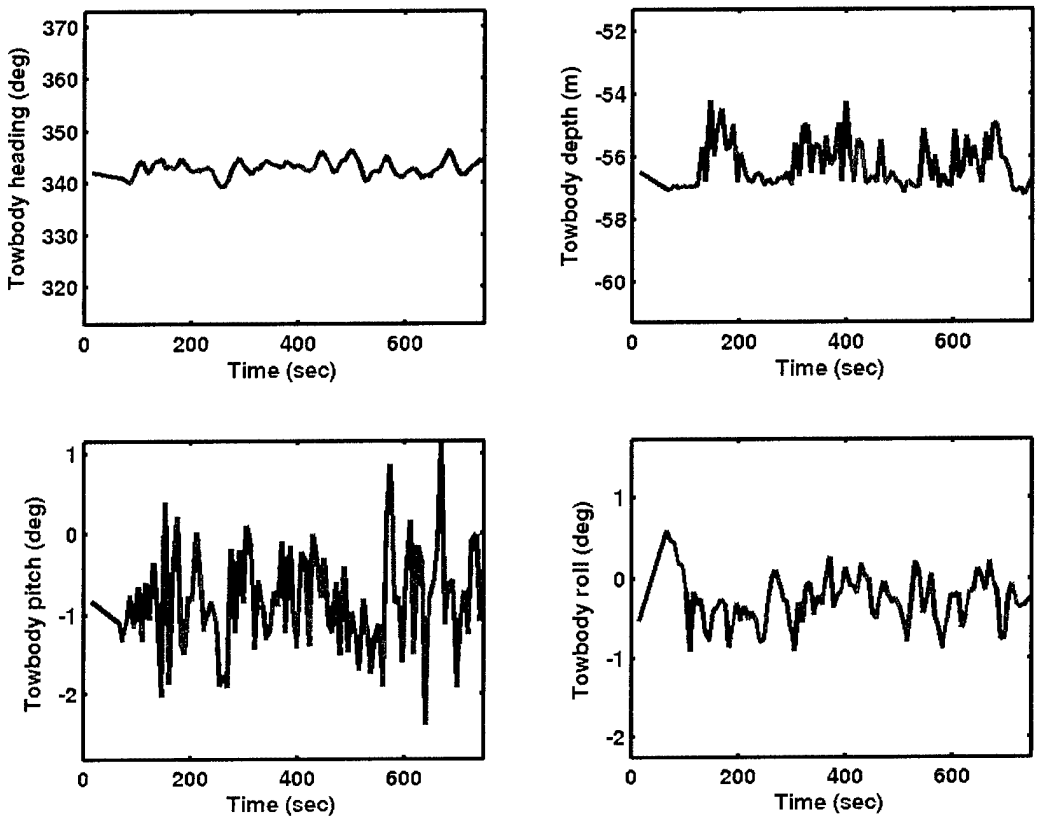

Figure D-4. Towbody motion for run S3. Note the extremely small heading changes during the run.

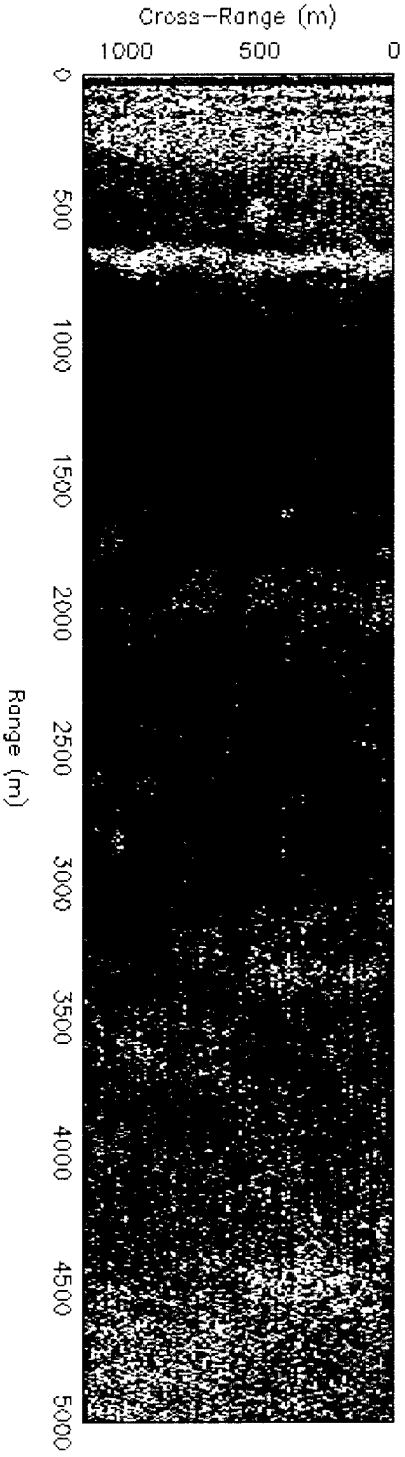

Figure D-5. SLS image for run S3. The Salmon is very cleanly present here. There is not obvious motion in the image. There is possible clutter or Salmon reflections at multiple ranges.

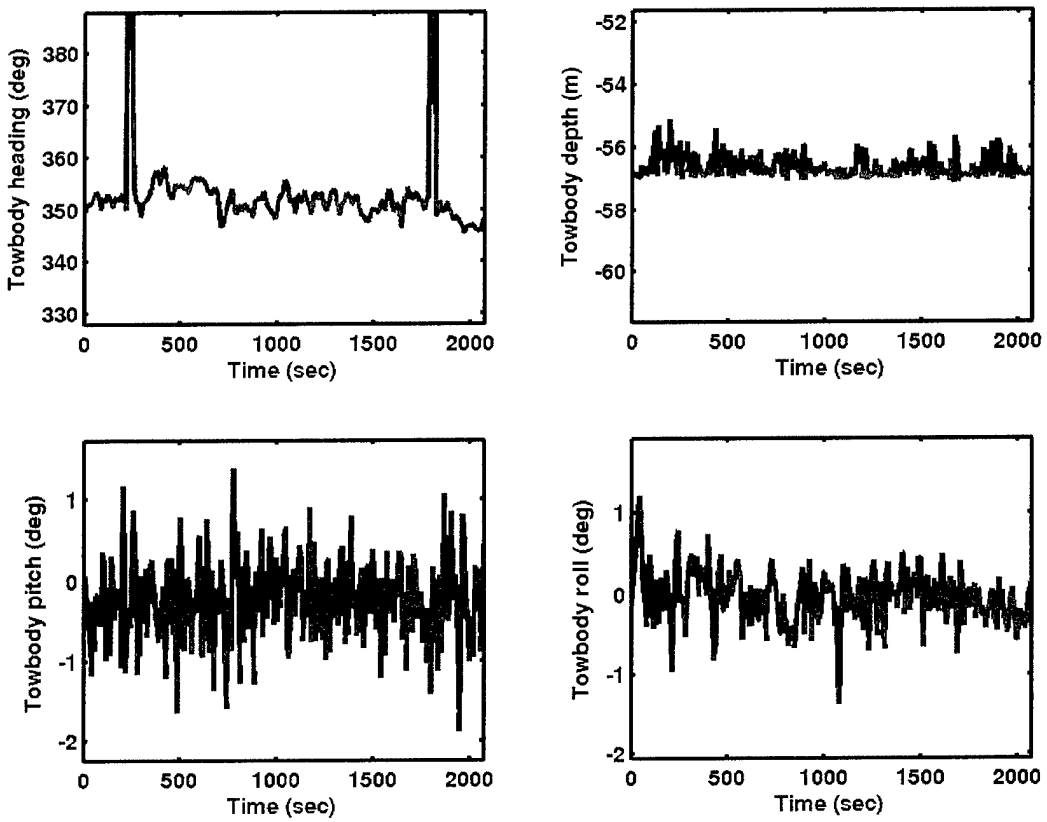

Figure D-6. Towbody motion for run S8. The two big excursions of the heading appear to be glitches in the system.

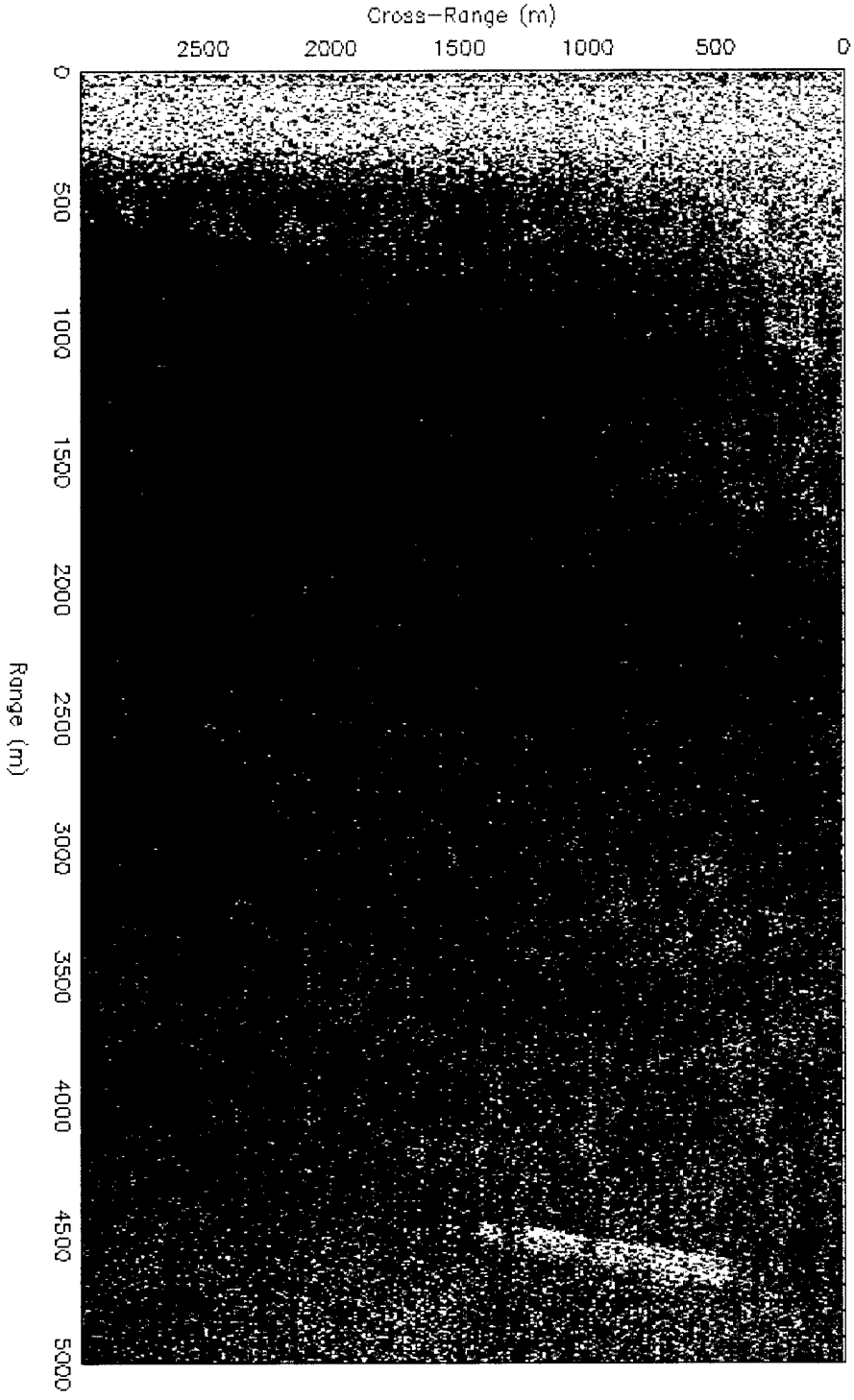

Figure D-7. SLS image for run S8. There appears to be strong yaw early in the run, or perhaps a crab throughout, causing extended returns early in the run.

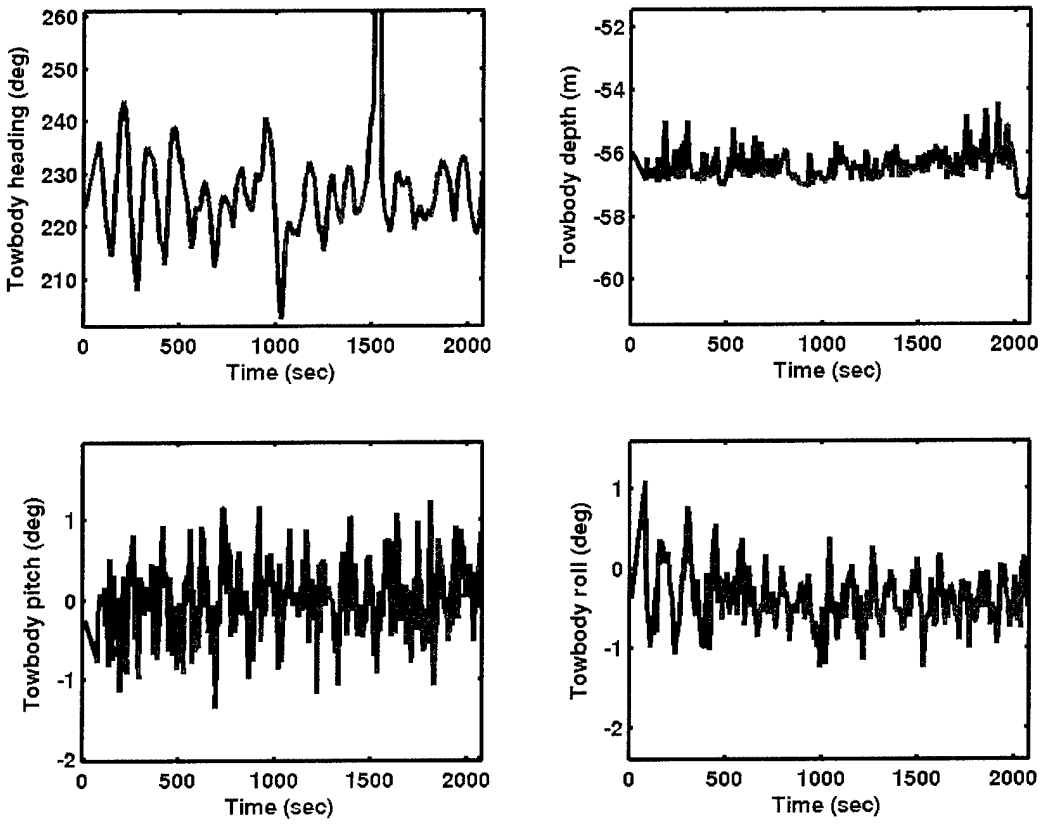

Figure D-8. Towbody motion for run S10. The heading oscillates quickly in this run.

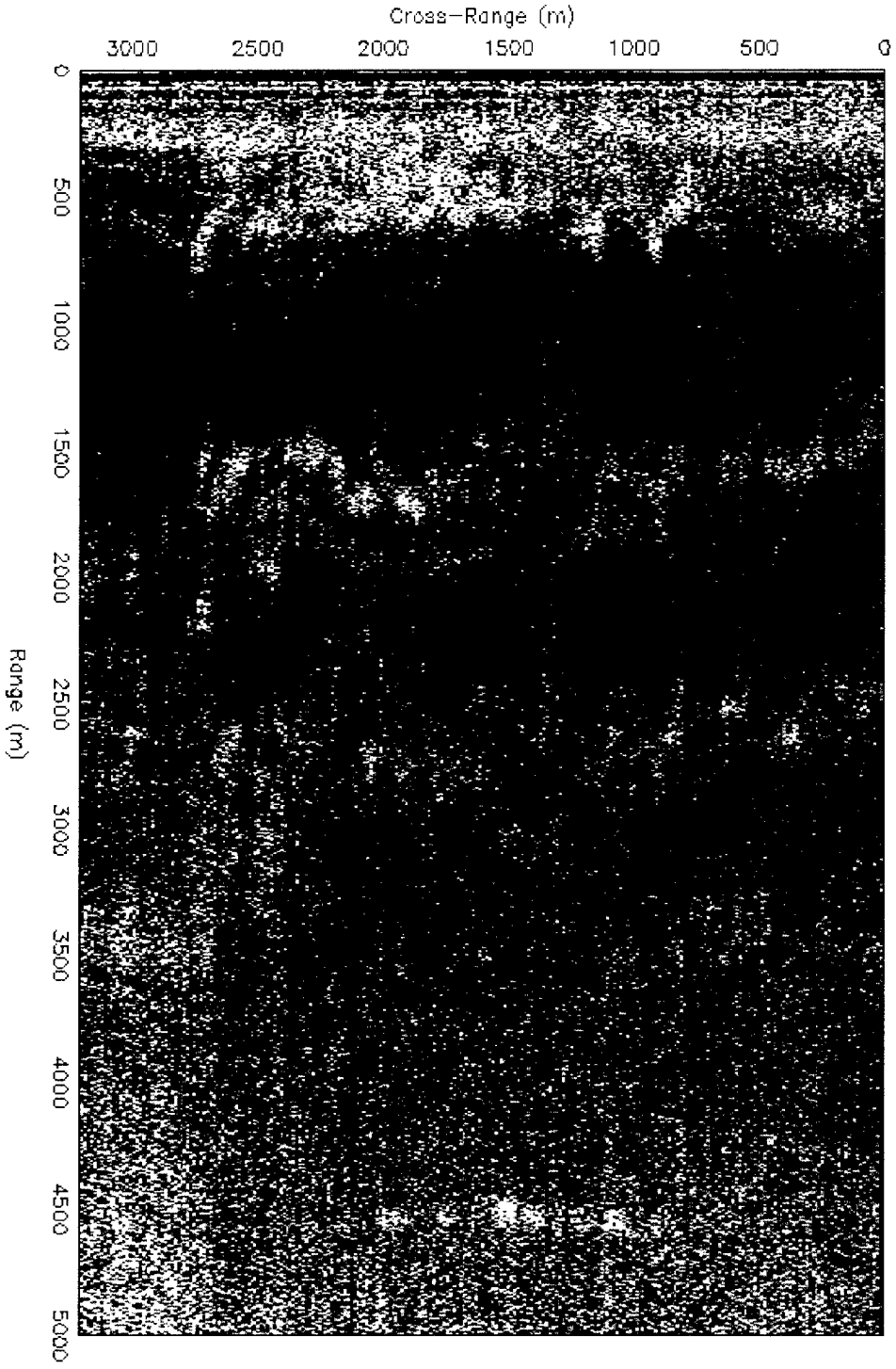

Figure D-9. SLS image for run S10. The on-off nature of the Salmon returns are indicative of the oscillating yaw seen in the towbody heading. The wavy pattern seen at ~500 m, ~1500 m and elsewhere may be due to motion or bathymetry changes.

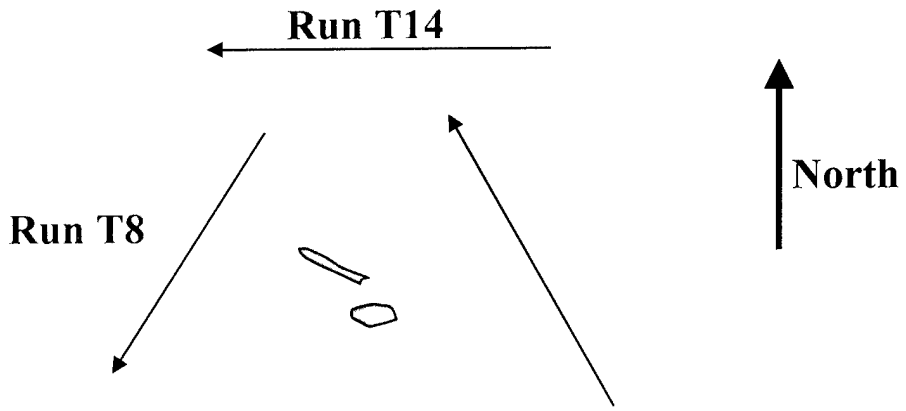

Figure D-10. Schematic of Bidevind site runs with SLS imagery in this appendix.

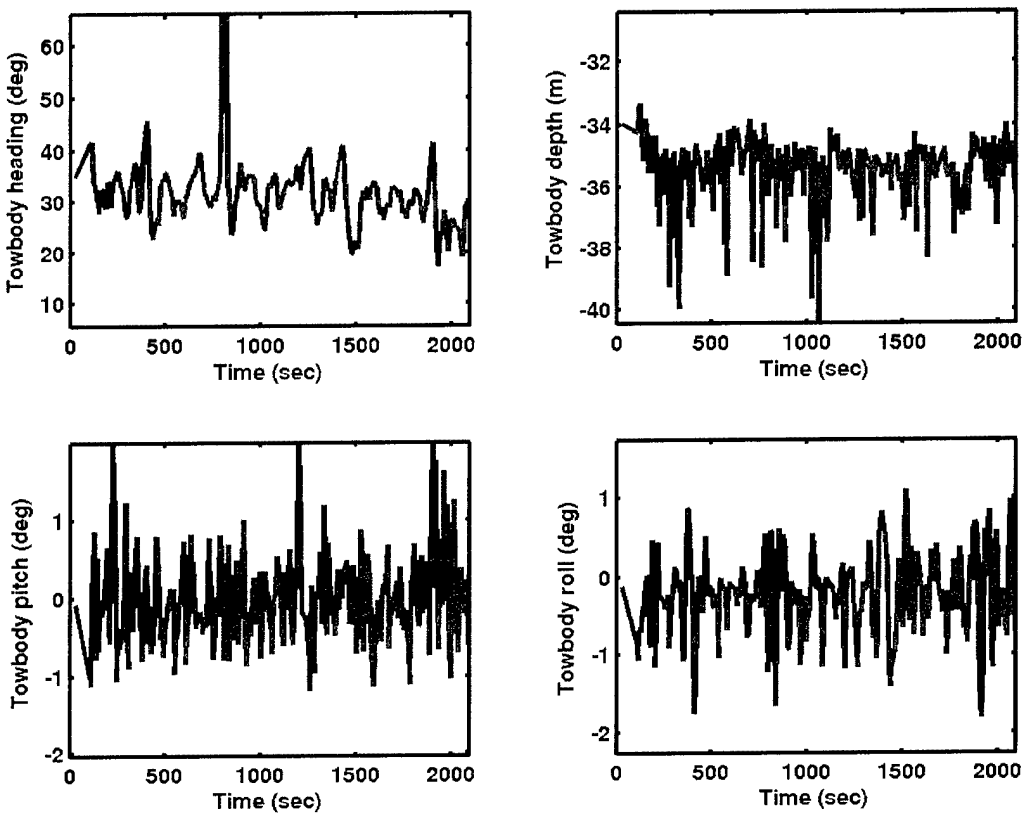

Figure D-11. Towbody motion for run T8. The strong heading change at ~800 s may be a glitch in the sensor. The slowly decreasing heading combined with the oscillations may explain the bright object changes in the SLS image. The depth changes were larger and more frequent than Salmon runs. The roll and pitch excursions are a little larger than in the Salmon runs.

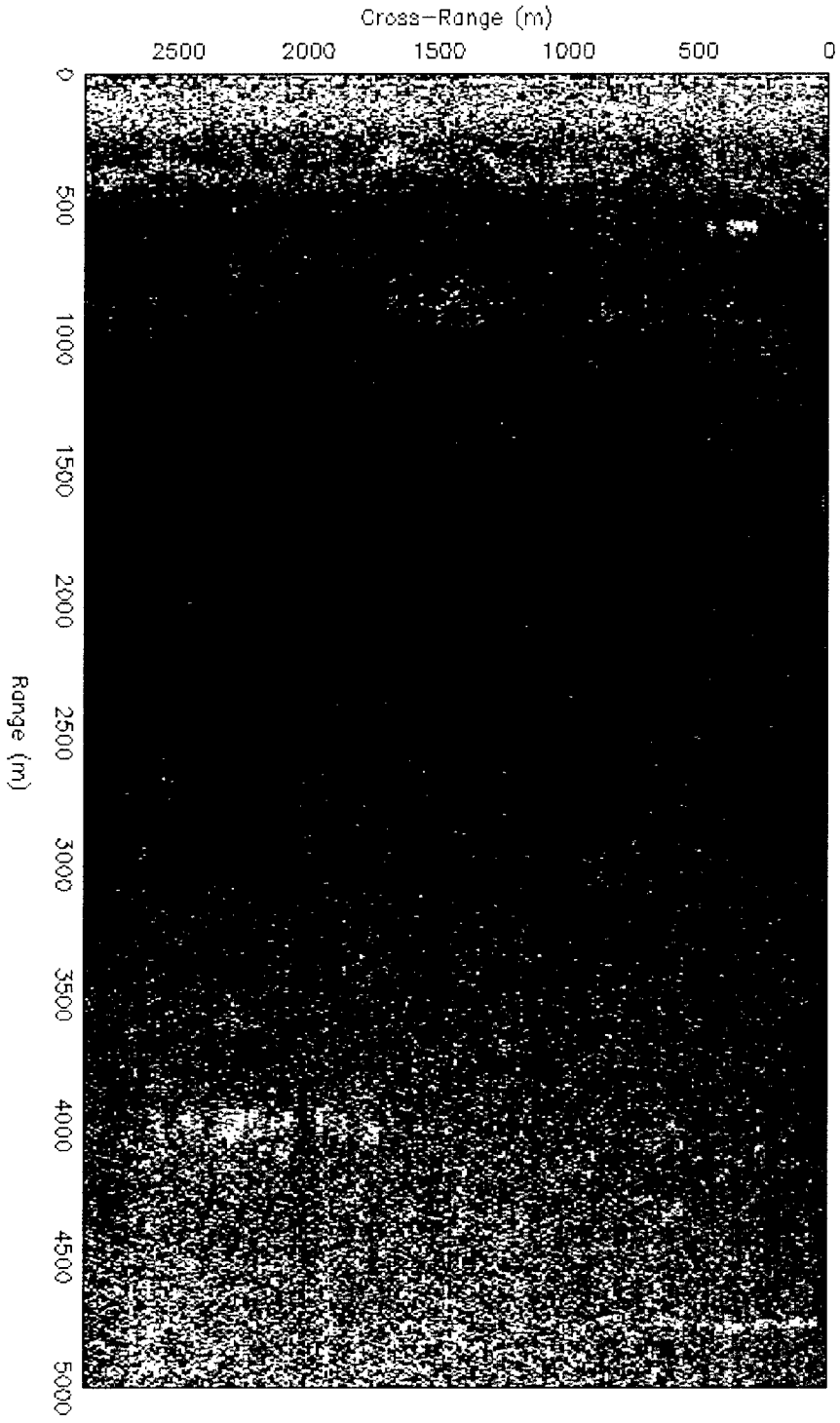

Figure D-12. SLS image for run T8. There appear to be objects at ~500 m and ~4700 m in addition to the Bidevind at ~4000 m. All objects have the on-off signature of yaw changes.

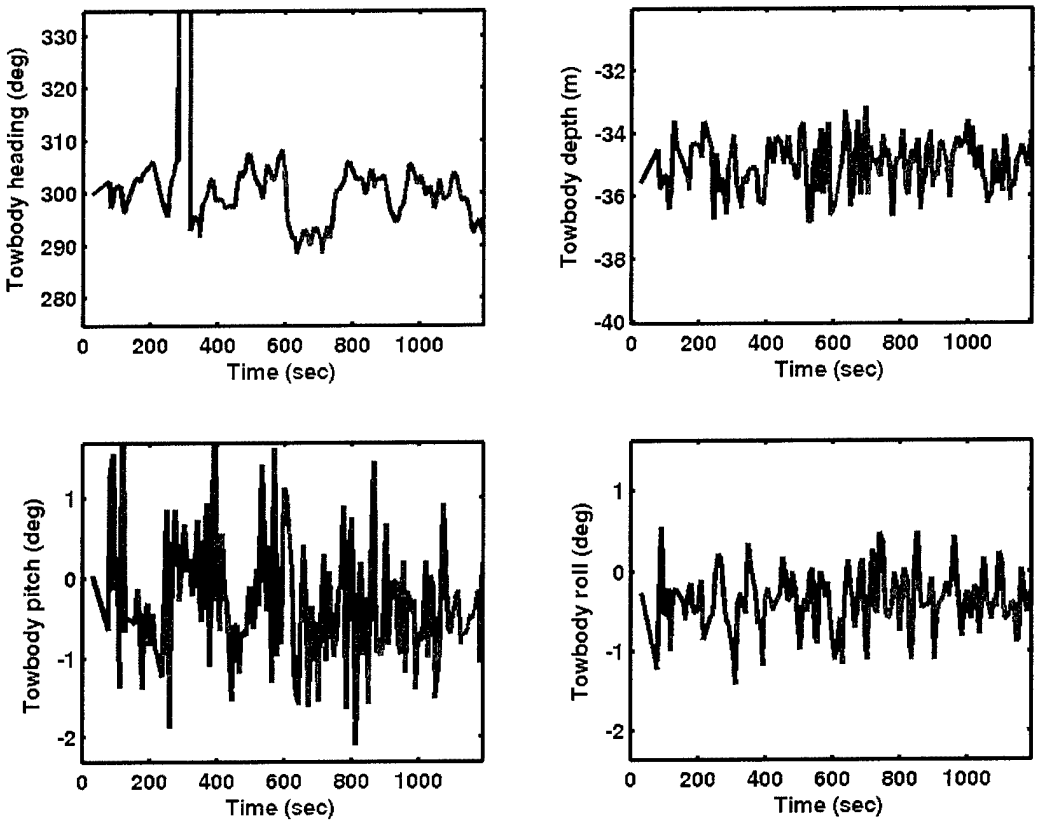

Figure D-13. Towbody motion for run T14. The large change in heading at ~300 s may be a sensor glitch. There are large, long changes in heading which may be affecting the image.

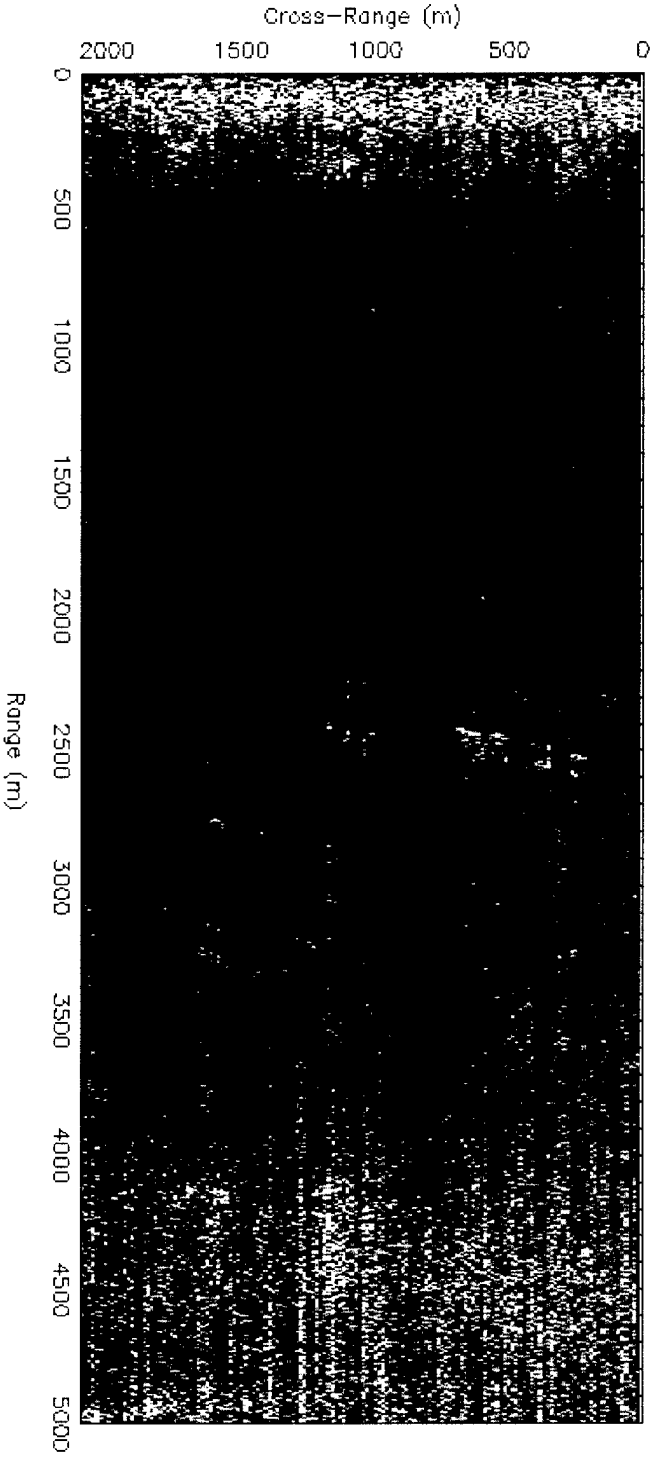

Figure D-14. SLS image for run T14. The on-off nature, in particular the strong returns early in the "smile" indicate strong yaw in the run.

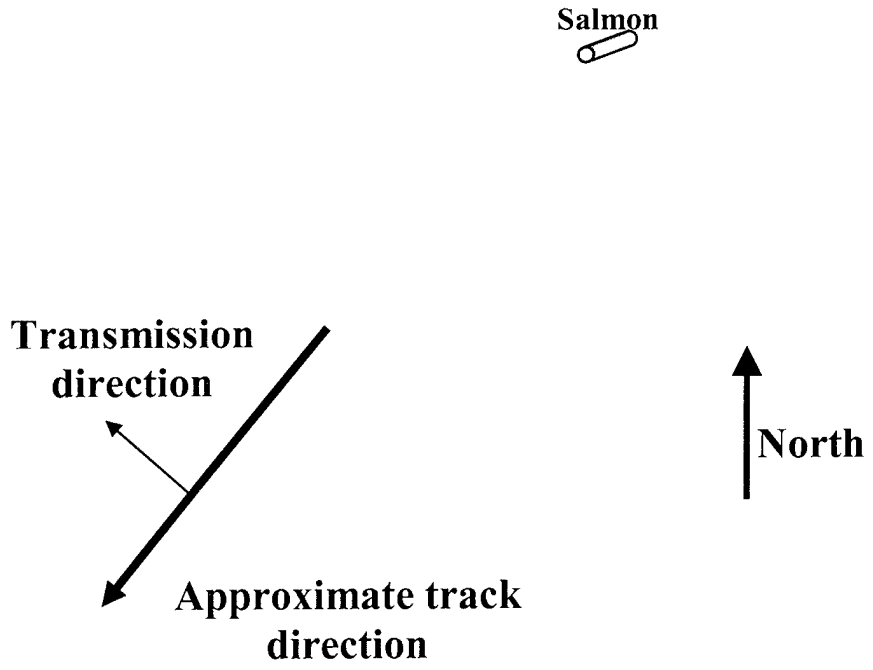

Figure D-15. Schematic of Clutter-only site run with SLS imagery in this appendix.

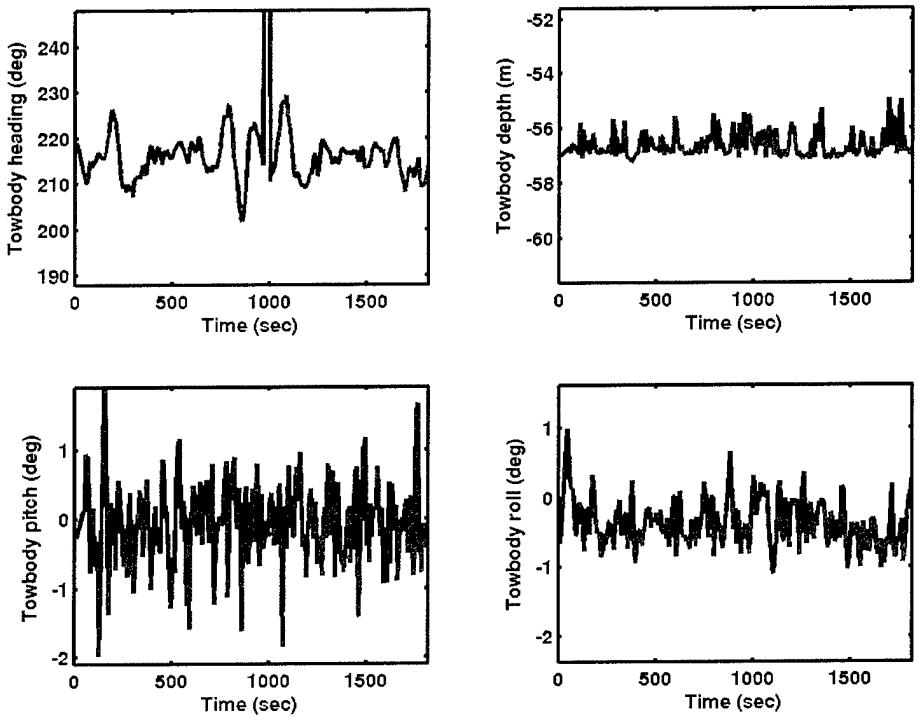

Figure D-16. Towbody motion for run C1. The large heading change at ~1000 s may be a glitch in the sensor. The occasional long deviations in the heading are probably due to course corrections by the Atlantic Surveyor.

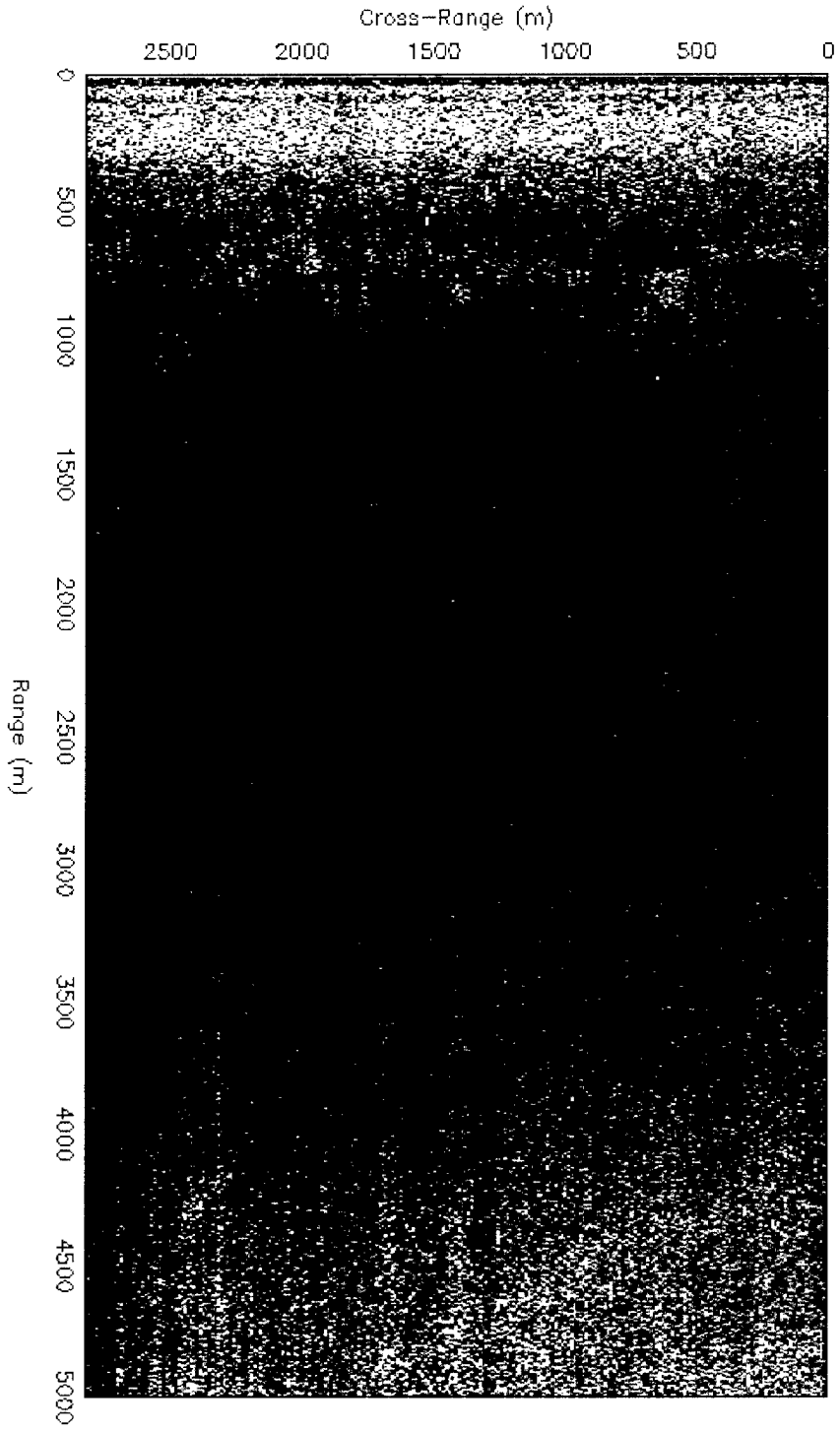

Figure D-17. SLS image for run C1. There are no apparent objects in these data and the scene appears empty aside from the last direct path returns. The current processing scheme cannot form images from this data set.

LIST OF SYMBOLS, ABBREVIATIONS, AND ACRONYMS

3-D	Three dimensional
ASW	Anti-Submarine Warfare
ATR	Automated Target Recognition
AWOIS	Automated Wreck and Obstruction Information System
CONOPS	Concept of Operations
CPA	Closest Point of Approach
DARPA	Defense Advanced Research Projects Agency
DOA	Direction of Arrival
DTI	Dynamics Technology, Inc.
DVD	Digital Video Disc
GDEMV	Generalized Digital Environment Model Variable resolution
GPS	Global Positioning System
IPR	Ideal Point Response
I/Q	In-phase and Quadrature
IRAD	Internal Research And Development
ISLR	Integrated Side-Lobe Ratio
L-3OS	L-3 Communications Ocean Systems
LFM	Linear Frequency Modulation
LRSAS	Long Range Synthetic Aperture Sonar (shortened name of program)
LSB	Least Significant Bit
MAI	Marine Acoustics, Inc.
MCM	Mine CounterMeasures
MMPE	Monterey-Miami Parabolic Equation
NAD	Non-Acoustic Data
NOAA	National Oceanic and Atmospheric Administration
NRL	Naval Research Laboratory
NUWC	Naval Undersea Warfare Center
OEA	Overseas Environmental Assessment
ONR	Office of Naval Research
PCSWAT	Personal Computer Shallow Water Acoustic Tool-set
PE	Parabolic Equation
PingNow	Name of circuit which measure moment of ping and bit the circuit sets.
PGA	Phase Gradient Autofocus
PRI	Ping Repetition Interval
PRO*SAS*™	Name of DTI's real-time SAS processor
RMA	Range Migration Algorithm
ROC	Receiver Operating Characteristic
RPC	Redundant Phase Center
SAR	Synthetic Aperture Radar
SAS	Synthetic Aperture Sonar
SLS	Side-Look Sonar
SNR	Signal to Noise Ratio
SSK	Conventional Submarine
SUPSALV	Supervisor of Salvage (Navy)

SVP	Sound Velocity Profile
VDS	Variable Depth Sonar
XBT	Expendable Bathytheromgraph
XSV	Expendable Sound Velocimeter

INDEX

P

R

S

T

DISTRIBUTION LIST

Douglas A. Abraham — 1 copy
Office of Naval Research
Code 321US - Undersea Signal Processing Team
800 North Quincy Street
Arlington, VA 22217

Dr. Ralph E. Chatham — 1 copy
Program Manager, Training Superiority
Defense Advanced Research Projects Agency
Defense Sciences Office
3701 North Fairfax Drive
Arlington, VA 22203

DCM Norwalk (GAODC) — 1 copy of transmittal letter only
12440 E. Imperial Highway
Suite 750, Box 17
Norwalk, CA 90650-3198

Director, Naval Research Laboratory — 1 copy
ATTN: Code 5227
Washington, D.C. 20375

Defense Technical Information Center — 2 copies
8725 John J. Kingman Road
STE 0944
Ft. Belvoir, VA 22060-6218